Phenotypic comparison of tendon, corneal and skin fibroblast populations

by

Jennifer R. Mackley B.Sc. (Hons)

A thesis submitted in partial fulfilment of the requirements

for the degree of

Doctor of Philosophy

University of Stirling
May 2005

Table of Contents

List of Figures

List of Tables

Acknowledgements

Declaration

I certify that this thesis is the result of my own work, and that I have not been assisted in its production, except where acknowledged in the text. No part of the manuscript has been submitted for consideration for any other higher degree, and all references cited have been consulted.

I certify that Jennifer R. Mackley is the author of this thesis and has complied with the regulations of the University of Stirling appropriate to its submission.

Professor Steven J. Winder   Dr. Michael Wyman
Supervisor   Co-Supervisor
University of Sheffield   University of Stirling

Abstract

Fibroblasts are connective tissue cells that are responsible for the synthesis and turnover of extracellular components, including collagens, proteoglycans and glycosaminoglycans, and adhesive proteins such as fibronectin or laminin. The ability of fibroblasts to regulate their extracellular environment is largely dependent upon the action of matrix metalloproteinases (MMPs), key proteolytic enzymes synthesised and secreted by fibroblasts. Fibroblasts regulate the synthesis of their surrounding extracellular matrix (ECM), which in turn has a profound effect on how cues are presented to and perceived by the cells themselves.

Fibroblasts are capable of synthesising diverse connective tissues and exhibit differences in growth characteristics, metabolism and morphology based upon their tissue of localisation. This thesis investigates the hypothesis that fibroblasts isolated from diverse connective tissues are phenotypically distinct. To test this, primary skin, corneal and tendon fibroblasts were subjected to shear stress produced by a parallel plate flow chamber. Prior to stimulation, the three fibroblast cell lines maintained discrete morphological differences based upon their tissue of origin. Upon stimulation, skin fibroblasts exhibited a larger cell area and all cell lines became increasingly rounded. Furthermore, corneal and skin fibroblasts demonstrated an increased number of focal adhesions per cell, while tendon fibroblasts exhibited a decrease in the number of focal adhesions with stimulation. All three cell lines demonstrated an increase in gelatinase (MMP-2 and MMP-9) activity, though each maintained cell line-specific regulation of gelatinase activity. Microarray analysis, validated by semi-quantitative RT-PCR and Western blotting, indicated that each cell line maintained unique, tissue-specific transcriptional and translational responses. Genes involved in these differential responses were functionally diverse and shown to be both up- and down-regulated with stimulation. Furthermore, levels of encoded proteins from four genes of interest – lumican, dyxin, Crp1 and neogenin – altered with stimulation, though their expression did not correlate with mRNA levels in all cases.

The data presented here provide unequivocal evidence that tendon, corneal and skin fibroblasts are morphologically and phenotypically distinct. Furthermore, this investigation provides an invaluable resource for further study of the factors that control fibroblast heterogeneity and may provide avenues for the manipulation and improvement of tissue engineered prostheses and implants for reconstructive surgery.

Abbreviations

ADAM33	A disintegrin & metalloprotease domain 33
Adamts5	A disintegrin & metalloprotease w/thrombospondin type 1 motif, 5
Akr1b3	Aldo-keto reductase family 1, member B3
Angptl4	Angiopoietin-like 4
Anln	Anillin, actin binding protein
APS	Ammonium persulphate
BCIP	5-bromo-4-chloro-3'-indolyphosphate *p*-toluidine
bp	Base pairs
BSA	Bovine serum albumin
Btbd11	BTB (POZ) domain containing 11
Car3	Carbonic anhydrase 3
Ccl20	Chemokine (C-C motif) ligand 20
Ccne2	Cyclin E2
cDNA	Complimentary DNA
Cebpd	CCAAT/enhancer binding protein delta
Centg2	Centaurin, gamma 2
COMP	Cartilage oligomeric matrix protein
CPD	Cumulative population doublings
cRNA	Complimentary RNA
Crp1	Cysteine and glycine-rich protein 1
Cspg4	Chondroitin sulphate proteoglycan 4
Cxcl5	Chemokine (C-X-C motif) ligand 5
Cxcl14	Chemokine (C-X-C motif) ligand 14
Cyb5	Cytochrome b-5
DAPI	4',6-Diamidino-2-phenylindole
DEPC	Diethylpyrocarbonate
DMEM	Dulbecco's modified Eagle's medium
DMSO	Dimethyl sulphoxide
DNA	Deoxyribonucleic acid
dNTP	Deoxyribonucleotide triphosphate
Dst	Dystonin
Dusp4	Dual specificity phosphatase 4
Dyn	Dynes
Dyxin	LIM and cysteine-rich domains 1
ECL	Enhanced chemiluminescence
ECM	Extracellular matrix
Edn1	Endothelin 1
Ednrb	Endothelin receptor type B
EDTA	Ethylenediaminetetraacetic acid
EGF	Epidermal growth factor
Egr2	Early growth response 2
Egr3	Early growth response 3
Elavl2	ELAV-like 2 (Hu antigen B)
Enpp2	Ectonucleotide pyrophosphatase/phosphodiesterase 2
ER	Endoplasmic reticulum
ERK	Extracellular signal-regulated protein kinase
F-actin	Filamentous actin

FAK	Focal adhesion kinase
FC	Fold-change
FC*nom*	Nominal fold-change
FCS	Foetal calf serum
FDR	False discovery rate
FPCL	Fibroblast-populated collagen lattice
Foxp2	Forkhead box P2
Frmd3	FERM domain containing 3
Fst	Follistatin
Gabarapl1	Gamma-aminobutyric acid receptor-associated protein-like 1
GAPDH	Glyceraldehyde-3-phosphate dehydrogenase
Gas5	Growth arrest specific 5
Gclm	Glutamate-cysteine ligase , modifier subunit
GPI	Glycophosphatidyl inositol
Gsta2	Glutathione S-transferase, alpha 2
Gsta4	Glutathione S-transferase, alpha 4 (Gsta4)
Gulp1	GULP, engulfment adaptor PTB domain containing 1
HBSS	Hank's Balanced Salt Solution
HCl	Hydrochloric acid
Hmox1	Heme oxygenase (decycling) 1
HRP	Horseradish peroxidase
Hsp72	Heat shock protein 1A
iGA	Iterative Group Analysis
ITS	Insulin, transferrin, selenium
IVT	*In vitro* transcription
JNK	c-Jun N-terminal kinase
kb	kilobases
kDa	kilo Daltons
Lcn2	Lipocalin 2
Lpp	LIM domain containing preferred translocation partner in lipoma
Lum	Lumican
MAP	Mitogen-activated protein
MAPK	Mitogen-activated protein kinase
Map3k4	Mitogen activated protein kinase kinase kinase 4
Mlck	Myosin, light polypeptide kinase
MMP	Matrix metalloproteinase
mRNA	Messenger RNA
MSC	Mesenchymal stem cell
MSF	Migration stimulating factor
MSM	Mechanical stimulation medium
NBT	Nitro-blue tetrazolium chloride
N-CAM	Neural cell adhesion molecule
NCBI	National Center for Biotechnology Information
Neo	Neogenin
NGAL	Neutrophil gelatinase B-associated lipocalin
Npn3	Neoplastic progression 3
Nrk	Nik-related kinase
OD	Optical density
Osr1	Odd-skipped related 1 (*Drosophila*)
Pa	Pascal

PAGE	Polyacrylamide gel electrophoresis
PBS	Phosphate Buffered Saline
PCR	Polymerase Chain Reaction
PGE	Prostaglandin E_2
Plf	Proliferin
PLL	Poly L-lysine
PMSF	Phenylmethylsulphonylfluoride
Ptx3	Pentaxin related gene
PVDF	Polyvinylidene fluoride
Rad51	RAD51 homolog (*S. cerevisiae*)
RANKL	Receptor activator of NF-κB Ligand
RER	Rough endoplasmic reticulum
RMA	Robust Multichip Average
RP	Rank Products
RT-PCR	Reverse transcription polymerase chain reaction
RNA	Ribonucleic acid
SAPE	Streptavidin Phycoerythrin
SDS	Sodium dodecyl sulphate
SDS-PAGE	Sodium dodecyl sulphate polyacrylamide gel electrophoresis
SE	Standard error of the mean
Serpinb1b	Serine (or cysteine) proteinase inhibitor, clade B, member 1b
Slc4a4	Solute carrier family 4 (anion exchanger), member 4
Slpi	Secretory leukocyte protease inhibitor
Sphk1	Sphingosine kinase 1
TAME	*p*-toluenesulfonyl-L-arginine methyl ester
TAE	Tris-acetate-EDTA
TBST	Tris-buffered saline with Tween-20
TEMED	N, N, N', N'-tetramethylethylenediamine
TIMP	Tissue inhibitor of matrix metalloproteinase
TNF	Tumour necrosis factor
TPCK	N-tosyl-L-phenylalanylchloromethyl ketone
Tris	Tris(hydroxymethyl)aminomethane
Tslp	Thymic stromal lymphopoietin
UV	Ultraviolet
v/v	volume per volume
VASP	Vasodilator-stimulated phosphoprotein
w/v	weight per volume
Xdh	Xanthine dehydrogenase

CHAPTER 1

Chapter 1

Introduction

1.1 General

Fibroblasts are usually defined as cells of mesenchymal origin that are widely distributed in most vertebrate organisms and are responsible for the production of connective tissue components, including the extracellular matrix (ECM) (Camelliti *et al.*, 2005; Sappino *et al.*, 1990). The ECM has been shown to undergo dramatic degradation and re-synthesis during early development and post-natal growth. While this metabolic turnover diminishes with age, ECM maintenance remains crucial throughout life in numerous connective tissues, as is the case after injury, for example (Kjaer, 2004; Walker *et al.*, 2001). Consequently, it is imperative that fibroblasts not only synthesise and secrete ECM, but also maintain homeostasis of the resultant connective tissue. This has been shown to occur by the fibroblastic production of numerous factors, including cytokines, growth factors, and proteases, all of which are involved in sustaining a balance between the synthesis and degradation of ECM components (Camelliti *et al.*, 2005).

The diversity of connective tissues, each of which is adapted to the functional requirements of the particular tissue, is a direct consequence of the ability of fibroblasts not only to synthesise a wide variety of ECM macromolecules, but also regulate their secretion and organisation (Bron, 2001; Chichester *et al.*, 1993; Gabbiani and Rungger-Brandle, 1981; Kessler *et al.*, 2001; Sappino *et al.*, 1990). The very fact that fibroblasts are capable of synthesising and maintaining such diverse tissues *in vivo* is intriguing and has raised significant interest in recent years. Ongoing research into this capacity has led to the hypothesis that strong variation exists between fibroblasts isolated from different tissues, arising from the cell phenotype as well as its

environment. This introduction will provide a background to the identification, function, origin and diversity of fibroblasts, as well as the mechanisms by which such diversity is thought to arise, in order to put the work presented in this thesis into context.

1.2 Identification of the fibroblast

The term "fibroblast" was first proposed by Schwann, a German microscopist who described the "fibre-cells of areolar tissue" as "being spindle-shaped or longish corpuscles which are thickest in the middle and gradually elongated in both extremities into minute fibres" (Schwann, 1847). From his observations, Schwann ultimately concluded that these cell bodies split into the fibres he observed in the extracellular milieu. Schwann's theory was challenged by subsequent researchers, who believed that the fibres were actively secreted by the fibroblast; this hypothesis was eventually substantiated by Stearns, upon her observation that fibres were never found until fibroblasts had first appeared (Stearns, 1940).

1.3 Fibroblast morphology and behaviour in culture

Fibroblasts were the first cells to be isolated in pure cultures and have subsequently become one of the most widely used cell types to be maintained *in vitro*. Consequently, numerous morphological and ultrastructural studies have been performed on these cells. *In vivo*, fibroblasts occur as single cells surrounded by an extensive ECM; they are irregularly shaped, with stellate, polygonal or spindle-shaped outlines, contain substantial cytoplasm around the nucleus, and possess long, filopodial extensions of the plasma membrane (Conrad *et al.*, 1977b; Maximow, 1927). From ultrastructural studies, fibroblasts were observed to have prominent rough endoplasmic

reticulum (RER) and Golgi apparatus, and their cytoplasm appeared to contain numerous vesicles, vacuoles, mitochondria and intermediate filaments (Chapman, 1962). While fibroblasts do not appear to establish extensive contacts amongst themselves *in vivo* (Gabbiani and Rungger-Brandle, 1981), at least one instance of cell-cell communication via gap junctions has been previously observed (Banes *et al.*, 1999b).

When fibroblasts are cultured, however, their morphology changes rather substantially. *In vitro*, fibroblasts are characterised by their ability to proliferate in culture with attached, well-spread morphology. The cells demonstrate a flattened and polarised morphology and contain numerous actin stress-fibres (Ross and Greenlee, Jr., 1966). Moreover, cultured fibroblasts show close physical apposition and can be interconnected via integrins, adherens junctions and gap junctions (Banes *et al.*, 1999b; Konttinen *et al.*, 2000; Sappino *et al.*, 1990).

Furthermore, when cultured, two populations of fibroblasts have been observed to exist, one of which is made up of larger, more epithelioid cells that are capable of only one or two divisions and another which is comprised of smaller, more proliferative cells (Martin *et al.*, 1974). This phenomenon was later qualified by Bayreuther and colleagues, who observed that primary fibroblast cultures had definite mitotic lifespans, after which cellular degeneration occurred (Bayreuther *et al.*, 1988). They observed that, in a given population of primary fibroblasts, both mitotic and post-mitotic cells existed. The mitotic fibroblast population was observed to include three cell types: FI, a small, spindle-shaped cell; FII, a small, epithelioid cell; and FIII, a larger pleiomorphic epithelioid cell. The post-mitotic population, on the other hand, was found to consist of four cell populations: FIV, which was large in appearance, with an overall spindle-shape; FV, a large cell with epithelioid morphology; FVI, an even larger

cell with epithelioid appearance; and FVII, which corresponded to a degenerating fibroblast. In their study, Bayreuther and colleagues cultured a primary fibroblast cell line for 52 cumulative population doublings (CPD) and observed that, up to CPD 14, the population consisted of mainly FI and FII fibroblasts. As the population progressed to CPD 52, there was an increasing occurrence of FII and FIII fibroblasts. After CPD 52, when the growth rate was less than 0.2 population doublings per day, fibroblasts were termed post-mitotic. At this point, cells were maintained for a further 315 days in culture without any further passaging. As the time in culture increased, there was an increasing appearance of FIV-FVI fibroblasts before degenerating fibroblasts were seen after approximately 280 days in stationary culture.

1.4 Developmental origin of fibroblasts: the relationship between mesenchymal stem cells and fibroblasts

Connective tissues, as well as the cells that synthesise them, arise from the mesoderm. The cells that synthesise these connective tissues are all characterised as being mesenchymal, due to their ability to spread and migrate in early embryonic development between the ectodermal and endodermal layers (Caplan, 1991). Such mesenchymal cells include members of the connective tissue cell family, such as fibroblasts, osteoblasts, chondrocytes, adipocytes and myoblasts. Together, these cells are capable of synthesising and regenerating all types of mesenchymal tissues, including bone, cartilage, ligament, tendon, adipose, muscle and stroma (Pittenger *et al.*, 1999).

All of the aforementioned connective tissue cells are thought to share a common progenitor cell, currently termed the mesenchymal stem cell (MSC). MSCs are fibroblastic in appearance and can be isolated from bone marrow, around blood vessels,

in adipose tissue, skin, muscle and various other locations, based upon their adherence in culture (Caplan and Bruder, 2001; Prockop, 1997). MSCs cultured *in vitro* can be induced to differentiate into osteoblasts, chondrocytes, adipocytes and myoblasts, and as a consequence, are thought to represent a unique cell population that is capable of differentiating along multiple mesenchymal cell lineages (Phinney *et al.*, 1999).

This raises an obvious question: are fibroblasts the common connective tissue progenitor cell? Until this question was answered recently (Pittenger *et al.*, 1999), interpretation following the observation of connective tissue cells in culture was sometimes difficult. For example, when Movat and Fernando were conducting the first systematic ultrastructural study of fibroblasts in various connective tissues, the difficulty of determining whether a given connective tissue cell was an "undifferentiated" mesenchyme cell, a fibroblast, a fibrocyte (meaning a terminally differentiated fibroblast), a chondrocyte, or osteoblast was discussed (Conrad *et al.*, 1977b).

Recently, however, in an elegant experiment performed by Pittenger *et al.*, it was shown that fibroblasts and MSCs are not one and the same, despite their somewhat uncanny morphological similarities (Pittenger *et al.*, 1999). In their study, the differentiation potential of MSCs isolated from bone marrow was tested alongside two strains of human fibroblasts under conditions known to promote adipogenic, chondrogenic or osteogenic lineages (Pittenger *et al.*, 1999). According to their study, MSCs gave rise to adipocytes, chondrocytes and osteocytes after 1-3 weeks, whereas normal human fibroblasts did not undergo any such differentiation when cultured for as long as 28 days. It is clear from this evidence that MSCs have a differentiation capacity that is not present in primary fibroblasts, which are suggested to be "mature" mesenchymal cells. Nonetheless, it remains unknown when, where, and how

mesodermal cells differentiate first into mesenchymal cells and then into fibroblasts (Shimizu and Yoshizato, 1992).

1.5 Fibroblasts exist in biochemically and morphologically distinct subpopulations

Despite the fact that fibroblasts were shown to be incapable of interconverting into other members of the connective tissue cell family by Pittenger and colleagues (Pittenger *et al.*, 1999), evidence has accumulated which indicates that they are, nonetheless, a highly diverse population of cells, which exhibit a considerable degree of phenotypic heterogeneity. Such variability has been observed in overall morphology, as well as numerous, fundamental aspects of cell behaviour, such as growth rate, proliferative potential and protein synthesis. Since differentiative cell behaviour has been identified in fibroblasts isolated from different regions of the same tissues, or different tissues altogether, fibroblasts are currently hypothesised to demonstrate both intra- and inter-site heterogeneity. Evidence for this hypothesis follows.

1.5.1 Inter-site heterogeneity

Phenotypic heterogeneity, as well as the possibility that fibroblasts were not homogeneous populations, as so many studies presumed, was discussed in very early investigations of fibroblast-like cells *in vitro* (Parker and Fischer, 1929; Parker, 1932; Porter and Vanamee, 1949). In one of the earliest reports, for example, Parker and Fischer demonstrated that fibroblasts isolated from the same embryo and maintained under identical culture conditions displayed different proliferation rates and varying responses to increasing embryonic serum concentration (Parker and Fischer, 1929). In order to investigate this apparent fibroblast heterogeneity more rigorously, Parker went on to compare directly nine different fibroblast strains from various tissues of the same

organism and found that the cells could be distinguished based upon differing growth rates as well as the relative amount of free acid that accumulated in the culture medium (Parker, 1932).

While the results obtained from the early studies of Parker and Porter were compelling, their isolation procedures were not rigorous, and hence could not rule out the possibility that the heterogeneity they were observing was due to contamination by non-fibroblastic cells, which can assume fibroblastic morphologies *in vitro*. Consequently, numerous studies followed, which used increasingly stringent isolation protocols in order to investigate the possibility that fibroblasts exist as heterogenous populations *in vitro*, and by implication, *in vivo*.

In one such investigation, Conrad and colleagues illustrated that corneal, heart and skin fibroblasts exhibited unique morphology and behaviour in culture (Conrad *et al.*, 1977a; Conrad *et al.*, 1977b). For example, the three fibroblast cell lines demonstrated differing cell density at saturation, behaviour upon reaching confluency, sensitivity to trypsin and EDTA, ability to be subcultured, and glycosaminoglycan synthesis. In the same year, embryonic skin and lung fibroblasts were compared, which revealed differences in proliferation, cell density at confluence, and DNA synthesis (Schneider *et al.*, 1977).

The possibility of inter-tissue fibroblast heterogeneity was carried further by the work of Garret and Conrad. In this study, fibroblasts isolated from cornea, skin and heart were used as antigens to produce a series of antibodies that were subsequently cross-absorbed for specificity. Based upon a series of experiments including immunodiffusion, immune agglutination, immune cytotoxicity and indirect immunofluorescence, the three fibroblast cell lines were determined to be antigenically distinct (Garrett and Conrad, 1979). Furthermore, Shimizu and Yoshizato showed that

heart, skin and lung fibroblasts demonstrate unique morphology and proliferative capacity. The same study also illustrated that the proteome of the cell lines, despite being largely similar, contained proteins that were produced in an organ-dependent manner (Shimizu and Yoshizato, 1992).

1.5.2   Intra-site heterogeneity

Not only do fibroblasts appear to display differences when isolated from diverse tissues, but evidence also exists suggesting that "subpopulations" of fibroblasts exist within different regions of the same tissue. Two early studies demonstrated, for example, the presence of subpopulations of skin fibroblasts derived from single foreskin explants, based upon variations in lysosomal enzyme activity (Milunsky *et al.*, 1972) and testosterone metabolism (Kaufman *et al.*, 1975). Martin and colleagues corroborated these observations with data indicating that subclones of human skin fibroblast cultures displayed differences in growth rates and morphology (Martin *et al.*, 1974).

Harper and Grove carried these investigations further, by directly comparing skin fibroblasts isolated from either the papillary or reticular dermis. Their investigation indicated that the two cultures demonstrated a subtle difference in cell density at saturation; indeed, papillary cultures were found to have greater saturation levels as opposed to reticular cultures, which was rationalised by the distinct physiological roles of these cell populations *in vivo* (Harper and Grove, 1979). These reports were corroborated by the isolation and characterisation of synovial and internal tendon fibroblasts by Riederer-Henderson and colleagues (Riederer-Henderson *et al.*, 1983). Based upon their investigations, it became apparent that synovial cells had lower attachment efficiencies when compared to internal tendon fibroblasts. These

findings were later substantiated by Banes *et al.* in a study that reported synovial and internal tendon fibroblasts maintained distinct morphology, adherence and proliferation in culture (Banes *et al.*, 1988a).

Carrying these investigations of intra-site heterogeneity further, Irwin and colleagues investigated the possibility of fibroblasts existing in culture as either migrating or synthesising fibroblasts (Irwin *et al.*, 1994). In their study, fibroblasts isolated from the papillary tips or the deeper reticular region of the gingival tissue were compared. These two fibroblast populations were found to maintain differential expression of migration stimulatory factor (MSF), a novel protein previously identified in their laboratory and found to be responsible for migratory phenotypes present in foetal fibroblasts that was otherwise missing in adult cells (Schor *et al.*, 1988). Consequently, Irwin and colleagues reported that papillary fibroblasts displayed more foetal-like characteristics of migration in conjunction with persistent MSF production (Irwin *et al.*, 1994).

1.6 Fibroblast heterogeneity appears to be modulated by soluble factors and cell-matrix interactions

While it appears, from the evidence presented above, that fibroblasts display inter- and intra-site heterogeneity, it is nonetheless difficult to identify the precise mechanisms whereby this "differentiation" occurs, namely because there is no known universal marker for fibroblasts, much less fibroblast subpopulations. Consequently, it is difficult to determine whether a true population of fibroblasts is being studied, without any contaminating fibroblast-like mesenchymal precursors and/or committed fibroblast subpopulations.

Nonetheless, differentiation of a variety of cell types has been shown to be mediated by soluble factors, such as growth factors or hormones, as well as cell-cell and cell-matrix interactions. While it is entirely possible that cell-cell interactions are important in fibroblast heterogeneity, this has not been validated to date. There does exist, however, a substantial body of evidence that suggests that both soluble factors and cell-matrix interactions play a role in driving and maintaining inter- and intra-site fibroblast heterogeneity.

1.6.1   The role of soluble factors in fibroblast heterogeneity

One of the earliest reports to suggest that soluble factors, such as hormones or growth factors, could be used to distinguish fibroblast subpopulations came from Kaufman and colleagues, in which three populations of skin fibroblasts isolated from the same explant were distinguished based upon testosterone metabolism (Kaufman *et al.*, 1975). Several years later, cultures of isolated gingival fibroblasts were found to contain subpopulations based upon the fact that prostaglandin E_2 (PGE$_2$), a hormone-like substance known to elicit a range of functions in various cell types, was found to inhibit protein synthesis, membrane transport, and DNA synthesis in only 50% of the cell population (Ko *et al.*, 1977). Smith and colleagues substantiated these findings by demonstrating that only approximately 22-50% of a given population of human orbital fibroblasts demonstrated a PGE$_2$-dependent shape change (Smith *et al.*, 1995). Finally, Lee and Eun revealed that the amount of collagen synthesised by dermal and oral mucosa fibroblasts could be altered after stimulation with transforming growth factor (TGF)-β1; oral fibroblasts were found to synthesise more collagen than dermal fibroblasts after stimulation (Lee and Eun, 1999).

1.6.2   The role of cell-matrix interactions in fibroblast heterogeneity

In addition to soluble factors, cell-matrix interactions also appear to be important in fibroblast heterogeneity. This is not surprising, given that fibroblasts are usually a sparse population surrounded by an extensive ECM *in vivo* (see sections 1.7.1-1.7.3). Cell-matrix interactions are dependent upon transmembrane receptors, which are themselves capable of transducing chemical, topographical or mechanical cues to the actin cytoskeleton, thus eliciting an intracellular response (see section 1.7).

Chemical and topographical cues arise from the macromolecular composition and precise organisation of the surrounding ECM. Numerous studies indicate that fibroblasts can be distinguished based upon the types of matrix macromolecules produced. For example, Conrad and colleagues identified that corneal, heart and skin fibroblasts maintain differences in the amounts of synthesised glycosaminoglycans (Conrad *et al.*, 1977a). Such reports were corroborated by the isolation and characterisation of synovial and internal tendon fibroblasts by Riederer-Henderson and colleagues. Based upon their investigations, it became apparent that synovial cells secreted less collagen and sulphated glycosaminoglycans when compared to internal tendon fibroblasts. Furthermore, the types of collagen produced by each cell line was found to differ; synovial cells synthesised types I and III collagen, while internal tendon fibroblasts only synthesised type I collagen (Riederer-Henderson *et al.*, 1983). Banes *et al.* identified differential synthesis and localisation of yet another matrix macromolecule, fibronectin (Banes *et al.*, 1988b). In this study, synovial and tendon fibroblasts were distinguished based upon staining with an anti-fibronectin antibody; it was found that synovial fibroblasts were principally responsible for the synthesis of this protein.

Several years later, Breen and colleagues presented evidence that lung fibroblasts could be separated into two subpopulations based upon the ratios of associated type I to type III collagens to their plasma membranes. According to their results, generated by flow cytometry, one population demonstrated a high density of type I collagen receptors in conjunction with elevated cellular steady-state levels of pro-α1(I) and pro-α2(I) mRNA. In contrast, the other population had a higher density of type III collagen surface receptors with higher cellular steady-state levels of pro-α1(III) mRNA (Breen *et al.*, 1990). Finally, collagen and fibronectin secretion was also found to vary between skin, heart and lung fibroblasts, with heart cells demonstrating the highest levels of secretion for both proteins (Shimizu and Yoshizato, 1992).

In addition to chemical and topographical cues, transmembrane receptors are also capable of transducing mechanical cues, which arise from both the endogenous tension generated by the cytoskeleton as well as exogenous forces produced by or conveyed through the surrounding connective tissue. These mechanical cues also appear to influence and/or reinforce heterogeneity, as apparent from several studies that have observed the ability of fibroblasts from different tissues to generate altered magnitudes of internal cytoskeletal tension *in vitro*. As shown by Shimizu and Yoshizato, heart fibroblasts, when cultured in three-dimensional collagen gels, were capable of contracting the matrix more effectively than skin or lung fibroblasts (Shimizu and Yoshizato, 1992). Similar differential contractile capabilities were substantiated by Lee and Eun. In this study, fibroblasts isolated from the oral mucosa and normal skin demonstrated differential proliferation rates and also exhibited different contraction potencies when cultured in collagen gels. In this case, dermal fibroblasts demonstrated the greatest contractile potency (Lee and Eun, 1999). Evans

and Trail carried these investigations further by presenting an exogenous mechanical stimulus to fibroblasts isolated from distinct regions of tendon. In this study, the group examined the response of flexor and extensor tendon fibroblasts to mechanical strain in the form of a stretched, three-dimensional collagen matrix (Evans and Trail, 2001). Both cell lines were found to have similar morphology, though flexor tendon fibroblasts demonstrated increased cell numbers in comparison to extensor cells.

1.7 Fibroblasts synthesise the extracellular matrix

Since the early observations of Schwann and Stearns (Schwann, 1847; Stearns, 1940), it has become apparent that fibroblasts synthesise and secrete several proteins, including various types of collagen, adhesive proteins such as fibronectin and laminin, and proteoglycans, a class of macromolecules consisting of a protein core onto which numerous polysaccharide units, termed glycosaminoglycans, are bound (Breen *et al.*, 1990; Chichester *et al.*, 1993; Dunphy, 1963; Gabbiani and Rungger-Brandle, 1981; Herrmann *et al.*, 1980). Together, these macromolecules constitute the ECM, an organized meshwork that exists in close association to the connective tissue cells that produced it, namely fibroblasts, osteoblasts, adipocytes or chondrocytes.

The ECM is broadly defined as all secreted molecules that are immobilised outside of cells, which collectively function to: (1) help regulate spatial and temporal properties of growth factors, chemotropic agents, and other soluble factors (Kaname and Ruoslahti, 1996); (2) activate intracellular signalling pathways upon the binding of ECM ligands to these factors (Burridge and Chrzanowska-Wodnicka, 1996; Schwartz *et al.*, 1995); (3) permit the migration of cells and movement of growth cones (Reichardt and Tomaselli, 1991); and (4) contribute to the overall mechanical integrity, rigidity, and elasticity of connective tissues such as skin, tendon, ligaments,

vasculature, bone, and cartilage (Hynes, 1996). Consequently, the ECM has been implicated in the regulation of diverse cellular processes, such as proliferation, migration, cell survival, and differentiation.

The ECM consists of three major macromolecular constituents: (1) fibrillar proteins; (2) adhesive glycoproteins; and (3) proteoglycans. The fibrillar proteins present in the ECM, such as collagen and elastin, provide a largely structural role and impart strength and resilience to the tissue (Canty and Kadler, 2002). Adhesive glycoproteins, such as laminin and fibronectin, aid in the attachment of cells to, and the organisation of, the ECM. Adhesive proteins usually have multiple domains, each with binding sites for other matrix macromolecules, cell-surface proteins, signalling molecules, and/or proteases or protease inhibitors (Hynes, 1999). Consequently, adhesive proteins are capable of attaching cells to the ECM, as well as initiating various cellular responses through classical signal-transduction pathways. Proteoglycans, on the other hand, are a group of diverse glycoproteins, with functions mediated by both their protein cores and glycosaminoglycan side chains (Danielson *et al.*, 1997; Kanwar *et al.*, 1980). The protein core of proteoglycans contains numerous domains, including putative hyaluronic acid binding domains, calcium-dependent lectin (sugar-binding) domains, leucine-rich repeats, epidermal growth factor (EGF) repeats, and immunoglobulin-like domains. Collectively, these diverse domains hint toward the adhesive and mitogenic functions sometimes displayed by proteoglycans (Lander, 1999). Overall, however, these proteins, and the charged polysaccharides which are attached to them, form a highly hydrated, swelled structure that is largely responsible for the volume of the ECM, allows for the diffusion of small molecules between cells and tissues, and offers compressive resilience to the tissue (Comper, 1996).

Based upon the synthesis and secretion of such a wide variety of molecules, fibroblasts, and other members of the connective tissue cell family, are capable of synthesising a striking diversity of connective tissues, including bone, cartilage, muscle, ligament, tendon, adipose and stroma. This study has focused on fibroblasts isolated from three structurally diverse connective tissues: tendon, cornea and skin. A brief description of each follows.

1.7.1 *Extracellular matrix of the tendon*

Tendons are soft connective tissues with a densely packed and highly organised ECM, consisting of approximately 85% collagen, 1-5% proteoglycan, and 2% elastin, by dry weight (Figure 1.1) (Lin *et al.*, 2004). Tendon is comprised of predominantly type I collagen, though collagen types III, IV, V and VI are also present, albeit in much smaller quantities (Dressler *et al.*, 2002; Hanson and Bentley, 1983; Vogel and Meyers, 1999). In tendon, collagen is organised into tensile-resistant fibrils, fibres, fibre bundles, and eventually fascicles (Silver *et al.*, 2003a). This hierarchical organisation of collagen increases its structural strength and helps to protect the tissue as a whole from minor damage that might occur from the high tensile forces that result from the transmission of forces between muscle and bone (Rack and Westbury, 1984; Raspanti *et al.*, 1990). A number of proteoglycans have been identified in tendon, including decorin, cartilage oligomeric matrix protein (COMP), fibromodulin, biglycan, lumican, syndecan, perlecan, agrin, versican, and aggrecan. When hydrated, water is thought to account for 60-80% of the tendon's total weight, a substantial amount of which is thought to be associated with proteoglycans (Lin *et al.*, 2004). Tendon ECM has also been found to contain several adhesive proteins, such as laminin and fibronectin (Kjaer, 2004).
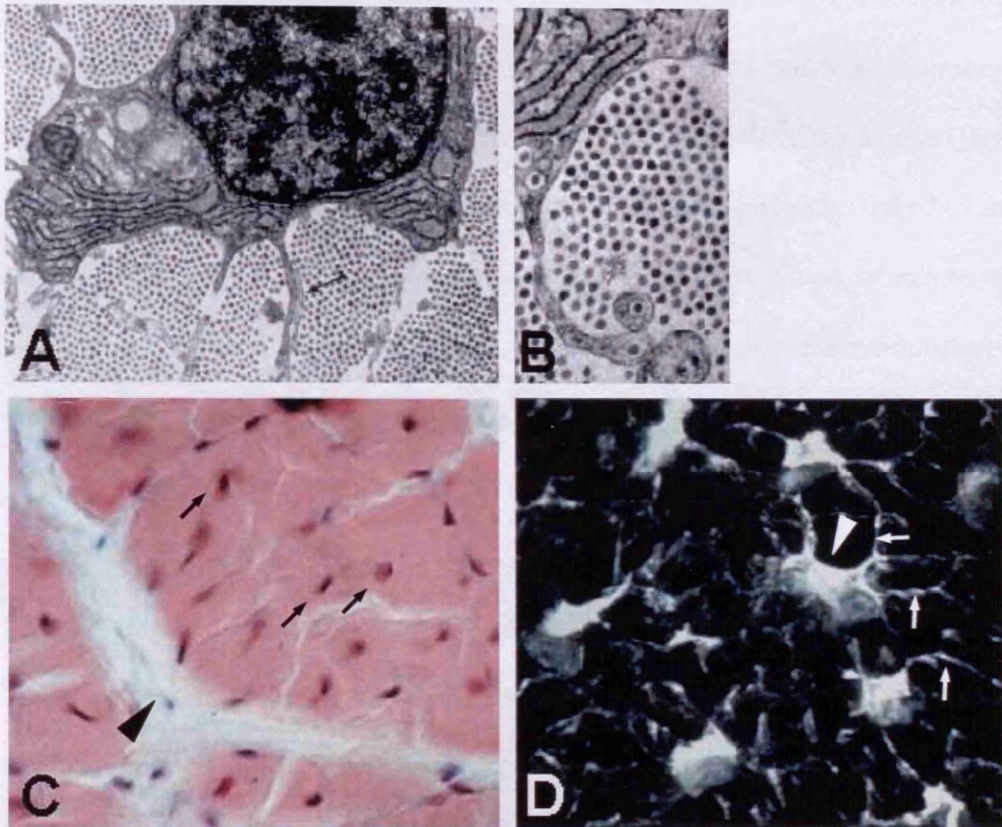
Figure 1.1: Extracellular matrix of the tendon. (A) Transmission electron micrograph showing the arrangement of collagen fibrils in tendon. (B) Higher magnification view of a collagen fibril bundle (A). (C) Transverse section of a hematoxylin and eosin stained tendon fascicle, illustrating the longitudinal arrangement of fibroblasts (arrows) *in vivo*. The fascicle is seen surrounded by loose connective tissue (arrowhead). (D) Confocal image of a transverse section of tendon illustrating adjacent fibroblasts (arrowhead) within a fascicle. The fibroblasts all contain sheet-like processes (arrows) that extend into the surrounding ECM. (A) and (B) modified from (Silver *et al.*, 2003a); (C) and (D) modified from (Kjaer, 2004).

Tendons contain relatively few cells (Figure 1.1) (Lin *et al.*, 2004). Of these, the fibroblast is the most predominant cell type, though other cell types such as epithelial cells, mast cells and axons are also present within the ECM (Kjaer, 2004; McNeilly *et al.*, 1996). *In vivo*, tendon fibroblasts demonstrate a fusiform morphology, possess abundant, sheet-like extensions that extend into the ECM, and have been shown to be oriented along the lines of tension that exist in the long axis of the tendon (Banes *et al.*, 1988a; McNeilly *et al.*, 1996). Fibroblasts have been found to be linked to each other via gap junctions, and are thought to assist in the transduction of mechanical signals into biochemical responses, a phenomenon referred to as mechanotransduction (see section 1.8) (Banes *et al.*, 1999b).

The mechanical properties of tendon are dependent on the properties and axial alignment of the collagenous network as well as cell-matrix interactions. This connective tissue serves to connect muscle to bone and hence forms a musculotendinous unit, whose primary function is to transmit tensile loads generated by muscle to move and stabilise joints (Banes *et al.*, 1999a; Lin *et al.*, 2004).

1.7.2   *Extracellular matrix of the cornea*

The cornea is the only transparent connective tissue and is responsible for the majority of the refractive power of visible light in the eye (Karring *et al.*, 2004). The bulk of the cornea consists of the corneal stroma, which itself is a hydrated ECM consisting of collagen and proteoglycans. Most collagens present in the stoma exist in the fibrillar form and are composed mostly of types I, III and V collagen, though some non-fibrillar collagens are also present, with types VI and XII being the most prominent (Marshall *et al.*, 1991; Michelacci, 2003). In addition to collagen, the corneal stroma is also characterised by the prevalence of proteoglycans in its ECM, the most abundant of

which are decorin, lumican, keratocan and mimecan (Bron, 2001; Funderburgh *et al.*, 2003).

Similar to that of the tendon, the ECM of the corneal stroma is highly organised (Figure 1.2). Collagen fibrils within the corneal stroma are arranged in broad lamellae that are aligned with corneal surface (Radner *et al.*, 1998). Whilst fibrils in the same lamella run approximately parallel to one another, those in adjacent lamellae tend to lie at perpendicular angles; the fibrils within the lamellae have uniform diameter, and regular spacing (*ibid.*). This high degree of organisation, which is thought to be responsible for both the strength and transparency of the cornea (Bron, 2001), is a consequence of both the fibroblasts that synthesise it, as well as the biochemical properties of the matrix macromolecules themselves. For example, it is thought that the overall negative charge possessed by glycosaminoglycan side chains is capable of some degree of ordering, due to repulsive electrostatic forces. Furthermore, the mix of collagen types in this ECM seems to determine the ultimate size to which the collagen fibrils can grow laterally. Molecules of collagen type V, for example, serve to limit growth when incorporated into a growing type I fibril (Marchant *et al.*, 1996).

The corneal stroma is populated by quiescent corneal fibroblasts, also called keratocytes, which are flattened, stellate-shaped cells interspersed between the collagen lamellae (Pei *et al.*, 2004). Keratocytes can be maintained in their quiescent state by culturing in the absence of serum. If cultured with serum, however, keratocytes become "activated" and transform into spindle-shaped fibroblasts, which is reminiscent of the activation of keratocytes *in vivo* after injury (Matsuda and Smelser, 1973).
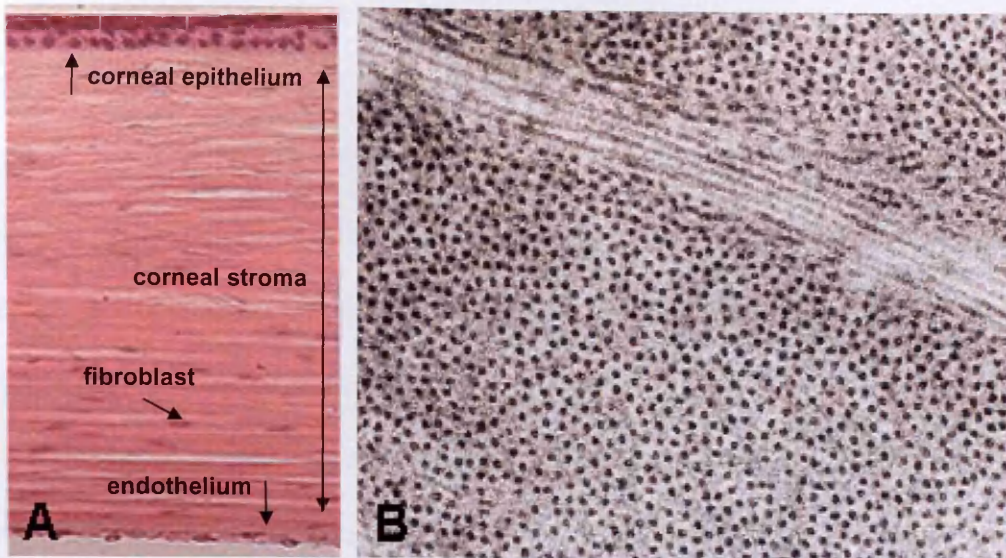
Figure 1.2: Extracellular matrix of the corneal stroma. (A) Micrograph of hematoxylin and eosin stained cornea. The corneal epithelium and endothelium delineate the corneal stroma, which makes up the bulk of the cornea. Corneal fibroblasts can be seen within the collagen fibrils of the stroma (arrow). (B) Transmission electron micrograph illustrating the arrangement of collagen fibrils in the corneal stroma. Fibrils are of fixed diameter, regularly spaced, and ordered in broad lamellae that are perpendicular to one another. (A) modified from http://www.siumed.edu/~dking2/intro/IN022b.htm; (B) modified modified from http://www.optometry.co.uk/files/377a0e69e398a201252a0bb3680f7f88_quantock20001215.pdf.

1.7.3 Extracellular matrix of the skin

Skin is a multilayered composite consisting of an upper cellular layer and a lower connective tissue layer, called the epidermis and dermis, respectively (Figure 1.3). The dermis, consisting of both cells and ECM, is organised into a further two regions based upon the density and arrangement of the connective tissue. The papillary dermis is the upper region, which appears as a feltwork of randomly oriented, small-diameter collagen fibres, while the deeper region, known as the reticular dermis, consists of loosely interwoven, large, wavy, randomly oriented collagen bundles

(Sorrell and Caplan, 2004; Silver *et al.*, 2003b). The somewhat random arrangement of the collagen fibrils in the dermal tissue is in stark contrast to that seen in the tendon or cornea (see sections 1.7.1, 1.7.2).

Collagen is reported to compose approximately 66% and 69% of the total volume of the papillary and reticular dermis, respectively (Lavker *et al.*, 1987). The dermis, as a whole, contains fibrillar collagens, the majority of which are types I and III collagen (Light, 1985), as well as non-fibrillar forming collagens, such as types IV, VI, and VI (Silver *et al.*, 2003b). Though collagen accounts for the bulk of the dermal ECM, a number of other matrix macromolecules are also present. For example, elastic tissue, consisting of elastin, fibrillins and microfibrillar-associated glycoproteins, forms a three-dimensional network which spans the papillary and reticular dermis and helps impart elasticity to dermal tissue (Pasquali-Ronchetti and Baccarani-Contri, 1997). In addition, glycosaminoglycans, such as hyaluronan, and proteoglycans, including heparin, versican, lumican, decorin, and biglycan, are also present (Hassell *et al.*, 1980; Iozzo and Murdoch, 1996).

Fibroblasts constitute the dominant cell type in the dermal tissue and appear to be associated with the surface of collagen fibrils (Silver *et al.*, 2003b). Fibroblasts have been found to be more abundant, have higher rates of metabolic activity, display enhanced proliferation, and a exhibit longer replicative life spans in the papillary dermis (Harper and Grove, 1979; Sorrell and Caplan, 2004; Tajima and Pinnell, 1981).

The organisation of this ECM and, hence, the connective tissue of skin results from the internal and external forces to which the tissue is regularly subjected. External forces are defined as those that result from either tension, when skin is compressed or stressed, or shear, which results from friction. Such external forces arise
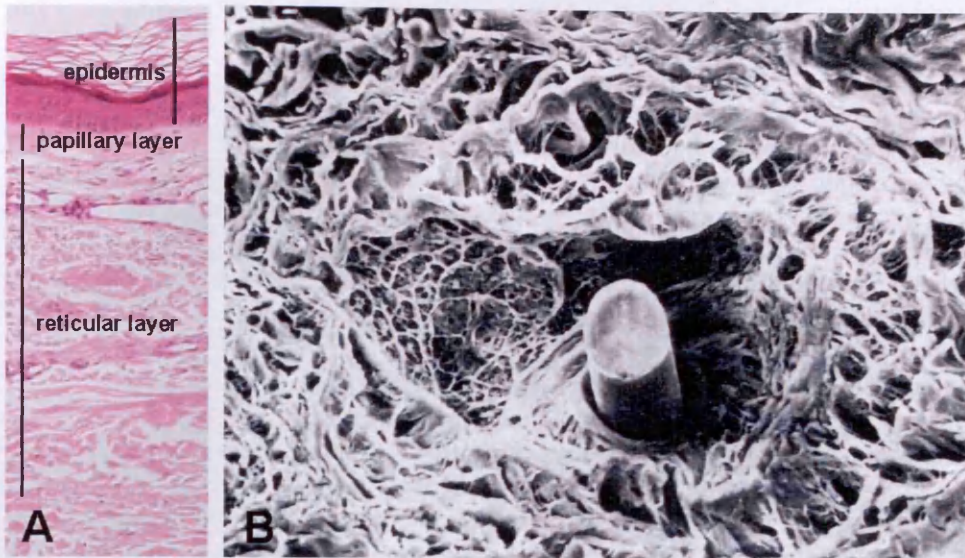
Figure 1.3: Extracellular matrix of skin. (A) Transverse section of hematoxylin and eosin stained skin. The layers of skin are indicated, including the epidermis and the papillary and reticular layers of the dermis. (B) Electron micrograph demonstrating the arrangement of collagen fibrils in human skin. (A) modified from http://cellbio.utmb.edu/microanatomy/skin/cskin.jpg; (B) courtesy of Professor Peter Purslow, University of Guelph, Canada.

during physiological processes, such as wound healing (Silver *et al*., 2003b), or by environmental stimuli, such as gravity (Ingber, 1999). Internal forces, on the other hand, result from inherent tension incorporated into the collagen fibril network (Grinnell, 2000). Collagen is thought to prevent premature mechanical failure of the tissue by aligning in the direction of the load (Dunn and Silver, 1983; Daly, 1982), and elastic fibres are believed to contribute to the recovery of the collagen networks when skin is subjected to such internal or external forces (Oxlund *et al*., 1988).

1.7.4 Fibroblasts regulate the ECM by secreting proteolytic enzymes

Extracellular matrices are dynamic structures and thus are subject to diverse influences from external stimuli and internal changes, cell-matrix interactions and genetic regulation (Carlson and Hockfield, 1996). In addition to the macromolecules

21

already mentioned, fibroblasts have also been shown to be capable of synthesising and secreting various proteolytic enzymes, including serine proteases and matrix metalloproteinases (MMPs), as well as some of their specific inhibitors, whose function is to modulate the formation of the ECM (Sappino *et al.*, 1990). The ability of fibroblasts to degrade ECM macromolecules is essential for the cell to be able to interact properly with its microenvironment. Furthermore, the selective synthesis, secretion and activation of MMPs allows fibroblasts to exert fine control over the composition and turnover of the surrounding ECM (Sternlicht and Werb, 2001).

1.7.4.1 Matrix metalloproteinases

Matrix metalloproteinases are a family of zinc-containing proteases synthesised and secreted by fibroblasts that serve to alter the composition and structural organisation of the ECM, which is essential for various cell processes including migration, morphogenesis, tissue resorption and remodelling, embryonic development, and disease (Nelson *et al.*, 2000; Phillips *et al.*, 2003). MMPs can potentially influence cell behaviour by cleaving cell-cell adhesion proteins, releasing bioactive cell surface molecules, or cleaving cell surface molecules that transduce signals from the extracellular environment (Sternlicht and Werb, 2001).

MMPs belong to the metzincin superfamily of endopeptidases, which is characterised by two highly conserved sequence motifs: (1) three histidines that bind zinc at the catalytic site; and (2) a conserved methionine turn ("Met turn") that sits beneath the active site zinc (Stocker *et al.*, 1995). The metzincin superfamily is further subdivided into four multigene families – the serralysins, astacins, ADAMs/adamalysins, and MMPs – based upon the exact amino acid sequence of the

MMP family	MMP	Common Name	Domain organisation
Collagenases	MMP-1	collagenase-1	B
	MMP-8	collagenase-2	B
	MMP-13	collagenase-3	B
	MMP-18	collagenase-4	B
Gelatinases	MMP-2	gelatinase-A	C
	MMP-9	gelatinase-B	C
Stromelysins	MMP-3	stromelysin-1	B
	MMP-10	stromelysin-2	B
	MMP-11	stromelysin-3	D
Matrilysin	MMP-7	matrilysin	A
Transmembrane	MMP-14	MT1-MMP	E
	MMP-15	MT2-MMP	E
	MMP-16	MT3-MMP	E
	MMP-17	MT4-MMP	F
	MMP-24	MT5-MMP	E
	MMP-25	MT6-MMP	F

Table 1.1: Common vertebrate MMPs, indicating their family (based on substrate specificity), common name, major substrates and domain organisation (see Figure 1.4). Adapted from (Nagase and Woessner, Jr., 1999).

zinc-binding motif: HEBXHXBGBXHZ, where histidine (H), glutamic acid (E) and glycine (G) residues are invariant, (B) is a bulky hydrophobic amino acid, (X) is a variable residue and (Z) is a family-specific amino acid. Vertebrate MMPs are characterised by containing a serine residue in the Z position of their conserved zinc binding motif (Stocker *et al.*, 1995).

To date, 25 vertebrate, as well as several nonvertebrate, MMPs have been identified, each of which has distinct but often overlapping substrate specificities (Sternlicht and Werb, 2001). This functional redundancy, which most likely exists to compensate for any losses of regulatory control, enables MMPs, collectively, to cleave virtually all ECM proteins (Coussens and Werb, 1996).

1.7.4.1.1 Domain structure

In addition to the conserved zinc binding and "Met turn" motifs, vertebrate MMPs also share stretches of sequence homology including a pre- and pro-peptide domain, a catalytic domain, and a C-terminal hemopexin domain that is linked to the catalytic domain by a flexible hinge region (Figure 1.4) (Nagase and Woessner, Jr., 1999). Domain organisation is usually conserved within members of given MMP families (Table 1.1).

The pre-domain is an N-terminal signal sequence, which is cleaved after it directs the synthesis of the protein to the endoplasmic reticulum (ER). As a consequence, most MMPs are secreted. There are, however, six MMPs that also contain a transmembrane domain or a glycosylphosphatidyl inositol (GPI)-anchoring domain, such that they are eventually expressed as cell surface enzymes (Sternlicht and Werb, 2001).

The pro-peptide domain, on the other hand, consists of approximately 80 amino acids and has a conserved PRCG(V/N)PD sequence (Nagase and Woessner, Jr., 1999). The cysteine within this sequence, also termed the "cysteine switch," maintains the latency of pro-MMPs by ligating the catalytic zinc until it is removed or disrupted (see section 1.7.4.1.2) (Van Wart and Birkedal-Hansen, 1990).

Following on from the pro-peptide domain is a catalytic domain, which dictates cleavage site specificity through its active site cleft, comprises approximately 170 amino acids, and contains the conserved zinc binding and "Met turn" motifs that characterise MMPs. The catalytic domains of MMPs contain an additional structural zinc ion and several calcium ions, which are required for the stability and expression of enzymatic activity (Bode *et al.*, 1993).
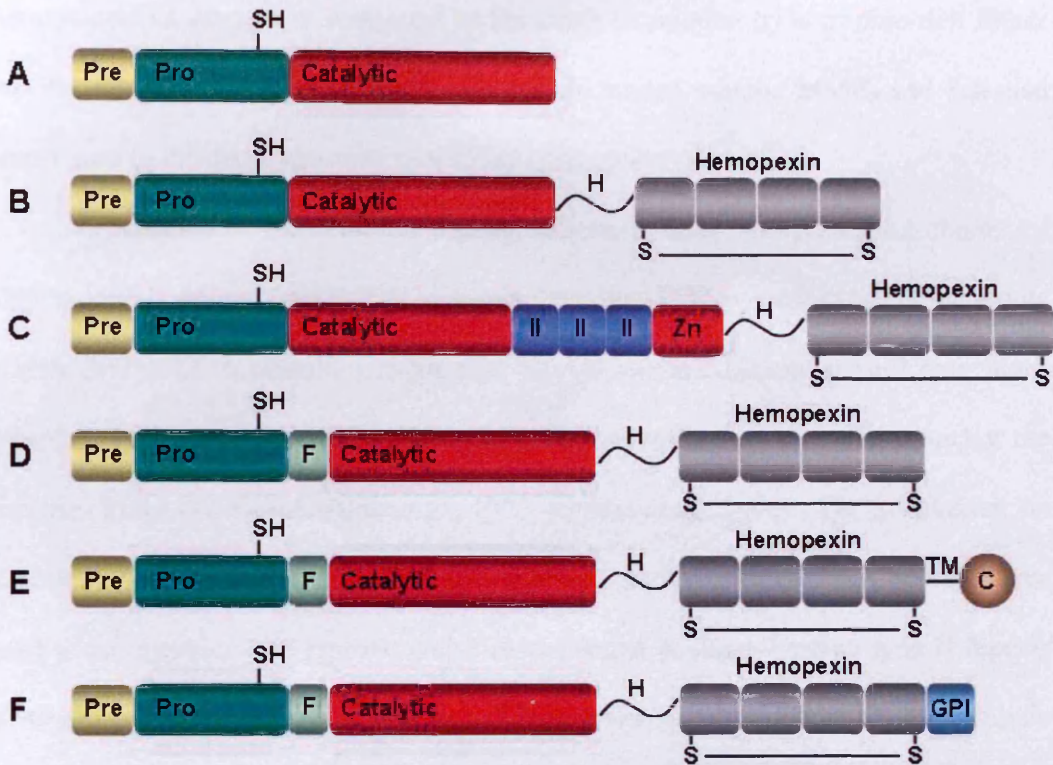
Figure 1.4: Domain organisation of common vertebrate MMPs, including a signal sequence (Pre), propeptide (Pro) with a free zinc thiol group (SH), furin-susceptible site (F), zinc-binding site (Zn), collagen-binding fibronectin type II inserts (II), hinge region (H), transmembrane domain (TM), cytoplasmic tail (C), glycophosphatidyl inositol-anchoring domain (GPI) and hemopexin/vitronectin-like domain with the first and last repeats linked by a disulphide bond (S-S). (A) Minimal domain MMPs; (B) simple hemopexin domain-containing MMPs; (C) gelatin-binding MMPs; (D) furin-activated secreted MMPs; (E) transmembrane MMPs; (F) GPI-linked MMPs. Adapted from (Sternlicht and Werb, 2001).

The C-terminal hemopexin-like domain is an absolute requirement for collagenases to cleave triple helical interstitial collagens, although the catalytic domains alone retain proteolytic activity toward other substrates (Bode, 1995). Additionally, this domain has been found to influence the binding of the tissue inhibitors of matrix metalloproteinases (TIMPs) as well as certain other substrates and

appears to play a role in MMP activation (Nagase and Woessner, Jr., 1999). The hemopexin-like domain is connected to the catalytic domain by a proline-rich linker peptide, which varies in length and composition among various MMPs and has also been found to influence substrate specificity (Knauper *et al.*, 1997).

In addition to the common domain structures listed above, several classes of MMPs contain unique stretches of sequence homology. For example, membrane-type MMPs (MT-MMPs) contain a single-pass transmembrane domain as well as a short, cytoplasmic tail or a C-terminal hydrophobic region, both of which serve to anchor the enzymes to the cell surface (Itoh *et al.*, 1999; Kojima *et al.*, 2000). The gelatinases, on the other hand, are unique from other MMP family members in that they possess three head-to-tail cysteine-rich repeats, which resemble the collagen-binding type II repeats of fibronectin (Murphy *et al.*, 1994). These domains are inserted in the catalytic domain and are required to bind and cleave collagens, gelatins and elastin (Shipley *et al.*, 1996).

1.7.4.1.2   Activation of latent metalloproteinases

Most MMPs are secreted from the cell as inactive zymogens, which are subsequently activated *in vitro* by proteinases and non-proteolytic agents such as SH-reactive agents, mercurial compounds, reactive oxygen and denaturants (Nagase and Woessner, Jr., 1999). *In vivo*, most MMPs can be activated by other, already activated, MMPs or by several serine proteinases that can cleave peptide bonds within MMP pro-domains (Sato *et al.*, 1994). In all cases, activation requires the disruption of the unpaired sulphydryl group near the C-terminal end of the pro-peptide domain, which acts as a fourth ligand for the active site zinc ion (Nagase, 1997). MMP activation requires that this cysteine-to-zinc switch be opened by normal proteolytic removal of

the propeptide domain or by ectopic perturbation of the cysteine-zinc interaction (Van Wart and Birkedal-Hansen, 1990). Once displaced, the sulphydryl group is replaced by a water molecule that can subsequently attack the peptide bonds of MMP targets (Nagase, 1997).

1.7.4.1.3 Inhibition

MMPs are reversibly inhibited by a family of 20-29 kDa secreted proteins, known as the tissue inhibitors of matrix metalloproteinases (TIMPs) (Sternlicht and Werb, 2001). Four TIMPs have been identified to date, all of which share 37-51% overall sequence identity, a conserved gene structure, and 12 similarly separated cysteine residues (Gomez *et al.*, 1997). TIMPs are not only important regulators of matrix turnover but have also been implicated in a variety of cellular activities *in vitro*, which are independent of their MMP-inhibitory activities (Nagase and Woessner, Jr., 1999). For example, TIMP-1 and -2 have been shown to have mitogenic activities on number of cell types (Gomez *et al.*, 1997) and TIMP-2 alone has been seen to inhibit fibroblast growth factor (FGF)-induced endothelial cell growth (Murphy *et al.*, 1993). Additionally, TIMP-1 has been found to stimulate fibroblasts to produce MMP-1 and appears to accumulate in the nuclei of human fibroblasts in a cell-cycle dependent manner, suggesting a role in cell growth (Clark *et al.*, 1994; Zhao *et al.*, 1998).

1.8 Mechanotransduction

While one of the major functions of connective tissues is to sustain mechanical stresses, they also appear to require such stresses for tissue maintenance and homeostasis (Chiquet *et al.*, 2003). As discussed in sections 1.7.1-1.7.3, tendon, corneal and skin connective tissues are constantly subjected to a wide range of

27

mechanical cues, which can ultimately alter the behaviour of the fibroblasts within these tissues. The process whereby cells can transduce such physical, force-induced signals into biochemical responses is termed mechanotransduction and is critical, since connective tissues are invariably subjected to different mechanical environments during development, growth and aging (Ko and McCulloch, 2001). The evidence for the process of mechanotransduction is far reaching and is presented in section 1.9. This section, therefore, will focus on the ways in which cells are thought to sense such mechanical cues.

Overall, four basic types of mechanical cues exist: tension, compression, fluid shear, and torsional shear (Eastwood *et al.*, 1998). Generally, fibroblasts are considered in terms of tensile forces, vascular endothelial cells in terms of fluid shear, and chondrocytes in terms of compression. The complexity of the response of cells to mechanical cues is immense. For example, the basic types of mechanical cues mentioned above can be further differentiated based upon the velocity of loading or whether the force is cyclical or static. Furthermore, mechanical cues can be directional or non-directional, which is particularly important when cellular responses are polarised. The final level of complexity arises from the interplay between fibroblasts and the ECM that they not only synthesise, but also remain surrounded within. By its very nature, the ECM is capable of having a dramatic effect on the way mechanical cues are presented to the fibroblasts within it. Hence, a complicated feedback mechanism exists, whereby fibroblasts synthesise an ECM based upon the mechanical requirements of the given connective tissue, and the ECM, in turn, alters the way subsequent mechanical cues are presented to the cell.

In general, cells are capable of sensing mechanical stress via cell-cell and cell-matrix adhesions. The finding that fibroblasts are sparsely populated within an

extensive ECM in most connective tissues *in vivo* (see sections 1.7.1-1.7.3) suggests

that mechanotransduction in fibroblasts relies largely on cell-matrix adhesions. Such

adhesions form the physical link from the ECM across the plasma membrane to the

actin cytoskeleton, and are thought to be dependent on two particular proteins based

upon their strategic locations within such matrix adhesions: (1) integrins and (2)

mechano-sensitive ion channels (Chiquet *et al.*, 2003). Both integrins and ion channels

have been implicated in the transduction of mechanical signals in fibroblasts, in studies

using functionally blocking antibodies directed toward β_1-integrins and inhibitors of

stretch sensitive ion channels (Chiquet *et al.*, 2003; Eastwood *et al.*, 1998).

Furthermore, integrins have been shown to be capable of triggering intracellular signals

in response to pulling forces applied to their ECM ligands (Choquet *et al.*, 1997), the

immediate consequences of which are three-fold: (1) a Rho-dependent assembly and

growth of focal adhesion complexes at these sites (Geiger and Bershadsky, 2001); (2)

an increase in cytoskeletal tractional force (Choquet *et al.*, 1997); and (3) an initiation

of mitogen-activated protein (MAP) kinase and NF-κB pathways (MacKenna *et al.*,

2000; Schmidt *et al.*, 1998).

Transmembrane receptors that interact with ECM components on the outside of

the cell, such as integrins, are often aggregated at focal adhesions, regions where the

surface of the cell comes into close proximity to the substrate. In addition to their

interaction with ECM macromolecules, such transmembrane receptors are also capable

of interacting with bundles of actin filaments, or stress fibres, on the inside of the cell

(Geiger and Bershadsky, 2001). Numerous proteins have been identified in focal

adhesions, the majority of which appear to be localised at their cytoplasmic face and

either play structural roles or function in signal transduction. The relative abundance of

such proteins is highly variable, with vinculin and talin being most prominent, and

focal adhesion kinase (FAK), α-actinin, paxillin, tensin, zyxin, and many other components with signalling roles being less abundant (Zamir *et al.*, 1999). Not surprisingly, a number of proteins found to be localised to focal adhesions, including talin, α-actinin, filamin and tensin, have direct actin-binding capabilities which is important in maintaining and stabilising the microfilament attachment in focal adhesions (Bershadsky *et al.*, 2003).

Focal adhesions appear to evolve from small dot-like focal complexes, less than 1 μm in diameter, into mature focal adhesions. Immature focal contacts appear to be formed during lamellipodial protrusions of the plasma membrane, which contain dense, rapidly polymerising branching networks of actin filaments and are induced by the small Rho-family G-protein, Rac (Geiger and Bershadsky, 2001). The transition of focal contacts to mature focal adhesions is accompanied by the transition of the associated actin mesh into densely packed, straight bundles of filaments known as stress fibres, which themselves contain many actin-associated proteins, including myosin II. Stress fibres are contractile structures that function to apply tension to the membrane-bound adhesion plaque, which are then transmitted to the ECM via transmembrane receptors such as integrins (Bershadsky *et al.*, 2003). This internal cytoskeletal tension has been shown to be crucial in mechanotransduction; fibroblasts only seem capable of sensing external mechanical stresses if a certain amount of resistance by internal cytoskeletal tension is retained. This has been illustrated previously by culturing fibroblasts on soft type I collagen matrices; it was found that cellular force was reduced considerably by actin depolymerising agents (Kolodney and Wysolmerski, 1992).

1.9 Use of mechanical stimulation to investigate cell behaviour

Fibroblasts are the main source for the production, maintenance and turnover of connective tissues (see section 1.7), the very function of which is mechanical in nature. Consequently, observations that fibroblasts contain a wide variety of mechanical responses are not surprising. In general, fibroblasts are thought to respond to the generation of endogenous mechanical loads in tissues, as well as react to externally applied mechanical loading (Eastwood *et al.*, 1998). The ability of fibroblasts to respond to mechanical force was first described in 1940, when Stearns demonstrated that fibroblasts, together with the fibres they secrete, aligned in the direction of stress "like iron filings to a magnet" (Stearns, 1940).

Since this initial observation, fibroblasts have also been shown to be capable of generating endogenous tensional forces (Elsdale and Bard, 1972). The ability of fibroblasts to generate such forces has been measured by the use of fibroblast-populated collagen lattices (FPCL), which have been adapted in numerous studies in order to quantitate fibroblast contraction (Eastwood *et al.*, 1998). From studies such as these, it has been calculated that fibroblasts are capable of producing average forces of 10^{-10} N, assuming that all the resident fibroblasts within the FPCL participate (Eastwood *et al.*, 1996). In addition to their contractile ability, fibroblasts populated in mechanically loaded FPCLs have been shown to increase synthesis of both MMP-2 and MMP-9, with MMP-9 being more sensitive to tension than its gelatinase counterpart (Prajapati *et al.*, 2000a).

Since the discovery that fibroblasts could both create and respond to endogenous and external mechanical loads, a number of studies have been published which reveal that mechanical stimulation of fibroblasts *in vitro* results in a variety of cellular responses, including induction of intra-cellular signalling pathways, changes in

31

morphology and organisation of the actin cytoskeleton, altered gene and protein expression, as well as variations in focal adhesion formation.

1.9.1   Effect of mechanical stimulation on cell signalling

Several reports have indicated that mechanical stimulation can lead to the activation of several intracellular signalling pathways, such as the mitogen-activated protein (MAP) kinase and the NF-κB pathways (Chiquet, 1999; Yamamoto *et al.*, 1999). The MAPKs are intracellular kinases, whose signalling pathways appear to consist of three major phosphorylation cascasdes: (1) extracellular signal-related protein kinases (ERKs); (2) c-Jun NH_2-terminal kinases (JNK); and (3) p38 MAP kinases (Yamamoto *et al.*, 1999). MAP kinases have been shown to respond to physical stimuli such as UV light, heat shock, osmotic challenge, and mechanical stimulation (Hung *et al.*, 2000). For example, ERK 1 and 2 were demonstrated to be activated to a greater extent in chondrocytes subjected to shear stress (Hung *et al.*, 2000). Moreover, the JNK and p38 pathways have also been shown to be activated by various stress-related stimuli and, as such, are collectively known as stress-activated protein kinases (Force *et al.*, 1996).

It has also been shown that the NF-κB pathway is induced upon mechanical stimulation. For example, various types of stresses are known to induce phosphorylation and degradation of I-κB, the cytoplasmic inhibitor of the transcription factor, NF-κB, which is consequently activated and translocated to the nucleus (Mercurio and Manning, 1999). Furthermore, the I-κB kinase complex has been recently shown to interact with two enzymes of the MAP kinase kinase kinase family, suggesting that there is functional crosstalk between the MAP kinase and NF-κB pathways during mechanotransduction. (Chiquet, 1999). Activation of the NF-κB

pathway, via protein kinase C, is also required for the integrin-dependent ability of fibroblasts to contract collagen gels (Xu *et al.*, 1998).

1.9.2   *Effect of mechanical stimulation on cell morphology*

Cell morphology has also been found to alter with stimulation in cultured connective tissue cells. Van Kooten and colleagues reported that human skin fibroblasts subjected to pulsations of shear stress adopted an elongated morphology, aligned in the direction of flow, and demonstrated more abundant filopodia (van Kooten *et al.*, 1993). A similar response was also observed in mechanically stimulated osteoblasts (Pavalko *et al.*, 1998). In this particular cell type, fluid shear resulted in the development of prominent stress fibres that were oriented roughly parallel to the long axis of the cell. The effect of fluid shear stress on connective tissue cells was investigated further by Billotte and Hofmann, who showed that NIH-3T3 fibroblasts acquired a more spindle-like morphology and demonstrated cytoskeletal reorganisation upon 12 hours of exposure to fluid flow (Billotte and Hofmann, 1999). More recently, tendon fibroblasts were confirmed to align in the direction of flow after being subjected to six hours of shear stress (Archambault *et al.*, 2002b), and the actin cytoskeleton was shown to reorganise into distinct stress fibres that traversed the cell body (Kessler *et al.*, 2001) upon the application of mechanical tension to skin fibroblasts.

1.9.3   *Effect of mechanical stimulation on gene and protein expression*

Given that mechanical stimulation has been shown to alter intracellular signalling pathways as well as gross cell morphology, it is not at all surprising that numerous genes and proteins demonstrate altered expression with stimulation. Fluid

flow, for example, has been shown to alter the gene and protein expression of matrix macromolecules as well as focal adhesion proteins. In one of the first reports to indicate that the synthesis of ECM macromolecules alters with mechanical stimulation, the production of type I and III collagen, as well as proteoglycan synthesis, was shown to be up-regulated in vascular smooth muscle cells in response to cyclic strain (Leung *et al.*, 1976). This phenomenon has since been corroborated by numerous studies. In one such report, Kessler *et al.* compared fibroblasts cultured in tensioned FPCLs to those cultured in free retracting lattices or in a monolayer (Kessler *et al.*, 2001). According to their study, synthesis of collagen, as well as steady-state mRNA levels of procollagen types I, III, and VI, fibronectin, elastin, and β-actin, were highest in the fibroblasts cultured in the tensioned FPCL. Not surprisingly, proteins such as vinculin, zyxin and integrin-linked kinase were also altered in fibroblasts subjected to mechanical tension (Kessler *et al.*, 2001).

Mechanical stimulation has also been found to alter MMP synthesis, secretion and activity (Archambault *et al.*, 2002b; Archambault *et al.*, 2002a; Blain *et al.*, 2001; Lambert *et al.*, 2001; Magid *et al.*, 2003; Prajapati *et al.*, 2000b). More specifically, levels of MMP-2, -3, -9, -13, and -14 have shown to alter in response to shear stress, tensile forces, and compressive loading in a variety of cell types (Archambault *et al.*, 2002b; Lambert *et al.*, 2001), and collagenase activity has been shown to be inversely regulated to collagen synthesis, with the highest activities and mRNA levels observed in fibroblasts cultured in free retracting FPCLs (Kessler *et al.*, 2001).

Several studies have also reported the increased expression of cyclooxygenase II (COX-2) mRNA and protein levels. This key enzyme is responsible for the formation of prostaglandins, which themselves have been shown to be released in fibroblasts and osteoblasts in response to fluid flow (Archambault *et al.*, 2002b; van der

Pauw *et al.*, 2000). COX-2 has been shown to respond quickly to mechanical stimulation in numerous cell types, including osteoblasts and fibroblasts (Archambault *et al.*, 2002b; Chen *et al.*, 2000; Pavalko *et al.*, 1998). Interestingly, COX-2 up-regulation did not necessarily result in an increase in prostaglandin expression, as shown by Archambault and colleagues, indicating that mechanotransduction in these cells contains numerous regulatory pathways that have yet to be elucidated (Archambault *et al.*, 2002b).

Growth factors, and in particular transforming growth factor (TGF)-β1, has also been found to be induced upon mechanical stimulation in fibroblasts (Brown *et al.*, 2002; Kessler *et al.*, 2001). TGF-β1 has been classified as a potent "profibrotic" agent, since it promotes rapid deposition of collagenous matrix in wound repair and stimulates collagen, fibronectin and TIMP synthesis while suppressing MMP production in fibroblasts (Brown *et al.*, 2002).

1.9.4 Effect of mechanical stimulation on cell adhesion

Not surprisingly, mechanical stimulation has also been found to alter the prominence and composition of focal adhesions. Pavalko and colleagues demonstrated that β_1-integrin and α-actinin became concentrated in focal adhesions after subjecting osteoblasts to fluid shear, which was in stark contrast to the diffuse localisation of both proteins in control cells (Pavalko *et al.*, 1998). Kessler *et al.* made a similar observation after they subjected skin fibroblasts to mechanical tension. In this case, vinculin was found to be localised to focal adhesions in skin fibroblasts that were subjected to mechanical tension, whereas the protein was more diffused throughout the cytoplasm in control cells (Kessler *et al.*, 2001).

1.10 Aims and Hypothesis

As described above, fibroblasts are responsible for the synthesis, maintenance and turnover of a wide variety of connective tissues. Despite the fact that all fibroblasts, irrespective of their tissue of origin, maintain similar morphological features, numerous studies have begun to identify inter- and intra-site heterogeneity in fibroblast populations. Such heterogeneity is manifested in differences in subtle morphological characteristics, behaviour in culture, protein synthesis, gene expression, proliferation rate, cell surface antigen presentation, *in vitro* life spans, responses to hormones and growth factors, migration and mechanosensation.

In order to test inter-site fibroblast heterogeneity, tendon, corneal and skin fibroblasts were subjected to a well defined shear stress produced by a parallel plate flow chamber. Following stimulation, cell morphology and gelatinase activity were examined, to determine if the three cell lines maintained differential cellular responses to an identical mechanical stimulus. Furthermore, microarray technology, semi-quantitative RT-PCR and Western blotting were employed to investigate gene and protein expression in stimulated and control cells, in order to provide a comprehensive analysis of any tissue-specific responses to mechanical stress.

CHAPTER 2

Chapter 2

Materials and Methods

2.1 Materials

2.1.1 Mammalian cell culture vessels and reagents

HeLa, C2C4 and NIH 3T3 cells were obtained from laboratory stocks, and the bovine skin fibroblasts (BOVS-1) used in production of the gelatinase standard were generously supplied by Dr. Emma Blain (University of Cardiff, Wales, UK).

All reagents used in the isolation and culture of cell lines, including collagenase type II, Hank's Balanced Salt Solution (HBSS) without calcium and magnesium, trypsin-ethylenediaminetetraacetic acid (EDTA), foetal calf serum (lot # 40Q9021F), phosphate buffered saline (PBS), Dulbecco's Modified Eagle's medium (DMEM), penicillin/streptomycin, and EDTA, were all manufactured by Gibco and obtained from Invitrogen, Ltd. (Paisley). Cells were frozen in a cryo freezing container manufactured by Nalgene and obtained by Fisher Scientific UK, Ltd. (Loughborough).

Poly-L-lysine, porcine skin gelatin, tissue culture grade dimethyl sulphoxide (DMSO), and insulin, transferrin, selenium (ITS) liquid media supplement were all obtained from Sigma-Aldrich Company, Ltd. (Dorset). Cell culture flasks, dishes, six-well plates, cryovials, and centrifuge tubes were manufactured by Greiner (Stonehouse). Serological pipettes were manufactured by Corning and obtained from Fisher Scientific (UK), Ltd. The single-well plates used in mechanical stimulation experiments were manufactured by Nunc and obtained from VWR International (Lutterworth).

2.1.2 Molecular Biology Reagents

Total RNA was isolated from cells using the Absolutely RNA RT-PCR miniprep kit, Stratagene, Inc. (La Jolla, CA, USA). Contaminating RNases were inactivated with

RNaseZap (Ambion (Europe) Ltd., Huntingdon) and diethylpyrocarbonate (DEPC) (Sigma-Aldrich Company, Ltd.). RT-PCR was based around the Titan One-Tube RT-PCR System, which was obtained from Roche Diagnostics, Ltd. (Lewes). Deoxyribonucleotide triphosphates (dNTPs) were from Bioline, Ltd. (London), and oligonucleotides were synthesized by Operon Biotechnologies GmbH, (Cologne, Germany).

DNA gels were cast and run in a Mini Sub Cell GT electrophoresis tank (Bio-Rad Laboratories, Ltd.). Electrophoresis grade, high gel strength agarose was purchased from Melford (Ipswich), and ethidium bromide was obtained from VWR International. Hyperladder 1 was from Bioline, Ltd. Agarose gels were visualised with a gel documentation system, comprised of a transilluminator (BST-15.M), camera, viewer, and video copy processor (Mitsubishi P91), all of which were obtained from UVItec, Ltd. (Cambridge).

2.1.3 *Antibodies and additional immunofluorescence reagents*

Primary antibodies directed toward vinculin (V-9131), desmin (D-1033), keratin (K-4252), and vimentin (V-4630) were obtained from Sigma-Aldrich Company, Ltd., while neogenin (sc-15337) and β-actin (sc-1616) anti-sera were manufactured by Santa Cruz Biotechnology, Inc. and supplied by Autogen Bioclear UK, Ltd. (Wiltshire). Anti-CRP-1 was from BD Biosciences, Ltd. (Oxford). The anti-lumican rabbit polyclonal antibody was kindly provided by Dr. Åke Oldberg (Division of Cell and Matrix Biology, University of Lund, Sweden) (Svensson *et al.*, 1999), while anti-dyxin rabbit polyclonal was a generous gift from Dr. Rachelle Crosbie (Department of Physiological Science, University of California, Los Angeles, CA, USA) (Yi *et al.*, 2003). All HRP- and alkaline phosphatase-conjugated anti-rabbit, anti-mouse, anti-goat and anti-guinea pig secondary antibodies were purchased from Sigma-Aldrich Company, Ltd.

Glass coverslips, slides and paraformaldehyde were purchased from VWR International. Vectashield was obtained from Vector Laboratories (Peterborough). Rhodamine phalloidin and 4',6-Diamidino-2-phenylindole (DAPI) were manufactured by Molecular Probes, Inc. and obtained from Invitrogen, Ltd.

2.1.4 SDS-PAGE, Zymography and Western Blotting

All protease inhibitors, including aprotinin, pepstatin, phenylmethylsulphonylfluoride (PMSF), N-tosyl-L-phenylalanylchloromethyl ketone (TPCK), *p*-toluenesulfonyl-L-arginine methyl ester (TAME), and benzamidine were obtained from Sigma-Aldrich Company, Ltd. The Micro BCA Protein Assay Kit was obtained from Perbio Science UK, Ltd. (Cramlington).

Broad range prestained protein molecular weight standards were purchased from New England Biolabs (Beverly, MA, USA). SDS-PAGE gels were cast and run using the Mini Protean II gel system, which was obtained from Bio-Rad Laboratories, Ltd. (Hemel Hempstead), while gradient zymograms were poured and electrophoresed in the EF100 Rapid PAGE System from Cambridge Electrophoresis, Ltd. (Cambridge). Protein transfer was achieved using the Trans-Blot SD Semi-Dry Transfer Cell (Bio-Rad, Ltd.). Porcine skin gelatin, bromophenol blue, and N, N, N', N'-tetramethylethylenediamine (TEMED) were purchased from Sigma-Aldrich Company, Ltd, while ammonium persulphate (APS) was obtained from VWR International. Acrylamide:bisacrylamide (37.5:1) was purchased from GeneFlow, Ltd (Fradley), whereas polyvinylidene fluoride (PVDF) membrane (0.2 μm), and Coomassie Brilliant Blue R-250 were obtained from Bio-Rad, Laboratories, Ltd. Marvel non-fat dry milk powder was purchased from a local supermarket.

Western blots developed with enhanced chemiluminescence were exposed on Kodak MXB film purchased from Xograph Imaging Systems, Ltd. (Tetbury). X-ray films

were fixed in Kodak RP X-OMAT LO, developed in Kodak X-OMAT EX II, both of which were obtained from VWR International, and film was processed in an Optimax 1170 film processor from IGP UK, Ltd. (Chelmsford). Western blots detected with chromogenic substrates were scanned with a UMAX Powerlook 1000 transmissive scanner.

2.1.5 Miscellaneous

Cells in culture were visualized on a Ceti Versus inverted brightfield microscope, while all morphological images were captured on a Leica DM IRE2 inverted fluorescence microscope in conjunction with a 1.3 megapixel CCD camera (DC 350F). Conditioned media was concentrated in Amicon Centricon YM-30 centrifugal filter devices, which were obtained from Millipore (UK), Ltd. (Watford). The parallel plate flow chamber used in the mechanical stimulation of fibroblasts was kindly provided by Dr. Joji Ando (Department of Biomedical Engineering, University of Tokyo, Japan), which was interfaced with a P-1 peristaltic pump obtained from Amersham Biosciences (UK), Ltd. (Little Chalfont).

All other chemicals used were of standard or AnalaR reagent grade and were purchased from Sigma-Aldrich Company, Ltd., or VWR International.

2.2 Methods

Methods for all of the protocols utilised in this study are detailed in this section; the recipes for stock solutions, buffers and media compositions are listed the Appendix.

2.2.1 Isolation of fibroblast cell lines

Isolation of primary, murine fibroblasts was carried out according to the method of Spector *et al.* (Spector *et al.*, 1998), using 19-day gestation foetal CD1 mice (term = 21 days). The pregnant mother was euthanized by carbon dioxide asphyxiation and immediately swabbed with 70% ethanol in a sterile hood. With the mouse on its back, an incision was made down its midsection with sterile scissors, thereby exposing the uterus and amniotic sacs. The embryos and uterine horns were pulled away from the abdomen, detached from the animal, and placed in a dish of sterile PBS. The uterine horns were then opened, thus releasing the embryos into the PBS. Embryos were detached from the amniotic sac, decapitated, and placed in a fresh dish of PBS in an attempt to eradicate as many red blood cells as possible. At this point, the corneas, tendons from the tail, and skin were isolated from the embryos and placed in sterile PBS. PBS was then carefully removed and tissues were overlaid with approximately 2 ml of HBSS, 0.25% trypsin, and 0.25% collagenase type II. Tissues were minced and overlaid with an additional 10 ml of HBSS solution. To aid in collagenase digestion, the tissue homogenate was incubated at 37 °C for 45 minutes. The suspension was transferred to sterile centrifuge tubes and the large tissue allowed to settle by gravity. The crude supernatant containing suspended cells was removed to a fresh sterile centrifuge tube containing 1 ml foetal calf serum (FCS) per 10 ml of suspension to inactivate the trypsin. The solution was then centrifuged at 1200 rpm for five minutes in a bench-top Sigma 204 centrifuge with a swing-out rotor (# 11030) and the supernatant discarded. The resultant pelleted cells were resuspended in approximately 13 ml working medium (DMEM, 15% FCS), transferred to a fresh, sterile Petri dish, and incubated in a humidified incubator (5% CO_2) at 37 °C. Cells at this stage were designated passage zero. When cultures reached confluence, culture medium was removed and the cells were washed with 10 ml of warm 0.53 mM EDTA in PBS. EDTA

was removed and replaced with 10 ml of warm 0.05% trypsin-EDTA, and the cells incubated at 37 °C for five minutes. Using a sterile pipette, the cell suspension was transferred to a sterile centrifuge tube containing 1-2 ml of FCS and centrifuged at 1200 rpm for five minutes. After discarding the supernatant, the pellet was resuspended in 15 ml working medium, aliquoted into two tissue culture flasks, and designated passage one. Cells were maintained under standard tissue culture conditions (37 °C; 5% CO_2).

2.2.2 Subculturing fibroblast monolayers

Primary murine fibroblasts were cultured in a humidified 5% CO_2 atmosphere at 37 °C in working medium. Cells were maintained until they reached approximately 80% confluence, at which point the cell sheet was rinsed with sterile PBS and the cells dissociated from the substrate upon treatment with trypsin-EDTA. Cells were re-suspended in an appropriate volume of working medium and seeded in tissue culture flasks to yield the desired level of confluency. Because cultures were maintained in pre-confluent conditions, cells were kept in the active log phase of growth and were only subcultured until passage number five. In all cases, splitting ratios ranged from 1:2 to 1:4, leading to 5-6 cumulative population doublings prior to experimentation.

2.2.3 Cryopreservation of cell lines

In order to preserve cell lines in liquid nitrogen, cells in the log phase of growth were washed with sterile PBS and overlaid with trypsin-EDTA to dissociate the cell monolayer. Cells were resuspended in working medium, transferred to a 15 ml conical centrifuge tube and centrifuged at 1500 rpm for three minutes (Sigma 204 centrifuge; rotor #11030). After aspirating the supernatant, the cell pellet was resuspended in working medium supplemented with 5% DMSO and transferred to a sterile cryovials. Cryovials

were placed in a cryo freezing container containing isopropanol and allowed to cool to at a rate of -1 °C/minute until samples reached -70 °C, at which point they were transferred to liquid nitrogen.

2.2.4 Thawing cells following cryopreservation

To revive cells frozen in liquid nitrogen, cryovials were rapidly thawed in a 37 °C waterbath. After the cell suspension was transferred to a sterile centrifuge tube, cold working medium was added drop-wise while shaking gently. The cell suspension was spun at 1500 rpm (Sigma 204 centrifuge; rotor #11030) for three minutes and the supernatant discarded. The cell pellet was resuspended in 10 ml fresh working medium, placed in a fresh, sterile tissue culture flask and allowed to grow under standard tissue culture conditions.

2.2.5 Immunofluorescence

Murine fibroblasts grown on sterile, ethanol-washed coverslips were rinsed with PBS and fixed in freshly prepared 3.7% (v/v) paraformaldehyde/PBS for 10 minutes at room temperature. After washing three times in PBS, coverslips were incubated in permeabilising buffer and blocking buffer at room temperature for five minutes and one hour, respectively. Primary antibody was diluted in blocking buffer at the appropriate concentrations (see Table I, Appendix) and added to the coverslips for one hour at room temperature, after which coverslips were washed for five minutes in blocking buffer followed by 3 x 5 minute washes in PBS.

For indirect immunofluorescence, coverslips were subsequently incubated with secondary antibodies diluted in blocking buffer for one hour at the supplier's recommended dilution. Filamentous actin (F-actin) was detected using rhodamine

phalloidin, which was added with the secondary antibody at 0.2 U/µl per coverslip. After subsequent washes in blocking buffer and PBS, coverslips were mounted onto glass slides with Vectashield mounting medium containing DAPI. Images were obtained with a Leica fluorescence microscope and processed through Adobe Photoshop 6 software.

2.2.6 Quantification of Focal Adhesions

After visualising with immunofluorescence (see section 2.2.5), focal adhesions were quantified by manually counting the number of focal contacts (< 1 µm^2), focal adhesions (> 1 µm^2) or fibrillar adhesions (> 1 µm in length) in sub-confluent cells. Fibroblasts that were in contact with other cells were disregarded for the purpose of this quantification. Counts were subsequently used in determining the total number of focal adhesions (focal contacts, focal adhesions and fibrillar contacts) per cell or per cell area. Cell area was measured using the public domain ImageJ program, developed at the U.S. National Institutes of Health and available on the Internet at http://rsb.info.nih.gov/ij/.

2.2.7 Measuring cell morphology

Quantification of morphological parameters, including area and circularity of cells, was performed using ImageJ. Circularity was calculated based upon the following equation:

$$circularity = 4\pi\left(\frac{A}{P^2}\right) \tag{1}$$

where A is area (µm^2) and P is perimeter (µm). A circularity value of 1.0 indicates a perfect circle, whereas values approaching 0 indicate an increasingly elongated polygon.

2.2.8   Total Cell Lysates

Adherent fibroblasts were rinsed with PBS prior to the addition of modified sample buffer to lyse the cells. Cells were harvested using a cell scraper and transferred to an Eppendorf tube before being sonicated on ice. Protein concentration was determined using the Micro BCA assay kit (section 2.2.9), and adjusting solution was added to the samples prior to boiling and loading onto SDS-PAGE gels (section 2.2.10).

2.2.9   Determination of Protein Concentration

Protein concentrations were determined using the Micro BCA Protein Assay Kit following the manufacturer's instructions. Briefly, 10 µl of the sample to be tested, or the buffer in which the proteins were solubilised (control), was added to 490 µl of distilled water and incubated at 60°C for one hour with 500 µl of the Micro BCA reaction solution. After cooling to room temperature, the absorbance of the samples was measured at a wavelength of 562 nm, using the control reaction as the reference. Protein concentration was quantified by use of a standard curve, which was generated using known concentrations of bovine serum albumin (BSA) in the relevant sample buffer.

2.2.10   Polyacrylamide Gel Electrophoresis

SDS-PAGE was carried out according to Laemmli (Laemmli, 1970) in the Mini-Protean II system with 1 mm spacers using the components listed (Table II, Appendix). Resolving gels were typically 10% polymer, unless otherwise stated, and stacking gels were always 5% polymer, using the components listed. Prior to loading onto the gel, an equal volume of 2x SDS-PAGE sample buffer was added to samples, after which they were boiled for two minutes. Gels were electrophoresed in SDS-PAGE running buffer at a constant voltage of 150 V until the bromophenol blue tracking dye reached the bottom of

the gel. Broad range pre-stained molecular weight markers were run in parallel to monitor the process of electrophoresis and ultimately aid in size determination.

2.2.11 SDS-PAGE gel staining

Proteins were visualized directly on SDS-PAGE polyacrylamide and zymogram gels following staining with Coomassie Blue stain for approximately 30 minutes. Gels were then rinsed in distilled water and washed in destaining solution.

2.2.12 Gelatin Zymograms

Gradient SDS-PAGE gelatin zymograms were produced using the components listed (Table III, Appendix), an adaptation of Kleiner and Stetler-Stevenson (Kleiner and Stetler-Stevenson, 1994), which provides a method by which to analyse MMP activity on denaturing, but non-reducing, gels. A solution of dissolved porcine gelatin was co-polymerised with 7.5 and 15% polyacrylamide gels, yielding a final gelatin concentration of 1 mg/ml. TEMED and APS were added to catalyse polymerisation of the acrylamide, at which point the 7.5% and 15% polyacrylamide solutions were transferred to a gradient gel mixer and poured into a gradient mould containing sufficient numbers of glass plates and 1 mm spacers for the simultaneous casting of eight gradient zymograms (Cambridge Electrophoresis Ltd, Cambridge, UK). The addition of bromophenol blue into the 15% gel allowed the visualisation of the polyacrylamide gradient. After casting, zymograms were overlaid with water-saturated butanol and allowed to polymerise for approximately 40 minutes before removal of the butanol and addition of the 5% stack. Sample wells were created upon insertion of combs into the stack prior to polymerization. Conditioned media isolated from mechanically stimulated and control fibroblasts were concentrated (as described in 2.2.19), prepared by dilution into zymogram sample buffer and allowed to

incubate at room temperature for 10 minutes prior to loading. Determination of the concentration of proteins in conditioned media was not possible using classical methods because of the presence of interfering substances in DMEM. Consequently, the loading volume of individual samples was calculated as described in section 2.2.13. Protein molecular weight markers and a gelatinase standard (section 2.2.14) were loaded to aid in protein identification and determination of molecular sizes. In some cases, the loading volume of a given sample exceeded 20 µl, in which case the sample was double-loaded. In order to ensure that double-loading did not result in the presence of erroneous doublets within the gel, molecular weight markers were also double-loaded. Zymograms were electrophoresed using the Rapid PAGE System in SDS-PAGE running buffer at a constant voltage of 250 V for two hours.

Following electrophoresis, gels were incubated at room temperature for 30 minutes in zymogram renaturation buffer, in order to remove SDS and allow for subsequent protein refolding. The renaturation buffer was decanted, and the gels were then incubated in two changes of zymogram developing buffer: the first for 30 minutes at room temperature and the second for 48 hours at 37 °C. Zymograms were washed briefly in distilled water prior to staining as described in section 2.2.11.

2.2.13 Normalisation, quantification and statistical analysis of MMP activity

Determination of protein concentration in conditioned media samples was not possible due to the presence of interfering substances, such as phenol red, tyrosine, tryptophan, and iron, in the working medium. Consequently, loading volumes of samples were normalised for (1) the volume of medium remaining at the end of the 14-hour period, since a small amount of the original 30 ml perfusate evaporated during the course of the experiment; (2) fold-concentration of the conditioned medium; and (3) differences in

growth area, given that the stimulated glass plate was surrounded by a Teflon gasket, which reduced the growth area by approximately 20 cm^2 compared to the static culture dish.

Prior to analysis, zymograms were scanned at 300 dpi on a UMAX PowerLook 1000 scanner using Adobe Photoshop 6 and the UMAX Magic Scan software interface. The volume integration of cleared zones of gelatinolytic activity was subsequently quantified using the public domain NIH Image program (http://rsb.info.nih.gov/nih-image/). Resultant values were further normalized by subtracting the background gelatinase activity present in the mechanical stimulation working medium. Statistical analysis of all samples was performed with a Students *t*-test. Data represent the mean ± standard error (SE) from at least three experiments, and differences with $p < 0.05$ were considered to be significant.

2.2.14 Production of gelatinase standard

Conditioned media, used as a positive control for MMP-2 and MMP-9 activity in gelatin zymography, was prepared by subculturing a bovine skin fibroblast secondary cell line (BOVS-1), kindly provided by Dr. Emma Blain (School of Biosciences, University of Cardiff). A frozen stock of BOVS-1 was thawed and maintained for five days under standard tissue culture conditions in DMEM supplemented with 10% FCS, at which point cells were subcultured at a dilution of 1:10. Following a further five days of incubation, culture media was removed from each tissue culture flask and replaced with 10 ml of ITS liquid media supplement. Cells were allowed to grow in ITS for a further five days, at which point the resultant conditioned culture media was harvested and stored at -20 °C.

2.2.15 Western Blotting

Protein transfer to PVDF was performed using a semi-dry blotter in transfer buffer at a constant voltage of 25 V for 50 minutes. Following transfer, membranes were blocked in 5% (w/v) Marvel/Tris buffered saline with Tween-20 (TBST) for one hour at room temperature. Incubation with primary antibodies in 5% (w/v) Marvel/TBST was performed for one hour at room temperature at concentrations indicated in Table I (Appendix). Following extensive washing in TBST, blots were incubated with alkaline phosphatase- or horseradish peroxidase (HRP)-conjugated secondary antibodies diluted in 5% (w/v) Marvel/TBST, according to the manufacturer's instructions, for 1 hour at room temperature. After extensive washing in TBST, immunoreactive bands were detected by enhanced chemiluminescence (ECL) or chromogenic substrates.

2.2.16 Western Blot Detection Using Enhanced Chemiluminescence

Proteins were transferred to PVDF and the membranes probed with the appropriate primary antibody and a HRP-conjugated secondary antibody as described (see section 2.2.15). Equal volumes of ECL solutions I and II were mixed and added to the membranes for one minute with minor agitation. Membranes were transferred to autoradiography cassettes and exposed to Kodak medical film. Film was developed in an Optimax 1170 film processor.

2.2.17 Western Blot Detection using Chromogenic Substrates

Proteins were transferred to PVDF and the membranes probed with the appropriate primary antibody and an alkaline phosphatase-conjugated secondary antibody as described (see section 2.2.15). 132 µl NBT stock was mixed with 10 ml of alkalkine phosphatase buffer, to which 66 µl BCIP stock was added. Membranes were incubated with this

solution until immunoreactive bands were of the desired intensity, at which point the membranes were washed with distilled water and allowed to dry.

2.2.18 Stripping and re-probing western blots

In cases where western blots were quantified, β-actin was used as a loading control. After probing membranes with anti-sera directed toward a protein of interest and visualizing the immunoreactive bands with ECL, primary and secondary anti-sera directed to the protein of interest were removed from membranes by washing in TBST and incubating in stripping buffer after for one hour at room temperature. Stripped blots were then washed extensively in TBST, re-blocked for 1 hour with 5% (w/v) Marvel/TBST, and re-probed with anti-sera directed against β-actin.

2.2.19 Concentrating conditioned media

Conditioned media isolated from mechanically stimulated and control fibroblasts were concentrated using Amicon Centricon YM-30 centrifugal filter devices according to the manufacturer's instructions. Briefly, 2 ml of conditioned media was placed in the sample reservoir and the Centricon device assembled after weighing each component with and without the sample. The device was then spun at 2500 rpm in a Sigma 4K15 table-top centrifuge using a spin-out rotor (# 11150) for 30 minutes at 4 °C. This resulted in an approximate two-fold concentration of the sample. The exact magnitude of concentration was determined by calculating the proportion of sample retentate compared to filtrate after spinning by weight. The filter device used had a molecular weight cut-off of 30 kDa, such that any molecules with a molecular weight exceeding 30 kDa were retained.

2.2.20 RNA extraction and purification

RNA extractions were carried out with the Absolutely RNA RT-PCR Miniprep kit (Stratagene, La Jolla, CA, USA) according to the manufacturer's instructions. Briefly, mechanically stimulated and control fibroblasts were lysed directly on a glass plate in 600 μl of lysis buffer containing guanidine thiocyanate to denature proteins and prevent RNA degradation by ribonucleases. Because of the high viscosity of the lysates, samples were homogenised prior to purification by passing the lysate through a 19.5 gauge syringe needle. Homogenised lysates were then prefiltered to remove particles and contaminating DNA. The resulting filtrate was subsequently transferred to a spin cup containing a silica-based fibre matrix to which the RNA bound, making it possible to remove remaining protein and DNA contaminants upon a series of washes and treatment with DNase. Purified RNA was eluted from the matrix after two successive washes in 40 μl of a low-ionic-strength buffer. Isolated total RNA was quantified and qualified by measuring its optical density at 260 nm and 280 nm, according to the equation:

$$C = A_{260} \times D_F \times C_F \tag{2}$$

where C is the concentration in μg/μl, A_{260} is the optical density (OD) of the sample at 260 nm, D_F is the dilution factor used to measure the A_{260} of the RNA sample, and C_F is the conversion factor for RNA (0.040 μg/μl per OD_{260} unit). Contaminating RNases were inactivated in solutions upon treatment with 0.1% (v/v) DEPC, and RNaseZap was used according to the manufacturer's instructions to eliminate RNase contamination on work surfaces and pipettes.

2.2.21 RNA Amplification and Preparation

Amplification and processing of total RNA was carried out at the Sir Henry Wellcome Functional Genomics Facility (SHWFGF) at the University of Glasgow.

Initially, total isolated RNA (see section 2.2.20) was subjected to two controls: quantity was determined using the NanoDrop ND-1000 spectrophotometer (NanoDrop Technologies, Wilmington, DE, USA) and quality verified using the BioAnalyzer2100 (Agilent, Palo Alto, CA, USA). While RNA was of sufficient quality, the quantity was too low to obtain sufficient amounts of labelled complementary RNA (cRNA) targets for subsequent analysis with probe arrays.

Consequently, RNA was subjected to two rounds of amplification using the Superscript RNA Amplification system (Invitrogen). In the first round of amplification, complementary DNA (cDNA) was synthesised from total RNA using SuperScript II Reverse Transcriptase, which synthesises a cDNA strand, primed with an anchored oligo(dT) primer containing a T7 promoter, from single stranded RNA. Following second-strand cDNA synthesis with *Escherichia coli* (*E. coli*) DNA polymerase and ligase, the cDNA template was amplified by an *in vitro* transcription (IVT) reaction. In this reaction, a bacteriophage T7 RNA polymerase was used to transcribe cRNA from the cDNA template.

The second round of amplification was carried out using the BioArray HighYield RNA Transcript Labelling kit (Enzo Life Sciences, Farmingdale, NY, USA) in order to produce high levels of hybridisable, biotin-labelled cRNA targets. In this case, 400 ng of cRNA generated in the first round of amplification was reverse transcribed using random primers, after which the T7-Oligo(dT) primer was used to facilitate double-stranded cDNA synthesis. This resultant double-stranded cDNA template containing T7 promoter sequences was then subjected to a second IVT reaction, but this time incorporating biotinylated ribonucleotides. The labelled cRNA was then purified using RNeasy mini columns (Qiagen, Crawley, West Sussex) and fragmented by metal-induced hydrolysis to

generate 35-200 base fragments, which served to improve the kinetics of hybridisation to the gene chip.

2.2.22 Microarray Analysis

Microarray analysis was carried out at the SHWFGF, University of Glasgow. RNA samples from three separate control and stimulated experiments for each of the three tissue types were analysed on the Affymetrix GeneChip Mouse Expression Set 430, using standard Affymetrix protocols. Briefly, after amplification and preparation of target cRNA (see section 2.2.21), a hybridisation cocktail was prepared, which contained fragmented target cRNA, probe array controls, BSA, and herring sperm DNA to competitively block non-specific hybridisation. The probe array controls used were bio-B, bio-C and bio-D, all of which are implicated in the biosynthesis pathway of *E. coli*, as well as Cre from the recombinase gene of bacteriophage P1. A synthetic control oligo (B2) was also added to the hybridisation solution to generate a grid pattern at the border of the chip, which was ultimately used by the analysis software. The hybridisation cocktail was then allowed to hybridise to the GeneChip for 16 hours in a 45 °C oven rotating at 60 rpm.

After hybridisation to either the standard (Mouse Expression Set 430) or test arrays (discussed further in section 2.2.23), the chips were washed to remove any cRNA that had not hybridized to its complementary oligonucleotide probe. Bound cRNA was then fluorescently labelled with phycoerythrin-conjugated streptavidin (SAPE). After the initial staining with SAPE alone, the chips were incubated with a biotinylated antibody followed by additional staining with SAPE, in order to amplify the fluorescent signal. All washing and staining was carried out in the GeneChip Fluidics Station 400 (Affymetrix). Washed and stained chips were then scanned at 570 nm with the Agilent Gene Array Scanner 2500 (Affymetrix).

2.2.23 Statistical Analysis of Microarrays

After hybridisation of cRNA to the gene chips, several methods were employed for quality control and data analysis. First, test arrays were used to assess target quality and labelling efficiency for each sample. Following hybridisation, washing, staining, and scanning of the test arrays, images were analysed according to five quality control parameters: (1) the 3'/5' ratio of housekeeping genes to assess the efficiency of the cDNA synthesis reaction; (2) the presence of control cRNAs (bio-B, C, D and Cre), which were spiked into the hybridization cocktail at varying concentrations and served as hybridization controls; (3) the background values of the signal intensity caused by autofluorescence of the array surface, as well as nonspecific binding of target or stain molecules (SAPE); (4) the noise (Q value), which resulted from small variations in the digitized signal observed by the scanner as it sampled the probe array's surface; and finally (5) the scaling factor, which provided a measure of the brightness of the array, which can vary from array to array. In all cases, the data obtained from the test arrays were deemed satisfactory.

Information provided by the positions and intensities of the fluorescent emissions on scanned chips was converted into data relating to levels of gene expression in the original samples. This gene expression data, corresponding to the stimulated and control groups for tendon, corneal and skin fibroblasts, was compared using FunAlyse, a newly-established automated pipeline in SHWFGF (http://www.gla.ac.uk/functionalgenomics/rp/affy_analysis.html). As a first step of this analysis, all 18 samples were normalized using the Robust Multichip Average (RMA) method (Irizarry *et al.*, 2003) and differentially expressed genes were subsequently identified using the Rank Products (RP) method (Breitling *et al.*, 2004b). For every comparison, the RP method ranked the genes according to differential expression measured

by the non-parametric RP-statistic and assessed the statistical significance by producing false discovery rates (FDR). This method is particularly powerful for experiments involving small numbers of replicated samples. Differentially expressed functional gene classes were identified by iterative Group Analysis (iGA) (Breitling *et al.*, 2004a) and assigned using GeneOntology annotations (http://www.geneontology.org/). The A and B arrays of the Affymetrix GeneChip Mouse Expression Set 430 were analysed separately.

The RP-generated list of differentially expressed genes (Table 4.2) was cut using FDR 10% and was further compared manually to identify the highest up- and lowest down-regulated genes in one or more cell lines. Indicated fold-change values correspond to the nominal fold-change (FC*nom*), which is itself obtained from the RMA fold-changes. It has been previously demonstrated that fold-changes calculated after RMA analysis are significantly lower than the nominal fold-changes calculated from the spiked-in control gene concentrations (Cope *et al.*, 2004). Consequently, the relationship between these two fold-changes was calculated by a fitting procedure:

$$\log_2(rmaFC) = 0.61 \times \log_2(FCnom) \tag{3}$$

Equation (3) was used over all possible between-chip comparisons and, hence, contributed to between-group comparisons. Altered genes were manually classified into one of nine broad functional groups based upon their functional annotation in the SOURCE (Diehn *et al.*, 2003), GenBank (Benson *et al.*, 2004), and Mouse Genome Informatics (Blake *et al.*, 2003) databases.

2.2.24 Semi-Quantitative RT-PCR

RNA isolated from mechanically stimulated and control fibroblasts (section 2.2.20) was reverse transcribed and amplified using the Titan One Tube RT-PCR System (Roche, Lewes, East Sussex, UK) according to the manufacturer's instructions. 10 ng of total RNA

was used as the template in all reactions. The reverse transcription reaction was carried out at 50 °C for 30 minutes in a Biometra T-Gradient thermocycler, followed by denaturation for two minutes at 94 °C. The thermocycling conditions included 35 cycles of 10 seconds at 94 °C, 30 seconds at 45-65 °C (depending upon the melting temperature of the primer pairs used), 45 seconds at 68 °C, which was increased by five seconds for each cycle during cycles 11-25, and a final, prolonged elongation cycle of seven minutes at 68 °C. RT-PCR was performed using primers specific for each target gene (Table IV, Appendix) and conditions were chosen such that all of the RNAs analysed were in the exponential phase of amplification.

2.2.25 Primer Selection

The sequences of all primers used in this study were determined using the software Primer3 (Rozen and Skaletsky, 2000). Primers were always chosen according to the following parameters: length between 18 and 27 bases, optimal 20 bases; melting temperature (T_m) between 57 and 63°C, optimal T_m 60°C; length of amplification product between 200 and 800 bp; C+G content above 20% and below 80%; maximum self-complimentarity 8.0; maximum 3' self-complimentarity 3.0; stretches of > 5 mononucleotide repeats were avoided. Sequences were homologous to the RNA of interest, as compared with the GenBank database available at the National Center for Biotechnology Information (NCBI). All oligonucleotides were synthesized by Operon Biotechnologies (Cologne, Germany). Details of these primers are listed in Table IV (Appendix).

2.2.26 Agarose Gel Electrophoresis

DNA samples were separated by non-denaturing electrophoresis on 1% (w/v) agarose/tris-acetate-EDTA (TAE) horizontal gels at a constant voltage of 100 V for 20 minutes. Approximately 80 ng/ml ethidium bromide was incorporated into the agarose/TAE solution prior to casting to allow visualization of DNA under UV light following electrophoresis. Before dispensing samples on the gel, they were mixed with 1x Orange G loading buffer. A DNA size ladder (5 µl) was loaded alongside the samples for molecular weight determination of the separated bands. Gels were visualized under UV light and images captured using a gel documentation system (UVItec, Ltd.).

2.2.27 Mechanical Stimulation

A parallel plate flow chamber, kindly provided by Dr. J. Ando, was used to introduce a laminar fluid flow (rate = 0.88 ml/min) over fibroblasts to produce a chamber wall shear stress of 0.1 dyn/cm^2. Prior to stimulation, fibroblasts were seeded onto gelatin-coated glass plates (7 cm x 10 cm) (see section 2.2.28) at an approximate density of 10,000 cells/cm^2. Cells were seeded in WM and allowed to adhere for approximately seven hours. Fibroblast-seeded plates were rinsed three times with PBS and transferred to mechanical stimulation medium (DMEM, 2% FCS, 500 U/ml penicillin, 500 µg/ml streptomycin) prior to incorporation into the flow chamber (Figures 2.1, 3.4). A fluid flow of 0.88 ml/min, resulting in a steady shear stress of 0.1 dyn/cm^2 (0.01 Pa), was applied to monolayer fibroblasts for a duration of 14 hours with the aid of a peristaltic pump (Amersham Biosciences). The wall shear stress is proportional to the flow rate and the geometry of the channel and can be calculated according to the equation:

$$\tau = \frac{6\mu Q}{bh^2} \tag{4}$$

where τ is shear stress in dyn/cm^2, μ is the fluid viscosity (0.01 dyn/cm^2), Q is flow rate in ml/s, b is the flow channel width (5.5 cm) and h is the flow channel height (0.04 cm). The flow perfusate was mechanical stimulation medium and the volume of the perfusate was 30 ml. Studies were performed in a 37 °C incubator. Static controls were performed similarly except the fibroblast-seeded glass plate was transferred to a single-well plate for the duration of the experiment. Each experiment was performed at least three times.

2.2.28 Coating Stimulation Plates

Glass plates used in mechanical stimulation reactions were coated with 0.1% (w/v) porcine gelatin or 0.1% (w/v) poly-L-lysine (PLL) prior to use. Glass plates were overlaid with approximately 7 ml of the gelatin or PLL solution and incubated for 30 minutes at room temperature in a sterile tissue culture hood, after which the plates were washed 3 x with sterile PBS. Glass plates were seeded with fibroblasts immediately after coating.
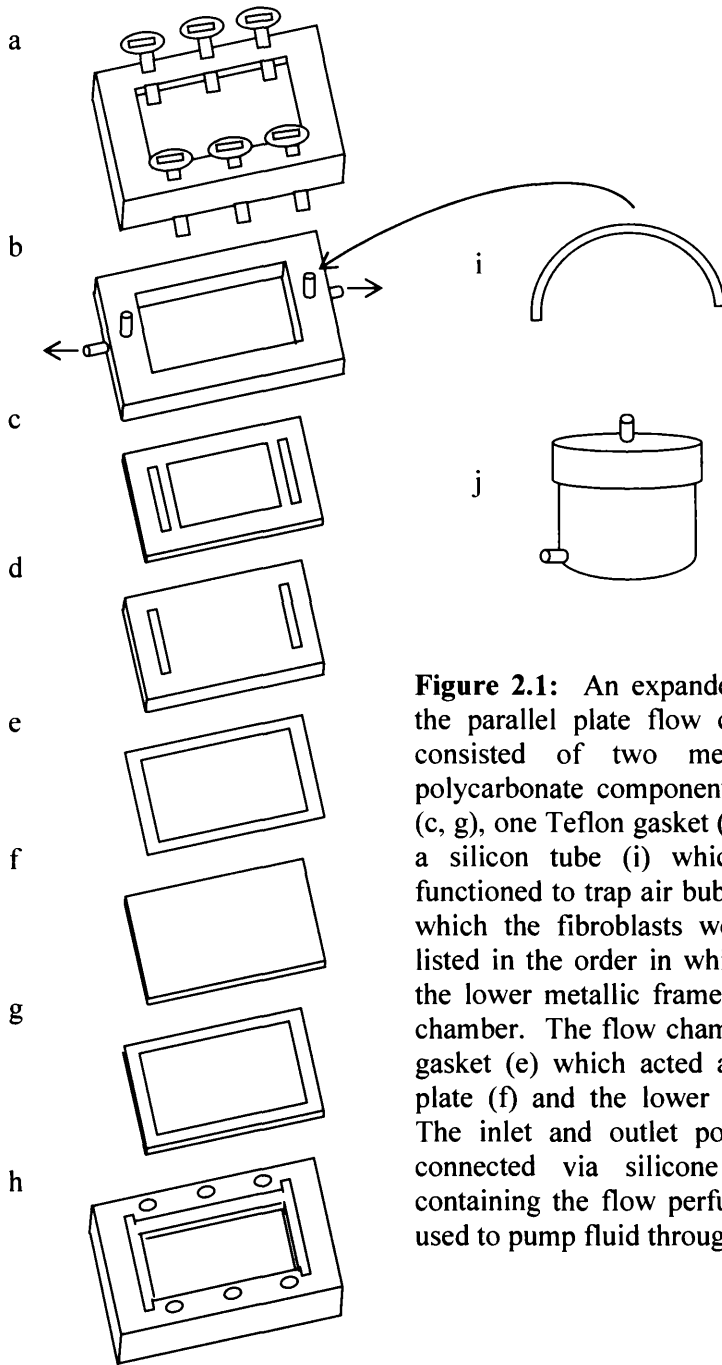
Figure 2.1: An expanded view of the components of the parallel plate flow chamber. The flow chamber consisted of two metallic frames (a, h), two polycarbonate components (b, d), two silicone gaskets (c, g), one Teflon gasket (e) with a thickness of 0.04 cm, a silicon tube (i) which was attached to (b) and functioned to trap air bubbles, and a glass plate (f) onto which the fibroblasts were seeded. Components are listed in the order in which they were assembled, with the lower metallic frame forming the base of the flow chamber. The flow chamber was created by the Teflon gasket (e) which acted as a spacer between the glass plate (f) and the lower polycarbonate component (d). The inlet and outlet ports of the chamber (b) were connected via silicone tubing to a reservoir (j) containing the flow perfusate. A peristaltic pump was used to pump fluid through the channel.

CHAPTER 3

Chapter 3

Morphological characterisation of mechanically stimulated fibroblasts

3.1 Introduction

Despite their broad functional roles and widespread use in culture, fibroblasts are very poorly defined. To date, there are no known markers for fibroblasts, mainly due to the fact that all potential markers have also been identified in other members of the connective tissue cell family, such as osteoblasts, smooth muscle cells, and adipocytes (Wolf *et al.*, 2003). To make matters more complicated, the term "fibroblast" has often been used to refer to the morphology of a fibroblast-like cell, rather than a specific cell type. This definition is based upon the fact that fibroblasts are traditionally considered to have a relatively uniform morphology, appearing elongated and spindle-shaped, with clear leading and trailing edges, characteristics sometimes shared in cells that are not of fibroblastic origin.

The observation that all fibroblasts are created morphologically equal has since been shown to be untrue, however, as demonstrated by the morphological differences detected between fibroblasts analyzed *in vivo* and those cultured *in vitro* (Gabbiani and Rungger-Brandle, 1981; Herrmann *et al.*, 1980; Pinto and Gilula, 1972; Ross and Greenlee, Jr., 1966). Phenotypic plasticity in fibroblasts is further supported by findings that fibroblast populations derived from the same or distinct tissues demonstrate unique behaviour and morphology (see Table 3.1). Based upon their tissue localisation, fibroblasts have been shown to demonstrate unique responses in culture, such as sensitivity to trypsin and EDTA, replication rate, saturation density, attachment efficiency, and proliferative capacity (Banes *et al.*, 1988a; Conrad *et al.*, 1977b; Harper and Grove, 1979; Riederer-Henderson *et al.*, 1983), discernible morphology (Banes *et al.*, 1999a; Conrad *et al.*, 1977b; Smith *et al.*, 1995), differential synthesis of ECM

60

Cell Populations	Distinguished by	Reference
Skin fibroblasts	Proliferation rates, morphology	(Martin *et al.*, 1974)
Skin and lung fibroblasts	Replication rates, [^{3}H]thymidine incorporation into DNA, saturation density, cell volume, cellular RNA and protein contents, *in vitro* life spans	(Schneider *et al.*, 1977)
Gingival fibroblasts	Cellular response to prostaglandin E$_2$	(Ko *et al.*, 1977)
Corneal, heart and skin fibroblasts	Glycosaminoglycan synthesis, morphology, behaviour in monolayer (i.e. directionality, contact inhibition), saturation densities, sensitivity to trypsin and EDTA, cell-surface antigen presentation	(Conrad *et al.*, 1977a), (Conrad *et al.*, 1977b), (Garrett and Conrad, 1979)
Papillary and reticular skin fibroblasts	Saturation density, proliferative capacity	(Harper and Grove, 1979)
Synovial and internal tendon fibroblasts	Attachment efficiency, amount and type of collagen synthesis, glycosaminoglycan synthesis	(Riederer-Henderson *et al.*, 1983)
Synovial and internal tendon fibroblasts	Morphology, presence of cytoplasmic, lipid-containing vesicles, decreased sensitivity to trypsin, reduced generation time	(Banes *et al.*, 1988a), (Banes *et al.*, 1988b)
Skin, lung and heart fibroblasts	Morphology at confluence, protein synthesis, proliferation rate, contraction potency in collagen gels, ECM protein secretion	(Shimizu K. and Yoshizato K., 1992)
Papillary and reticular gingival fibroblasts	Migration, saturation density	(Irwin *et al.*, 1994)
Orbital fibroblasts	Differential expression of surface glycoproteins, change in shape in response to prostaglandin E$_2$, morphology	(Smith *et al.*, 1995)
Orbital and dermal fibroblasts	Morphology after treatment with compounds that increase endogenous cAMP production	(Reddy *et al.*, 1998)
Oral mucosa and skin fibroblasts	Proliferation rate, contraction potency in collagen gels, effect of TGF-β1 on contraction and collagen synthesis	(Lee and Eun, 1999)
Flexor and extensor tendon fibroblasts	Synthesis of ECM proteins, effect of mechanical strain on cell proliferation	(Evans and Trail, 2001)
Myometrial and endometrial fibroblasts	Differential expression of surface glycoproteins, cytokine production	(Koumas *et al.*, 2001)

Table 3.1: Phenotypic plasticity demonstrated by various fibroblast populations. Phenotypic variations are found in subpopulations of fibroblasts isolated from the same tissue or distinct populations of fibroblasts isolated from diverse tissues. Fibroblasts have been shown to demonstrate differences in morphology, proliferation rates, saturation density, protein synthesis, antigen presentation, sensitivity to trypsin, response to growth factors, and *in vitro* life spans.

proteins (Conrad *et al.*, 1977a; Evans and Trail, 2001; Riederer-Henderson *et al.*, 1983), and distinct cell-surface antigen presentation and surface receptors (Garrett and Conrad, 1979; Koumas *et al.*, 2001).

The aforementioned studies all suggest that fibroblasts from different tissues, as well as fibroblast populations within a given tissue, are somehow differentiated. Thus far, however, such studies have been largely qualitative. Fibroblasts from different tissues have often been compared on a morphological or biochemical level, but only few reports exist which have characterised the transcriptional responses of fibroblast cell lines to an exogenous stimulus, and in these cases, the fibroblast populations were all derived from the same tissue (Banes *et al.*, 1999a). While this type of investigation has been crucial in furthering the body of knowledge surrounding the possible differentiation of fibroblasts, the scope of techniques currently available, ranging from quantification of cell morphology to microarray technology, enable a much more in-depth analysis of fibroblast populations.

In order to determine if fibroblasts from distinct tissues exhibit differential responses to an identical mechanical stimulus, tendon, skin and corneal fibroblasts were subjected to shear stress by fluid flow using a parallel plate flow chamber. This method of stimulation is well-documented in the literature, and is characterised by producing well-defined, replicable shear stresses (Brown, 2000). Furthermore, the parallel plate flow chamber has been successful in eliciting a variety of cellular responses, ranging from changes in morphology to gene and protein expression (Table 3.2).

The following chapter details the isolation and characterisation of the cell lines used throughout this study, as well as the optimization of the method of mechanical stimulation. In addition, this work qualitatively and quantitatively assesses cell morphology, including cell size, shape, multinucleation, proliferation rate and focal

Stimulation regime	Parameters measured	Cell Type	Magnitude (dyn/cm^2)	Reference
Single shear stress for maximum of 210 min; incremental stress for 165 and 195 min	Cell adhesion	Skin fibroblasts	4.4, 8.8, 17.6, 26.3	(van Kooten *et al.*, 1992)
Pulsatile stress applied for 180 min	Morphology	Skin fibroblasts	44 (min); 176 (max)	(van Kooten *et al.*, 1993)
Single stress for 1 min with rest period of 3 min	Ca^{2+} transients	Ligament fibroblasts	25	(Hung *et al.*, 1997)
Single stress applied for 1 h	Morphology, adhesion, gene and protein expression	Osteoblasts	12	(Pavalko *et al.*, 1998)
Stress applied for 12 h	Morphology and proliferation	Osteoblasts, 3T3 fibroblasts	0.1-4.0	(Billotte and Hofmann, 1999)
Single stress applied for 5, 15, 30, 60, and 180 min	Gene expression	Osteoblasts	12	(Chen *et al.*, 2000)
Single stress applied for 2, 5 or 15 min	Protein expression	Chondrocytes	16	(Hung *et al.*, 2000)
Stress applied for 1-3 min with rest period of 15 min	Ca^{2+} transients, protein expression	Intervertebral disc cells	1, 3, 5, 10, 15, 20, 25	(Elfervig *et al.*, 2001)
6 h at lowest magnitude; 3 h at higher magnitudes	Gene expression, cell alignment, protein secretion	Tendon fibroblasts	1-25	(Archambault *et al.*, 2002b)

Table 3.2: Published instances of the use of parallel plate flow chamber to mechanically stimulate cells. The presentation of shear stress to a cell monolayer has been successful in stimulating a wide variety of cells, ranging from connective tissue cells to endothelial cells. Cell responses to such mechanical stimulus is varied, including both morphological responses to changes in gene and protein expression.

adhesion formation, as well as gelatinase activity. This data provides strong evidence that tendon, corneal and skin fibroblasts are morphologically distinct and respond in unique ways to an identical mechanical stimulus.

3.2 *Results*

3.2.1 *Isolation of primary murine tendon, corneal and skin fibroblasts*

In order to investigate the morphology of fibroblasts from diverse tissues, the present study utilised primary, as opposed to transformed, cell lines. While the use of transformed cells is sometimes advantageous, due to higher growth rates and general ease of maintenance, transformed cells, and even primary cells that have been cultured extensively, display a loss of morphology and phenotype from the donor tissue (Herrmann *et al.*, 1980; Majumdar *et al.*, 1998). To ensure, as much as possible, that the cells used in this study reflected their *in vivo* phenotype, primary tendon, corneal and skin fibroblasts were isolated and used at low population doublings throughout this study.

Primary embryonic murine fibroblasts were obtained from a time mated CD1 mouse, which was euthanized at 19 days post-conception. Embryos were detached from the embryonic sac, whereupon tail tendon, cornea, and skin were isolated and used in production of three fibroblast cell lines (as described in 2.2.1). The isolation procedure used here relied upon the rapid adhesion of fibroblasts, in order to accomplish their separation from non-fibroblast-like cells (Spector *et al.*, 1998). Isolated cells were grown under standard tissue culture conditions and examined microscopically. As shown in Figure 3.1, the isolated cell lines all displayed typical fibroblast morphology; cells appear elongated and spindle-like and possess long, filopodial extensions. In addition, cells are very clearly polarised, with a distinct leading and trailing edge, and

appear flattened with an irregular outline. All three cell lines exhibited contact inhibition, after which cells maintained the same overall morphology.

While tendon, corneal, and skin fibroblast-like cells were isolated by techniques previously demonstrated to generate populations of authentic fibroblasts (Spector *et al.*, 1998) and displayed typical fibroblast morphology (Figure 3.1), the fibroblastic origin of the isolated cells was further substantiated. In lieu of a universal marker for fibroblasts, the presence or absence of tissue-specific intermediate filament proteins was used to distinguish fibroblasts from other contaminating cell types that could have survived the isolation process. This method is based upon the fact that epithelial cells have been found to predominantly express keratins (Moll *et al.*, 1982), whereas cells of muscular origin express desmin, and mesenchymal cells express vimentin (Osborn and Weber, 1982).

Primary tendon, corneal and skin fibroblasts, as well as HeLa cells, C2C4 myoblasts and 3T3 fibroblasts, were lysed directly in their tissue culture vessels and subjected to immunoblotting. HeLa cells, C2C4 myoblasts and 3T3 fibroblasts served as both positive and negative controls. As shown in Figure 3.2, the cell lines isolated from tendon, cornea and skin are devoid of desmin and keratin intermediate filaments, but are rich in vimentin. This indicates that the isolated cell lines are not contaminated by epithelial or muscle-derived cells and confirms the mesenchymal origin of the isolated cell lines. While the presence of vimentin does not itself distinguish fibroblasts from other mesenchymal cells, such as monocytes, macrophages and lymphocytes, the existence of this intermediate filament, in conjunction with the isolation protocol and fibroblastic morphology of the isolated cell lines, is sufficient in confirming that these cells are likely to be fibroblasts.
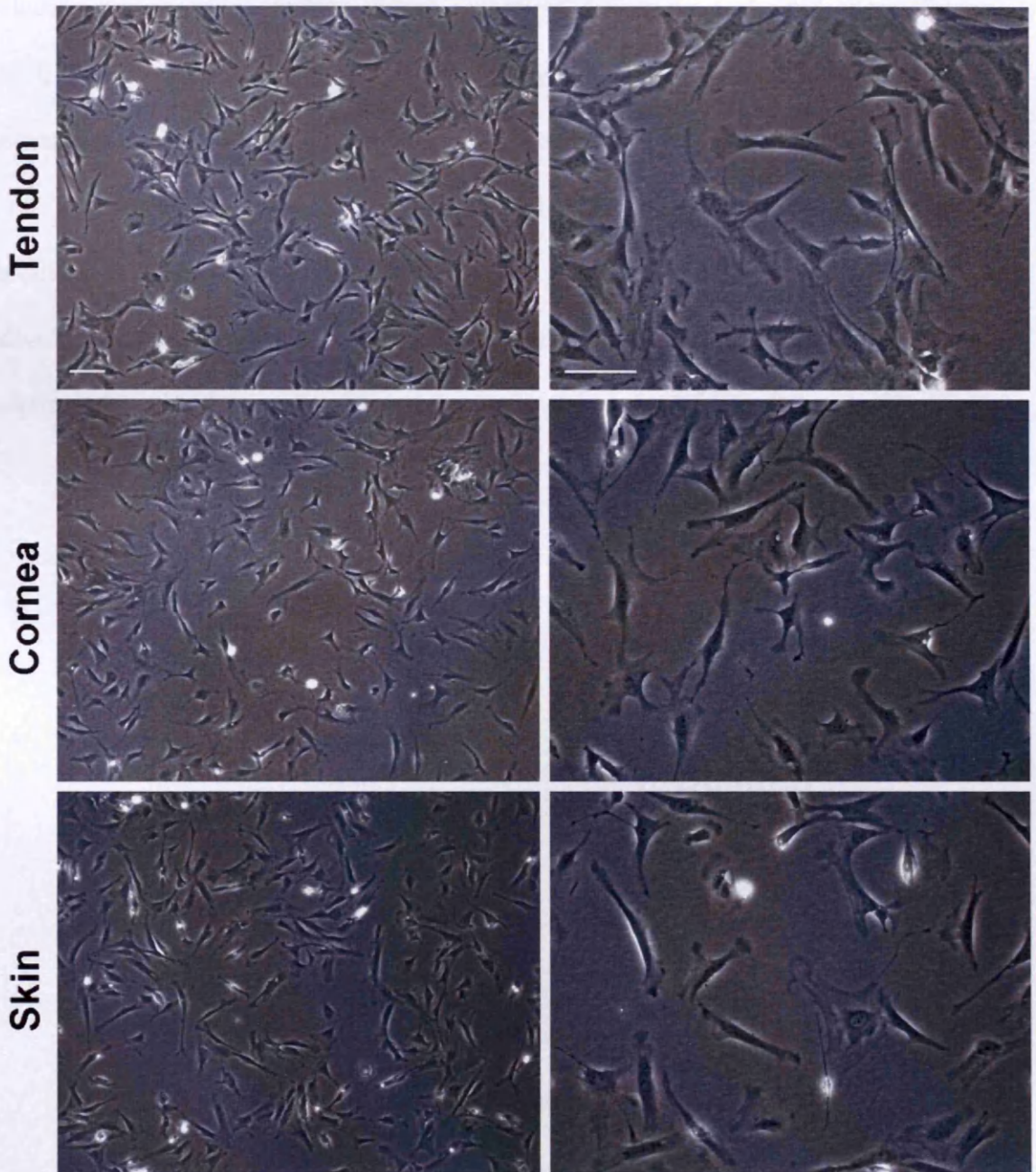
Figure 3.1: Phase contrast images of isolated tendon, corneal and skin fibroblasts. Cells were isolated as described in section 2.2.1, cultured under standard tissue culture conditions, and imaged. Scale bars = 100 μm.

3.2.2   Determination of method of mechanical stimulation

There are numerous ways in which to mechanically stimulate cells *in vitro*, including compressive loading, stretch, substrate distension and fluid shear (Brown, 2000). In this study, we have chosen to employ fluid shear as the method by which to mechanically stimulate primary tendon, corneal and skin fibroblasts. While this method is not necessarily physiologically relevant to all three tissues, it is thought that tendon fibroblasts may experience shear stress as the tendon moves within its sheath or as individual fascicles move past one another (Archambault *et al.*, 2002b; Benjamin and Ralphs, 1997). Furthermore, tendon and skin fibroblasts have been shown previously to
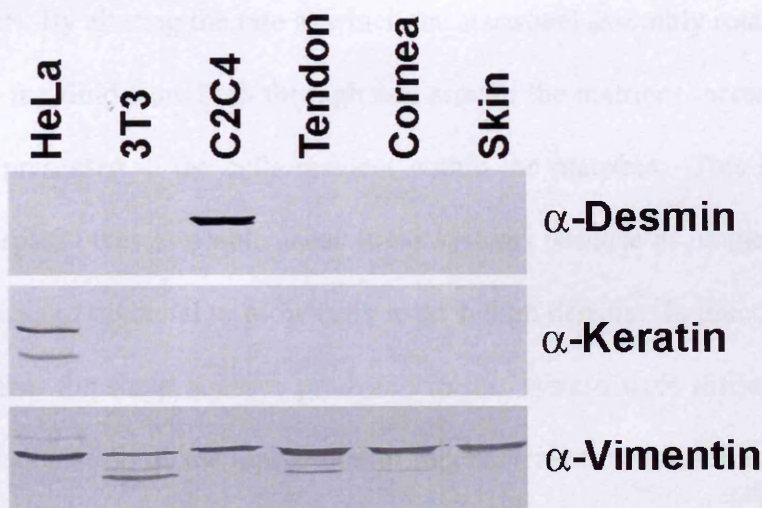
Figure 3.2: Western blot indicating the presence of intermediate filament proteins in various cell lines. Fibroblasts were isolated (as described in 2.2.1) and maintained under standard tissue culture conditions. Total cell lysates were prepared from tendon, corneal and skin fibroblast cell lines, as well as HeLa cells, 3T3 fibroblasts, and C2C4 myoblasts. Proteins were separated by SDS-PAGE, transferred to PVDF, and probed with the indicated anti-sera.

respond to fluid flow (Archambault *et al.*, 2002a; Grierson and Meldolesi, 1995). Regardless, the fact that this type of stimulation may not be experienced by each of these cells *in v*ivo is not necessarily relevant; this study aims to compare the response of three cell lines to an identical mechanical cue in order to determine if the generated responses are similar or distinct.

In order to generate fluid flow, two mechanical stimulation systems were tested. In the first instance, the Starwheel cell culture system was used, which is a novel three-dimensional culturing system capable of generating shear stresses by fluid flow (Figure 3.3). This system consisted of three-dimensional matrices in which cells could be seeded and, theoretically, cultured to high densities. The matrices were immobilised in a star-wheel assembly, which was rotated through the growth medium with the aid of a magnetic stirrer. By altering the rate at which the starwheel assembly rotated through the growth media, the fluid flow both through and around the matrices increased, as did the shear stresses presented to the cells resident within the matrices. This system initially appeared to surpass other available shear stress systems because of its three-dimensional growth substrate and potential to grow cells to such high density. In practice, however, it became clear that the shear stresses produced in this system were difficult to quantify. For example, calculation of the magnitude of mechanical stimulation being presented to the cells cultured in the system was difficult, given that each cell occupied a unique and distinct location in the three-dimensional matrix, and hence would sense completely unique mechanical cues. Moreover, imaging cells in the three-dimensional scaffold was difficult, the volumetric fluid requirement was high, the three-dimensional matrices were difficult to clean, and trypsinisation or cell lysis resulted in low yields.
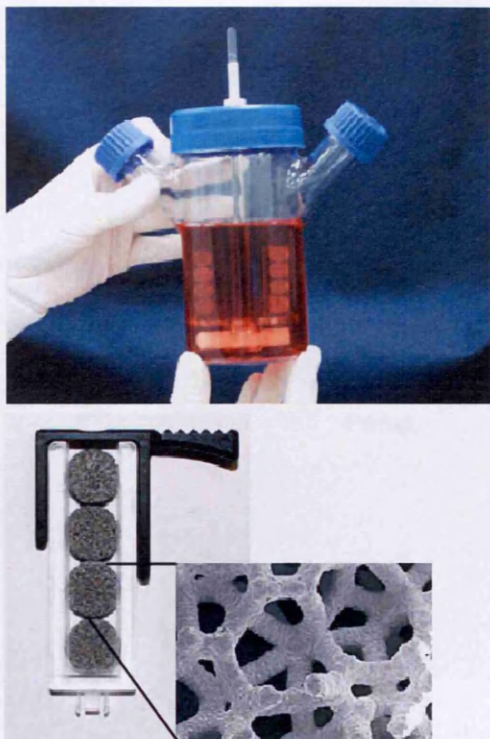
Figure 3.3: The Starwheel cell culture system, used initially as a method by which to subject primary tendon, corneal and skin fibroblasts to shear stress. The system is composed of a two-armed flask containing a star-wheel assembly, onto which tuning fork assemblies are mounted. Cells grow within porous disks, whose three-dimensional structure is said to mimic the three-dimensional structure of bone marrow. (Images adapted from http://www.cygenics.com/cellsciences)

In order to overcome these difficulties, subsequent mechanical stimulation was achieved using the parallel plate flow chamber. This system is well-documented and used to apply a well-defined, reproducible laminar flow over cell monolayers based upon a pressure differential between two slit openings at either end of a rectangular chamber (Figure 3.4) (see section 2.2.27) (Brown, 2000). Despite the fact that the parallel plate flow chamber had a two-dimensional growth surface, it provided significant advantages over the Starwheel system, in that the stress stimulus was homogenous across the monolayer, perceived stresses were easy to calculate, the system had a small volumetric requirement, and sampling and exchange of medium was easy. Furthermore, the parallel plate flow chamber is well documented in the literature and has been used in the production of mechanical stimulus for a wide variety of cell types, including members of the connective tissue cell family (Table 3.1).
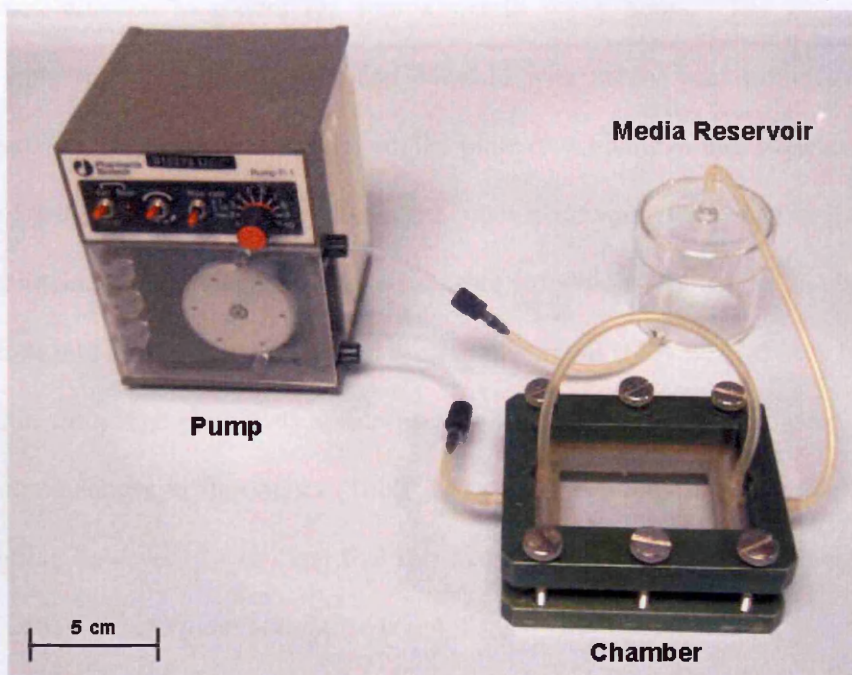
Figure 3.4: Parallel plate flow chamber used to produce laminar fluid flow over fibroblast monolayers. The system was interfaced with a paristaltic pump, which created a pressure differential between two slit openings in the rectangular chamber, thus creating laminar flow of medium over the cell monolayer. The flow perfusate was contained within a glass reservoir. The chamber's components are detailed in section 2.2.27 or Figure 2.1.

3.2.3   Optimising mechanical stimulation by laminar fluid flow

After determining the method of stimulation to be used throughout this study, it was necessary to optimise the magnitude of stimulation and culture conditions, in order to maximise the mechanical cue presented to the cells while minimising potential cell damage.

3.2.3.1 Magnitude of stimulation

In initial mechanical stimulation experiments, primary fibroblasts were subcultured until passage number five, at which point they were seeded onto two glass

plates and allowed to adhere for approximately seven hours. The fibroblast-seeded plates were then rinsed with PBS and overlaid with mechanical stimulation medium. One plate was incorporated into the parallel plate flow chamber and subjected to a shear stress of 1 dyn/cm^2 for 24 hours, while the other plate was placed in a single well plate and maintained under standard tissue culture conditions to act as a control. The magnitude and duration of stimulation used in this initial study were chosen because they lie within the range previously observed to elicit morphological and gene and protein expression changes in fibroblasts (Table 3.1). Upon examination of the cells following stimulation, however, it was clear that this magnitude of fluid flow resulted in complete loss of cells from the glass substrate (data not shown).

Consequently, lower magnitudes of stimulation were tested, and the glass plate onto which fibroblasts were seeded was coated with either 0.1% poly-L-lysine or 0.1% gelatin to facilitate cell adhesion (section 2.2.28). As illustrated in Figure 3.5, the number of adherent cells after stimulation varies with the magnitude of fluid flow. Stimulation at 0.5 dyn/cm^2 results in a decrease in cell density compared to the control, in which cells not only remained adhered but also appear to have proliferated.

While there were notably more adherent cells remaining after 24 hours at 0.5 dyn/cm^2 as opposed to the higher magnitude of 1 dyn/cm^2, this was, nonetheless, an unacceptable reduction in cell number. In contrast, cells stimulated with a fluid flow of 0.1 dyn/cm^2 display comparable cell density to the control. Because fibroblasts remained adhered to the substrate and still demonstrated typical fibroblast morphology after 24 hours of fluid flow, the magnitude of stimulation used hereafter in this study was 0.1 dyn/cm^2.
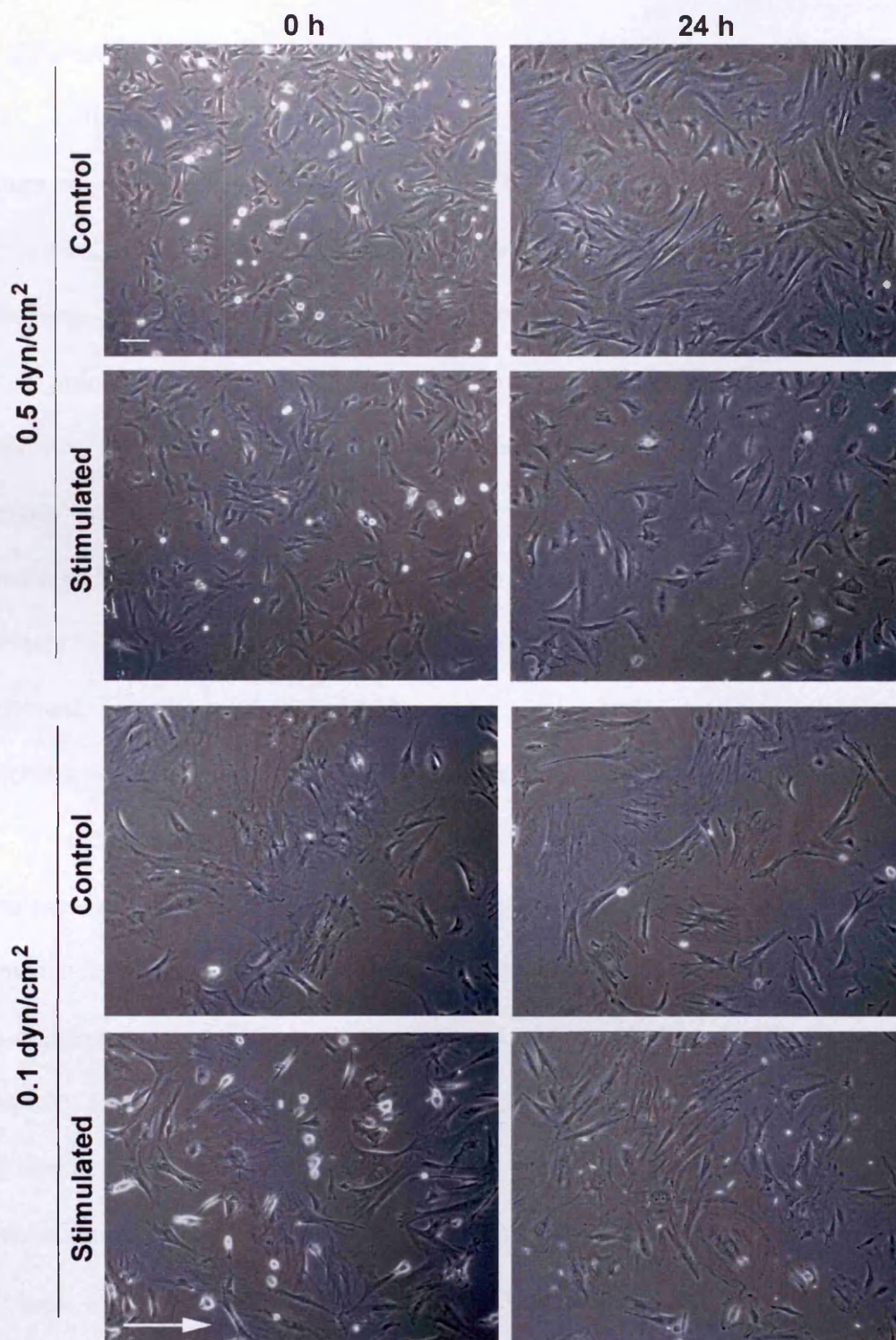
Figure 3.5: Phase contrast images of control and stimulated tendon fibroblasts at two magnitudes of fluid flow. Fibroblasts were cultured until passage number five under standard tissue culture conditions, at which point they were seeded onto gelatin-coated glass plates. Cells were imaged after being allowed to adhere for approximately seven hours, but before stimulation (0 h). Cells were then placed either in a single well plate (control) or subjected to 24 hours of fluid flow at the indicated magnitudes (stimulated). Cells were subsequently imaged (24 h) to examine the effect of flow rate on cell density. The arrow indicates the direction of fluid flow. Scale bar = 100 μm.

3.2.3.2 Foetal calf serum concentration

Following the determination of a suitable magnitude for stimulation, specific cell culture conditions were analysed in order to facilitate analysis of cellular responses to stimulation, while still maintaining healthy cells. Prior to stimulation, primary embryonic fibroblasts were maintained in DMEM supplemented with 15% FCS. In initial stimulation experiments, this working medium was also used as the flow perfusate. With this level of serum supplementation, however, subsequent proteomic analysis was increasingly difficult, because the levels of secreted proteins in the conditioned medium were overshadowed by the high protein levels already present in the medium. Consequently, the concentration of FCS used in the flow perfusate was optimised, in order to minimise background protein levels, while maintaining healthy fibroblast populations and eliciting quantifiable mechanical responses.

In this series of experiments, primary fibroblasts were transferred from DMEM supplemented with 15% FCS to DMEM supplemented with either 0.1% or 2% FCS immediately prior to stimulation. According to Figure 3.6, it is evident that decreasing the concentration of FCS to 0.1% results in a dramatic loss of fibroblasts from the substrate, either with or without stimulation. When supplemented with 0.1% FCS, the cell density of control fibroblasts at 24 h was approximately half of that seen prior to the stimulation experiment, while virtually all stimulated cells appear to have washed off the substrate. With the higher concentration of FCS, however, the cell density both before and after the stimulation experiment is comparable, and cells remained adhered to the substrate even in the presence of fluid flow. Consequently, the flow perfusate used in subsequent stimulation experiments was DMEM supplemented with 2% FCS, which enabled adhesion to the substrate while facilitating subsequent examination of protein levels in the conditioned medium. Furthermore, previous reports have shown that serum
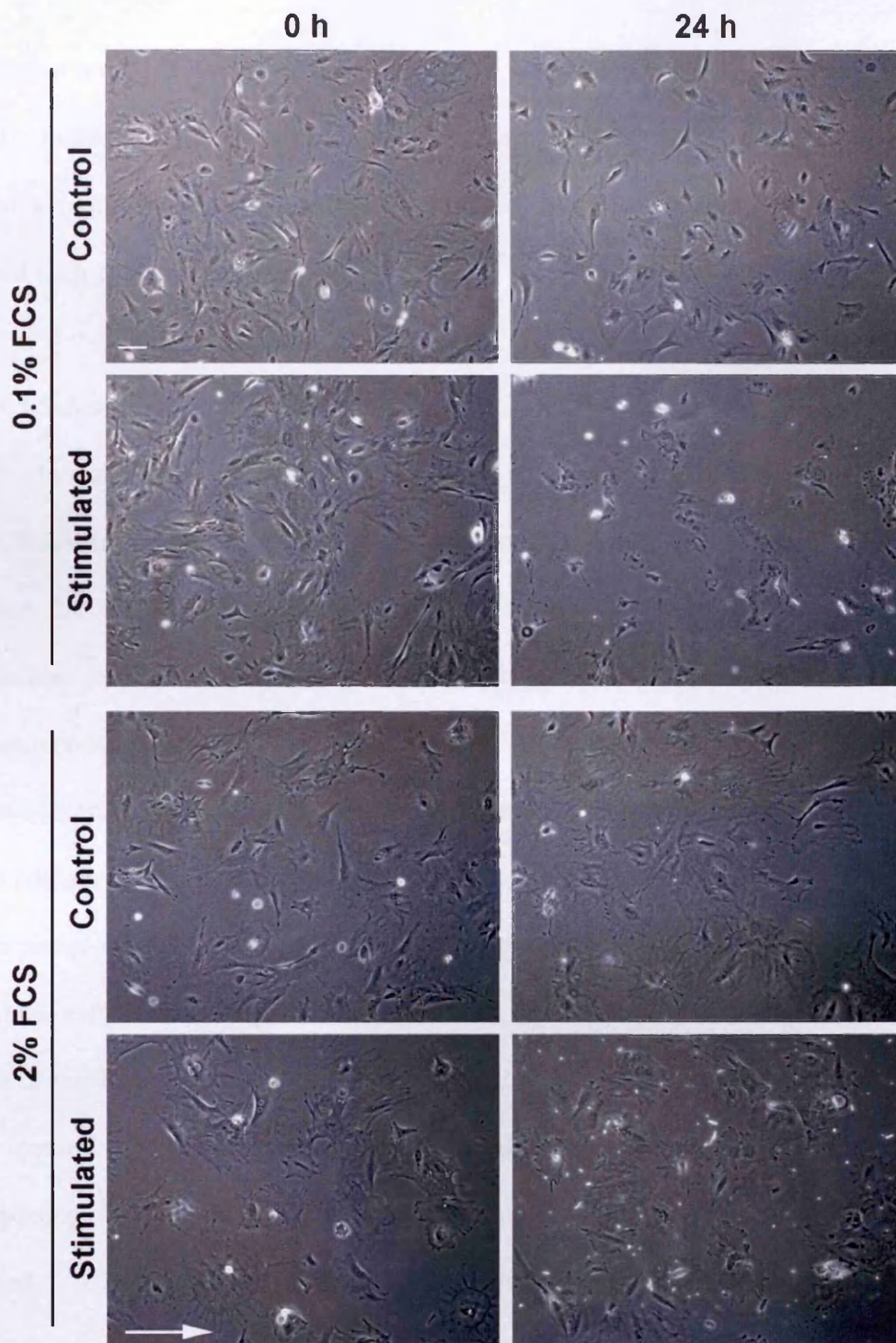
Figure 3.6: Phase contrast images of control and stimulated embryonic fibroblasts. Fibroblasts were cultured until passage number five, at which point they were seeded onto gelatin-coated glass plates. Cells were imaged after being allowed to adhere for approximately seven hours (0 h) and were then overlaid with DMEM supplemented with either 0.1% or 2% FCS. Control cells were placed in a single well plate, while stimulated cells were subjected to 24 hours of fluid flow at 0.1 dyn/cm^2. Cells were imaged after the stimulation experiment (24 h) to examine the effects of serum levels on cell adhesion after stimulation. The arrow indicates the direction of fluid flow. Scale bar = 100 µm.

levels can modulate the mechanosensitivity of connective tissue type cells (Allen *et al.*, 2000). In this study, bone cells pre-treated with 2% serum prior to flow stimulation were found to demonstrate the maximal mechanical response in comparison to cells pre-treated with 10% or 0% serum.

3.2.3.3 Substrate coating

In order to aid in cell attachment, glass stimulation plates were coated with either poly L-lysine (PLL) or gelatin. PLL was employed to provide a positively charged surface that would allow for non-specific fibroblast attachment. However, proteins sometimes lose biological activity when they bind to surfaces in a non-specific manner. Consequently, gelatin was also used, which allows for specific fibroblast attachment to the substrate. In order to test these two substrates, corneal fibroblasts were subcultured until passage number five, at which point they were seeded onto PLL- or gelatin-coated glass plates and allowed to adhere for approximately seven hours. Fibroblasts were then overlaid with DMEM supplemented with 2% FCS and either placed in a single well plate or mechanically stimulated at 0.1 dyn/cm^2 for 24 hours. As apparent from Figure 3.7, control corneal fibroblasts appear healthy and demonstrate typical fibroblast morphology at both time points, irrespective of the substrate onto which the cells were seeded. After 24 hours of stimulation, however, cells seeded onto PLL exhibit a dramatic decrease in cell density and those that remain exhibit an increasingly rounded morphology. Corneal fibroblasts plated on gelatin, however, still appear healthy and demonstrate typical elongated, spindle-like morphology after 24 hours of fluid flow. As a consequence, glass stimulation plates were coated with 0.1% gelatin prior to seeding cells for the duration of the mechanical stimulation experiments in this study.
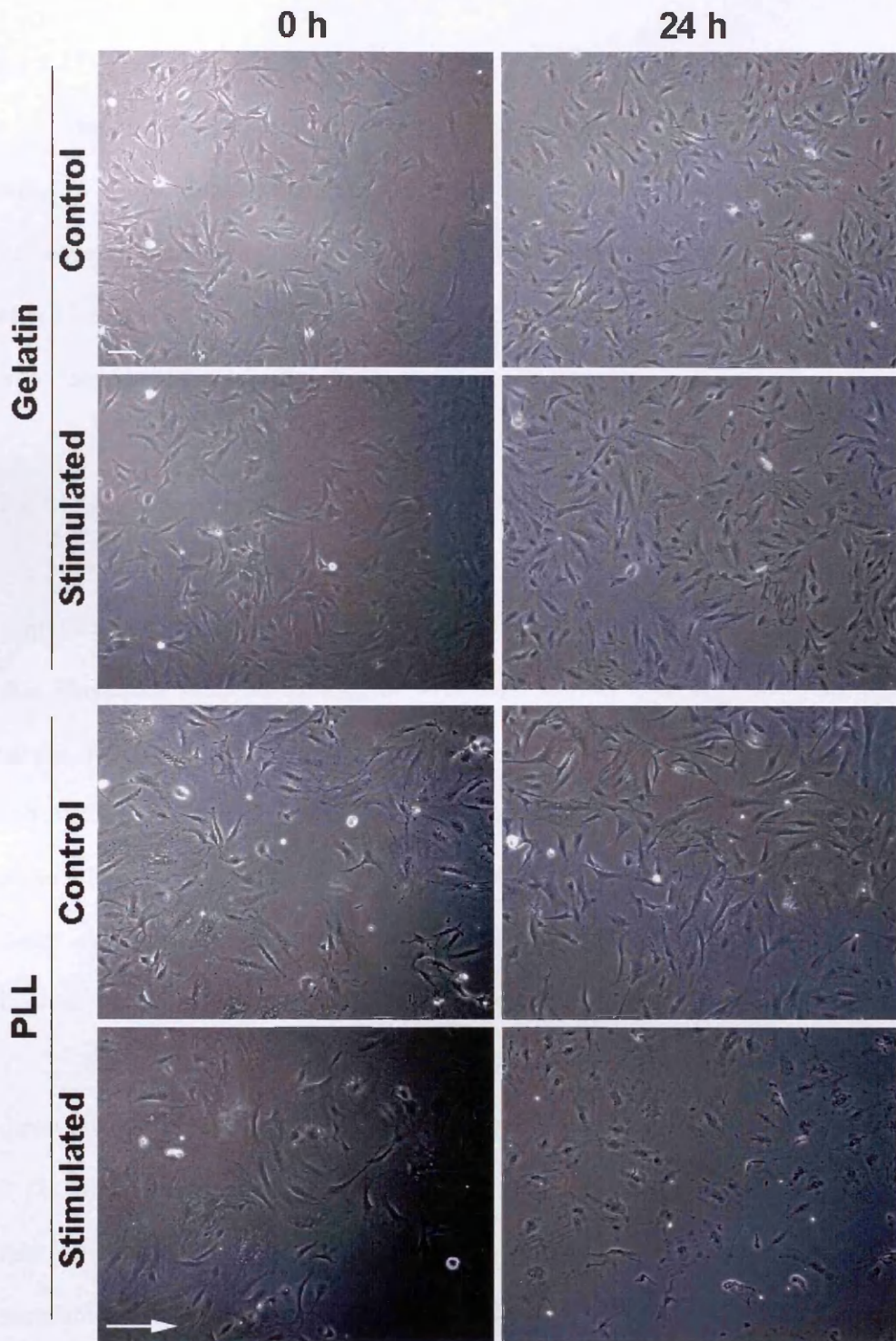
Figure 3.7: Phase contrast images of control and stimulated corneal fibroblasts. Fibroblasts were cultured until passage number five, at which point they were seeded onto either 0.1% gelatin- or 0.1% PLL-coated glass plates. Cells were allowed to adhere for approximately seven hours, at which point they were transferred to mechanical stimulation medium. Control cells were placed in a single well plate, while stimulated cells were subjected to 24 hours of fluid flow at 0.1 dyn/cm^2. Cells were imaged both before (0 h) and after (24 h) the stimulation experiment. The arrow indicates the direction of fluid flow. Scale bar = 100 μm.

3.2.3.4 Duration of stimulation

Initially, the duration of mechanical stimulation was chosen to be 24 hours, in order to allow measurement of both gene and protein expression changes. It was subsequently determined, however, that protein expression changes could be measured after 14 hours (see sections 3.2.6, 4.2.12, 4.2.13), so subsequent stimulation experiments were carried out accordingly.

3.2.4 Qualitative morphological examination of mechanically stimulated fibroblasts

After optimising stimulation conditions (section 3.2.3), all subsequent mechanical stimulation experiments were carried out in the following manner: tendon, corneal and skin fibroblasts were subcultured until passage number five, at which point they were seeded onto 0.1% gelatin-coated glass plates. Cells were imaged after being allowed to adhere for approximately seven hours, at which point they were shifted into mechanical stimulation medium. Control cells were placed in a single well plate and maintained under standard tissue culture conditions, while stimulated cells were subjected to 0.1 dyn/cm^2 of shear stress in a parallel plate flow chamber for 14 hours.

Initially, the effect of mechanical stimulation on the gross morphology and directionality of tendon, corneal and skin fibroblasts was investigated (Figures 3.8-3.10, 3.12-3.15), after which the effect of stimulation on the actin cytoskeleton (Figure 3.11) and focal adhesion formation (Figures 3.15-3.16) was examined. In the case of the gross morphological studies, live cells were imaged either just prior to or just following the 14-hour stimulation experiment. To enable visualisation of the actin cytoskeleton and focal adhesion formation, however, cells were fixed immediately after the simulation experiment and stained with rhodamine phalloidin or anti-sera directed against vinculin, respectively.

3.2.4.1 Gross morphology of tendon fibroblasts

Prior to stimulation, tendon fibroblasts demonstrate a large variability in cell size and shape with irregular, yet smooth, cell outlines (Figure 3.8). Based upon morphology alone, two populations of tendon fibroblasts appear to exist: the first comprises elongated, spindle-like cells, while the other population consists of larger and more rounded cells. After 14 hours, cell density of both control and stimulated cells appears to increase. Furthermore, both control and stimulated cells appear to be more rounded after 14 hours, which may have resulted from the decreased serum levels in the flow perfusate (MSM). There does not appear, however, to be a gross morphology change with stimulation and cells do not seem to align in the direction of flow (see section 3.2.5.2).
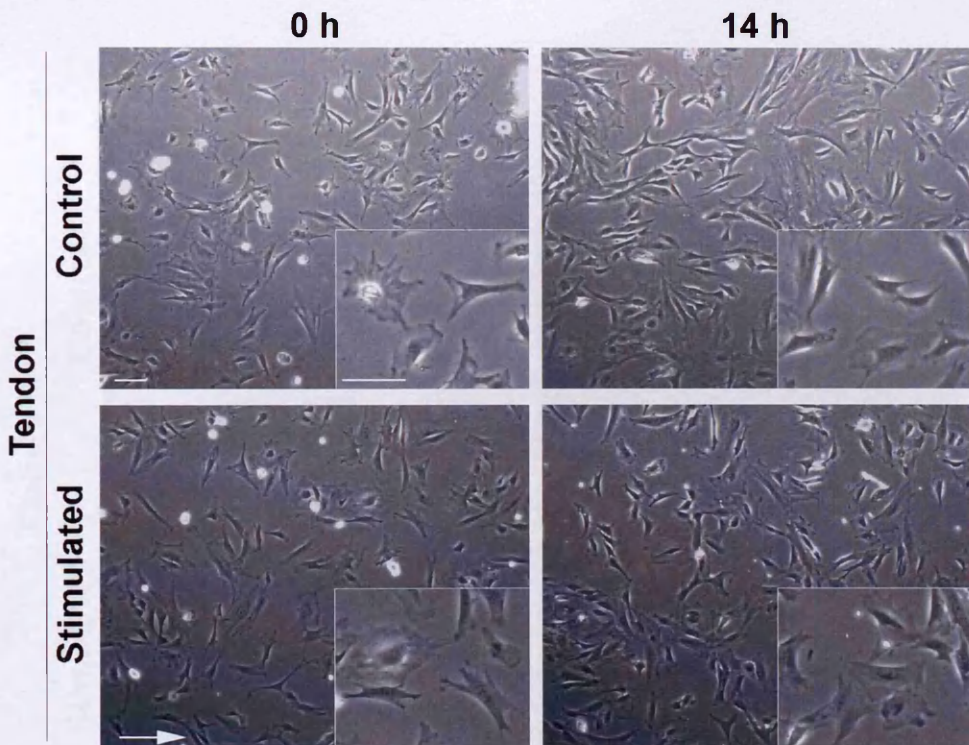
Figure 3.8: Phase contrast images of control and stimulated tendon fibroblasts before (0 h) and after (14 h) being subjected to 0.1 dyn/cm^2 of fluid flow for 14 hours. Arrow indicates direction of flow. Scale bars = 100 μm.

3.2.4.2 Gross morphology of corneal fibroblasts

In contrast to tendon cells, which demonstrate relatively smooth cell outlines, pre-stimulated corneal fibroblasts contain long, hair-like protrusions, which make their cell outline considerably more "jagged" in appearance (Figure 3.9). Additionally, there appear to be fewer rounded corneal fibroblasts; instead, the cell population seems to contain more elongated cells. After 14 hours, the "jagged" morphology seems to have lessened and the presence of rounded cells appears to have increased in control fibroblasts, perhaps a consequence of decreased serum levels. As seen with tendon fibroblasts, the cell density of control cells appears to have increased slightly. In stimulated corneal fibroblasts, cell shape appears even smoother and more rounded than in controls, and it is difficult to identify any hair-like protrusions.
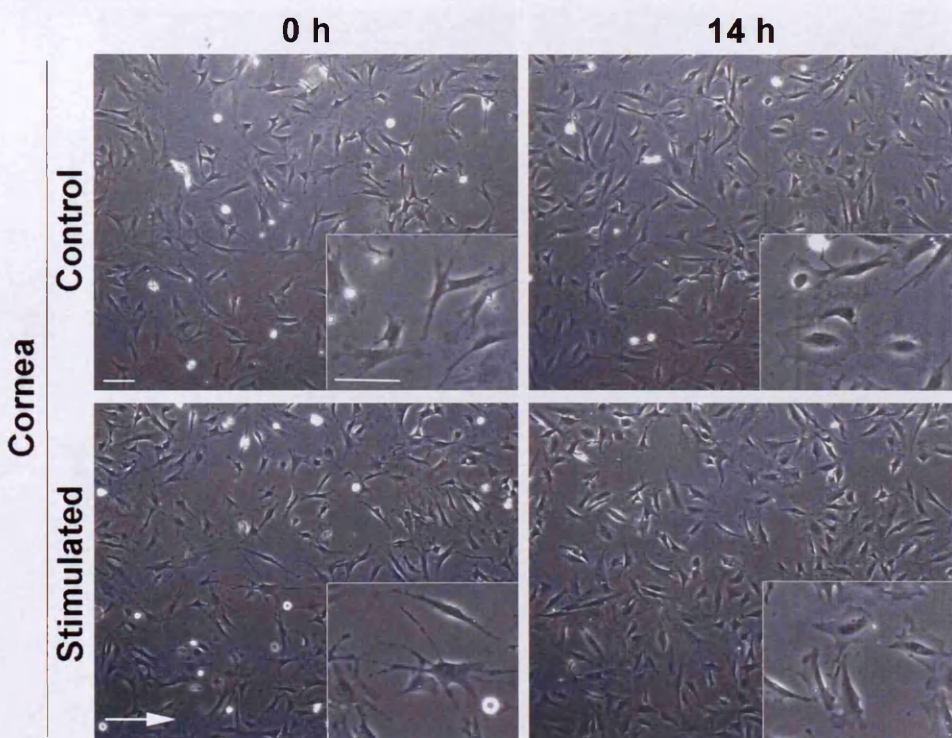
Figure 3.9: Phase contrast images of control and stimulated corneal fibroblasts before (0 h) and after (14 h) being subjected to 0.1 dyn/cm^2 of fluid flow for 14 hours. Arrow indicates direction of flow. Scale bars = 100 μm.

3.2.4.3 Gross morphology of skin fibroblasts

As with tendon and corneal fibroblasts, skin cells prior to simulation demonstrate variable cell size and irregular cell shape (Figure 3.10). In this case, a greater population of rounded cells seems to exist, with a notable number of stellate-shaped cells. On the whole, there are very few elongated, spindle-like cells in this population. The morphology of skin fibroblasts appears to lie somewhere between that demonstrated by tendon and corneal cells; the outline of skin cells is somewhat jagged, and some cells demonstrate the hair-like protrusions mentioned previously (3.2.4.2). Cell morphology seems to become more rounded and flattened in control cells after 14 hours, and there appears to be a slight increase in cell density. As with tendon and corneal fibroblasts,
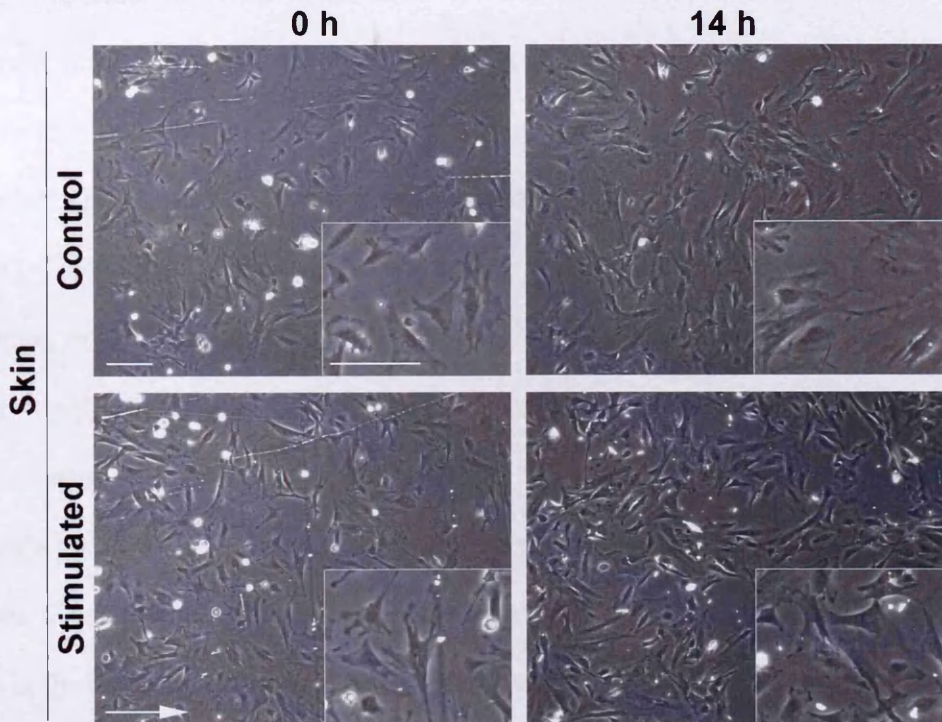
Figure 3.10: Phase contrast images of control and stimulated skin fibroblasts before (0 h) and after (14 h) being subjected to 0.1 dyn/cm^2 of fluid flow for 14 hours. Arrow indicates direction of flow. Scale bars = 100 μm.

there does not seem to be any gross morphological change upon stimulation. There do, however, appear to be confluent regions where cells share similar alignment. This is unlikely to be due to stimulation, however, since alignment does not correlate with the direction of flow and similar regions are also seen in control cells.

3.2.4.4 Effect of stimulation on the actin cytoskeleton

The actin cytoskeleton functions in a wide variety of cellular processes, including movement, shape determination, formation of surface structures, such as filopodia and microvilli, adhesion, and cytokinesis. It is not surprising, then, that organisation of the actin cytoskeleton has been previously shown to alter with fluid shear stress (Davies *et al.*, 1994; McGarry *et al.*, 2005; Pavalko *et al.*, 1998).

In order to visualise the actin cytoskeleton in control and stimulated tendon, corneal and skin fibroblasts, cells were fixed and subsequently stained with rhodamine phalloidin, which allowed for the visualisation of F-actin. Prior to stimulation, all three primary fibroblast cell lines show very prominent, highly organised stress fibres (Figure 3.11). Tendon and corneal fibroblasts appear to demonstrate more intense cortical actin staining as opposed to skin fibroblasts, which have more uniform staining. Somewhat surprisingly, mechanical stimulation does not seem to have an effect on the gross organisation or abundance of stress fibres; in all three cell lines, phalloidin staining reveals prominent, organised stress fibres, very similar to that seen in control cells. In all cases, F-actin stress fibres were oriented roughly parallel to the long axis of the cell, but not in the direction of flow as seen in previous studies (Birukov *et al.*, 2002; Pavalko *et al.*, 1998).
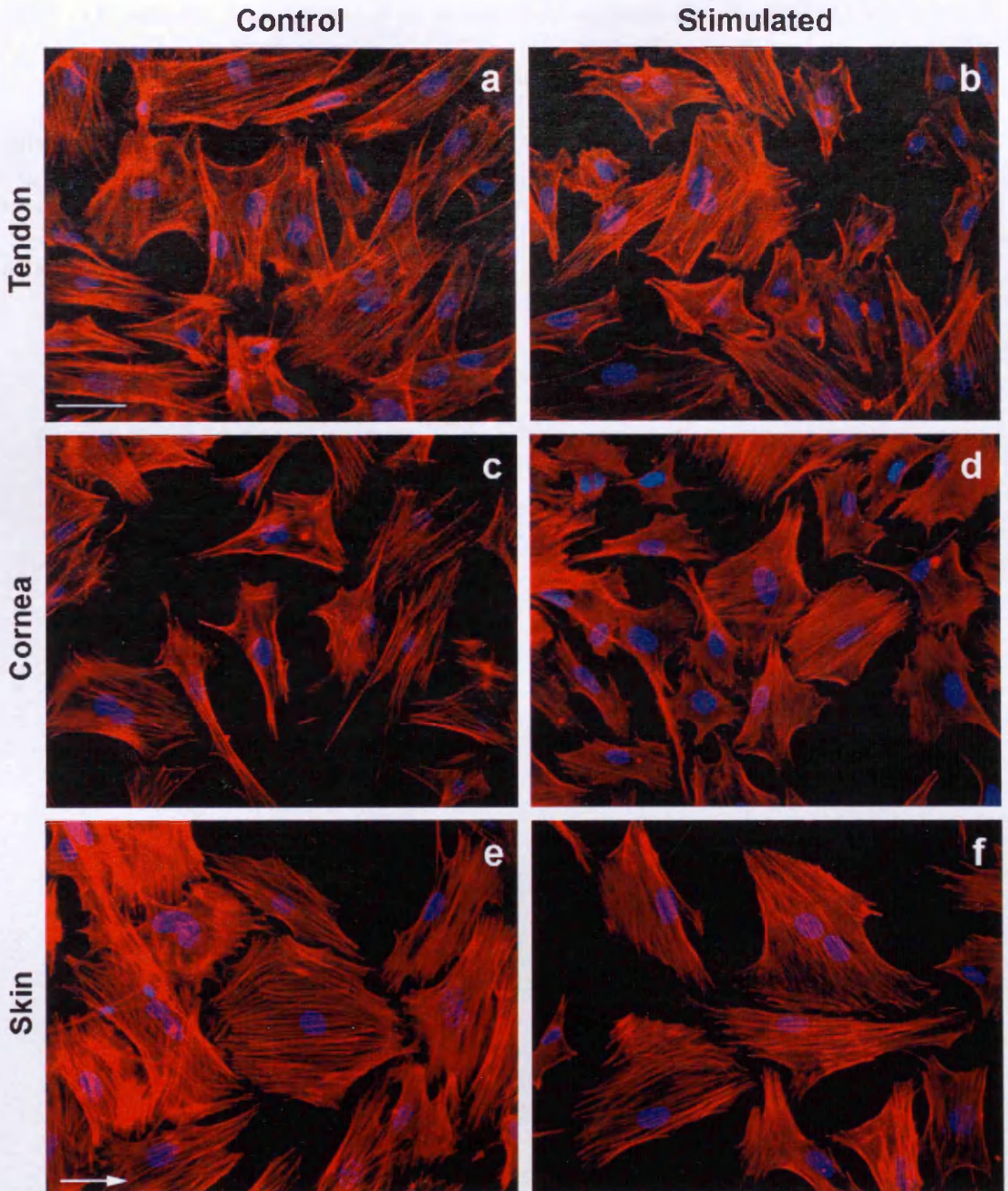
Figure 3.11: Organisation of the actin cytoskeleton in mechanically stimulated tendon, corneal and skin fibroblasts. Cells were seeded onto gelatin-coated glass plates and allowed to adhere for approximately seven hours. Control cells were placed in a single well plate for the duration of the experiment, while stimulated cells were subjected a shear stress of 0.1 dyn/cm^2 for 14 hours. Control (a, c, and e) and stimulated (b, d, and f) fibroblasts were fixed and stained with rhodamine phalloidin and DAPI to visualise F-actin and the nucleus, respectively. Arrow indicates direction of flow. Scale bar = 50 μm.

3.2.5 *Quantitative morphological examination of mechanically stimulated fibroblasts*

In addition to the qualitative assessment of cell morphology in control and stimulated tendon, corneal and skin fibroblasts, several morphological parameters, including multinucleation of cells, proliferation rate, cell area and circularity, and focal adhesion formation, were quantified.
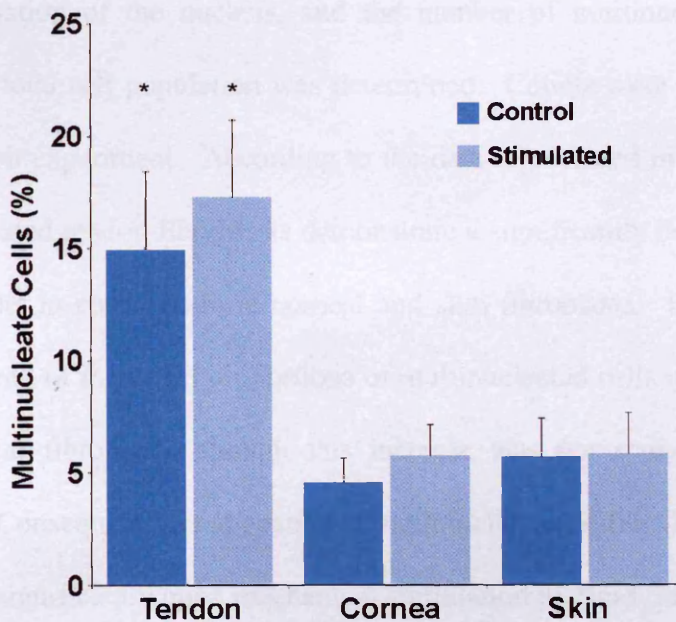
Figure 3.12: Effect of mechanical stimulation on multinucleation of primary fibroblasts. After seeding fibroblasts onto gelatin-coated glass plates and allowing cells to adhere, stimulated cells were subjected to a constant shear stress of 0.1 dyn/cm^2 for 14 hours. Cells were then fixed, stained with DAPI to enable visualisation of the nucleus, and the proportion of multinucleated cells determined. Values are represented as mean percentage of multinucleated cells (±SE). Both control and stimulated tendon fibroblasts contain significantly more multinucleated cells than the other two cell lines. Significant differences between means are indicated. *, $p < 0.01$ (n = 2; for each experiment, approximately 1300 cells were counted per sample).

3.2.5.1 Multinucleation alters with cell type but not with mechanical stimulation in primary fibroblasts

During culture and following stimulation of primary tendon, corneal and skin fibroblasts, it was observed that a notable proportion of cells contained multiple nuclei. Consequently, the multinucleated cell population was quantified, in order to determine if the number altered with cell type or upon the application of mechanical stimulation. To achieve this, control and stimulated fibroblasts were fixed and stained with DAPI to allow for visualisation of the nucleus, and the number of multinucleated cells as a percentage of the total cell population was determined. Counts were obtained after the 14-hour stimulation experiment. According to the data represented in Figure 3.12, both control and stimulated tendon fibroblasts demonstrate a significantly larger proportion of multinucleated cells in comparison to corneal and skin fibroblasts. Furthermore, there appears to be a trend of increased proportions of multinucleated cells with stimulation in tendon and corneal fibroblasts, though this increase was not statistically significant (Students *t*-test). Consequently, it appears that multinucleation differs between cell lines, but does not alter significantly upon mechanical stimulation by fluid flow.

3.2.5.2 Mechanical stimulation does not alter the cell density of primary fibroblasts

The effect of mechanical stimulation by fluid flow on the cell density of tendon, corneal and skin fibroblasts was assessed by observing the change in cell number after the 14-hour stimulation experiment. Live cells were imaged and manually counted before and after stimulation, and the change in cell density determined. According to Figure 3.13, control cells demonstrate approximately 20-30% increases in cell density. Stimulated tendon and skin cells display slightly lower cell numbers, with an approximate 10% increase in cell density. In contrast, corneal fibroblasts demonstrate a

slight reduction in cell density with stimulation. While there appears to be a general trend of a reduction in cell density with stimulation, neither the differences observed between control and stimulated cells, nor the variations between cell lines, are statistically significant.
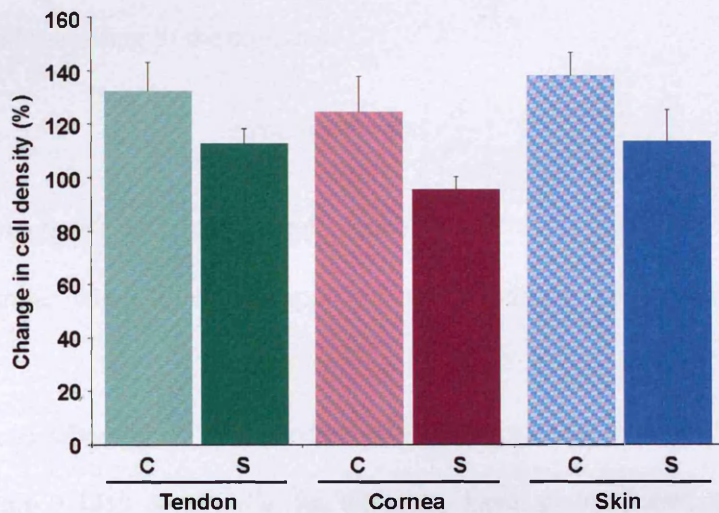
Figure 3.13: Effect of mechanical stimulation on cell density of control (C) and stimulated (S) tendon, corneal and skin fibroblasts. After seeding fibroblasts onto gelatin-coated glass plates and allowing cells to adhere, stimulated cells were subjected to a constant shear stress of 0.1 dyn/cm^2 for 14 hours. Live cells were imaged before and after the stimulation experiment and the change in cell density determined. Values are represented as mean change in cell density (± SE). Differences between means are not significant (Students *t*-test). n = 4, n = 5 and n = 3 for tendon, corneal and skin cell lines, respectively; approximately 1300 cells were counted per sample.

3.2.5.3 Mechanical stimulation does not alter the area but increases the roundedness of

tendon, corneal and skin fibroblasts

Following examination of the effect of stimulation on multinucleation and proliferation rates, changes in cell morphology were also quantified. In order to achieve this, live cells were imaged before and after the stimulation experiment, and various morphological parameters, including cell area and circularity were measured using ImageJ (Abramoff M.D. *et al.*, 2004). As previously stated in section 2.2.7, circularity was calculated according to the equation:

$$circularity = 4\pi\left(\frac{A}{P^2}\right)$$ (1)

where A is area (μm^2) and P is perimeter (μm). A circularity value of 1.0 corresponds to a perfect circle, whereas values approaching 0 indicate an increasingly elongated polygon.

Prior to stimulation, it is evident that the three cell lines are morphologically distinct (Figure 3.14). Skin cells, for example, have a significantly larger area than tendon or corneal fibroblasts. Furthermore, tendon and skin fibroblasts are significantly more rounded as compared to corneal cells. This data is in agreement with the visual, morphological assessment of the three fibroblast cell lines discussed previously (3.2.4.1-3.2.4.3).

Following the 14-hour stimulation experiment, however, it becomes possible to observe differences within and between cell lines, both as a result of mechanical stimulation and also serum deprivation, since the mechanical stimulation medium contains reduced FCS levels. In considering control cells before and after the stimulation experiment, all three cell lines demonstrate an increase in cell area (Figure 3.14). Because this increase is seen in both control and stimulated cells, it is likely to be
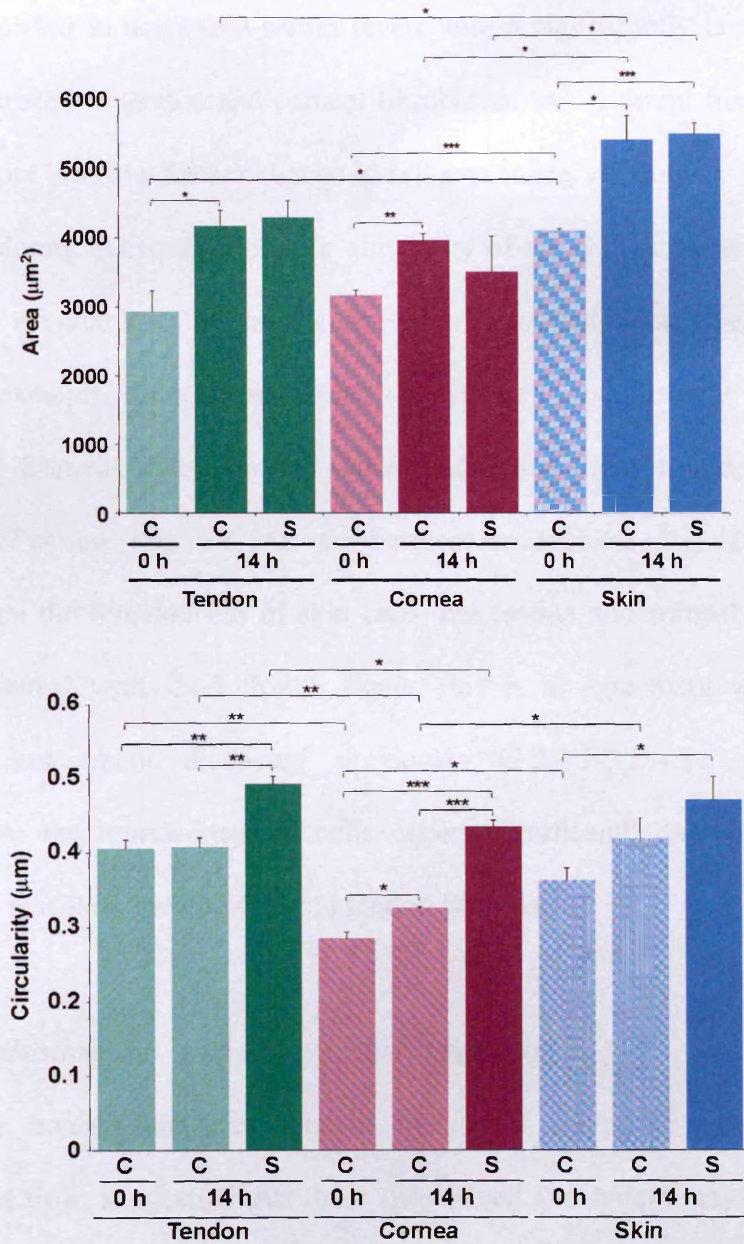
Figure 3.14: Effect of serum levels and mechanical stimulation on the area and circularity of control (C) and stimulated (S) tendon, corneal and skin fibroblasts. Cells were imaged both before (0 h) and after being subjected to a shear stress of 0.1 dyn/cm^2 for 14 hours (14 h). Control cells were maintained in a single well plate for the duration of the experiment. Area and circularity were measured using ImageJ (Abramoff M.D. *et al.*, 2004). Data is represented as mean area or circularity (± SE). Significant differences between means are indicated, as determined by a Students *t*-test. *, $p < 0.05$; **, $p < 0.01$; ***, $p < 0.001$; n = 3 and approximately 200 cells were counted per sample.

a serum deprivation response. Nonetheless, this observation is interesting since skin fibroblasts responded to decreased serum levels with a significantly larger increase in cell size as compared to tendon and corneal fibroblasts. As apparent from Figure 3.14, fluid flow does not induce a further change in cell area in any cell line.

In considering the roundedness or circularity of the cells, it appears that serum-deprivation has a variable effect on the three fibroblast cell lines. Tendon and skin fibroblasts, for example, do not demonstrate any change in roundedness with decreased serum levels. Corneal cells, on the other hand, are more rounded with lower concentrations of serum (Figure 3.14). Furthermore, mechanical stimulation appears to have no effect on the roundedness of skin cells, but tendon and corneal fibroblasts are increasingly rounded with fluid flow. Again, this is in agreement with the visual morphological assessment discussed previously (3.2.4.1-3.2.4.3), which further substantiates that the roundedness of cells differs significantly between tendon and corneal, corneal and skin, but not skin and tendon fibroblasts.

3.2.5.4 Focal adhesions vary with cell type and stimulation

Previous investigators have shown that focal adhesions are remodelled in response to fluid flow, suggesting that these sites of cell attachment may be important in mechanotransduction (Butcher *et al.*, 2004; Haier and Nicolson, 2002). Several "types" of focal adhesions have been identified and can be classified based upon their protein constituents and their size (Wozniak *et al.*, 2004). For the purpose of this study, focal adhesions were classified into three broad types based upon size alone: focal complexes, which are small in size (< 1 μm) and typically exist at the periphery of spreading or migrating cells; focal adhesions, which are "mature" adhesions (> 1 μm) typically found both at the cell periphery and more centrally, associated with the ends of stress fibres;
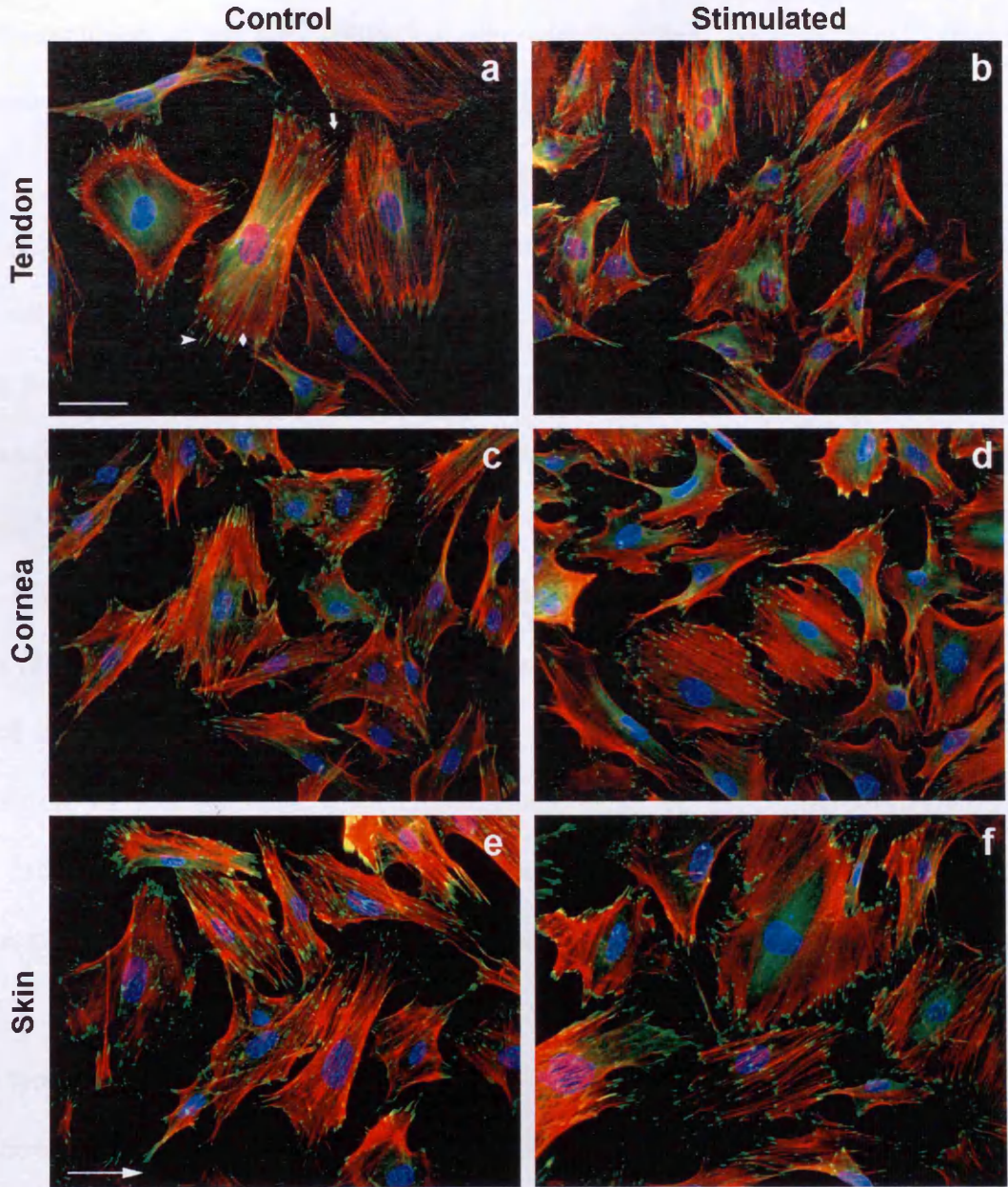
Figure 3.15: Effect of mechanical stimulation on the abundance of focal contacts (arrow), focal adhesions (diamond) and fibrillar adhesions (arrowhead), as shown in (a). Fibroblasts were seeded onto gelatin-coated glass plates and allowed to adhere for approximately seven hours. Control cells were placed in a single well plate for the duration of the experiment (a, c, and e), while stimulated cells were subjected a shear stress of 0.1 dyn/cm^2 for 14 hours (b, d, and f). Control and stimulated fibroblasts were fixed and stained with an anti-vinculin monoclonal antibody (green) and counterstained with rhodamine phalloidin (red) and DAPI (blue) to visualise focal adhesions, F-actin and the nucleus, respectively. Arrow indicates direction of flow. Scale bar = 50 μm. See Figure A (Appendix) for mouse secondary antibody controls.

and fibrillar adhesions, which appear as elongated focal adhesions and are usually found at the periphery of the cell. When not otherwise specified, the term "focal adhesion" refers to focal contacts, focal adhesions and fibrillar adhesions, collectively.

Because of the implication of focal adhesions in mechanotransduction, the effect of cell type and mechanical stimulation on the abundance of focal adhesions in tendon, corneal and skin fibroblasts was investigated. To achieve this, control and stimulated cells were fixed and stained with an antibody directed against vinculin, a universal focal adhesion marker (Figure 3.15). Focal adhesions were then manually quantified using ImageJ (Figure 3.16).

As is apparent from Figure 3.15, both control and stimulated tendon, corneal and skin fibroblasts show abundant focal complexes, focal adhesions and fibrillar adhesions. Focal contacts and fibrillar adhesions appear at the periphery of control and stimulated cells from all three cell lines, whereas focal adhesions appear both at the periphery and in the centre of the cell. In most cases, focal contacts, focal adhesions and fibrillar adhesions associate with the ends of stress fibres.

From visual inspection alone, however, it is difficult to ascertain if stimulation or cell type impacts the abundance of focal adhesions. Consequently, the number of focal contacts, focal adhesions and fibrillar adhesions present on sub-confluent cells was determined manually, by counting the focal adhesions present in sub-confluent control and stimulated cells. According to Figure 3.16, mechanical stimulation does not appear to have an effect on the number of focal adhesions per cell in tendon and skin fibroblasts. By contrast, corneal fibroblasts show a marked increase in the abundance of focal adhesions with stimulation. Interestingly, there is also a significant difference in the number of focal adhesions per cell between the three cell lines. Control tendon cells demonstrate increased numbers of focal adhesions per cell when compared to corneal
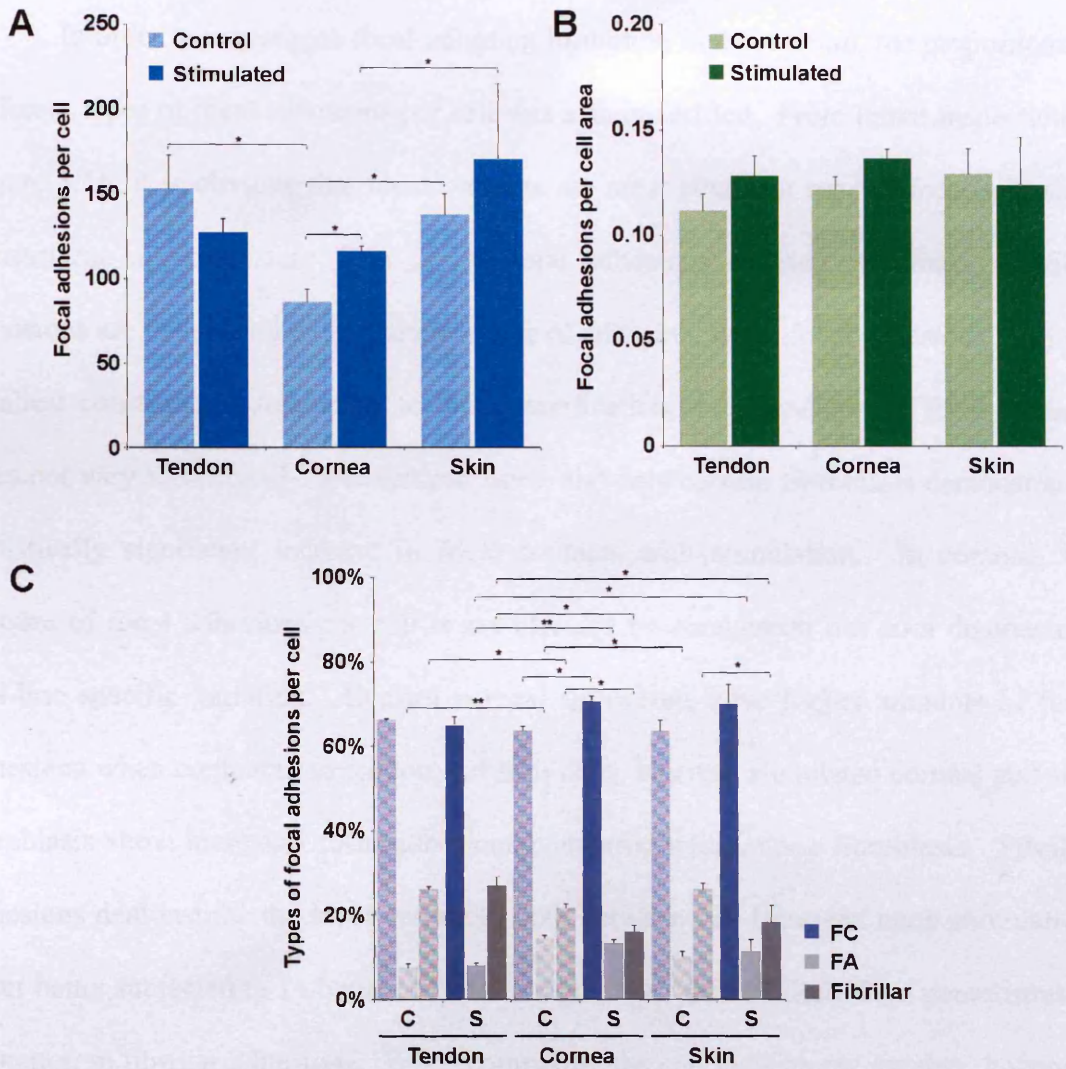
Figure 3.16: Total number and classification of focal adhesions in control and stimulated tendon, corneal and skin fibroblasts. Fibroblasts were seeded onto gelatin-coated glass plates and allowed to adhere for approximately seven hours. Control cells were placed in a single well plate for the duration of the experiment, while stimulated cells were subjected a shear stress of 0.1 dyn/cm^2 for 14 hours. Control and stimulated fibroblasts were stained with an anti-vinculin monoclonal antibody and focal contacts (FC; $< 1 \mu m^2$), focal adhesions (FA; $>1 \mu m^2$) and fibrillar adhesions (Fibrillar; $> 1 \mu m$ in length) were counted. Data is represented as the mean number of focal adhesions per cell (A), mean number of focal adhesions per cell area (B), and percent composition of the different types of focal adhesions per cell (C) ($\pm$ SE). Means that differ significantly are indicated. *, $p < 0.05$; **, $p < 0.01$; ***, $p < 0.001$; n= 3 and the focal adhesions in 20 cells were measured for each sample.

fibroblasts, while both control and stimulated skin fibroblasts display increased numbers of focal adhesions when compared to corneal fibroblasts.

In order to investigate focal adhesion formation in more detail, the proportions of different types of focal adhesions per cell was also quantified. From initial inspection of Figure 3.16, it is obvious that focal contacts are most abundant type of focal adhesion, constituting approximately 70% of the total adhesions in each cell line. Fibrillar adhesions are the second most abundant type of adhesion, while focal adhesions form the smallest constituent. According to this quantification, the abundance of focal contacts does not vary significantly between cell lines, and only corneal fibroblasts demonstrate a statistically significant increase in focal contacts with stimulation. In contrast, the amount of focal adhesions per cell is not affected by stimulation but does demonstrate cell-line specific variation. Control corneal fibroblasts have higher amounts of focal adhesions when compared to tendon and skin cells, whereas stimulated corneal and skin fibroblasts show increased focal adhesions compared with tendon fibroblasts. Fibrillar adhesions demonstrate the most variation, both between cell lines and upon stimulation. After being subjected to 14 hours of laminar fluid flow, corneal fibroblasts demonstrate a reduction in fibrillar adhesions. When comparing the cell lines to one another, however, it is apparent that control and stimulated tendon fibroblasts have larger numbers of fibrillar adhesions in comparison to control and stimulated corneal and skin cells.

3.2.6   *Gelatinase activity increases with mechanical stimulation in primary fibroblasts*

In addition to morphological changes discussed above, matrix metalloproteinase activity has also been shown to alter with mechanical stimulation in a variety of cell types (Archambault *et al.*, 2002b; Blain *et al.*, 2001; Prajapati *et al.*, 2000a; Lambert *et al.*, 2001). Consequently, the effect of shear stress on gelatinase (MMP-2, MMP-9)
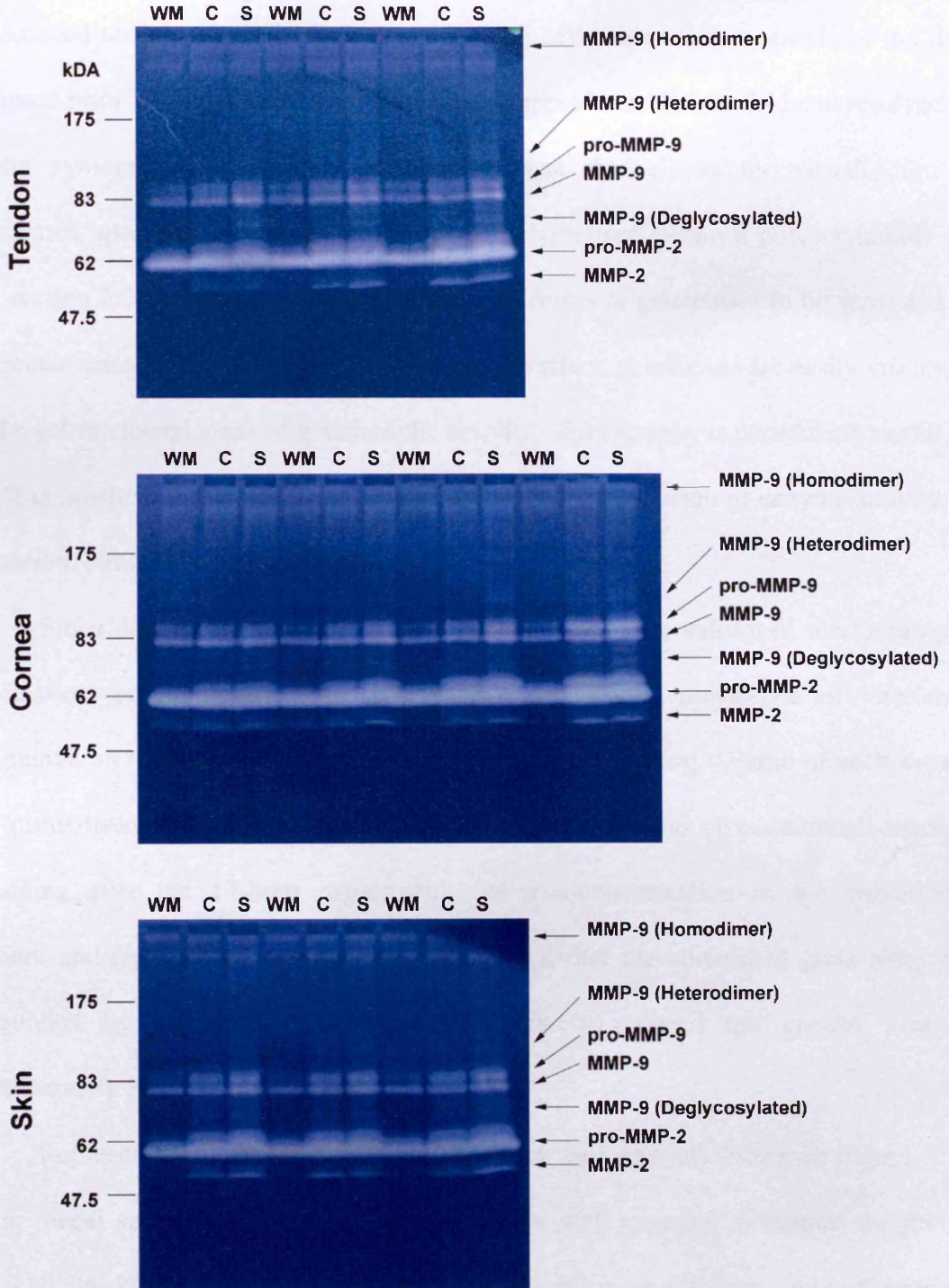
Figure 3.17: Detection of MMP-2 and MMP-9 activity by gelatin zymography. Samples of conditioned medium from control (C) and stimulated (S) tendon, corneal and skin fibroblasts were resolved on 7.5-15% gradient gelatin zymograms. A sample of mechanical stimulation medium (WM) was also resolved to indicate background levels of gelatinase activity. Tendon and skin zymograms contain WM, C and S samples from three replicate experiments, while the corneal zymogram contains samples from four replicate experiments.

activity in tendon, corneal and skin fibroblasts was investigated. To achieve this, conditioned medium from control and stimulated cells, as well as a sample of the flow perfusate prior to stimulation, was concentrated approximately two-fold and resolved by gelatin zymography, an electrophoretic technique that allows the visualisation of gelatinases upon their digestion of gelatin co-polymerised within a polyacrylamide gel (see section 2.2.12). Zymograms allow multiple forms of gelatinases to be separated by molecular mass and, after incubation in suitable buffers, gelatinases are easily visualised on the gel as cleared areas of gelatinolytic activity. Zymography is particularly useful, in that it is sensitive to picomolar range and allows the visualisation of enzyme activity, as opposed to straightforward quantification.

Since determination of the protein concentration of conditioned media samples by classical protein assays was not possible due to the prevalence of interfering compounds in the mechanical stimulation medium, the loading volume of each sample was normalised according to several factors: (1) the volume of conditioned medium remaining after the 14-hour experiment, (2) fold-concentration of the conditioned medium and (3) differences in growth area, given that the stimulated glass plate was surrounded by a Teflon gasket which effectively reduced the growth area by approximately 20 cm^2 (as described in 2.2.13).

Representative gelatin zymograms for each cell line are shown in Figure 3.17, which reveal seven prominent gelatinolytic bands with apparent molecular weights of 227, 120, 96, 83, 79, 64 and 54 kDa under non-denaturing conditions. According to the literature, the five highest molecular weight species correspond to different forms of MMP-9. The 227 kDa species corresponds to an MMP-9 homodimer, while the 120 kDa species most likely corresponds to a MMP-9 heterodimer, where the enzyme is complexed with a TIMP or the neutrophil gelatinase B-associated lipocalin (NGAL)
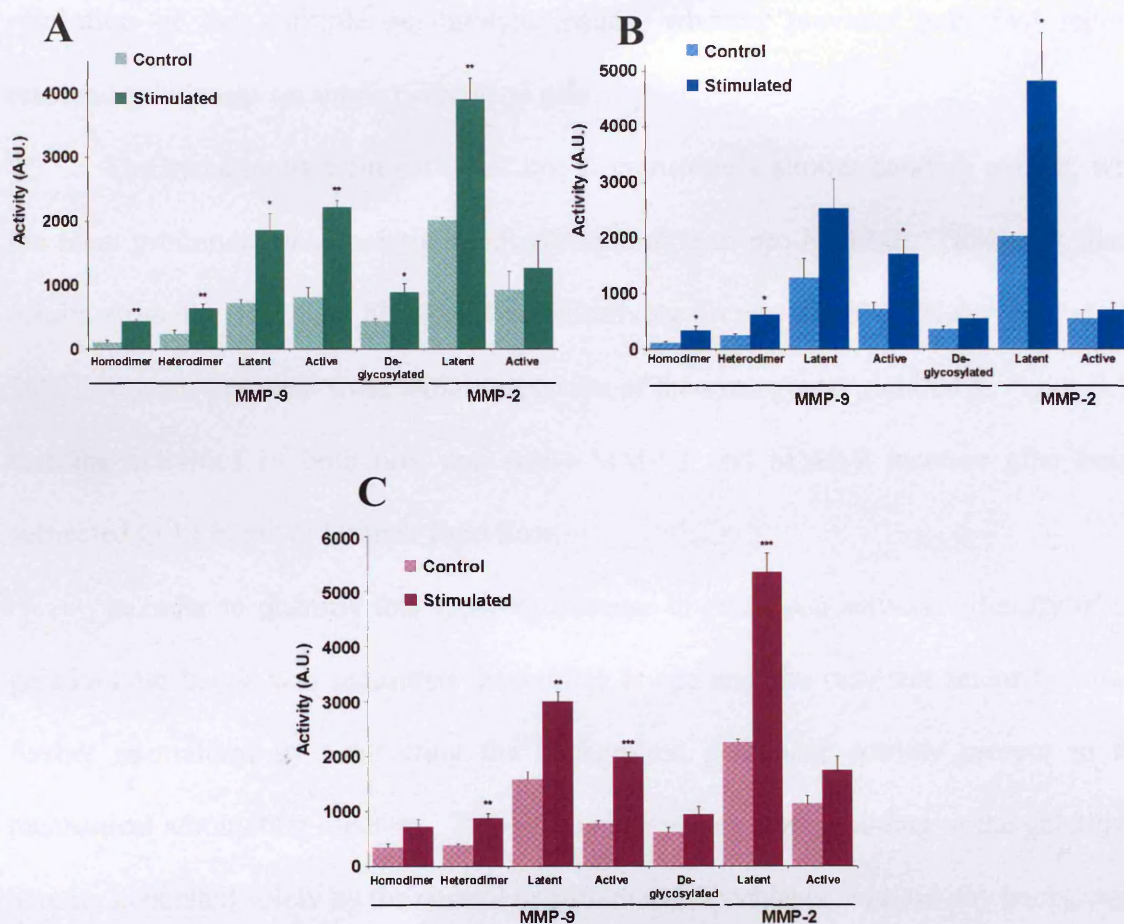
Figure 3.18: Quantification of gelatinase activity in control and stimulated tendon (A), corneal (B) and skin (C) fibroblasts. Data is represented as mean activity (± SE). Means that differ significantly are indicated. *, $p < 0.05$; **, $p < 0.01$; ***, $p < 0.001$; n = 3 for tendon and skin cells; n = 4 for corneal fibroblasts.

(Waas *et al.*, 2002; Rudd *et al.*, 1999). The pro and active forms of MMP-9 have an apparent molecular weight of 94 and 83 kDa, respectively, which is agreement with previous reports (Waas *et al.*, 2002; Zhao *et al.*, 2003). The additional MMP-9 species with a molecular weight of approximately 120 kDa most likely corresponds to a deglycosylated form (Fiore *et al.*, 2002). The two remaining bands, with molecular weights of 64 and 54 kDa, correspond to pro- and active-MMP-2. The molecular weights of these MMP-2 species are approximately 10 kDa lower than that previously

reported (Waas *et al.*, 2002). This discrepancy most likely arises from the fact that samples in this study were resolved on 7.5-15% gradient zymograms in order to increase resolution of the multiple gelatinolytic bands, whereas previous published reports resolved gelatinases on single percentage gels.

The zymograms from each cell line demonstrate a similar banding pattern, with the most prominent gelatinolytic band corresponding to pro-MMP-2. This most likely results from the fact that fibroblasts constitutively secrete MMP-2 (Kobayashi *et al.*, 2003). It is also evident from initial inspection of the zymograms pictured in Figure 3.17 that the activities of both pro- and active-MMP-2 and MMP-9 increase after being subjected to 14 hours of laminar fluid flow.

In order to quantify this apparent increase in gelatinase activity, intensity of the gelatinolytic bands was measured using NIH Image and the resultant intensity values further normalised by subtracting the background gelatinase activity present in the mechanical stimulation medium. This resulted in values corresponding to the gelatinase activity generated solely by the control or stimulated fibroblasts, without any background contribution from the flow perfusate (Figure 3.18). According to Figure 3.18, all cell lines demonstrate the up-regulation of gelatinase activity with stimulation. In order to directly compare the gelatinase activity of tendon, corneal and skin fibroblasts, however, data were further normalised to a gelatinase standard (Figure 3.19).

Upon initial inspection, it appears that skin fibroblasts typically demonstrate the highest gelatinase activity. This tendency appears to be conserved in most cases; the highest gelatinase activity is exhibited by skin fibroblasts, followed by tendon and then skin cell lines. The only exception to this otherwise conserved trend is in respect to the active form of MMP-9, in which tendon fibroblast gelatinase activity supersedes that exhibited by skin cells. While these data indicate that all three cell lines generate similar
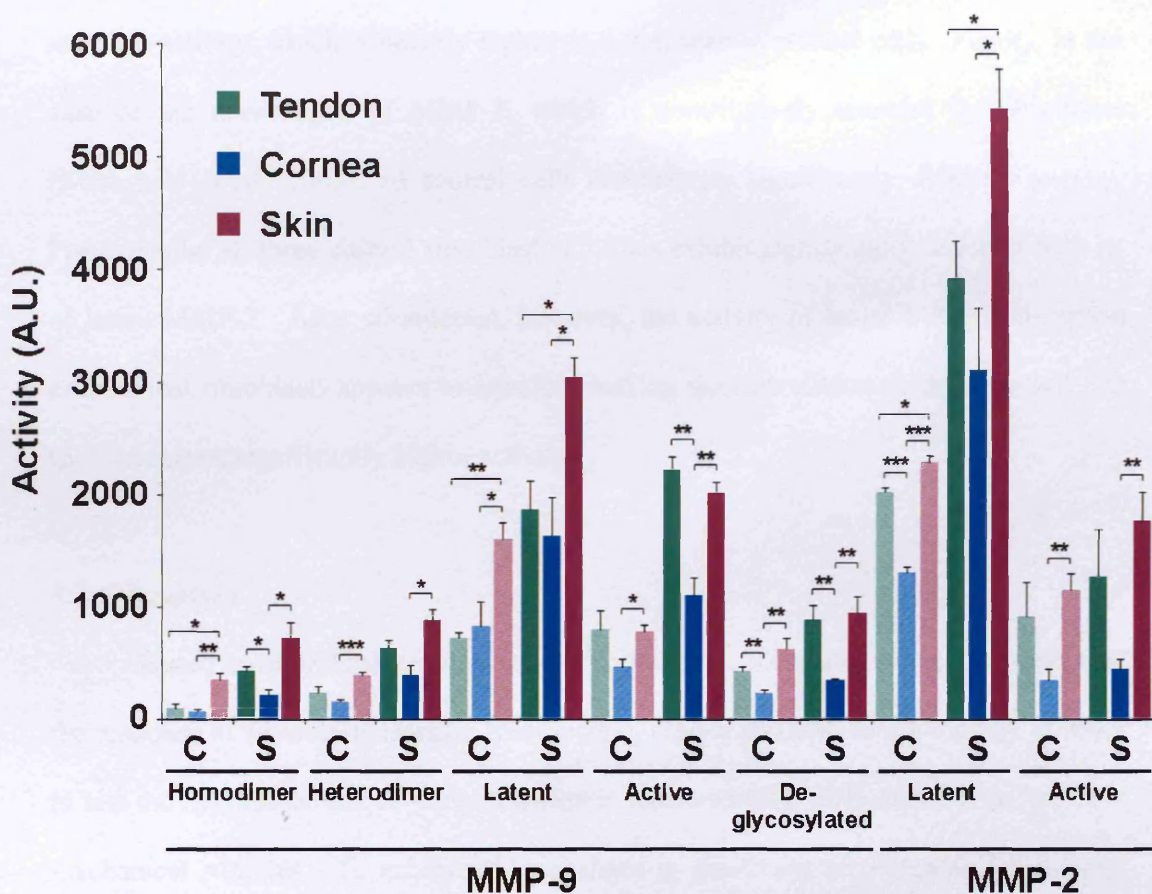
Figure 3.19: Direct comparison of gelatinase activity in mechanically stimulated tendon, corneal and skin fibroblasts. MMP activity visualised on gelatin zymograms was normalised to a gelatinase standard to enable direct comparison of gelatinase activity in the three cell lines; data are represented as normalised mean activity ($\pm$ SE). Statistically significant differences between means are indicated. *, $p < 0.05$, **; $p < 0.01$; ***, $p < 0.001$; n = 3 for tendon and skin cells; n = 4 for corneal fibroblasts.

increases in gelatinase activity in response to stimulation, there exist significant tissue-specific differences in the magnitude of this response. In the case of the homodimer of MMP-9, for example, control skin fibroblasts demonstrate higher activity than tendon or corneal cells, while stimulation results in both tendon and skin fibroblasts having higher activity than corneal cells. Similarly, both control and stimulated skin fibroblasts demonstrate increased activity of the heterodimer and latent forms of MMP-9, as well as active-MMP-2. When the active or glycosylated forms of MMP-9 are considered,

however, both control and stimulated tendon and skin fibroblasts display virtually identical activity, which is notably higher than that seen in corneal cells. Finally, in the case of the latent form of MMP-2, which is constitutively secreted by fibroblasts (Kobayashi *et al.*, 2003), all control cells demonstrate significantly different activity. For example, all three control fibroblast cell lines exhibit significantly different activity of latent MMP-2. After stimulation, however, the activity of latent MMP-2 in tendon and corneal fibroblasts appears to equalise, leaving skin fibroblasts as the only cell line to demonstrate significantly higher activity.

3.3 Discussion

Based upon preliminary data and evidence in the literature, we have investigated the response of fibroblasts isolated from tendon, cornea and skin to shear stress in order to test the hypothesis that fibroblasts maintain tissue-specific differences to an identical mechanical stimulus. To achieve this, changes in gelatinase activity and morphology were assessed qualitatively and quantitatively, including cell shape and size, multinucleation, proliferation rates, organisation of the actin cytoskeleton and abundance and organisation of focal adhesions.

Prior to stimulation, three fibroblast cell lines were isolated from tendon, cornea and skin. These connective tissues, in particular, were chosen because each demonstrate somewhat striking differences in the organisation of their ECM; tendon and corneal connective tissues both possess highly organised ECMs, while skin demonstrates a more disordered extracellular milieu (see sections 1.7.1-1.7.3). While, to date, there are no universal markers for fibroblasts, each of the three cell lines was shown to possess vimentin, an intermediate filament protein previously identified as being prevalent in mesenchymal cells (Osborn and Weber, 1982). Furthermore, the isolated cell lines were

shown to be free of contamination by muscle and/or epithelial cells since they did not contain intermediate filament proteins prevalent in these cell types, namely desmin and keratin. Together, the presence of vimentin, absence of desmin and keratin, and the typical fibroblast morphology demonstrated by the cell lines was indicative that the isolated cells were, indeed, fibroblasts.

Fibroblasts have been previously shown to demonstrate unique morphologies based upon their tissue location (see Table 3.1). In order to investigate this further, the present study examined the gross morphology of tendon, corneal and skin fibroblasts in cells subjected to a shear stress of 0.1 dyn/cm^2 and in static, no flow controls. Upon visual inspection, there appeared to be discrete differences between the three primary cell lines, which correlated with subsequent morphological quantification (Figures 3.8-3.10, 3.14). In particular, tendon fibroblasts displayed both elongated, spindle-like cells as well as a distinct population of more rounded cells. Upon stimulation, the number of cells demonstrating a more rounded morphology increased (Figures 3.8 and 3.14). Corneal fibroblasts, on the other hand, displayed a more jagged appearance, with more elongated cells containing long, hair-like protrusions. This observation was concurrent with a markedly reduced circularity index when corneal fibroblasts were compared with tendon or skin cells (Figures 3.9 and 3.14). After stimulation, the jagged morphology was reduced, leaving cells with a more rounded appearance. Finally, skin fibroblasts were unique, in that prior to stimulation, regions of the monolayer appeared to be arranged in somewhat parallel arrays and individual cells were significantly larger in area than the other two cell lines (Figures 3.10 and 3.14). Following stimulation, this increase in area became even more exaggerated. Because this increase in area was seen in both control and stimulated skin fibroblasts, it was most likely a consequence of reduced serum levels in the flow perfusate and not a direct response to stimulation.

Interestingly, skin fibroblasts did not become significantly more rounded with stimulation, a trend exhibited by both tendon and corneal cells. Perhaps this is a consequence of pre-stimulated skin fibroblasts demonstrating an inherently more rounded morphology.

While fibroblasts from tendon, cornea and skin have never been directly compared prior to this study, there are instances in the literature where the morphology of these cell types has been investigated. For example, the elongated morphology demonstrated by corneal fibroblasts in this investigation was observed previously when corneal fibroblasts were compared to those derived from heart and skin (Conrad *et al.*, 1977b). In the same study, Conrad *et al.* reported the alignment of confluent skin fibroblasts in parallel arrays, a tendency which was observed in sub-confluent skin cells (*ibid.*). Furthermore, distinct morphological populations of tendon fibroblasts have been discussed previously in the literature (Banes *et al.*, 1988a). The tendon fibroblasts in the present study appeared to consist of two discrete populations of cells, one that was more elongated and another that was more rounded in appearance. This fibroblast heterogeneity has been reported previously by Banes *et al.* when comparing fibroblasts isolated from internal and external (synovial) regions of the tendon. After isolation and culture, synovial tendon cells appeared as large, round cells with ruffling plasma membranes, whereas internal fibroblasts were smaller, more fusiform cells (Banes *et al.*, 1988a). It is possible that, since the isolation protocol used in this study did not distinguish between the discrete locations of fibroblasts within tendon, the tendon cells used in the present work contain both synovial and internal tendon fibroblasts.

All three cell lines appeared to contain roughly two populations of cells – one composed of smaller, spindle- or stellate-shaped cells and another consisting of larger, more rounded cells – though this was most obvious in tendon cells. Fibroblast

subpopulations have been reported previously and were characterised by Bayreuther and colleagues (Bayreuther *et al.*, 1988). According to their observations, fibroblasts exist as two distinct populations in culture: a mitotic, metabolically active population and a metabolically inactive, post-mitotic population, with the post-mitotic population becoming more prevalent with increasing age in culture. While the metabolism of the fibroblasts isolated in this study was not investigated directly, there appear to be distinct similarities in the gross morphology of the cell lines cultured here and those described by Bayreuther and colleagues. For example, pre-stimulated tendon, corneal and skin fibroblasts were seen to be composed of small spindle-like cells, stellate-like cells and slightly larger, more rounded cells (Figure 3.1, 3.8-3.10). These morphologies appear to correspond to the three cell types that predominantly comprise the mitotic fibroblast population, as classified by Bayreuther and colleagues (Bayreuther *et al.*, 1988). After culturing cells in decreased serum, however, there was a significant increase in the area of tendon, corneal and skin fibroblasts, and stimulation resulted in progressively more rounded fibroblasts. These morphologies, which appeared after serum deprivation and stimulation, closely resemble the large, spindle-like and epithelioid cells that Bayreuther *et al.* described as the post-mitotic fibroblast population.

The presence of these so-called mitotic and post-mitotic fibroblast populations was suggested by Bayreuther and colleagues to represent differentiating cell compartments along a terminal stem-cell-like fibroblast lineage (Bayreuther *et al.*, 1988). However, it is not clear from this study whether such fibroblast populations arise from true cell differentiation or an artefact of cell senescence induced by serum withdrawl. Since the prevalence of the larger post-mitotic cells increases with cumulative population doublings, the latter seems very likely. Nonetheless, the presence of these two distinct morphologies in the present study suggests that (1) the smaller spindle-like or stellate

fibroblasts used in the present work are predominantly metabolically active, mitotic, "young" cells and (2) serum deprivation and/or mechanical stimulation appears to increase the prevalence of the metabolically inactive, post-mitotic cell population, suggesting that fibroblasts are "differentiating" along the aforementioned fibroblast lineage and/or increasing senescent behaviour. The possibility that serum deprivation and/or mechanical stimulation can drive cell differentiation or accelerate cell senescence warrants further investigation.

In addition to the size and shape of the cells, there were other morphological differences which distinguished tendon, corneal and skin fibroblasts from one another. Tendon cells, for example, were shown to contain significantly higher numbers of multinucleated cells than the other two cell lines. Multinucleation has been found to be indicative of cell senescence, immortalisation, growth suppression, or serum deprivation. Because the cell lines used in this study were only cultured until passage number five, it is highly unlikely that multinucleation was a result of immortalisation. Furthermore, given that the proliferation rate of the cells does not differ significantly between control and stimulated (Figure 3.13), multinucleation is not likely to be due to suppression of cell growth. Consequently, the presence of multiple nuclei in tendon fibroblasts seen in this study is most likely a result of cell senescence induced by serum deprivation. Nonetheless, tendon fibroblasts responded to this deprivation with a marked increase in multinucleated cells when compared to corneal or skin fibroblasts, which further substantiates the differentiative capacity of fibroblasts isolated from different tissues.

Focal adhesions, the cell-matrix interactions that function in mechanotransduction, migration, and maintenance of cell morphology (Beningo *et al.*, 2001), were also shown to differ in control and stimulated tendon, corneal and skin fibroblasts. Such differences in the abundance of focal adhesions were difficult to

determine by microsope, however, since all three cell lines were observed to contain prominent focal adhesions (Figure 3.15). The fact that focal adhesions did not become more prominent nor display re-orientation with the direction of flow was somewhat surprising, given that local forces have been shown to correlate with the orientation, total fluorescence intensity and area of focal adhesions in previous investigations (Balaban *et al.*, 2001; Butcher *et al.*, 2004; Fini *et al.*, 1995; Haier and Nicolson, 2002). However, such studies have largely centred upon endothelial cells, since this cell type is routinely subjected to fluid flow *in vivo*. Perhaps the lack of gross focal adhesion reorganisation in this study is a consequence of unique cell type specific responses to shear stress.

While focal adhesions did not appear to re-orient with fluid flow, quantification revealed that the abundance of focal adhesions, as a whole, differed both amongst cell lines and with stimulation. Corneal fibroblasts, for example, demonstrated significantly fewer focal adhesions per cell when compared to tendon and skin fibroblasts and were the only cell line to exhibit an increase in the abundance of focal adhesions with stimulation (Figure 3.16). As mentioned previously, corneal fibroblasts were also the only cell line to demonstrate a reduction in cell number after stimulation. Perhaps this observation is a consequence of the reduced number of focal adhesions available to "anchor" corneal fibroblasts to the substrate during stimulation, thus resulting in a small proportion of cells being washed off the substrate.

In addition to the abundance of focal adhesions as a whole, the effect of stimulation on the specific types of focal adhesions was also examined. Small, dot-like focal contacts were the most abundant type of focal adhesion in all three cell lines, though the prevalence of these did not appear to vary significantly between cell lines and only corneal fibroblasts demonstrated an increase in focal contacts with stimulation (Figure 3.16). Elongated, fibrillar adhesions were the second most prominent type of

focal adhesion in all three cell lines and were found to vary significantly between cell lines and upon stimulation. Tendon fibroblasts, for example, demonstrated significantly more fibrillar adhesions when compared to corneal and skin fibroblasts, but was the only cell line that did not demonstrate a reduction in the abundance of fibrillar adhesions with stimulation. This reduction in elongated, fibrillar adhesions seems counter-intuitive, since cells subjected to a steady shear stress for 14 hours would presumably require additional larger, robust adhesions to act as "anchors" to the substrate.

However, previous studies have reported that the tractional force generated by adhesions at the leading edge of the cell is not directly related to the size of the adhesion (Beningo *et al.*, 2001; Geiger and Bershadsky, 2001). Beningo *et al.*, for example, demonstrated that focal contacts transmitted the largest forces in fish scale fibroblasts, and as focal contacts either disassembled or matured into larger adhesions, their traction stress decreased. Furthermore, mature focal adhesions were found to exert only resistive forces against forward migration and thus appear to function primarily as persistent anchors to the substrate. In the present study, the decrease in fibrillar adhesions in corneal and skin fibroblasts occurred with a concomitant increase in the abundance of focal contacts. Perhaps these two cell lines responded to fluid flow by generating focal contacts, which are capable of increased tractional forces in order to anchor them more securely to the substrate. This trend was not seen in tendon fibroblast, which further substantiates that fibroblasts isolated from distinct tissues respond to shear stress in unique ways.

The present study did not reveal any gross re-alignment of fibroblasts with fluid flow (Figures 3.5, 3.8-3.10), nor significant re-organisation of the actin cytoskeleton (Figure 3.11). This is in contrast to other mechanically stimulated cell lines: smooth muscle cells have been shown to re-align when the flexible substrate on which they are

grown is stretched (Hayakawa *et al.*, 2001); actin stress fibre formation has been reported to increase in endothelial cells subjected to fluid flow (Birukov *et al.*, 2002); and osteoblasts subjected to fluid shear demonstrate more prominent stress fibres when compared to static controls (Pavalko *et al.*, 1998). While alignment and/or reinforcement of the cell cytoskeleton in the direction of fluid flow seems somewhat intuitive, such behaviour has only rarely been demonstrated in fibroblasts (Archambault *et al.*, 2002b). There have been numerous instances, however, of fibroblasts aligning in response to mechanical strain, for example when the substrate onto which the cells are cultured is subjected to uniaxial stretching (Lee *et al.*, 2005; Neidlinger-Wilke *et al.*, 2002; Wang *et al.*, 2004a). In these cases, cytoskeletal reorganisation was observed within minutes, and reorientation of the cells in the direction of strain occurred within two to three hours (Neidlinger-Wilke *et al.*, 2002). Given that the cells in the present study were subjected to shear stress for 14 hours, cells would have had sufficient time to demonstrate reorganisation of the cytoskeleton and/or alignment in the direction of flow. The fact that such responses were not observed here suggests that fibroblasts elicit distinct cellular responses based upon the type of exogenous mechanical stimulation. Furthermore, it is important to note that the fluid flow-induced responses reported previously have been found to vary significantly with species, cell type, flow type and flow medium (Table 3.2).

Fibroblasts are capable of producing and secreting numerous proteolytic enzymes, including MMPs, which enable these cells to maintain and remodel their surrounding ECM in response to exogenous and endogenous biochemical, mechanical and topographical cues (Birkedal-Hansen *et al.*, 1976). Previous reports have shown that the amount and activity of MMPs secreted by fibroblasts alters with mechanical stimulation; moreover, this response has been found to be highly variable, and dependent

upon cell type as well as the method of mechanical stimulation. For example, tendon fibroblasts have been shown to increase expression of MMP-1 and MMP-3 in response to fluid flow (Archambault *et al.*, 2002b). By contrast, chondrocytes subjected to flow shear demonstrated decreased protein levels and activity of MMP-1 and MMP-13 (Yokota *et al.*, 2003). Furthermore, MMP-2 and MMP-9 were both found to increase with mechanical loading in fibroblasts (Prajapati *et al.*, 2000a) and in articular cartilage (Blain *et al.*, 2001). Here, the activity of MMP-2 and MMP-9 was shown to increase in tendon, corneal and skin fibroblasts upon mechanical stimulation by fluid flow (Figure 3.18). Interestingly, the magnitude of increase was shown to be cell line-dependent, with gelatinase activity, in general, being highest in skin fibroblasts and lowest in corneal cells (Figure 3.19). Perhaps the increase in gelatinase activity was generated by the fibroblast cell lines to counteract the effects of fluid flow. For example, increased activity in MMP-2 and MMP-9 could allow for increased degradation and turnover of the gelatin-coated substrate; fibroblasts could then secrete differential matrix macromolecules which could better "protect" them from shear stress and/or anchor them to the substrate more efficiently.

In summary, the data presented in this chapter clearly demonstrate that tendon, corneal and skin fibroblasts are morphologically distinct and respond in unique ways to both serum deprivation and an identical mechanical stimulus. Prior to stimulation, it was shown that the three cell lines were morphologically distinct, for example as determined by overall cell shape and multinucleation. Following stimulation, cells demonstrated specific changes in morphology, focal adhesion formation and gelatinase activity. Together, these data provide compelling evidence that fibroblasts isolated from distinct tissues are unique.

CHAPTER 4

Chapter 4

Mechanical stimulation alters mRNA and protein levels in fibroblasts

4.1 Introduction

From the data presented in Chapter 3, it is apparent that mechanical stimulation by shear stress induces morphological and biochemical alterations in tendon, corneal and skin fibroblasts. Furthermore, the response of these cells to fluid flow appears to be distinct based upon their tissue of localization. These investigations were subsequently carried further, upon analysis of mRNA expression levels, which were analysed in order to reveal the molecular mechanisms responsible for the tissue-specific responses of tendon, corneal and skin fibroblasts to an identical mechanical stimulus. Despite the fact that classical methods, such as RT-PCR and northern blotting, are reliable, they are time-consuming and, due to inherent experimental limitations, only allow the investigation of several genes in parallel. Differential display has also been employed in recent years to identify numerous differentially regulated genes in response to a given treatment, but the quantification of results gathered in this manner is difficult and the probability of false positives is undesirably high (Locklin *et al.*, 2001). Consequently, this study employed Affymetrix GeneChip probe arrays, in order to simultaneously quantify the expression of 34,000 genes in parallel. Gene chips offer an advantage over typical microarray analysis because each array contains multiple probe-sets, and hence offers multiple, independent measurements for a given transcript (Schena *et al.*, 1998). Semi-quantitative RT-PCR and Western blotting subsequently validated gene expression data.

While obtaining genetic expression information is important, it appears that such results only provide a correlative understanding of cellular responses to external stimuli. In order to understand the causative relationship between stimulation and cell behaviour, protein expression must also be investigated. This is due to the fact that, typically, only

minimal correlations have been found between mRNA and protein expression levels (Lichtinghagen *et al.*, 2002). This most likely results from (1) the possibility of regulating protein levels at either transcriptional or translational levels, and/or (2) the rate of protein turnover *in vivo* (Greenbaum *et al.*, 2003). In order to further extrapolate the gene expression data, this study has investigated the level of protein expression of several genes initially identified by microarray analysis as being differentially regulated with stimulation.

Data presented in the following chapter illustrate that gene expression alters in tendon, corneal and skin fibroblasts following 14 hours of shear stress. While the cell lines show some similarities in their response, they also clearly maintain tissue-specific genetic responses, which are functionally diverse and both up- and down-regulated with mechanical stimulation. In addition, this chapter details the validation of microarray data using both semi-quantitative RT-PCR and Western blotting, and reveals that protein levels also changed with stimulation, though their expression did not necessarily correlate with mRNA levels.

4.2 Results

4.2.1 Tendon, corneal and skin fibroblasts demonstrate differential gene regulation when subjected to an identical mechanical stimulus

In order to analyse comprehensively the genetic responses of tendon, corneal and skin fibroblasts to mechanical stimulation, gene regulation was examined in treated and non-treated cells by microarray analysis. Prior to this analysis, the three primary cell lines were subcultured until passage number five, seeded onto gelatin-coated glass plates, and were either subjected to 0.1 dyn/cm^2 of linear fluid flow for 14 hours (treated), or maintained under standard tissue culture conditions (non-treated). Following lysis of the

cells directly on the glass plate, total RNA was isolated and purified. Because the concentration of isolated total RNA was below that required for subsequent analysis, total cRNA was amplified from total RNA by two rounds of *in vitro* transcription and subsequently cleaned, labelled and fragmented prior to its hybridization to the probe array for 16 hours. In this case, the probe array used was the GeneChip Mouse Expression Set 430 (Affymetrix, High Wycombe, UK), which comprises more than 45,000 probe sets to analyse the expression of approximately 39,000 transcripts and variants and includes a set of mouse maintenance genes to facilitate normalization and scaling of array experiments. All RNA processing and preparation, as well as the subsequent microarray analysis, was performed at the SHWFGF, University of Glasgow.

The genes identified by microarray analysis were initially examined on a global scale, in order to better understand the commonality or individuality of the fibroblast cell lines demonstrated after being subjected to an identical stimulus. Approximately 344 genes, all of which have false discovery rates of less than 10%, were shown to be differentially regulated with stimulation (Figure 4.1). Of these altered genes, 14.8% were identified as being common to all three cell lines, 16.6% were identified in two of the three cell lines, and 68.6% were differentially regulated in one cell line only. Interestingly, 34.3% and 27.3% of the total genes identified were found to be unique to either tendon or corneal fibroblasts, respectively. In contrast, only 7.0% of the genes identified were unique to skin fibroblasts. This immediately indicates that tendon, corneal and skin fibroblasts, despite their common developmental origin, mounted a unique transcriptional response to an identical mechanical stimulus. Upon closer inspection, it is apparent that tendon and corneal fibroblasts have approximately 6.4% of the identified genes in common, while tendon and skin fibroblasts share 7.6% of differentially regulated genes. Given that corneal and skin fibroblasts maintain only

2.6% of the altered genes in common, this hints to the possibility that skin and corneal

fibroblasts demonstrate the most unique genetic response to stimulation.
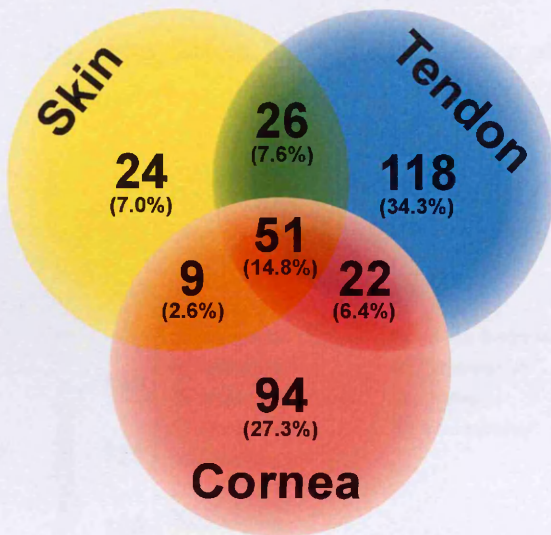
Figure 4.1: Venn Diagram representing the total number of up- and down-regulated genes in tendon, corneal and skin fibroblasts after mechanical stimulation. In total, 344 genes were identified as being differentially regulated with stimulation by microarray analysis. The number of genes identified in a given cell line are designated, and overlap regions denote genes common to the indicated cell lines.

4.2.2 *Differentially regulated genes identified by microarray are functionally diverse*

In order to place the transcriptional responses of these cell lines to stimulation in

a more biological and physiological context, altered genes were manually classified into

one of nine, broad functional groups based upon their functional annotation in the

SOURCE (Diehn *et al.*, 2003), GenBank (Benson *et al.*, 2004), and Mouse Genome

Informatics (Blake *et al.*, 2003) databases. Upon initial inspection, it is clear that the

functional spectrum of altered genes was diverse; transcripts were found to be implicated

in apoptosis, cell division, ECM and cytoskeletal remodelling, general cell maintenance

or housekeeping, cell signalling, stress response, transcription or cellular transport

(Figure 4.2). Furthermore, tendon fibroblasts demonstrated approximately equal

numbers of up- and down-regulated genes with stimulation, whereas the majority of

genes were down-regulated in corneal fibroblasts. When compared with the other two

cell lines, skin fibroblasts exhibited a significantly lower number of altered genes with stimulation, the majority of which were up-regulated. It appears that housekeeping genes comprise the major category of up-regulated genes, while a significant number of genes associated with cell division, ECM and cytoskeletal remodelling, as well as signalling factors, showed reductions in mRNA levels.
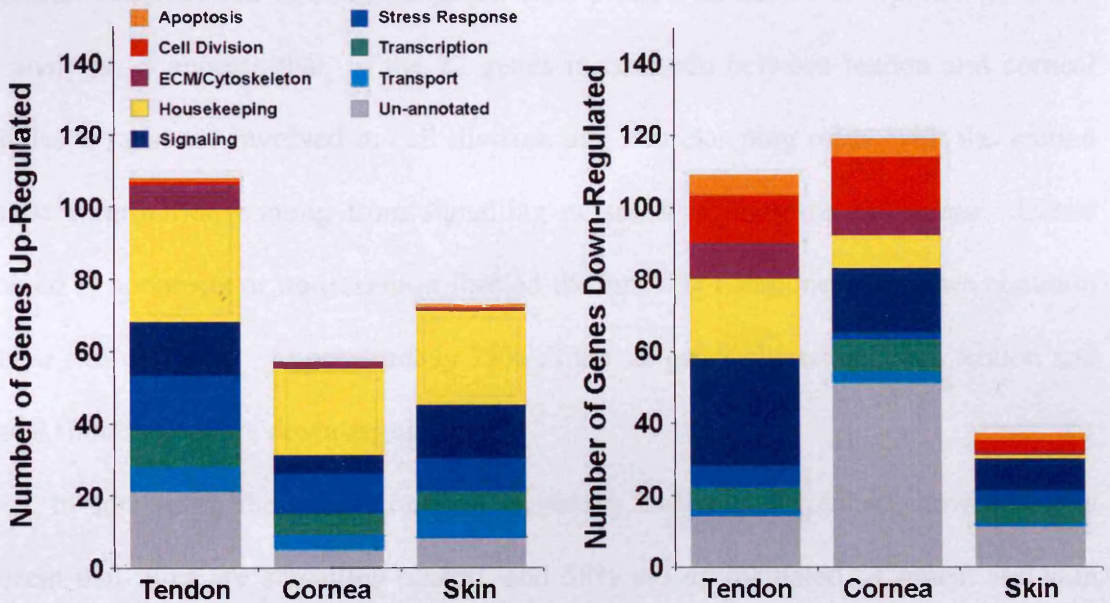
Figure 4.2: Total number and functional classification of genes up- and down-regulated following mechanical stimulation. Tendon, corneal and skin fibroblasts were subjected to 14 hours of fluid flow at a magnitude of 0.1 dyn/cm^2 for 14 hours. Control and stimulated cells were then lysed directly on the glass plate. Following purification, total RNA was processed and microarray analysis performed at the SHWFGF, University of Glasgow. Genes identified as being differentially regulated with stimulation, and having false discovery rates of less than 10%, were grouped into one of nine broad categories based upon their functional annotation in the SOURCE, GenBank, NCBI, and Mouse Genome Informatics databases.

4.2.3 The majority of genes identified in more than one cell line are classified as having housekeeping or signalling roles

Of the total number of genes altered in response to mechanical stimulation, the three cell lines maintained a number of altered genes in common. Corneal and tendon fibroblasts share approximately 45% of their altered genes with one of the other cell types, whereas skin fibroblasts share 78%, hinting that the response of the skin cell line to stimulation is less distinctive than its counterparts (Figure 4.1). In order to gain further insight into the types of genes shared between cell types, histograms of the functional classification of common genes were plotted, as shown in Figure 4.3. From this analysis, is appears that, of the 22 genes in common between tendon and corneal fibroblasts, most are involved in cell division and housekeeping roles, with the second greatest contribution coming from signalling or stress response-related genes. Genes involved in apoptosis or transcription formed the smallest component of genes common to these two cell lines. Approximately 73% of the 22 genes shared between tendon and corneal fibroblasts were down-regulated.

In comparing the genes common to tendon and skin fibroblasts, however, it is apparent that most are signalling-related, and 58% are up-regulated. Corneal and skin fibroblasts have the fewest altered genes in common, and of these, there appears to be a relatively even distribution of signalling, stress response, transcription, and transport-related genes. In this case, 78% of genes are down-regulated.

In addition to the genes found to be shared in two of the three cell lines, 51 genes were identified as being common to all three cell lines. Of these, the majority are thought to perform housekeeping functions within the cell and are up-regulated with stimulation. It is not surprising that housekeeping-related genes form the major
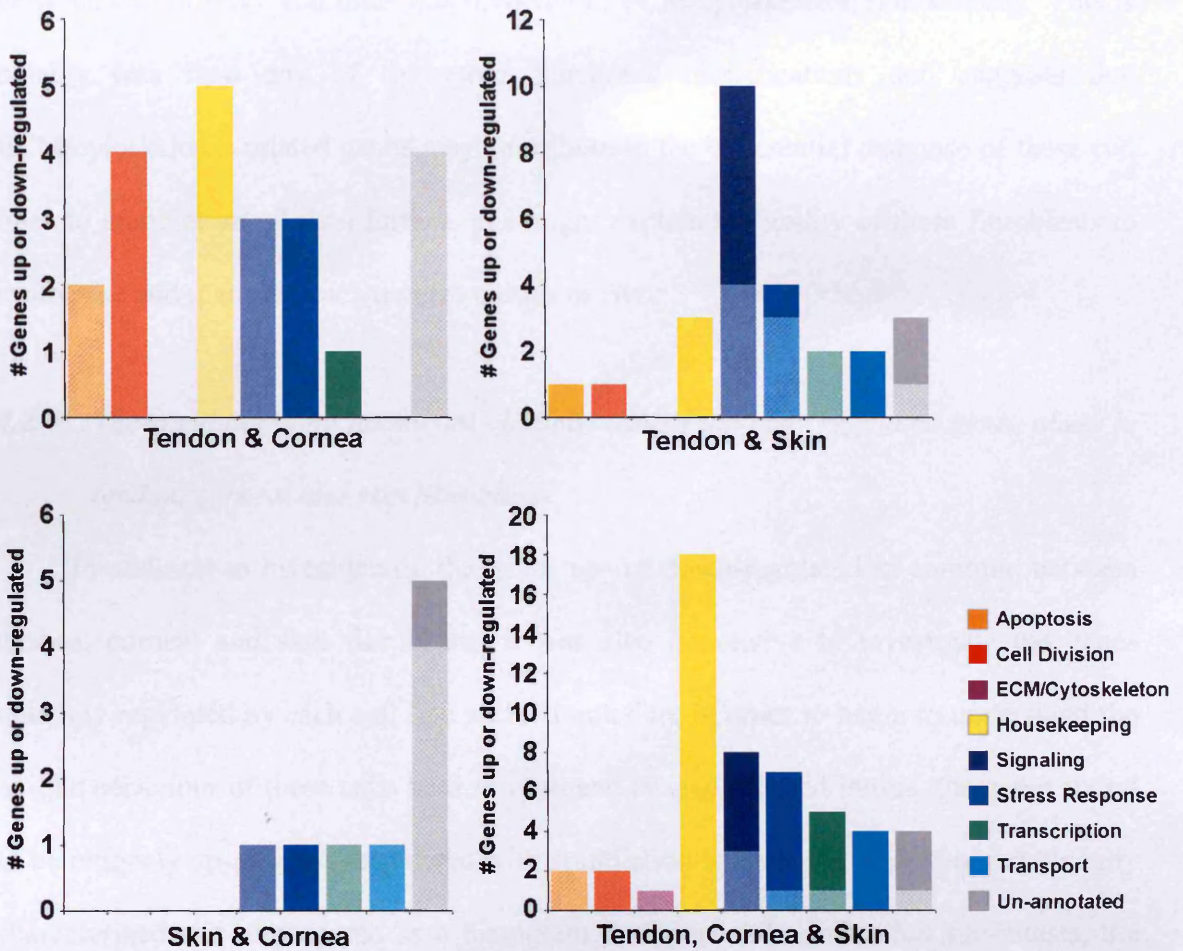
Figure 4.3: Number and functional classification of genes altered with stimulation and identified in more than one cell line. Histograms represent the total number of genes altered in the indicated cell lines, with the up-regulated genes appearing in full colour and down-regulated genes appearing muted.

functional classification common between the cell lines, since the genes controlling such fundamental activities essential for maintenance of cell function are likely to be highly conserved among similar cell lines. Genes involved in signalling or stress response formed the next highest contribution, but there were also contributions from genes classified as being involved in transcription, transport, apoptosis, cell division and ECM/cytoskeleton remodelling. Of the genes shared between all three cell lines, 78% were up-regulated with stimulation (Figure 4.3).

Surprisingly, only one gene out of the total possible 108 genes in common between two or more cell lines was involved in ECM/cytoskeleton remodelling. This is notably less than any of the other functional classifications and suggests that ECM/cytoskeleton-related genes may contribute to the differential response of these cell lines to stimulation. Taken further, this might explain the ability of these fibroblasts to synthesise and maintain such diverse tissues *in vivo*.

4.2.4 The regulation and functional classification of uniquely regulated genes alters in tendon, corneal and skin fibroblasts

In addition to investigating the genes up- or down-regulated in common between tendon, corneal and skin fibroblasts, it was also imperative to investigate the genes uniquely regulated by each cell line with stimulation, in order to begin to understand the unique behaviour of these cells both *in vitro* and *in vivo*. To aid in this, the genes found to be uniquely up- or down-regulated with stimulation in each cell line were functionally characterized and represented as a histogram in Figure 4.4. In tendon fibroblasts, the greatest proportion of genes uniquely regulated with stimulation fall into housekeeping or signalling roles. ECM or cytoskeleton-related genes form the next largest component, with a significant contribution also being made by genes involved in cell division, stress response, and transcription. Of the genes unique to tendon fibroblasts, 60% were down-regulated with stimulation.

Corneal fibroblasts demonstrate a very different trend, with similar proportions of genes involved in cell division, ECM and cytoskeletal remodelling, housekeeping, signalling, and transcription being uniquely altered with stimulation. Again, the majority of these genes were down-regulated with stimulation, with only 8.5% of the transcripts increasing with stimulation. Like tendon fibroblasts, the skin cell line demonstrates a relatively large contribution from housekeeping and signalling-related messages,

114
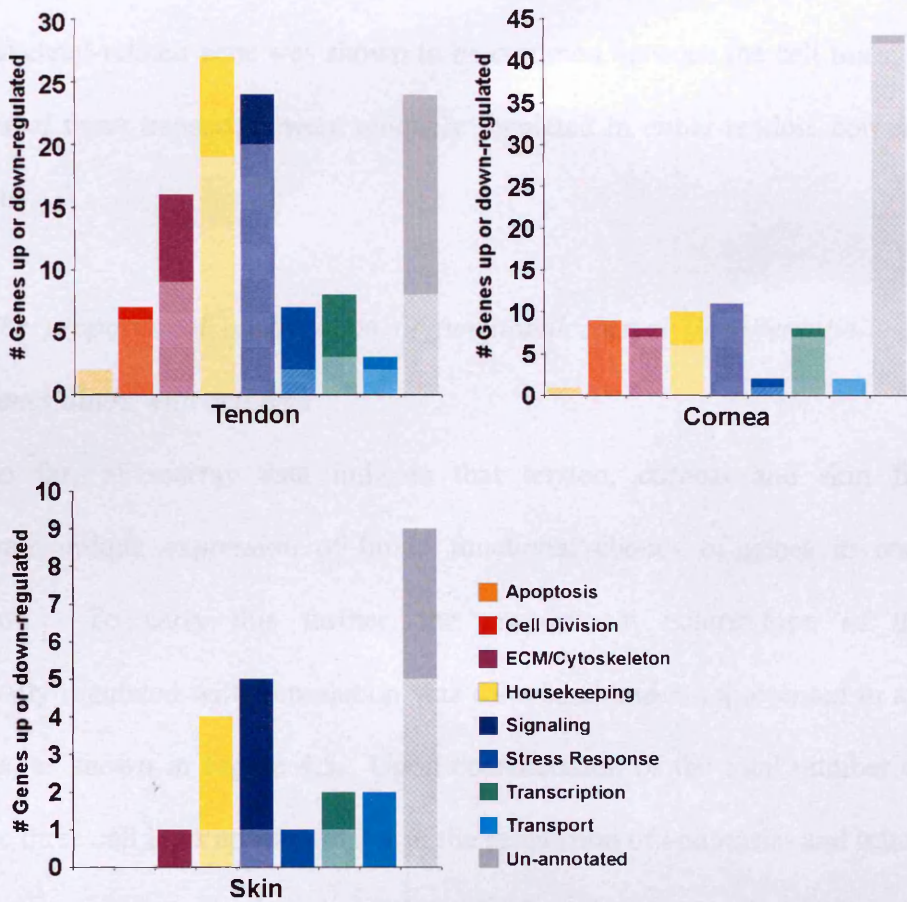
Figure 4.4: Number and functional classification of genes altered with stimulation and identified in only one cell line. Histograms represent the total number of genes altered in the indicated cell lines. Up-regulated genes appear in full colour and down-regulated genes appear muted.

followed by transcripts involved in transcription and cellular transport. Two-thirds of the transcripts unique to skin fibroblasts were up-regulated with stimulation. In contrast to tendon and corneal fibroblasts, the relative contribution of ECM- and cytoskeletal-related genes is somewhat lower in skin fibroblasts.

Overall, skin fibroblasts appeared distinct, in that the majority of its unique transcripts were up-regulated. This is in stark contrast to both tendon and corneal fibroblasts, in which uniquely altered genes were largely down-regulated with

stimulation. Furthermore, ECM and cytoskeleton-related genes appear to play an important role in the unique response of these cell lines to stimulation; only one ECM and cytoskeletal-related gene was shown to be common between the cell lines, while the remainder of these transcripts were uniquely regulated in either tendon, corneal or skin fibroblasts.

4.2.5 *The proportional contribution of functional classes in differentially regulated genes alters with cell type*

So far, microarray data indicate that tendon, corneal and skin fibroblasts demonstrate unique expression of broad functional classes of genes in response to stimulation. To carry this further, the proportional contribution of the genes differentially regulated with stimulation was calculated and is represented in a series of pie charts, as shown in Figure 4.5. Upon consideration of the total number of altered genes, the three cell lines appear similar in the proportion of apoptosis- and transcription-related genes that change with stimulation. In these two cases, the proportions of the genes altered were within 3% of the other two cell lines. Tendon and corneal fibroblasts show a significantly higher proportion of genes involved in cell division and ECM and cytoskeleton remodelling as compared with skin fibroblasts. Furthermore, corneal fibroblasts demonstrate a lower contribution of genes involved in signalling when compared with the other two cell lines. Of the genes differentially regulated with stimulation in tendon and corneal fibroblasts, approximately 4% were involved in transport. This is in contrast to an approximate 8% contribution demonstrated by skin fibroblasts. Signalling- and housekeeping-related genes were altered in similar proportions in tendon and skin fibroblasts, whereas the proportion of signalling-related genes in corneal fibroblasts changed with stimulation was markedly less.

116
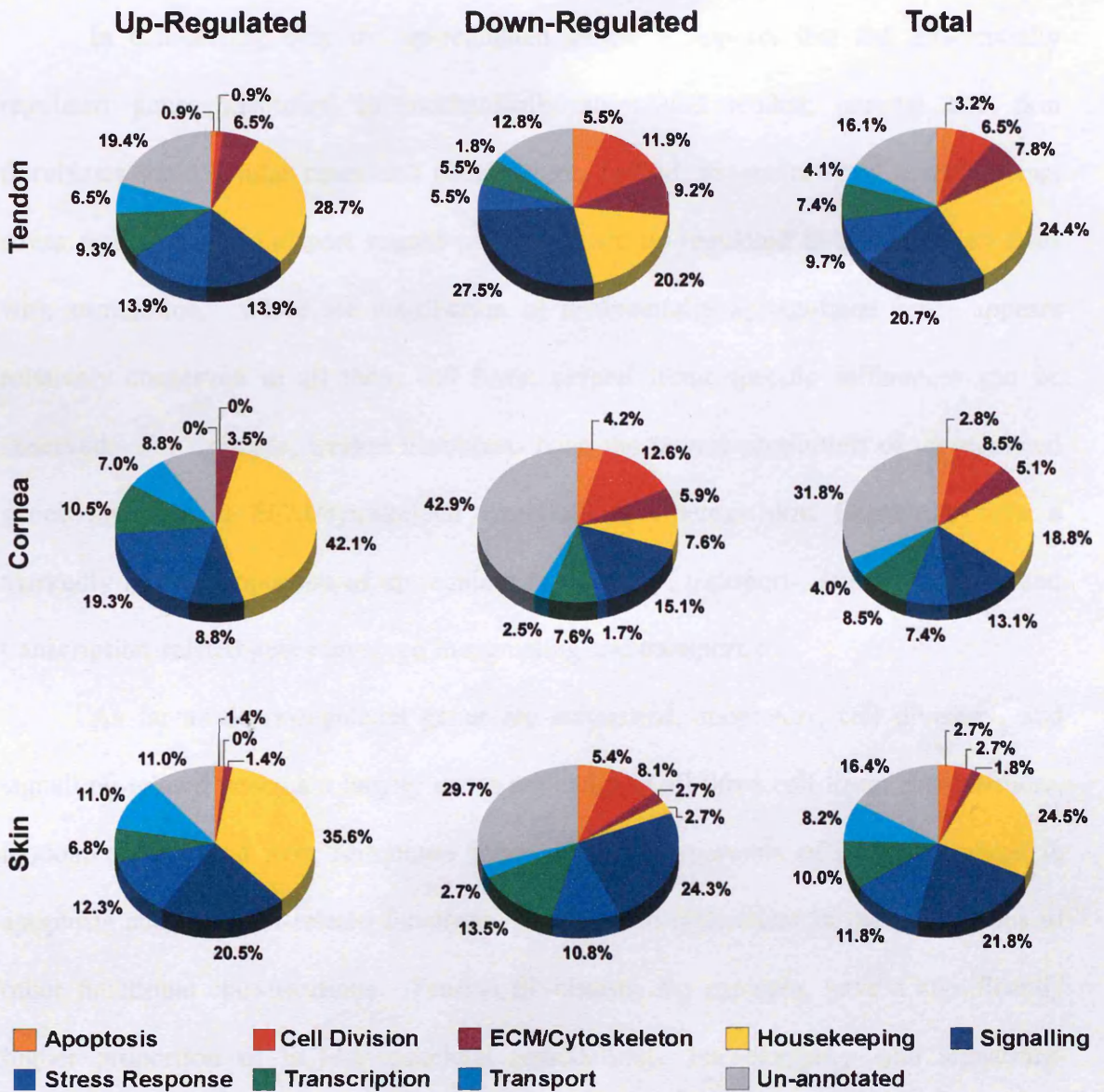
Figure 4.5: Proportional contribution of functional spectrum of total, up- or down-regulated genes differentially regulated with stimulation in tendon, corneal or skin fibroblasts. Differentially regulated genes identified by microarray analysis were categorized into broad functional groups and the proportion of functional classifications calculated.

Of the transcripts implicated in stress responses, skin fibroblasts demonstrated the largest proportion, followed by tendon and then corneal cells.

In considering only the up-regulated genes, it appears that the differentially regulated genes identified in mechanically stimulated tendon, corneal and skin fibroblasts share similar functional distributions. Indeed, the majority of housekeeping, stress response and transport related transcripts are up-regulated in all three cell lines with stimulation. While the distribution of differentially up-regulated genes appears relatively conserved in all three cell lines, several tissue-specific differences can be observed. For example, tendon fibroblasts have the largest proportion of up-regulated genes involved in ECM/cytoskeletal remodelling, whereas skin fibroblasts have a markedly higher proportion of up-regulated signalling-, transport-, stress response- and transcription-related genes involved in signalling and transport.

As far as down-regulated genes are concerned, apoptosis-, cell division-, and signalling-related genes are largely down-regulated in all three cell lines. Furthermore, tendon, corneal and skin fibroblasts show similar proportions of genes involved in apoptosis and transport-related functions, yet maintain differences in the proportions of other functional classifications. Tendon fibroblasts, for example, have a significantly higher proportion of ECM/cytoskeletal remodelling-, housekeeping- and signalling-related genes down-regulated with stimulation. In contrast to the fairly conserved distribution of up-regulated genes discussed previously, the functional distribution of down-regulated genes appears to reveal greater tissue-specific gene expression. Interestingly, this trend reinforces that already seen in Figure 4.4, where the genes identified as being differentially regulated with stimulation were shown to be largely down-regulated.

4.2.6   Iterative Group Analysis substantiates the manual classification of altered genes

In order to gain further information about the functional classes of genes that were significantly changed with stimulation, genes were subjected to Iterative Group Analysis (iGA) at the SHWFGF (University of Glasgow) (Breitling *et al.*, 2004a).   In contrast to the functional annotation discussed above (section 4.2.2), which was performed manually, iGA provides an automatic functional annotation for genes that are identified as being differentially regulated in microarray analysis, as well as a statistical confidence level for each.   Initially, genes were assigned to a functional class as annotated in GeneOntology (Ashburner *et al.*, 2000), after which individual genes were sorted according to fold-change in differential expression.   Finally, the members of a given functional class were counted and a probability of change (PC) value calculated. Table 4.1 represents groups of genes that were shown to be differentially regulated after stimulation and had confidence levels greater than 99%.   Only gene families in which at least 70% of the total number of family members altered with stimulation were included in this table, in order to preferentially identify the families in which most genes were altered with stimulation.   To aid in data analysis, gene families identified by iGA as being differentially regulated with stimulation were subsequently classified into one of seven broad functional roles based upon a consensus of database-derived searches, including GenBank, PubMed, GeneOntology and Reactome (Joshi-Tope *et al.*, 2005).

According to iGA, the gene families differentially regulated with stimulation were diverse and implicated in a variety of cellular functions, including cell division, ECM/cytoskeletal maintenance, general cell maintenance or housekeeping, stress response, transcription or translation, signalling, or mechanotransduction.   Of the six families differentially regulated with stimulation and identified in all three cell lines, three were implicated in cellular responses to oxidative stress.   This finding is in

119

Group	↑	↓	Function	Total	Changed	T	C	S
pentose-phosphate shunt, oxidative branch	✓		Housekeeping	4	4	✓	✓	✓
phosphogluconate 2-dehydrogenase activity	✓		Housekeeping	4	4	✓	✓	✓
activation of NF-kappaB-inducing kinase	✓		Mechanotransduction	2	2	✓	✓	✓
glutamate-cysteine ligase activity	✓		Oxidative Stress	2	2	✓	✓	✓
oxidoreductase activity, peroxide as acceptor	✓		Oxidative Stress	2	2	✓	✓	✓
catalase activity	✓		Oxidative Stress	2	2	✓	✓	✓
sterol 14-demethylase activity		✓	Housekeeping	3	3	✓	✓	
transforming growth factor beta receptor binding		✓	Mechanotransduction	7	5	✓	✓	
isopentenyl-diphosphate delta-isomerase activity		✓	Housekeeping	2	2	✓	✓	
carotenoid biosynthesis		✓	Housekeeping	2	2	✓	✓	
CoA-transferase activity		✓	Signalling	4	3	✓		✓
alpha DNA polymerase:primase complex		✓	Transcription/Translation	5	5	✓		✓
ribonucleoside-diphosphate reductase complex		✓	Transcription/Translation	5	5		✓	✓
ribonucleoside-diphosphate reductase activity		✓	Transcription/Translation	6	5		✓	✓
positive regulation of neuron differentiation		✓	Signalling	3	3		✓	✓
glutathione-disulfide reductase activity	✓		Oxidative Stress	2	2		✓	✓
'de novo' IMP biosynthesis	✓		Transcription/Translation	6	5	✓		
extrachromosomal circular DNA	✓		Transcripton/Translation	4	3	✓		
cyclooxygenase activity	✓		Mechanotransduction	4	4	✓		
phosphatidylserine decarboxylase activity	✓		Housekeeping	5	5	✓		
ornithine decarboxylase activity	✓		Housekeeping	3	3	✓		
regulation of interleukin-6 biosynthesis		✓	Transcription/ Mechanotransduction	2	2	✓		
malate dehydrogenase (NADP+) activity	✓		Housekeeping	2	2	✓		
glycogen debranching enzyme activity	✓		Housekeeping	2	2	✓		
bone mineralization		✓	Cell Division	3	3	✓		
nitric-oxide synthase regulator activity		✓	Mechanotransduction	5	4	✓		
activation of MAPKK	✓		Mechanotransduction	3	3	✓		
patterning of blood vessels	✓		Cell Division	2	2	✓		
procollagen-lysine 5-dioxygenase activity	✓		ECM/Cytoskeleton	4	4		✓	
centrosome separation		✓	Transcription/Translation	3	3		✓	
phenylalanyl-tRNA aminoacylation	✓		Transcription/Translation	5	5		✓	
delta-DNA polymerase cofactor complex		✓	Transcription/Translation	3	3		✓	
phenylalanine-tRNA ligase activity	✓		Transcription/Translation	5	5		✓	
phosphatidate cytidylyltransferase activity	✓		Housekeeping	5	4		✓	
cytoplasmic sequestering of transcription factor		✓	Transcription	3	3		✓	
Cajal body	✓		Transcription	7	6		✓	
carnitine metabolism	✓		Housekeeping	2	2			✓
deoxyribonucleotide metabolism		✓	Transcription/Translation	3	3			✓
deoxyribonucleoside diphosphate metabolism		✓	Transcription/Translation	3	3			✓
phosphatidylcholine biosynthesis		✓	Housekeeping	5	5			✓
aldehyde metabolism	✓		Housekeeping	4	4			✓
autophagic vacuole	✓		Housekeeping	4	4			✓
polynucleotide adenylyltransferase activity	✓		Transcription/Translation	6	5			✓
carboxylesterase activity	✓		Housekeeping	2	2			✓
DNA primase activity		✓	Transcription/Translation	4	4			✓
aminobutyraldehyde dehydrogenase activity	✓		Housekeeping	2	2			✓
semaphorin receptor activity	✓		Signalling	3	3			✓
methylthioadenosine phosphorylase activity	✓		Housekeeping	4	4			✓
protein amino acid nitrosylation		✓	Signalling	5	4			✓
oxidoreductase activity, acting on aldehyde or oxo group of donors, NAD or NADP as acceptor	✓		Housekeeping	2	2			✓
dimethylargininase activity		✓	Mechanotransduction	5	4			✓
microfibril		✓	ECM/Cytoskeleton	7	5			✓

Table 4.1: Iterative Group Analysis (iGA) of genes identified as being up- (↑) or down-regulated (↓) in tendon (T), corneal (C) or skin (S) fibroblasts by microarray analysis. Functional classes that altered with confidence levels greater than 99% are tabulated; only the groups in which the total number of family members altered with stimulation exceeded 70% are included. Functional annotation of the tabulated gene groups was obtained by a series of database-derived searches.

agreement with the trends observed after the manual functional classifications of genes differentially regulated (discussed further in section 4.3.1). The overwhelming majority of families differentially regulated in one cell line only, however, functioned in signalling, transcription, mechanotransduction or general housekeeping roles. This corroborates findings from the manual classification of genes discussed previously (Figure 4.4).

It is important to note that the manual functional classification of genes discussed previously (sections 4.2.2-4.2.4) was completed prior to iGA. Data was analysed in this manner in order to rule out the possible erroneous automatic classification of genes. For example, while GenBank may classify a gene as being implicated in DNA binding and transcription, only manual investigation will reveal if this transcription factor has been implicated in specific cellular processes, such as differentiation, division, or ECM biogenesis. Nonetheless, iGA is a valuable tool for both substantiating the manual classification of altered genes and visualising groups of genes with similar functions that are differentially regulated in tendon, corneal and skin fibroblasts after stimulation.

4.2.7 Microarray analysis is validated by semi-quantitative RT-PCR

In order to validate the changes in gene expression identified by microarray analysis, a subset of 14 genes was examined by semi-quantitative RT-PCR, representing eight down-regulated and six up-regulated genes. These particular genes were initially short-listed based upon their differential regulation in one or more cell lines and/or possible role in ECM biogenesis or cytoskeletal organization. Ultimately, these 14 genes were chosen because antibodies were available that were directed toward their protein products. This enabled the validation of the microarray analysis by both semi-quantitative RT-PCR and Western blotting (see section 4.2.8).

Prior to validation by semi-quantitative RT-PCR, however, it was necessary to determine empirically the number of cycles of RT-PCR needed to take samples during the linear range of amplification, prior to saturation of the product. To accomplish this, forward and reverse primers were designed in order to amplify cyclin E2 (Ccne2) and cysteine and glycine-rich protein 1 (Crp1) in mRNA samples from skin and corneal controls. An aliquot of each of the reverse transcription-PCR products was taken at various cycles and subsequently resolved by agarose gel electrophoresis. NIH Image was used to calculate the intensity of the resultant bands against background. These values were directly proportional to the amount of product that had formed at various time points, and could be subsequently compared to the amount of product that formed when the reaction was allowed to proceed to saturation. The cycle at which the RT-PCR product reached saturation yielded the highest integrated density value, and hence, was termed the "maximal density." Figure 4.6 represents the integrated density measurements as a proportion of this maximal density. From this, it appears that cycle 35 resulted in sufficient amplification of the desired RT-PCR product, while still falling within the linear portion of amplification. Consequently, each subsequent RT-PCR reaction was stopped at cycle 35, such that the amount of product produced was both proportional to the amount of transcript present after mechanical stimulation and directly comparable to the microarray data.

Semi-quantitative RT-PCR was performed on 14 genes initially identified by microarray analysis as being differentially regulated with shear stress. The primers for these genes of interest were designed using Primer3, as described in section 2.2.25. RNA previously isolated from three replicate mechanical stimulation experiments for each cell line was used as a template and the resultant products were electrophoresed and visualized by ethidium bromide staining. As with the empirical determination described
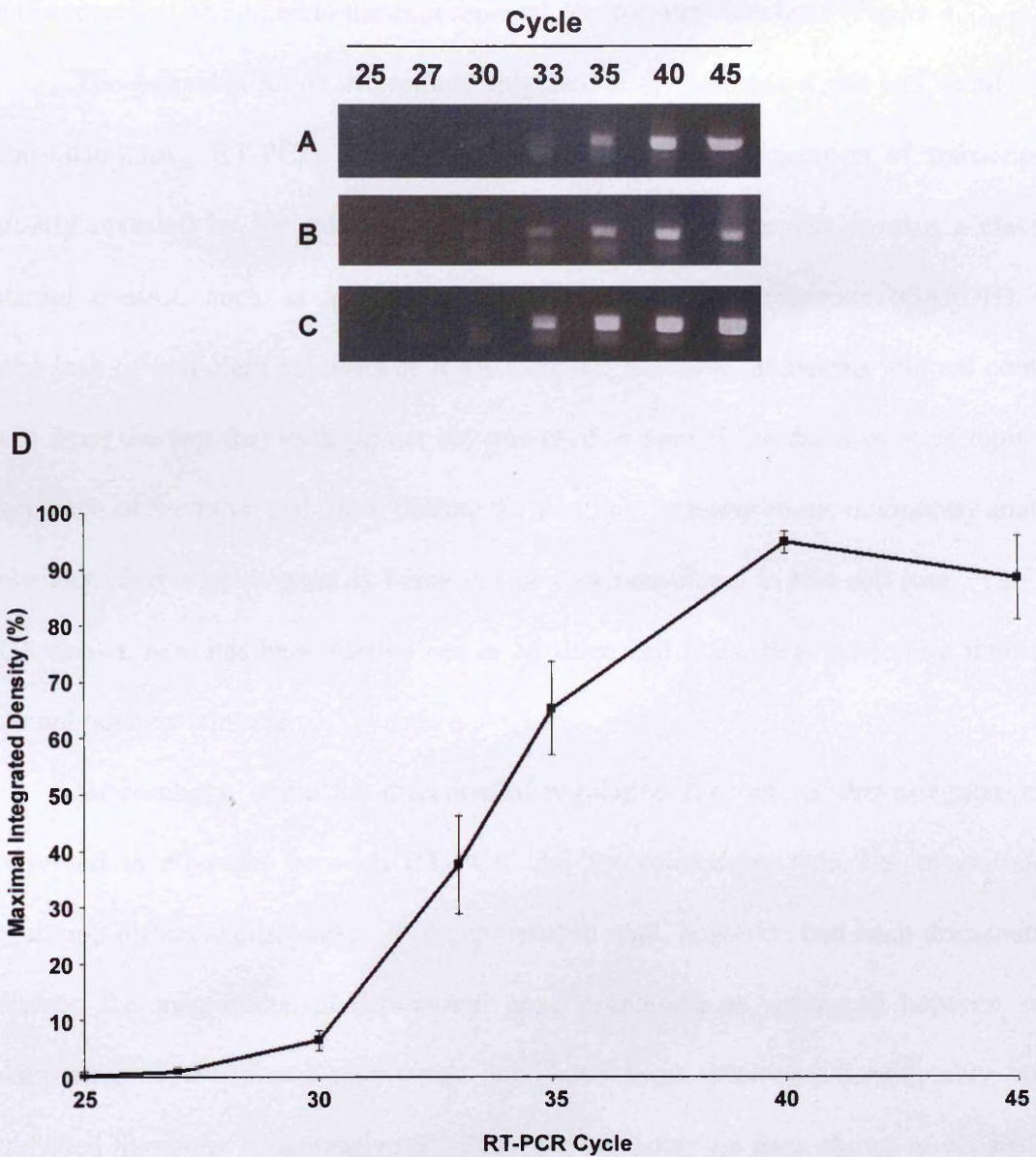
Figure 4.6: Empirical determination of the number of cycles to use in amplifying products for semi-quantitative RT-PCR validation of microarray data. mRNA isolated from skin (A, B) or corneal control fibroblasts (C) were subjected to RT-PCR with forward and reverse primers for Ccne2 (A, C) or Crp1 (B). Aliquots from these three RT-PCR products were taken at cycles 25, 27, 30, 33, 35, 40, and 45, resolved by electrophoresis, and visualized by ethidium bromide staining. NIH Image was used to calculate the intensity of the resultant bands. Data is represented as the mean maximal integrated density (± SE), calculated from three independent experiments, which were generated from two samples of mRNA and two unique forward and reverse primers (D).

above, the intensity of each band was quantified with NIH Image and the fold change in gene expression compared to the experimental control was calculated (Figure 4.7).

The generated RT-PCR products migrated at their expected size and, in all cases, semi-quantitative RT-PCR substantiated the up- or down-regulation of transcription initially revealed by the microarray data. The RT-PCR does not contain a classical internal control, such as glyceraldehyde-3-phosphate dehydrogenase (GAPDH), due tothe lack of sufficient amounts of RNA samples; however, numerous internal controls exist from the fact that each primer set was used to amplify products in three replicates from each of the three cell lines, despite the fact that, in many cases, microarray analysis only identified a given gene as being up- or down-regulated in one cell line. The RT-PCR shown here has been carried out in all three cell lines, thus generating numerous internal positive controls.

Interestingly, while the direction of regulation (i.e. up- or down-regulation) is conserved in all cases between RT-PCR and the microarray data, the magnitude of regulation differs significantly. It is important to note, however, that such discrepancies between the magnitudes of differential gene regulation as compared between semi-quantitative RT-PCR and microarray data have been discussed considerably within published literature. Quantitative RT-PCR, for example, has been shown to consistently reflect the up- and down-regulated status but will not accurately reflect the magnitude of the fold-changes as indicated by microarray (Marone *et al.*, 2001). Furthermore, it has been reported that microarrays frequently underestimate the fold-change with respect to absolute changes in transcript levels (*ibid.*).

Further discrepancies between the RT-PCR results and microarray data result from complications in quantifying the magnitude of up- or down-regulation. For example, in the case of the second replicate for neogenin in skin fibroblasts, the control
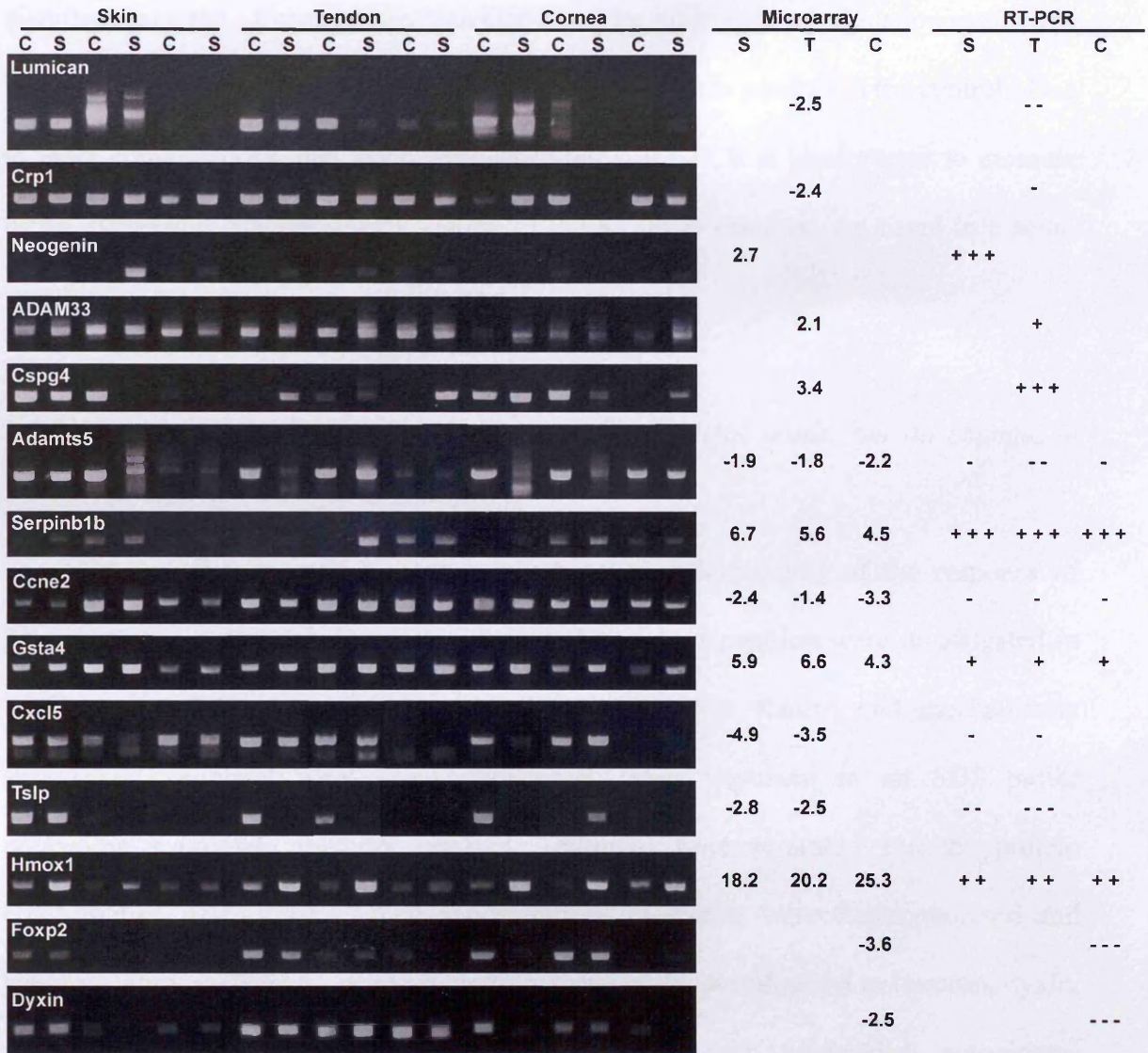
Figure 4.7: Validation of microarray data by semi-quantitative RT-PCR. 10 ng of RNA isolated from control (C) and mechanically stimulated (S) tendon, cornea and skin fibroblasts was subjected to 35 cycles of semi-quantitative RT-PCR using forward and reverse primers for 14 genes of interest. Samples were taken during the linear phase of amplification, resolved by electrophoresis and visualized by ethidium bromide staining. NIH Image was used to calculate the intensity of the resultant bands. Genes are represented as being up- or down-regulated in tendon (T), corneal (C), or skin (S) fibroblasts by less than 2-fold (-/+), greater than or equal to 2-fold, but less than 10-fold (- -/ + +), or greater than or equal to 10-fold (- - -/ + + +). As means of comparison, the fold-change in gene expression as determined by microarray analysis is listed alongside the semi-quantitative integrated density results from RT-PCR.

sample shows very little, if any product, whereas the stimulated sample exhibits a significant amount. Consequently, calculation of the magnitude of regulation resulted in an apparent infinite up-regulation, since there was no visible product in the control. Due to these complications, and since semi-quantitative RT-PCR is ideally used to measure broad expression changes, quantification of the RT-PCR reactions are listed in a semi-quantitative manner, as shown in Figure 4.7.

4.2.8 *Protein levels do not directly correlate with mRNA levels, but do change, in mechanically stimulated fibroblasts*

In an effort to gain a more comprehensive understanding of the response of fibroblasts to mechanical stimulation, levels of protein expression were investigated in addition to mRNA transcript levels. To achieve this, control and mechanically stimulated fibroblasts were lysed immediately after treatment in an SDS buffer containing a protease inhibitor cocktail. Samples were sonicated and the protein concentration determined. Equal concentrations of lysates were electrophoresed and subsequently visualized by Western blotting, using antibodies directed to lumican, dyxin, CRP1, and neogenin. Western blots were probed with horseradish peroxidase-conjugated secondary antibodies, and ultimately visualized by enhanced chemiluminescence at low exposures to ensure linearity of the response. The intensity of the resulting bands were quantified with NIH Image and normalized to the loading control (β-actin). Fold-changes in protein expression were calculated and the replicates of a given experiment averaged.

The lumican antibody identified four distinct bands, indicating proteins with apparent molecular weights of 73, 62, 30 and 26 kDa. According to the literature, the highest molecular weight species corresponds to the intact glycoprotein, the 62 kDa
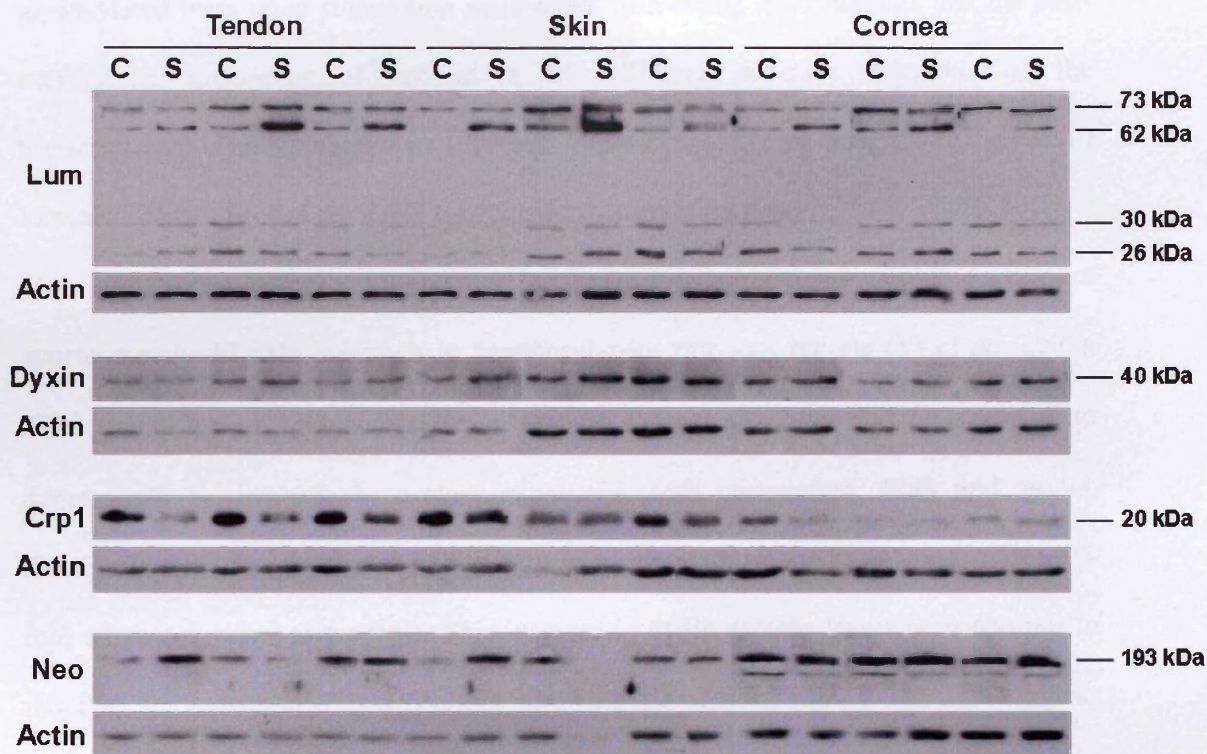
Figure 4.8: Expression of lumican (Lum), dyxin, cysteine and glycine-rich protein 1 (Crp1) and neogenin (Neo) in control (C) and mechanically stimulated (S) tendon, skin and corneal fibroblasts. Cell lysates were prepared from cultures of fibroblasts following stimulation, subsequently resolved by SDS-PAGE, and submitted to immunoblot analysis with the indicated antibodies. n = 3 for all proteins in all cell lines, with the exception of neogenin in skin fibroblasts. In this case, n = 2, since there was not sufficient quantities of one of the stimulated samples.

species represents an alternatively glycosylated form, and the lower molecular weight 30 and 26 kDa species denote the two isoforms of the core protein typically found in fibroblasts (Funderburgh and Conrad, 1990; Funderburgh *et al.*, 1991). After quantification, it appears that stimulation has no effect on the levels of the 73, 30 or 26 kDa species in either of the three cell lines (Table 4.2). However, the 62 kDa species, corresponding to the alternatively glycosylated form of lumican, shows an increase of approximately 6-, 3.5-, and 7-fold with stimulation in tendon, corneal and skin

fibroblasts, respectively. While this apparent increase in the 62 kDa lumican species is at odds with the decreased levels of lumican mRNA with stimulation, as determined by both microarray and RT-PCR (Figure 4.7, Table 4.2), the appearance of an alternative glycosylated form upon stimulation is, in itself, interesting. This suggests that the post-translational processing of lumican is affected in a different direction than the transcriptional control, which may reveal an important functional insight into the role of lumican. This aspect of the study warrants further investigation.

The dyxin antibody, kindly provided by Dr. Rachelle Crosbie, revealed a band of approximately 40 kDa, which is in agreement with previous reports (Yi *et al.*, 2003). After quantification and normalization against β-actin, all three cell lines appear to demonstrate an increase in protein expression with stimulation. Skin and tendon fibroblasts show the greatest change in protein levels, with an approximate increase of 2-fold when compared to controls. This increase in dyxin protein levels is in contrast to reducing amounts of mRNA transcripts following stimulation (Table 4.2). This suggests that tendon, corneal and skin fibroblasts differentially regulated the transcriptional or translational levels of dyxin upon stimulation.

Probing cell lysates with the CRP1 anti-sera revealed a band of approximately 20 kDa. Levels of transcripts encoding CRP1 were found to decrease in stimulated tendon fibroblasts, and this trend correlated with a concomitant 3.8-fold decrease in CRP1 protein levels (Figure 4.8, Table 4.2). Furthermore, despite the fact that differential expression of CRP1 mRNA was not shown to be significantly altered in stimulated corneal or skin fibroblasts, levels of CRP1 protein in these cell lines was also shown to decrease by approximately 3-fold.

Protein	Species	Tendon	Cornea	Skin
Lumican	62 kDa	6.07 ± 1.16	3.50 ± 0.49	7.21 ± 4.80
Dyxin	40 kDa	1.98 ± 0.44	1.24 ± 0.19	2.08 ± 0.69
Crp1	20 kDa	-3.79 ± 1.62	-3.08 ± 0.93	-2.78 ± 1.22
Neogenin	193 kDa	–	-2.98 ± 0.97	2.16 ± 1.15

Table 4.2: Quantification of immunoblotting of ECM/cytoskeleton-related proteins differentially regulated with stimulation. Values are represented as the mean fold change between stimulated and control cells ± SEM.

Neogenin immunoblots revealed a prominent band at approximately 193 kDa; this most likely differs from the protein's theoretical molecular weight of 150 kDa because of glycosylation (Vielmetter *et al.*, 1994). Shear stress resulted in the differential regulation of neogenin by skin and corneal fibroblasts. Neogenin was found to increase by approximately 2-fold upon the application of mechanical stimulation in skin fibroblasts, which correlated well with a 1.67-fold increase in neogenin transcript levels, as determined by microarray analysis (Figure 4.7, Table 4.3). Corneal fibroblasts, on the other hand, displayed an almost 3-fold decrease in neogenin following stimulation. In this case, the decrease in protein levels occurs without any apparent change in gene expression. Tendon fibroblasts did not show any change in neogenin protein levels with stimulation.

4.3 Discussion

4.3.1 Highest up-regulated genes are similar in tendon, corneal and skin fibroblasts

Following examination of the functional classifications of genes altered in common and unique to each cell line with stimulation, a number of genes of interest were selected based upon their functionality, magnitude of up- or down-regulation, or identification in one or more cell lines (Table 4.3). It is important to note that, while a

gene may be identified in Table 4.3 as being one of the highest up- or lowest down-regulated genes in a given cell line, its absence from the other cell lines is not necessarily indicative that the gene was not altered in that cell line. Rather, the gene may have demonstrated differential regulation with stimulation in numerous cell lines, but the magnitude was not sufficient to fall within the top five highest up- or lowest down-regulated genes for the given cell line.

Three of the top five highest-regulated genes, glutathione-S-transferase alpha 2 (GSTα2), heme oxygenease-1 (Hmox1), and glutamate-cysteine ligase modifier subunit (Gclm), were identical in all three cell lines. GSTα2 is a phase II detoxifying enzyme which, in collaboration with phase I enzymes such as members of the cytochrome P450 family, plays an important role in detoxification by catalyzing the conjugation of electrophilic compounds with reduced glutathione (Pearson *et al.*, 1988). Furthermore, GSTα2 has been shown to play an important role in the protection of cells against oxidative stress. Hmox1, one of three mammalian HO isoforms, is the rate-limiting enzyme in heme catabolism, which leads to the generation of carbon monoxide (CO), biliverdin, and free iron. In addition to its housekeeping role, Hmox1 is also a stress-responsive protein, has been shown to modulate cytokine production, cell proliferation, and apoptosis to protect organs and tissues from acute injury, and appears to be heavily involved in responses to oxidative stress (Choi *et al.*, 2003); more specifically, Hmox1 prevents cell death by regulating intracellular iron levels (Konttinen *et al.*, 2000). Gclm, also found to be highly up-regulated in all three cell lines, is the rate-limiting enzyme in the glutathione biosynthesis pathway and is another in the oxidative stress response (Yang *et al.*, 2002a; Yang *et al.*, 2002b).

In addition to the genes up-regulated in all cell lines, both tendon and skin fibroblasts showed a marked increase in expression of the angiopoietin-like 4 (Angptl4)

gene. Angptl4 has been shown to be involved in lipid metabolism or glucose homeostasis (Yoon *et al.*, 2000), and the recombinant protein has been shown to act as an apoptosis survival factor for vascular endothelial cells (Kim *et al.*, 2000). Furthermore, Angptl4 has also been implicated in adipocyte differentiation, which is of particular interest given the capability of "fibroblasts" to differentiate along various connective tissue cell-type lineages, such as to adipocytes (Mandard *et al.*, 2004; Yoon *et al.*, 2000).

In contrast to tendon and skin fibroblasts, corneal fibroblasts demonstrated an increase in the expression of the gene encoding heat shock protein 1A (Hsp72). Heat shock proteins, in general, serve as scaffolding or chaperone proteins that function to preserve the integrity of essential intracellular proteins during times of stress and have been found to be produced in response to a vast array of stimuli, including heat, heavy metals, oxidants, protein synthesis, and degradation inhibitors (Lindquist and Craig, 1988). It is not surprising, then, that Hsp72 has been found to inhibit cell necrosis and apoptosis (Kabakov and Gabai, 1995), or help protect cells against oxidant-mediated injury (Musch *et al.*, 2004).

Interestingly, Gsta2, Hmox1, Gclm, Angptl4 and Hsp72, all of which were all up-regulated to the highest magnitude in tendon, corneal and skin fibroblasts, are implicated in the protection of cells against oxidative stress, a phenomenon generated upon the production of reactive oxygen species (ROS) through endogenous processes and exogenous stimuli such as the mitochondrial electron transport chain, cytochrome P450 systems, nitric oxide synthetase, inflammation ultraviolet and ionizing radiation, and mechanical stress. Such oxidative stress can lead to subsequent changes to cellular macromolecules including nucleic acids, proteins and lipids (Yang *et al.*, 2002b). Given the method by which these cells were stimulated, it is not surprising that all three cell

lines responded by up-regulating oxidative response genes. An increase in these transcripts most likely serves to protect the cells from reactive oxygen species produced as a consequence of mechanical stimulation. Interestingly ROS have also been implicated in mechanotransduction (Yamamoto *et al.*, 1999). Perhaps, in this case, an increase in ROS assists in the transduction of exogenous shear stress cues into the cell, while the cell itself counteracts the potentially harmful increase in ROS by up-regulating oxidative response genes, as discussed above.

4.3.2 Down-regulated genes vary between tendon, corneal and skin fibroblasts

Unlike the highest up-regulated genes, in which the three cell lines shared significant overlap, there was greater variation in the functional classification of lowest down-regulated genes. In tendon, for example, levels of mRNA encoding the CCAAT/enhancer binding protein delta (Cebpd), carbonic anhydrase 3 (Car3), chemokine (C-C motif) ligand 20 (Ccl20), pentaxin related gene (Ptx3) and early growth response 3 (Egr3) were all shown to be down-regulated to the greatest extent with stimulation. Cebpd is a transcription factor, which has been implicated in diverse cellular functions including the acute phase response, mammary epithelial cell growth control and adipocyte differentiation (Huang *et al.*, 2004). Car3, in addition to its role in catalyzing the hydration of carbon dioxide, regulation of cellular pH and carbon dioxide transport (Kim *et al.*, 2001), has also been implicated in the differentiation of adipocytes, with levels of Car3 having been found to be negligible in pre-adipocytes. Genes implicated in adipocyte differentiation have emerged several times, such as the up-regulation of Angptl4 in tendon and skin fibroblasts (see section 4.3.1), and now with the down-regulation of Cebpd and Car3.

Of the five genes found to be down-regulated to the greatest extent with stimulation in tendon fibroblasts, two genes were identified as being in common with skin fibroblasts. The first encodes a low molecular weight cytokine, Ccl20, which has been found to play an important role in inflammation as well as differentiation (Shiba *et al.*, 2003; Shirane *et al.*, 2004). Interestingly, Ccl20 was found to be up-regulated in tumour necrosis factor (TNF)-activated endothelial cells subjected to shear stress (Meissner *et al.*, 2003). Perhaps its down-regulation in this case points to the differential response of diverse cell types to mechanical stresses. The second gene common to tendon and skin fibroblasts is Ptx3, which has been shown to be involved in the acute phase response (Goodman *et al.*, 1996).

In contrast to tendon cells, corneal fibroblasts demonstrated the down-regulation of forkhead box P2 (Foxp2), follistatin (Fst), cyclin E2 (Ccne2), engulfment adaptor PTB domain containing 1 (Gulp1), and solute carrier family 4, member 4 (Slc4a4) genes with stimulation, all of which have very diverse cellular functions. Foxp2 is a large multi-domain transcriptional regulator that belongs to the Fox family of winged helix-DNA binding proteins and functions as a transcriptional repressor (Li *et al.*, 2004). Fst, on the other hand, encodes a TGFβ superfamily binding protein, and has been shown to be an extracellular inhibitor or TGFβ signalling and a downstream component of Wnt4 signalling (Wang *et al.*, 2004b; Yao *et al.*, 2004). Ccne2, like other cyclins, is important in regulating cell cycle progression. Cyclin E2 levels have been shown to be low to undetectable in nontransformed cells and increased significantly in tumour-derived cells (Gudas *et al.*, 1999). Furthermore, overexpression in mammalian cells accelerates G1, so cyclin E2 is believed to be rate limiting for G1 progression. Corneal fibroblasts also demonstrated significant down-regulation of Gulp1, which encodes an adapter protein that is ultimately thought to mediate the specific recognition and engulfment of apoptotic

Gene description	Function	T	C	S	Assession #
A. Highest up-regulated genes					
heme oxygenase (decycling) 1 (Hmox1)	Housekeeping	20.2	25.3	18.2	NM_010442
glutathione S-transferase, alpha 2 (Gsta2)	Stress Response	18.7	27.9	13.3	NM_008182
neoplastic progression 3 (Npn3)	Transcription	11.9	9.8		NM_029688
angiopoietin-like 4 (Angptl4)	Housekeeping	11.4		8.6	NM_020581
glutamate-cysteine ligase , modifier subunit (Gclm)	Housekeeping	11.1	9.3	8.5	NM_008129
heat shock protein 1A (Hsp72)	Stress Response		9.0		NM_010479
proliferin (Plf)	Signalling			14.0	NM_031191
B. Lowest down-regulated genes					
CCAAT/enhancer binding protein delta (Cebpd)	Transcription	-4.3			NM_007679
carbonic anhydrase 3 (Car3)	Housekeeping	-4.3			NM_007606
chemokine (C-C motif) ligand 20 (Ccl20)	Signalling	-4.0		-2.5	NM_016960
pentaxin related gene (Ptx3)	Stress Response	-4.0		-2.6	NM_008987
early growth response 3 (Egr3)	Transcription	-3.5			NM_018781
forkhead box P2 (Foxp2)	Transcription		-3.6		NM_053242
follistatin (Fst)	Signalling		-3.4		NM_008046
cyclin E2 (Ccne2)	Cell Division		-3.3		NM_009830
GULP, engulfment adaptor PTB domain containing 1 (Gulp1)	Apoptosis		-3.3		BB138485
solute carrier family 4 (anion exchanger), member 4 (Slc4a4)	Transport		-3.1		NM_018760
chemokine (C-X-C motif) ligand 5 (Cxcl5)	Signalling			-4.9	NM_009141
thymic stromal lymphopoietin (Tslp)	Signalling			-2.8	NM_021367
lipocalin 2 (Lcn2)	Housekeeping			-2.6	NM_008491
C. Highest up-regulated genes found in only one cell line					
dual specificity phosphatase 4 (Dusp4)	Signalling	4.8			NM_176933
xanthine dehydrogenase (Xdh)	Housekeeping	4.5			NM_011723
mitogen activated protein kinase kinase kinase 4 (Map3k4)	Signalling	3.9			NM_011948
dystonin (Dst)	ECM/Cytoskeleton	3.7			NM_133833
growth arrest specific 5 (Gas5)	Cell Division	3.5			NM_013525
gamma-aminobutyric acid (GABA(A)) receptor-associated protein-like 1 (Gabarapl1)	ECM/Cytoskeleton		4.4		NM_020590
aldo-keto reductase family 1, member B3 (Akr1b3)	Housekeeping		3.7		BB469763
sphingosine kinase 1 (Sphk1)	ECM/Cytoskeleton		3.3		NM_011451
cytochrome b-5 (Cyb5)	Housekeeping		2.9		NM_025797
ectonucleotide pyrophosphatase/phosphodiesterase 2 (Enpp2)	Housekeeping		2.8		NM_015744
BTB (POZ) domain containing 11 (Btbd11)	Transcription			3.5	BC072592
neogenin (Neo)	ECM/Cytoskeleton			2.7	NM_008684
secretory leukocyte protease inhibitor (Slpi)	Stress Response			2.5	NM_011414
endothelin receptor type B (Ednrb)	Signalling			2.5	NM_007904
centaurin, gamma 2 (Centg2)	Transport			2.5	NM_178119
D. Lowest down-regulated genes found in only one cell line					
carbonic anhydrase 3 (Car3)	Housekeeping	-4.3			NM_007606
ELAV-like 2 (Hu antigen B) (Elavl2)	Cell Division	-3.0			NM_207685
chemokine (C-X-C motif) ligand 14 (Cxcl14)	Signalling	-3.0			NM_019568
early growth response 2 (Egr2)	Transcription	-3.0			NM_010118
receptor activator of NF-κB Ligand (RANKL)	Signalling	-2.9			NM_011613
forkhead box P2 (Foxp2)	Transcription		-3.6		NM_053242
solute carrier family 4, member 4 (Slc4a4)	Transport		-3.1		NM_018760
RAD51 homolog (*S. cerevisiae*) (Rad51)	Stress Response		-2.7		NM_011234
Nik-related kinase (Nrk)	Signalling		-2.7		NM_013724
anillin, actin binding protein (Anln)	ECM/Cytoskeleton		-2.6		NM_028390
lipocalin 2 (Lcn2)	Housekeeping			-2.6	NM_008491
odd-skipped related 1 (*Drosophila*) (Osr1)	Transcription			-2.3	NM_011859
endothelin 1 (Edn1)	Signalling			-2.3	NM_010104
E. Genes implicated in ECM/Cytoskeletal remodelling					
lumican (Lum)	ECM/Cytoskeleton	-2.5			NM_008524
LIM and cysteine-rich domains 1 (Dyxin)	ECM/Cytoskeleton		-2.5		NM_144799
cysteine and glycine-rich protein 1 (Crp1)	ECM/Cytoskeleton	-2.4			NM_007791
myosin, light polypeptide kinase (Mlck)	ECM/Cytoskeleton	-2.0			NM_139300
LIM domain containing preferred translocation partner in lipoma (Lpp)	ECM/Cytoskeleton		-2.1		NM_178665

134

Gene description	Function	Cell Line			Assession #
		T	C	S	
FERM domain containing 3 (Frmd3)	ECM/Cytoskeleton		-2.0		NM_172869
A disintegrin and metalloprotease domain 33 (ADAM33)	ECM/Cytoskeleton	2.1			NM_033615
chondroitin sulfate proteoglycan 4 (Cspg4)	ECM/Cytoskeleton	3.4			NM_139001
F. Genes of interest identified in all cell lines					
a disintegrin-like & metalloprotease with thrombospondin type 1 motif, 5 (Adamts5)	ECM/Cytoskeleton	-1.8	-2.2	-1.9	NM_011782
serine (or cysteine) proteinase inhibitor, clade B, member 1b (Serpinb1b)	Housekeeping	5.6	4.5	6.7	NM_173052
glutathione S-transferase, alpha 4 (Gsta4)	Stress Response	6.6	4.3	5.9	NM_010357

Table 4.3: Genes of interest identified based upon their functionality, magnitude of up- or down-regulation, or identification in tendon (T), corneal (C), or skin (S) fibroblasts. The tabulated genes were manually clustered into the indicated functional groups based upon their annotation. The numerical intensity values shown indicate the fold-expression change, as described in 2.2.23. Positive values correspond to up-regulation, whilst negative values correspond to down-regulation. Triplicate microarray experiments were performed with each fibroblast cell line.

cells (Banerjee *et al.*, 2003; Su *et al.*, 2002). Finally, Slc4a4 was shown to decrease in stimulated corneal cells. The protein encoded by this gene functions to regulate intracellular pH levels by mediating the coupled movement of Na^+ and HCO_3^- ions across the plasma membrane (Kim *et al.*, 2003b).

In addition to Ccl20 and Ptx3, which were also identified in tendon fibroblasts, chemokine (C-X-C motif) ligand 5 (Cxcl5), thymic stromal lymphopoietin (Tslp) and lipocalin 2 (Lcn2) were also found to be down-regulated to a large extent in skin fibroblasts. Cxcl5, in contrast to Ccl20, encodes a C-X-C type chemokine, but is also responsible for the recruitment of inflammatory cells (Sachidanandan *et al.*, 2002; Smith and Herschman, 1995). Tslp, which also functions as a signalling molecule, encodes a cytokine which controls murine B cell development (Vosshenrich *et al.*, 2004) as well as CD(+) T cell expansion and survival (Al Shami *et al.*, 2004). Finally, Lcn2 encodes lipocalin 2, a small, secreted acute-phase protein and functions in diverse biological processes by forming multimeric complexes of small, hydrophobic molecules and cell surface receptors (Kamezaki *et al.*, 2003; Shen *et al.*, 2004). Lipocalin 2 has been found

to be expressed highly in mature adipocytes (Kratchmarova *et al.*, 2002), and, when induced in hematopoietic cells, has been found to induce apoptosis (Kamezaki *et al.*, 2003). Of the five genes identified as being down-regulated to the greatest extent in skin fibroblasts, four have been implicated either the inflammatory or the acute-phase response. It is interesting that, in contrast to the other two cell lines, the genes down-regulated to the greatest extent in skin fibroblasts were predominantly involved in stress-related functions.

4.3.3 *Description of genes up-regulated with stimulation and identified in one line only*

In addition to the identification of the highest up- and lowest down-regulated genes found in more than one cell line, it is also crucial to investigate those genes with the greatest magnitude of differential regulation found in only one cell line. In contrast to the genes identified above, the following genes were found to be differentially up-regulated in one cell line only, which inevitably provides information on the specific differential response these three cell lines had to an identical mechanical stimulus.

4.3.3.1 *Tendon fibroblasts*

Of the five genes up-regulated to the largest extent in tendon cells, two are implicated in signalling. Dual specificity phosphatase 4 (Dusp4) encodes a member of the dual specificity protein phosphatase subfamily, which function to inactivate their target kinases by dephosphorylating both phosphoserine/threonine and phosphotyrosine residues. In addition, they have been found to negatively regulate members of the mitogen-activated protein (MAP) kinase superfamily, specifically ERK1, ERK2 and c-Jun N-terminal kinase (JNK), which themselves, are implicated in cellular proliferation and differentiation (Guan and Butch, 1995). The activity and abundance of the MKP-2

protein, but not MKP-2 mRNA levels, has been shown to increase in senescent fibroblasts when compared to their younger counterparts (Torres *et al.*, 2003). Mitogen activated protein kinase kinase kinase 4 (Map3k4) was also found to be up-regulated in tendon fibroblasts. Map3k4 is a component of sequential kinase cascades activated in response to various extracellular signals and has been found to specifically activate the JNK pathway, but not ERKs or p38, and binds to Cdc42 and Rac (Gerwins *et al.*, 1997). Map3k4 has been found to be involved in the regulation of JNK activation by Rac/Cdc42 independent of PAK and has also been shown to bind Axin, a multidomain protein that plays a critical role in Wnt signalling (Fanger *et al.*, 1997).

In addition to signalling-related genes, tendon fibroblasts also demonstrated an up-regulation of xanthine dehydrogenase (Xdh) with stimulation. This gene encodes for the rate-limiting enzyme in purine catabolism which converts hypoxanthine to xanthine and xanthine to urate/uric acid, a process which occurs in most cell types (Ohtsubo *et al.*, 2004). Xdh has been linked to conditions of cellular injury and was also found to be capable of regulating cellular levels of cyclooxygenase-2 (COX-2), a protein inducible by oxidative stress (Ohtsubo *et al.*, 2004). Tendon fibroblasts also demonstrated the up-regulation of dystonin (Dst), a cytoskeleton-related gene, which contains actin-binding and microtubule-binding domains at either end separated by a plakin domain and several spectrin repeats (Young *et al.*, 2003). The protein encoded by this gene has been found co-aligning with actin stress fibres and has also been detected in the nuclei, most likely a result of a functional nuclear localization signal within the plakin domain (Young *et al.*, 2003). This suggests that dystonin is not only an important cytoplasmic/membrane protein, but also serves a different functional role, given its localization in the nucleus (Young *et al.*, 2003).

4.3.3.2 Corneal fibroblasts

Three of the five differentially regulated genes shown to be highest up-regulated in corneal fibroblasts perform housekeeping roles within the cell. The first of which, aldo-keto reductase family 1, member B3 (Akr1B3), encodes for a protein that is the rate-limiting enzyme in the conversion of glucose to sorbitol, which is then converted to fructose by sorbitol dehydrogenase (Nishinaka and Yabe-Nishimura, 2005). Aldose reductase also catalyzes the reduction of a variety of aldehydes, and thus plays a protective role against the accumulation of toxic aldehydes derived from lipid peroxidation and steroidogensis that could otherwise affect cell growth and differentiation (Lefrancois-Martinez *et al.*, 2004). Expression of Akr1B3 has been found to be activated by osmotic and oxidative stress (Nishinaka and Yabe-Nishimura, 2005). Levels of cytochrome b-5 (Cyb5) transcripts were also shown to be up-regulated in corneal fibroblasts, the protein product of which plays a key role in sterol biosynthesis pathways (Kunic *et al.*, 2001). Finally, the ectonucleotide pyrophosphatase/phosphodiesterase 2 (Enpp2) gene was also shown to be up-regulated with stimulation in corneal fibroblasts. Despite its classical housekeeping role, it appears as though Enpp2 also functions in differentiation of mesenchymal cell lines. Levels of Enpp2 mRNA expression have been shown previously to be highly up-regulated during the differentiation in a primary culture of mouse pre-adipocytes (Ferry *et al.*, 2003). Furthermore, Enpp2 mRNA transcription was also induced during osteo/chondrogenic differentiation *in vitro* (Bachner *et al.*, 1999).

In addition to these three genes, corneal fibroblasts also demonstrated the up-regulation of two ECM/cytoskeletal-related transcripts. The first of which is the gamma-aminobutyric acid receptor-associated protein-like 1, which encodes a protein that acts as a linker between microtubules and the gamma2 subunit of GABA(A) receptors (Xin *et*

al., 2001). The second is sphingosine kinase 1 (Sphk1), a gene which encodes an enzyme that converts sphingosine into sphingosine-1-phosphate (S-1-P). S-1-P is the ligand for a family of G protein-coupled receptors that regulate a wide range of cellular functions, including growth, survival, cytoskeletal rearrangements and cell motility. Overexpression of Sphk1 has been shown to induce extensive stress fibres through the generation of excess S-1-P, which goes on to impair formation of the Src-focal adhesion kinase signalling complex, ultimately leading to aberrant focal adhesion turnover and impaired cell locomotion (Olivera *et al.*, 2003). This overexpression in corneal fibroblasts could be a result of the inherent shear stress being experienced by the cells, leading them to reinforce their contacts to the substrate with a concomitant reduction in locomotion.

4.3.3.3 Skin fibroblasts

In keeping with tendon and corneal fibroblasts, skin cells also demonstrated the up-regulation of a gene involved in the oxidative stress response. This gene encodes the secretory leukocyte protease inhibitor (Slpi), which is thought to act as an anti-inflammatory factor by inhibiting a wide spectrum of proteases and has also been implicated in antimicrobial activity and the suppression of cyclooxygenase-2 (COX-2) production leading to a reduction of prostaglandin E_2, MMP-1 and MMP-9 in monocytes (Kikuchi *et al.*, 2000). Slpi has also been shown to inhibit the collagen gel contraction by fibroblasts in *in vitro* models of wound healing, by causing poor cytoskeletal organization most likely by hindrance of cell-matrix interactions (Sumi *et al.*, 2000).

The remaining four genes shown to be most highly up-regulated in skin fibroblasts either have hitherto unknown functions or appear to play roles in the regulation of cell division or transcriptional regulation during development. The BTB

(POZ) domain containing 11 gene, encodes a protein containing the Bric-a-brac, Tramtrack, Broad complex (BTB) or Poxvirus zinc finger (POZ) domain, which is a widely distributed protein-protein interaction domain. Classically, if the downstream domain is a zinc finger, the protein most likely functions as a transcriptional regulator, whereas if the downstream domain is a kelch motif, the protein most likely binds to actin (Kang *et al.*, 2004; Melnick *et al.*, 2000). Based upon information from the NCBI Conserved Domain Database (Marchler-Bauer *et al.*, 2005), this gene does not contain any identifiable domains downstream of the BTB/POZ domain, so the function of the protein is unclear. Neogenin (Neo) was also shown to be up-regulated with stimulation in skin fibroblasts. Neogenin is a member of the family of neural cell adhesion molecules (N-CAM), but little is known of its function in non-neuronal tissues in vertebrates. Nonetheless, neogenin transcripts have been found to be widely expressed in a broad spectrum of tissues throughout embryogenesis, which implies that it may play a critical role in differentiation and/or cell migration events within embryonic tissues (Keeling *et al.*, 1997).

Endothelin receptor type B (Ednrb) gene was also up-regulated, which has been shown to activate a serum response factor via G proteins (Liu and Wu, 2003). Deletion of this gene leads to arrest at embryonic day 8.5 due to defects associated with mesoderm development (Welsh and O'Brien, 2000). Centaurin, gamma 2 (Centg2), which encodes for a bifunctional GTP-binding and GTPase-activating protein, has been found to alter cell morphology and activation of gene transcription upon its overexpression (Xia *et al.*, 2003).

Overall, and in keeping with the trends discussed previously, genes involved in the oxidative stress response were shown to be differentially regulated with stimulation in each of the cell lines. As mentioned previously, this is most likely a direct result of

the fact that the cells were subjected to 14 hours of fluid flow as a means of stimulation. What is particularly interesting is not so much the fact that the cells are all mounting a similar stress response, but rather the way in which they go about it, for example with the differential regulation of unique oxidative-stress genes.

4.3.4 Genes that were down-regulated with stimulation and identified in one cell line only

In order to complete the picture regarding the differential response of tendon, corneal and skin fibroblasts to fluid flow, the differentially down-regulated genes distinguished by their presence in only one cell line must also be discussed.

4.3.4.1 Tendon fibroblasts

The genes identified as being down-regulated to the greatest extent in tendon fibroblasts function in diverse cellular processes such as differentiation, proliferation and migration. Chemokine (C-X-C motif) ligand 14 (Cxcl14), for example, expresses a protein belonging to a family of cytokines that function in angiogenesis, inflammation, cell recruitment and migration. When Cxcl14 is overexpressed, however, tumour myoepithelial cells demonstrate enhanced proliferation, migration and invasion (Allinen *et al.*, 2004). It would be interesting to determine if the down-regulation of this gene in the context of mechanically stimulated tendon fibroblasts could lead to the reduction of cell density and migration in these cells upon treatment with shear stress. Egr2, a sequence specific DNA-binding transcription factor, appears to be involved in the modulation of cell proliferation (Chavrier *et al.*, 1988; Parkinson *et al.*, 2003). Egr2 has been shown to be transiently activated following serum stimulation of quiescent fibroblasts in culture (Chavrier *et al.*, 1989), and is activated during the G0/G1 transition

in cultured cells. Because serum stimulation of quiescent cells leads to a rapid and transient accumulation of Egr2 mRNA, perhaps the downregulation of Egr2 in tendon fibroblasts is a consequence of the lower serum levels present during stimulation.

In addition to Cxcl14 and Egr2, tendon fibroblasts also demonstrate the down-regulation of the receptor activator of NF-κB ligand (RANKL) as well as embryonic lethal, abnormal vision-like 2 (Elavl2), both of which are implicated in connective tissue maintenance and/or turn-over. RANKL, for example, encodes for a protein that is a member of the TNF superfamily of cytokines and is implicated in stimulating the differentiation and subsequent activation of osteoclast progenitor cells, the cells responsible for bone resorption (Quinn and Gillespie, 2005). Elavl2, on the other hand, encodes an mRNA binding protein belonging to the RNA recognition motif family, which serves to bind to adenine- and uracil-rich elements in the 3'-untranslated regions of various mRNAs, thus controlling the stability of the message (Jain *et al.*, 1997). Interestingly, one study proposes that Elavl2 functions in selecting mRNAs essential for establishing and maintaining the adipocyte phenotype, chaperones them to the cytosol, and controls their expression (Gantt *et al.*, 2004). Furthermore, Elavl2, has been shown to be down-regulated during the conversion of preadipocytes to adipocytes (Qi *et al.*, 2002).

4.3.4.2 Corneal fibroblasts

In corneal fibroblasts, the functional classification of the five genes down-regulated to the greatest extent was very diverse. The gene encoding solute carrier family 4, member 4 (Slc4a4) is an ion transporter known to contribute to intracellular pH regulation during agonist-induced stimulation (Kim *et al.*, 2003a). The anillin (Anln) gene, on the other hand, encodes a protein that has been found to localize to the nucleus

of interphase cells, in the cytoplasm during metaphase, and becomes highly enriched in the cleavage furrow along with myosin II during anaphase-telophase, but is absent from cells that have left the cell cycle. Anillin isolated from embryo extracts has been found to bind directly to actin filaments and be capable of actin bundling. Consequently, anillin is thought to play a role in organizing and stabilizing the cleavage furrow and other cell cycle regulated, contractile domains of the actin cytoskeleton (Field and Alberts, 1995).

The genes encoding Rad51 and Nik-related kinase (Nrk) also showed decreased levels of mRNA in response to mechanical stimulation in corneal fibroblasts. Rad51 plays a pivotal role in various types of DNA repair in mammalian cells (Stark *et al.*, 2002), whereas Nrk is homologous to NCK-interacting kinase (Nik) and is expressed during the late stages of embryogenesis (Nakano *et al.*, 2000). Nrk has been found to selectively activate the JNK pathway (Nakano *et al.*, 2000) and is thought to play a role in cell migration since its protein product is highly homologous to the *Drosophila* Misshapen protein (Su *et al.*, 1998). Misshapen has been found to function upstream of the JNK pathway to stimulate dorsal closure in the *Drosophila* embryo, a process known to involve cell migration (Su *et al.*, 1998). When Nrk was overexpressed in COS-7 cells, however, polymerized actin accumulated, thus implicating Nrk in cytoskeletal organization (Nakano *et al.*, 2003). In the same study, Nakano and colleagues identified cofilin, a protein involved in depolymerising and severing actin filaments, as a substrate for Nrk. This finding led the group to postulate that Nrk may function in cell migration by regulating actin cytoskeletal organization through the cofilin phosphorylation (Nakano *et al.*, 2003). Perhaps the downregulation of Nrk in corneal fibroblasts, as shown in this study, serves to decrease actin polymerization and/or migration in response to laminar fluid flow.

4.3.4.3 Skin fibroblasts

Unlike tendon and corneal fibroblasts, only three functionally annotated genes could be identified as being uniquely down-regulated in skin fibroblasts. The first of these, lipocalin 2 (Lcn2), is a gene expressed during the acute phase response and has been shown to induce apoptosis in haematopoietic and mammary epithelial cells when overexpressed (Bong *et al.*, 2004; Kamezaki *et al.*, 2003). The odd-skipped related 1 (Osr1) gene was also down-regulated in skin fibroblasts with stimulation. Osr1 is widely expressed in mammalian tissues and cell lines and is activated by oxidative stresses and most likely functions as a transcription factor (Chen *et al.*, 2004).

Finally, endothelin 1 (Edn1), which belongs to a multi-functional family of endothelium-derived peptides, was also down-regulated with stimulation in skin fibroblasts. In addition to its role as a potent vasopressor (Desmouliere, 1995), Edn1 has been shown to be capable of modifying ECM metabolism and stimulating proliferation in fibroblasts and osteoblasts (Kopetz *et al.*, 2002). Interestingly, *in vitro* studies have also revealed that Edn1 increases osteoblast-specific gene expression (Kasperk *et al.*, 1997) and serves to induce expression of alpha-smooth muscle actin, ezrin, moesin and paxillin in lung fibroblasts, thus enhancing their ability to contract the ECM (Clarke *et al.*, 2003; Lam *et al.*, 2000; Shi-Wen *et al.*, 2004). In this case, perhaps the down-regulation of Edn1 is either a consequence or indicative of the slower proliferation of skin fibroblasts under fluid flow. Taken further, perhaps the downregulation of Edn1 serves to reinforce the fibroblastic phenotype in these mechanically stimulated cells.

4.3.5 Mechanical stimulation altered genes involved in ECM maintenance and/or actin cytoskeleton organisation

Cells are constantly subjected to a barrage of extracellular chemical, topographical and mechanical signals that ultimately modulate cell function by activating signal transduction pathways. The conversion of mechanical signals into biochemical responses relies on direct or indirect connections between the internal actin cytoskeleton and the ECM. Not surprisingly, numerous studies have shown that cells subjected to mechanical stimuli alter both the gene and protein expression of ECM and cytoskeletal components (Table 3.2). Consequently, several genes implicated in ECM biogenesis and maintenance or cytoskeletal organization identified in one cell line were distinguished.

4.3.5.1 Tendon fibroblasts

Lumican (Lum) is a member of the small leucine rich proteoglycans that has been shown to bind collagen, limit fibril diameter and regulate the kinetics of collagen fibrillogenesis *in vitro* (Doane *et al.*, 1992; Vij *et al.*, 2004). In addition to its role in maintaining the integrity and function of connective tissues, Lum has also been shown to decrease proliferation and increase apoptosis in cells derived from a Lum -/- mouse (Vij *et al.*, 2004) and was shown to be down-regulated during corneal wound healing (Carlson *et al.*, 2003). In this study, lumican was found to be down-regulated in mechanically stimulated tendon fibroblasts, which may indicate that these cells are responding to shear stress by decreasing proliferation and, perhaps, increasing apoptosis.

Levels of transcripts for cysteine and glycine-rich protein 1 (Crp1) were also found to be down-regulated in tendon fibroblasts with stimulation. Crp1 belongs to a family of highly conserved proteins containing two LIM domains with associated glycine-rich repeats. The LIM domain, named after three homeodomain containing

proteins – lin-11, isl-1 and mec-3 – is implicated in protein-protein interactions, may target proteins to distinct subcellular locations, and is thought to mediate the assembly of multimeric protein complexes (Wang *et al.*, 1992). All CRP family members characterized thus far have been shown to interact with alpha-actinin, a filamentious actin cross-linking protein (Harper *et al.*, 2000), and Crp1 itself has also been found to associate with adhesion plaques through its binding to the adhesion complex protein zyxin (Sadler *et al.*, 1992). As a consequence, Crp1 has been implicated in cell proliferation and differentiation, and it is also thought to regulate the stability and structure of adhesion complexes (Sadler *et al.*, 1992). Crp levels have been shown to be induced by serum stimulation (Wang *et al.*, 1992).

Transcripts for the myosin light polypeptide kinase (Mlck) were also reduced in tendon fibroblasts upon stimulation. Mlck is a calcium/calmodulin-dependent serine/threonine protein kinase that activates myosin motor activity by phosphorylating the myosin II regulatory light chain (Blue *et al.*, 2002). Because it also binds actin filaments with high affinity, Mlck has also been identified as regulating diverse cellular functions that rely on interactions of myosin II with the actin cytoskeleton (Smith *et al.*, 2002). Mlck has been previously identified by Ando *et al.* as a shear stress-response gene in endothelial cells, however in this case, Mlck was up-regulated (Ando *et al.*, 1996). Furthermore, in Mlck-inhibited cells, MLC phosphorylation was blocked at the cell periphery but not at the centre of the cell, and zyxin-containing adhesions were not assembled at the periphery of the cell but focal adhesions were maintained in the centre. These cells continued to generate membrane protrusions, but turned over more frequently and migrated less effectively (Totsukawa *et al.*, 2004). Interestingly, despite the fact that transcript levels of Mlck decreased in mechanically stimulated tendon fibroblasts, these cells did not demonstrate a noticeable decrease in the abundance of

zyxin-containing focal contacts, as Totsukawa's study would suggest (see Figure 3.17, section 3.1.5.4). The downregulation of Mlck in tendon fibroblasts is nonetheless interesting and may result from reduced migration of these cells in the presence of fluid flow.

In contrast to Lum, Crp1 and Mlck, which were all down-regulated in tendon fibroblasts, a disintegrin and metalloprotease domain 33 (ADAM33) and chondroitin sulfate proteoglycan 4 (Cspg4) were up-regulated with stimulation. ADAM33 encodes for a relatively new protein, identified in 2002 (Yoshinaka *et al.*, 2002), that belongs to the ADAM family of membrane-anchored proteins, each of which contains a disintegrin and metalloprotease domain. ADAM family proteins are implicated in cell-cell interactions, cell fusion, cell signalling (Gunn *et al.*, 2002) and integrin-mediated signalling pathways (Umland *et al.*, 2004). Cspg4, on the other hand, encodes for a transmembrane chondroitin sulfate proteoglycan, a class of molecules containing a core polypeptide onto which numerous glycosaminoglycan chains are covalently attached. Proteoglycans have been implicated in various cellular roles, such as ECM assembly and structural organization, cellular response to growth and trophic factors, cell-matrix and cell-cell interactions, cell migration, metastasis, and axon outgrowth (Petrini *et al.*, 2003). Cspg4 is an integral membrane proteoglycan that has been shown to interact with ECM components and cell surface molecules (Petrini *et al.*, 2003); it is developmentally regulated, with the highest level of expression being in immature cells and decreasing upon differentiation (Petrini *et al.*, 2003).

4.3.5.2 Corneal fibroblasts

Of particular interest in corneal fibroblasts was the down-regulation of two genes which both encode LIM-domain containing proteins. The first is dyxin, a novel gene

147

encoding a protein containing a cysteine-rich domain at its N-terminus and two LIM domains in the C-terminal region. As above, the presence of LIM domains implies involvement in protein-protein interactions, whereas its prevalent expression in skeletal muscle, combined with the double zinc finger motif contained within the LIM domain has caused some speculation that dyxin could be involved in skeletal muscle development. The differential regulation of dyxin was of particular interest, however, since it is a potential binding partner for β-dystroglycan[1], an adhesion molecule and component of the dystrophin glycoprotein complex, which is itself implicated in muscular dystrophy, development, cell adhesion and signalling (Winder, 2001).

The second LIM domain-containing protein identified in corneal fibroblasts is the LIM domain containing preferred translocation partner in lipoma (Lpp), which contains three C-terminal LIM domains and has been found to localize to focal adhesions but can also be transiently translocated to the nucleus. At cell adhesions, Lpp interacts with the vasodilator-stimulated phosphoprotein (VASP) and alpha-actinin, suggesting that Lpp functions in cell motility and actin dynamics. In the nucleus, however, Lpp maintains transcriptional activation activity, which hints at a role in directly regulating gene expression (Petit *et al.*, 2003).

Corneal fibroblasts also demonstrated a decrease in the level of transcripts for the FERM domain containing 3 (Frmd3) gene. The encoded protein is structurally related to 4.1 proteins, all of which contain a FERM domain (F, 4.1; E, ezrin; R, radixin; M, moesin), which itself comprises binding sites for the cytoplasmic tails of integral membrane proteins, as well as an internal 8-10 kDa domain containing spectrin-actin binding activity required for membrane stability (Ni *et al.*, 2003). Other 4.1 proteins

---

[1] Very soon after the identification of dyxin by Bespalova and Burmeister (Bespalova and Burmeister, 2000), another group submitted a paper claiming dyxin was a novel intracellular binding partner of β-dystroglycan (Holt *et al.*, 1999). When this microarray data was first being compiled and analysed, this reference was accessible in PubMed, but appeared to have been "revoked" due to a publishing discrepancy detailed by the publisher. This reference has since been removed from the database.

have been found to be required for the maintenance of cell shape and membrane mechanical properties through lateral interactions with spectrin and actin in the cytoskeleton and vertical interactions with cytoplasmic domains of transmembrane proteins (Ni *et al.*, 2003).

4.3.6 Genes of interest identified in all three cell lines

In addition to the extracellular matrix and/or cytoskeletal-related genes identified in one cell line only, there were also several genes identified in all three cell lines that were of particular interest. The first, a disintegrin-like and metalloproteinase with thrombospondin type I motif 5 (Adamts5), is akin to the genes discussed previously because it has a role in extracellular matrix remodelling. Adamts5 encodes for a protein that belongs to the ADAM-TS family of metalloproteases. All members of the ADAM-TS family share common domain organization: a pre-pro region to direct synthesis of the protein to the endoplasmic reticulum and maintain the enzyme in its latent form prior to its proteolytic activation, a reprolysin-type catalytic domain, a disintegrin-like domain, and a thrombospondin type-1 module (Hurskainen *et al.*, 1999). Members of the ADAM-TS family have potential roles in embryonic development, cell migration, angiogenesis and ECM breakdown (Bevitt *et al.*, 2003). Adamts5, in particular, is an aggrecanase, capable of degrading the interglobular domain of aggrecan at a specific Glu-Ala bond (Kevorkian *et al.*, 2004). This action has been implicated in rheumatoid and osteoarthritis, where the increased expression of Adamts5 has been correlated with the degradation of aggrecan in cartilaginous tissues, as seen in osteoarthritis.

Genes encoding the serine (or cysteine) proteinase inhibitor, clade B, member 1b (Serpinb1b) and glutathione-S-transferase, alpha 4 (Gsta4) were up-regulated in all cell lines. Serpins are known to regulate intracellular and extracellular proteolytic events

such as apoptosis, complement activation, fibrinolysis and blood coagulation. Clade B serpins have a high degree of sequence identity and are implicated in the regulation of tumour progression, inflammation and cell death. Serpinb1b is known to be a potent inhibitor of the neutrophil granule proteases, which are responsible for the killing of phagocytosed pathogens. An excessive release of these proteases, however, impairs the clearance of apoptotic cells during the inflammatory process (Benarafa *et al.*, 2002). Consequently, an up-regulation in the gene encoding Serpinb1b could act as a mechanism by which to decrease the amount of neurophil proteases in the extracellular milieu, thus increasing the clearance of apoptotic cells.

4.3.7 *Genes implicated in adipogenesis are differentially regulated in mechanically stimulated fibroblasts*

All three cell lines demonstrated the differential regulation of genes implicated in adipocyte differentiation, which is of particular interest given the capability of fibroblast precursors to differentiate along various connective tissue cell-type lineages, such as adipocytes (Wolf *et al.*, 2003). In the case of carbonic anhydrase 3 (Car3) or lipocalin 2 (Lcn2), which have both been found to be expressed at high levels in mature adipocytes (Kim *et al.*, 2001; Kratchmarova *et al.*, 2002), it appears that stimulation is effectively reinforcing the fibroblast phenotype, since levels of these genes were down-regulated with fluid flow. In contrast, however, angiopoietin-like 4 (Angptl4) and ectonucleotide pyrophosphatase/phosphodiesterase 2 (Enpp2) have been shown to be up-regulated during adipocyte differentiation (Ferry *et al.*, 2003; Mandard *et al.*, 2004; Yoon *et al.*, 2000). Because Angptl4 and Enpp2 were both up-regulated in this study in response to stimulation, this hints to the possibility that shear stress is inducing an adipogenic shift in tendon, corneal and skin fibroblasts. While this picture is currently conflicting and

difficult to interpret, the implication of these genes in mesenchymal differentiation is nonetheless remarkable and should be investigated further.

4.3.8   Summary

In summary, we present data that demonstrates clearly that gene expression alters in tendon, corneal and skin fibroblasts following 14 hours of shear stress. The three cell lines show some similarities in their response to stimulation, in particular, with the production of stress-response, signalling- and housekeeping-related genes, but they also clearly maintain unique genetic responses based upon their tissue of localization. Genes involved in these differential responses are functionally diverse, and are shown to be both up- and down-regulated with mechanical stimulation. RT-PCR successfully validated the microarray data in the direction, but not the magnitude, of expression. Furthermore, the encoded proteins from several genes of interest were also shown to change with stimulation, though their expression did not necessarily correlate with mRNA levels. This study provides the first in-depth analysis of the tissue-specific transcriptional response of a cell type to a mechanical stimulus and its comparison to the same cell type in other tissues.

CHAPTER 5

Chapter 5

Final Discussion

Fibroblasts are stromal cells that constitute the predominant cell type in mesenchymal tissues and are considered to be the primary source of most ECM macromolecules. Despite their fundamental role in connective tissue synthesis and widespread use in culture, surprisingly little is known about fibroblasts themselves. The study of these cells is often compromised by several factors, including the accidental inclusion of nonfibroblastic cell types (Boone and Scott, 1980; Kuznetsov and Gehron, 1996), the fact that embryonic mesenchymal stem cells (MSCs) closely resemble fibroblasts themselves (Pittenger *et al.*, 1999), and the distinct lack of knowledge surrounding the differentiation of MSCs into fibroblasts as well as any subsequent "differentiation" that gives rise to heterogeneity in given fibroblast populations. Furthermore, there is no known universal marker for fibroblasts or their differentiation states. This lack of characterization has led to the assumption that cultured fibroblasts are homogeneous, despite increasing evidence that these cells exist as heterogeneous populations based upon their tissue of localisation. In the past, such assumptions have resulted in erroneous interpretation of data (Thompson *et al.*, 1983).

This study has attempted to characterise fibroblasts isolated from three diverse connective tissues based upon their differential responses to an identical mechanical stimulus. In order to circumvent the difficulties mentioned above, fibroblasts were isolated by an established and widely used method, which exploits the rapid adhesion of fibroblasts to facilitate their separation from nonfibroblast-like cells (Spector *et al.*, 1998). Furthermore, fibroblasts tend to overgrow any contaminating cell types after only relatively few cumulative population doublings (CPDs) (Gilbert and Migeon, 1975), so isolated cell lines were maintained in culture for approximately five CPD prior to

experimentation. Isolated cell lines were shown to be of mesenchymal origin based upon the presence and/or absence of tissue-specific intermediate filament types. Moreover, the probability of isolated cell lines consisting of "true" fibroblasts, as opposed to MSCs, was increased, since cells were obtained from 19-day old embryos; in contrast, MSCs are typically isolated from 12- to 13-day old embryos (Spector *et al.*, 1998).

5.1 Morphological characterisation of tendon, corneal and skin fibroblasts

These studies substantiate previous reports (Table 3.1) that tendon, corneal and skin fibroblasts, despite demonstrating typical "fibroblastic" morphology, maintain discrete morphological differences based upon their tissue of origin. According to this study, all cell lines demonstrated an increasingly rounded morphology upon stimulation. There did not, however, appear to be any gross alignment of cells in the direction of flow, nor did stimulation reveal any further morphological distinctions between cells lines that were not already evident in the pre-stimulated fibroblasts. All cell lines demonstrated abundant, focal adhesions and directional stress fibres, though there did not appear to be any gross rearrangement of either with stimulation. There were, however, quantifiable differences in the abundance and classification of focal adhesions both between cell types and with stimulation. Corneal fibroblasts, for example, exhibited fewer focal adhesions per cell and were the only cell line to demonstrate an increase in focal adhesions with stimulation.

The present work also corroborates previous reports that MMP activity alters with mechanical stimulation (Archambault *et al.*, 2002a; Lambert *et al.*, 2001; Prajapati *et al.*, 2000b), and reveals for the first time that tendon, corneal and skin fibroblasts display differential regulation of gelatinase activity, both with and without stimulation. Overall, there was a universal increase in gelatinase activity in each cell line after fluid

flow, and although the cell lines shared this same broad response to stimulation, the magnitude of up-regulation varied based upon the tissue localisation of fibroblasts. In addition to gelatinases, the activity of other MMP subfamilies should be quantified, in order to obtain a comprehensive view of the effect of mechanical stimulation on, and differential regulation of, MMPs in tendon, corneal and skin fibroblasts.

Collectively, these data substantiate previous observations that fibroblasts from different tissues are heterogeneous (Table 3.1) and indicate, for the first time, that tendon, corneal and skin fibroblasts maintain differential morphological and biochemical responses to an identical mechanical stimulus. Had there been no time constraints, it would have been interesting to investigate the effects of variation in the magnitude, duration and type of mechanical stimulation. For example, tendon, corneal and skin fibroblasts may have aligned in the direction of flow or displayed a reorganisation of the actin cytoskeleton, as seen in other cell types (Archambault *et al.*, 2002b; Birukov *et al.*, 2002; Pavalko *et al.*, 1998), if stimulated for a shorter period of time but with a higher magnitude of fluid flow. Moreover, different methods of mechanical stimulation, such as substrate distension or compressive loading, may have revealed further morphological distinctions between the three cell lines. Such studies could further characterise the responses each cell line demonstrated to different mechanical environments, which could provide further insight into the biochemical responses each cell generates after such mechanotransduction *in vivo*.

Additionally, the effect of mechanical stimulation on focal adhesions would be worthy of further study. Recent research has shown that focal adhesions exist as heterogeneous structures, which display variable morphology, protein composition and phosphorylation states in response to chemical or physical parameters, such as the specific types of ECM macromolecules to which integrins can attach or the rigidity of

the extracellular substrate (Katz *et al.*, 2000; Zamir *et al.*, 1999). It is possible, then, that the composition and phosphorylation states of focal adhesions also varies with mechanical stimulation. Although focal adhesions typically contain fundamental building blocks, such as vinculin, zyxin and paxillin, other proteins may positively correlate with exogenous mechanical forces. Investigation of these proteins could reveal possible roles in the regulation of cell-substrate mechanical interactions and shed more light on the process of mechanotransduction in fibroblasts.

5.2 Phenotypic expression of fibroblasts following mechanical stimulation

While numerous investigations have attempted to distinguish fibroblasts from different tissues, this is the first study to examine the large-scale transcriptional responses of tendon, corneal and skin cell lines to mechanical stimulation. From this work, it is apparent that each cell line maintained numerous genes differentially regulated with stimulation. After identification and classification of these genes, it became evident that, while the majority were housekeeping-, signalling-, or stress response-related genes, a substantial number were implicated in adipocyte differentiation, mechanotransduction, and/or the protection of cells against oxidative stress.

The differential regulation of genes shown previously to play roles in adipocyte differentiation was of particular interest, given the capability of fibroblast precursors to differentiate along various connective tissue cell-type lineages (Wolf *et al.*, 2003). In some cases, the differential regulation of these genes with stimulation appeared to be effectively reinforcing the fibroblast phenotype, whereas in others, the direction of regulation suggested some sort of adipogenic shift in tendon, corneal and skin fibroblasts. Consequently, the effect of shear stress on possible fibroblastic and

adipogenic conversions is difficult to interpret, especially since mature fibroblasts are thought to be incapable of differentiating into adipocytes (Pittenger *et al.*, 1999). While it is unlikely that the fibroblasts in this study are exhibiting inter-lineage plasticity, it would be interesting to investigate these and other such genes implicated in adipocyte, chondrogenic and osteogenic differentiation further. For example, since genes previously implicated in adipogenesis were identified as being differentially regulated in mechanically stimulated tendon, corneal and skin fibroblasts, perhaps the mechanical environment of connective tissue cells serves to drive and/or reinforce their differentiation and possibly form the basis for connective tissue specialisation *in vivo*. Indeed, the implication of these genes in mesenchymal differentiation, and possibly mechanotransduction, is significant and requires further investigation.

Interestingly, this study revealed that numerous genes implicated in oxidative stress responses were up-regulated after stimulation, though differing oxidative stress response pathway genes were up-regulated among the cell lines. The production of reactive oxygen species (ROS) has been implicated previously in the activation of MAP kinase signalling pathways in various cell types (Baas and Berk, 1995; Bao *et al.*, 2001), (Hojo *et al.*, 2002; Kamata *et al.*, 2005; Stevenson *et al.*, 1994; Yamamoto *et al.*, 1999). The present study corroborates such findings and suggests that ROS production also modulates mechanotransduction in tendon, corneal and skin fibroblasts. The effect of mechanical stimulation on such signalling pathways, as well as the possible tissue-specific modulation of these pathways in fibroblasts from different tissues, warrants further investigation.

Not surprisingly, a number of other genes that are thought to function in mechanotransduction, either through interactions with the cytoskeleton or providing links from the cytoskeleton to the ECM, were differentially regulated with stimulation.

156

These genes were found to be both up- and down-regulated, and differed based upon the tissue localisation of the given cell lines. Furthermore, a substantial number of genes known to encode proteins that function in ECM/cytoskeletal remodelling were altered with stimulation. While this, perhaps, is to be expected, only one such gene was common to two or more cell lines after mechanical stimulation, with the rest being unique to one of the three lines tested. This trend is seen only in this functional classification and suggests that ECM/cytoskeleton-related genes may make a substantial contribution to the differential response of tendon, corneal and skin cell lines to stimulation, but in a tissue-specific manner.

Although this study has discussed the possible role of a number of differentially transcribed genes, their functions need to be investigated further, particularly in the context of mechanotransduction and maintenance of fibroblast heterogeneity. For example, overexpression or knock-down techniques could be used to probe further the function of genes implicated in mechanical stress responses. Similar techniques could also be used to try to reinforce or revert fibroblast phenotypes to that demonstrated by fibroblasts in other tissues or other connective tissue cells altogether. Prior to these kinds of studies, however, additional research into the differentiation of connective tissue cells from MSCs is necessary, in particular in the identification of suitable markers for the differentiation states of MSCs, fibroblasts and other connective tissue cells. Furthermore, a comprehensive proteomic investigation of stimulated and control tendon, corneal and skin fibroblasts would complement this research. The present study demonstrated that levels of four proteins were altered in the fibroblast cell lines in response to stimulation, though these levels did not necessarily correlate with the microarray data. This occurrence has been documented elsewhere (Lichtinghagen *et al.*, 2002) and is most likely attributable to the regulation of protein levels at both the

transcriptional and translational levels as well as the rate of protein turnover *in vivo*. Nonetheless, this variability indicates that cells possess very complex mechanisms by which they respond to external stimulation, and reinforces the importance of investigating gene as well as protein levels in the cell, in order to gain a comprehensive understanding of cell behaviour to a given stimulus.

While this study provides intriguing insights into both fibroblast heterogeneity and mechanotransduction, the results presented here are nonetheless very complex. For example, it is difficult to ascertain whether shear stress causes tendon fibroblasts to assume a more skin-like phenotype. This, and similar questions, are challenging to answer, given the indisputable gap in information regarding fibroblast heterogeneity and mesenchymal cell differentiation. In hindsight, perhaps these two processes should have been considered independently, for example, by first studying the genetic and proteomic mechanisms that drive and reinforce fibroblast heterogeneity. Perhaps mechanotransduction in different fibroblast cell lines should be investigated only after this heterogeneity was understood and organ- and differentiation-specific markers for fibroblast were identified. By approaching these questions independently, the identification of precise effects of shear stress on tendon, corneal and skin cells might have been more straightforward.

5.3 Summary and implications of fibroblast heterogeneity

In summary, the present study provides evidence that fibroblasts isolated from tendon, cornea and skin are morphologically and phenotypically distinct and respond in unique ways to an identical mechanical stimulus. While these three cell lines show some similarities in their response to stimulation, in particular, with increasingly rounded morphology, elevated gelatinase activity, and the production of stress-response,

signalling- and housekeeping-related genes, they also maintain unique responses based upon their tissue of localisation. It is clear, from the results presented here, that the traditional definition of the fibroblast, which is too often based solely on morphological criteria, needs reappraisal. These findings will provide an invaluable resource for further study of the factors that control cell- and tissue-specific mechanotransduction, and may provide avenues for the manipulation and improvement of tissue engineered prostheses and implants for reconstructive surgery.

APPENDIX

Appendix

A.1 Stock solutions, buffers and media compositions

Adjusting Solution (10x)	Tris-HCl (pH 6.8)	80 mM
	SDS	50% (w/v)
	Glycerol	30% (v/v)
	β-mercamptoethanol	40% (v/v)
	Bromophenol blue	
Alkaline Phosphatase Buffer	NaCl	100 mM
	MgCl$_2$	5 mM
	Tris-HCl (pH 9.5)	100 mM
BCIP Stock	BCIP	57.7 mM
	Made up in	
	dimethylformamide	
Blocking Buffer	Foetal Calf Serum	5% (v/v)
	BSA	1% (w/v)
	Made up in PBS	
Coomassie Blue Stain	Coomassie Blue R250	0.1% (w/v)
	Methanol	40% (v/v)
	Acetic Acid	10% (v/v)
Destaining Solution	Methanol	5% (v/v)
	Acetic Acid	10% (v/v)
Developing Buffer	Tris-HCl	500 mM
	NaCl	2 M
	CaCl2	50 mM
	Brij 35	0.2% (w/v)
	pH 7.8 (adjusted with HCl)	
ECL Solution I	Tris-HCl (pH 8.5)	100 mM
	Luminol	25 mM
	p-Coumaric Acid	396 µM
ECL Solution II	Tris-HCl (pH 8.5)	100 mM
	H$_2$O$_2$	0.02% (v/v)
Mechanical Stimulation Medium	FCS	2% (v/v)
	Penicillin/Streptomycin	1% (v/v)
	in DMEM	

Modified Sample Buffer	Tris-HCl (pH 6.8)	50 mM
	SDS	1% (w/v)
	Glycerol	10% (v/v)
	Pepstatin	1 μM
	PMSF	1 mM
	TPCK	100 μM
	TAME	260 μM
	Benzamidine	10 mM
NBT Stock	NBT	30.6 mM
	Dimethylformamide	70% (v/v)
Orange G Loading Buffer	Ficoll	30% (w/v)
	EDTA (pH 8.0)	100 mM
	Orange G to colour	
Permeabilising Buffer	Glycine	20 mM
	Triton X-100	0.05% (v/v)
	Made up in PBS	
Phosphate Buffered Saline	NaCl	137 mM
	KCl	2.68 mM
	Na_2HPO_4	10 mM
	KH_2PO_4	1.76 mM
Renatuation Buffer	Triton X-100	25% (v/v)
Resolving Gel Buffer	Tris-HCl (pH 8.8)	1.5 M
	SDS	0.4% (w/v)
SDS-PAGE Running Buffer (10x)	Tris	250 mM
	SDS	1% (w/v)
	Glycine	1.92 M
	pH 8.3	
SDS-PAGE Sample Buffer (2x)	Tris-HCl (pH 6.8)	62.5 mM
	SDS	2% (w/v)
	Glycerol	30% (v/v)
	Bromophenol Blue	0.01% (w/v)
	β-mercamptoethanol	710 mM
Stacking Gel Buffer	Tris-HCl (pH 6.8)	0.5 M
	SDS	0.4% (w/v)
Stripping Buffer	Glycine	0.2 M
	SDS	1% (w/v)
	pH 2.5 (adjusted with HCl)	

TAE (50x)	Tris Base	2 M
	Acetic Acid	1 M
	EDTA	50 mM
TBST	Tris-HCl	50 mM
	NaCl	150 mM
	Tween-20	0.05% (v/v)
	pH 8	
Transfer Buffer	Bicine	1.25 mM
	Bis-Tris	1.25 mM
	EDTA	50 μM
	Methanol	10% (v/v)
	pH 7.2	
Working Medium	FCS	15% (v/v)
	in DMEM	
Zymogram Sample Buffer (2x)	Tris-HCl (pH 6.8)	62.5 mM
	SDS	2% (w/v)
	Glycerol	30% (v/v)
	Bromophenol Blue	0.01% (w/v)

A.2 Antibodies, polyacrylamide gel recipes and primers used in RT-PCR

Antibody	Raised In (Species)	Raised Against (Species)	Working dilution	Source
β-actin	Goat	Human	1:500	Santa Cruz
CRP-1	Mouse	Mouse	1:100	BD Biosciences
Desmin	Mouse	Pig	1:200	Sigma
Dyxin	Rabbit	Mouse	1:50	R. Crosbie
Keratin	Guinea Pig	Cow	1:200	Sigma
Lumican	Rabbit	Mouse	1:500	A. Oldberg
Neogenin	Rabbit	Human	1:50	Santa Cruz
Vimentin	Goat	Human	1:400	Sigma
Vinculin	Mouse	Human	1:400	Sigma

Table I: Primary antibodies used in Western blotting and immunofluorescence.

Reagents	Resolving Gel			Stacking Gel
	10%	12%	15%	5%
Acrylamide	4.1 ml	5 ml	6.2 ml	1.5 ml
Resolving Gel Buffer	3.1 ml	3 ml	3 ml	-
Stacking Gel Buffer	-	-	-	2.5 ml
H_2O	5.15 ml	4.3 ml	4.3 ml	5.7 ml
APS (10%)	125 μl	125 μl	125 μl	125 μl
TEMED	10 μl	10 μl	10 μl	10 μl

Table II: Regents used in casting SDS-PAGE gels. Buffer compositions are detailed in section 2.3.

Reagents	Resolving Gel		Stacking Gel
	7.5%	15%	5%
Acrylamide	6.25 ml	12.6 ml	3.32 ml
Resolving Gel Buffer	6.25 ml	6.25 ml	-
Stacking Gel Buffer	-	-	5 ml
Gelatin (10 mg/ml)	2.5 ml	2.5 ml	-
Glycerol	1.4 ml	2.8 ml	-
H_2O	8.5 ml	2.16	11.52 ml
APS (10%)	150 μl	135 μl	120 μl
TEMED	12. 5 μl	12.5 μl	40 μl
Bromophenol Blue	-	+	+

Table III: Reagents used in the production of 7.5-15% gradient gelatin zymograms. Buffer compositions are listed in section 2.3.

163

Gene	F	R	Sequence (5' to 3')	Start	Len	T_m (°C)	GC%	Any	3'	Size
Lumican	✓		ttctctcttgccttggcatt	103	20	58.35	45	6	2	378
		✓	ggactcggtcaggttgttgt	480	20	62.45	55	4	0	
Crp1	✓		gacacctgagcccacatctt	983	20	62.45	55	4	0	538
		✓	gtgaggacttggggttcaaa	1520	20	60.4	50	3	2	
Mylk	✓		gacgtgttcaccctggttct	2397	20	62.45	55	4	0	535
		✓	agtcaacctgctgagggcta	2931	20	62.45	55	4	2	
Marcks	✓		tgggtgggtcaaaaggaata	1702	20	58.35	45	2	2	619
		✓	ttccacgtatcacagcttgg	2320	20	60.4	50	4	3	
Cspg2	✓		agacccactgttttgccaac	3211	20	60.4	50	5	3	442
		✓	gtgactttccaggagcttcg	3652	20	62.45	55	5	2	
Neogenin	✓		ctctaccgctgcattgttga	865	20	60.4	55	4	2	502
		✓	cactggggataaccacatcc	1366	20	62.45	55	6	2	
ADAM33	✓		aacccactacaggccagatg	585	20	62.45	55	4	2	541
		✓	gtcctgagtgatgcgactga	1125	20	62.45	55	3	2	
Cspg4	✓		tgattccttctccctggatg	4032	20	60.4	50	4	2	669
		✓	agggctcctctgtgtgagaa	4700	20	62.45	55	4	1	
Adamts5	✓		gctggacctggagagagatg	317	20	64.5	60	3	0	531
		✓	gagtcagccaccaagaggag	847	20	64.5	60	3	0	
Serpinb1b	✓		ccacacactgaaggaaagca	116	20	60.4	50	3	0	683
		✓	taagacccgtggactcatcc	798	20	62.45	55	4	3	
Ccne2	✓		ggcatgttcacaggaggttt	318	20	60.4	50	4	0	539
		✓	cgatggctagaatgcacaga	856	20	60.4	50	4	0	
Gsta4	✓		gccaagtacccttggttgaa	229	20	60.4	50	6	3	503
		✓	caggacaatcctgaccacct	731	20	62.45	55	7	0	
Cxcl5	✓		gaaagctaagcggaatgcac	413	20	60.4	50	5	2	474
		✓	ggtccccatttcatgagaga	886	20	60.4	50	6	3	
Tslp	✓		ccaggctaccctgaaactga	312	20	62.45	55	8	1	578
		✓	cacctcatcatggcagtgac	889	20	62.45	55	5	3	
Hmox1	✓		aagaggctaagaccgccttc	730	20	62.45	55	5	3	591
		✓	gtcgtggtcagtcaacatgg	1320	20	62.45	55	4	2	
Foxp2	✓		tctaaggaacgcgaacgtct	1801	20	60.4	50	4	2	849
		✓	cacgggttcttccttgacat	2649	20	60.4	50	3	2	
Dyxin	✓		tacatcgtcaccaagggtca	1163	20	60.4	50	3	3	430
		✓	aggcaaacaaatgggagttg	1592	20	58.35	45	3	3	

Table IV: Primers used in semi-quantitative RT-PCR reactions. For each primer, the sequences for the forward (F) and reverse (R) primers are listed, along with the start position (Start), length (Len) in base pairs, melting temperature (T_m), percent of G or C bases (GC%), self-complimentarity score (Any) according to the rodent mispriming library (http://frodo.wi.mit.edu/cgi-bin/primer3/cat_rodent_ref.cgi), the 3' self-complimentarity and the size of the expected product in base pairs is listed.

A.3 Secondary anti-sera controls
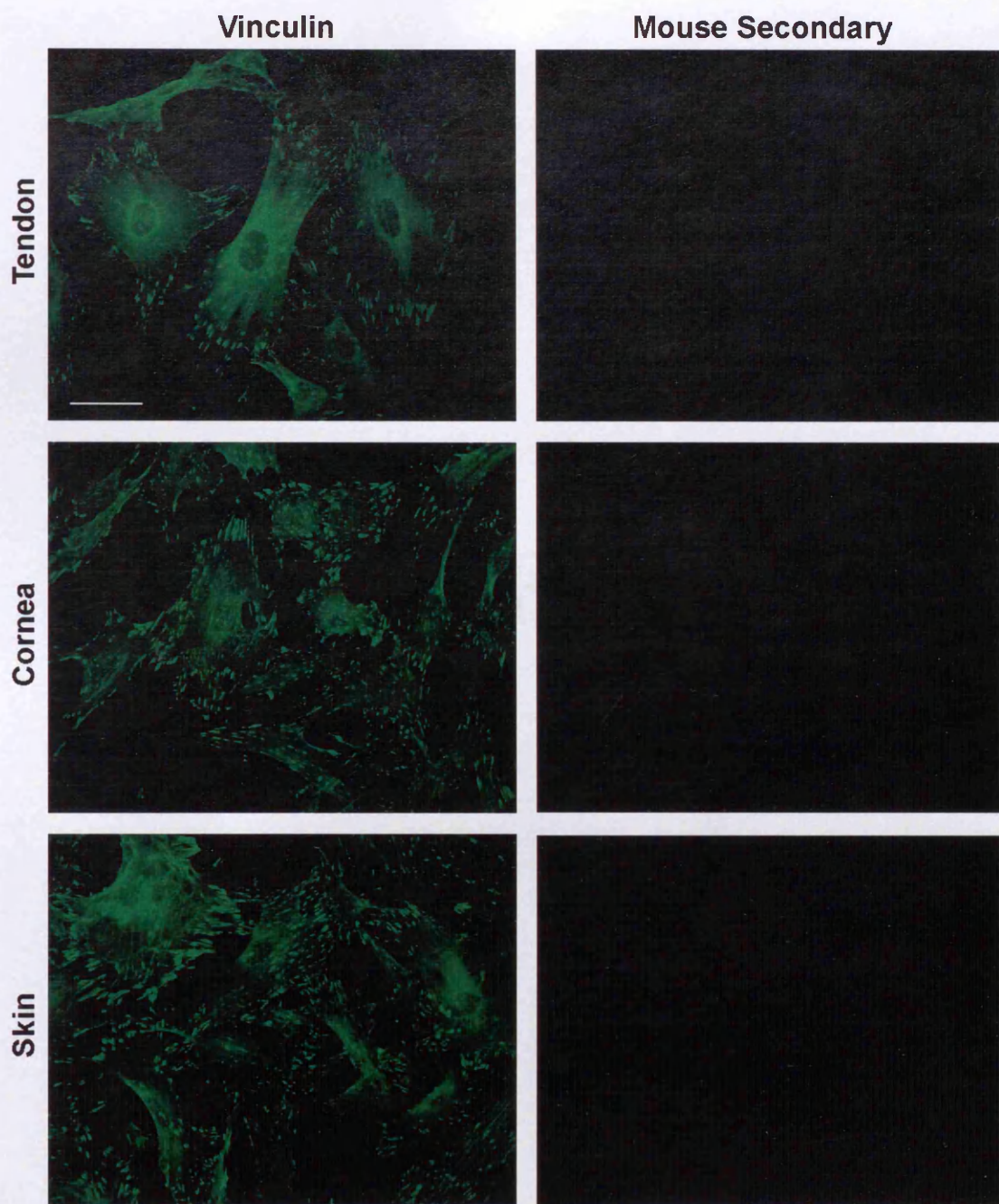
Figure I: Secondary antibody control. Sub-confluent tendon, corneal or skin fibroblasts were stained with either anti-vimentin monoclonal antibody or a mouse secondary antibody alone. Scale bar = 50 μm.

REFERENCES

References

Abramoff M.D., Magelhaes,P.J., and Ram,S.J. (2004). Image Processing with ImageJ. Biophotonics International *11*, 36-42.

Al Shami,A., Spolski,R., Kelly,J., Fry,T., Schwartzberg,P.L., Pandey,A., Mackall,C.L., and Leonard,W.J. (2004). A role for thymic stromal lymphopoietin in CD4(+) T cell development. J. Exp. Med. *200*, 159-168.

Allen,F.D., Hung,C.T., Pollack,S.R., and Brighton,C.T. (2000). Serum modulates the intracellular calcium response of primary cultured bone cells to shear flow. J Biomech. *33*, 1585-1591.

Allinen,M., Beroukhim,R., Cai,L., Brennan,C., Lahti-Domenici,J., Huang,H., Porter,D., Hu,M., Chin,L., Richardson,A., Schnitt,S., Sellers,W.R., and Polyak,K. (2004). Molecular characterization of the tumor microenvironment in breast cancer. Cancer Cell *6*, 17-32.

Ando,J., Tsuboi,H., Korenaga,R., Takahashi,K., Kosaki,K., Isshiki,M., Tojo,T., Takada,Y., and Kamiya,A. (1996). Differential display and cloning of shear stress-responsive messenger RNAs in human endothelial cells. Biochem. Biophys. Res. Commun. *225*, 347-351.

Archambault,J., Tsuzaki,M., Herzog,W., and Banes,A.J. (2002a). Stretch and interleukin-1beta induce matrix metalloproteinases in rabbit tendon cells in vitro. J Orthop. Res *20*, 36-39.

Archambault,J.M., Elfervig-Wall,M.K., Tsuzaki,M., Herzog,W., and Banes,A.J. (2002b). Rabbit tendon cells produce MMP-3 in response to fluid flow without significant calcium transients. J Biomech *35*, 303-309.

Ashburner,M., Ball,C.A., Blake,J.A., Botstein,D., Butler,H., Cherry,J.M., Davis,A.P., Dolinski,K., Dwight,S.S., Eppig,J.T., Harris,M.A., Hill,D.P., Issel-Tarver,L., Kasarskis,A., Lewis,S., Matese,J.C., Richardson,J.E., Ringwald,M., Rubin,G.M., and Sherlock,G. (2000). Gene ontology: tool for the unification of biology. The Gene Ontology Consortium. Nat. Genet. *25* , 25-29.

Atkinson,J.J. and Senior,R.M. (2003). Matrix metalloproteinase-9 in lung remodeling. Am. J. Respir. Cell Mol. Biol. *28*, 12-24.

Baas,A.S. and Berk,B.C. (1995). Differential activation of mitogen-activated protein kinases by H2O2 and O2- in vascular smooth muscle cells. Circ. Res. *77*, 29-36.

Bachner,D., Ahrens,M., Betat,N., Schroder,D., and Gross,G. (1999). Developmental expression analysis of murine autotaxin (ATX). Mech. Dev. *84*, 121-125.

Balaban,N.Q., Schwarz,U.S., Riveline,D., Goichberg,P., Tzur,G., Sabanay,I., Mahalu,D., Safran,S., Bershadsky,A., Addadi,L., and Geiger,B. (2001). Force and focal adhesion assembly: a close relationship studied using elastic micropatterned substrates. Nat. Cell Biol. *3*, 466-472.

Banerjee,H., Hawkins,Z., Johnson,T., Eley,S., Alikhan,A., Mcdaniel,M., Singh,I., and Raymond,J. (2003). Identification of a mouse orthologue of the CED-6 gene of Caenorhabditis elegans. Plasmid *49*, 30-33.

Banes,A.J., Donlon,K., Link,G.W., Gillespie,Y., Bevin,A.G., Peterson,H.D., Bynum,D., Watts,S., and Dahners,L. (1988a). Cell populations of tendon: a simplified method for isolation of synovial cells and internal fibroblasts: confirmation of origin and biologic properties. J Orthop. Res *6*, 83-94.

Banes,A.J., Horesovsky,G., Larson,C., Tsuzaki,M., Judex,S., Archambault,J., Zernicke,R., Herzog,W., Kelley,S., and Miller,L. (1999a). Mechanical load stimulates expression of novel genes in vivo and in vitro in avian flexor tendon cells. Osteoarthritis. Cartilage. *7*, 141-153.

Banes,A.J., Link,G.W., Bevin,A.G., Peterson,H.D., Gillespie,Y., Bynum,D., Watts,S., and Dahners,L. (1988b). Tendon synovial cells secrete fibronectin in vivo and in vitro. J Orthop. Res *6*, 73-82.

Banes,A.J., Weinhold,P., Yang,X., Tsuzaki,M., Bynum,D., Bottlang,M., and Brown,T. (1999b). Gap junctions regulate responses of tendon cells ex vivo to mechanical loading. Clin. Orthop. S356-S370.

Bao,X., Lu,C., and Frangos,J.A. (2001). Mechanism of temporal gradients in shear-induced ERK1/2 activation and proliferation in endothelial cells. Am. J Physiol Heart Circ. Physiol *281*, H22-H29.

Bayreuther,K., Rodemann,H.P., Hommel,R., Dittmann,K., Albiez,M., and Francz,P.I. (1988). Human skin fibroblasts in vitro differentiate along a terminal cell lineage. Proc. Natl. Acad. Sci. U. S. A *85*, 5112-5116.

Benarafa,C., Cooley,J., Zeng,W., Bird,P.I., and Remold-O'Donnell,E. (2002). Characterization of four murine homologs of the human ov-serpin monocyte neutrophil elastase inhibitor MNEI (SERPINB1). J. Biol. Chem. *277*, 42028-42033.

Beningo,K.A., Dembo,M., Kaverina,I., Small,J.V., and Wang,Y.L. (2001). Nascent focal adhesions are responsible for the generation of strong propulsive forces in migrating fibroblasts. J Cell Biol *153*, 881-888.

Benjamin,M. and Ralphs,J.R. (1997). Tendons and ligaments--an overview. Histol. Histopathol. *12*, 1135-1144.

Benson,D.A., Karsch-Mizrachi,I., Lipman,D.J., Ostell,J., and Wheeler,D.L. (2004). GenBank: update. Nucleic Acids Res. *32*, D23-D26.

Bershadsky,A.D., Balaban,N.Q., and Geiger,B. (2003). Adhesion-dependent cell mechanosensitivity. Annu. Rev. Cell Dev. Biol. *19*, 677-695.

Bespalova,I.N. and Burmeister,M. (2000). Identification of a novel LIM domain gene, LMCD1, and chromosomal localization in human and mouse. Genomics *63*, 69-74.

Bevitt,D.J., Mohamed,J., Catterall,J.B., Li,Z., Arris,C.E., Hiscott,P., Sheridan,C., Langton,K.P., Barker,M.D., Clarke,M.P., and McKie,N. (2003). Expression of

ADAMTS metalloproteinases in the retinal pigment epithelium derived cell line ARPE-19: transcriptional regulation by TNFalpha. Biochim. Biophys. Acta *1626*, 83-91.

Billotte,W.G. and Hofmann,M.C. (1999). Establishment of a shear stress protocol to study the mechanosensitivity of human primary osteogenic cells in vitro. Biomed. Sci. Instrum. *35*, 327-332.

Birkedal-Hansen,H., Cobb,C.M., Taylor,R.E., and Fullmer,H.M. (1976). Synthesis and release of procollagenase by cultured fibroblasts. J. Biol. Chem. *251*, 3162-3168.

Birukov,K.G., Birukova,A.A., Dudek,S.M., Verin,A.D., Crow,M.T., Zhan,X., DePaola,N., and Garcia,J.G. (2002). Shear stress-mediated cytoskeletal remodeling and cortactin translocation in pulmonary endothelial cells. Am. J. Respir. Cell Mol. Biol. *26*, 453-464.

Blain,E.J., Gilbert,S.J., Wardale,R.J., Capper,S.J., Mason,D.J., and Duance,V.C. (2001). Up-regulation of matrix metalloproteinase expression and activation following cyclical compressive loading of articular cartilage in vitro. Arch. Biochem Biophys. *396*, 49-55.

Blake,J.A., Richardson,J.E., Bult,C.J., Kadin,J.A., and Eppig,J.T. (2003). MGD: the Mouse Genome Database. Nucleic Acids Res. *31*, 193-195.

Blue,E.K., Goeckeler,Z.M., Jin,Y., Hou,L., Dixon,S.A., Herring,B.P., Wysolmerski,R.B., and Gallagher,P.J. (2002). 220- and 130-kDa MLCKs have distinct tissue distributions and intracellular localization patterns. Am. J. Physiol Cell Physiol *282*, C451-C460.

Bode,W. (1995). A helping hand for collagenases: the haemopexin-like domain. Structure. *3*, 527-530.

Bode,W., Gomis-Ruth,F.X., and Stockler,W. (1993). Astacins, serralysins, snake venom and matrix metalloproteinases exhibit identical zinc-binding environments (HEXXHXXGXXH and Met-turn) and topologies and should be grouped into a common family, the 'metzincins'. FEBS Lett. *331*, 134-140.

Bong,J.J., Seol,M.B., Kim,H.H., Han,O., Back,K., and Baik,M. (2004). The 24p3 gene is induced during involution of the mammary gland and induces apoptosis of mammary epithelial cells. Mol. Cells *17*, 29-34.

Boone,C.W. and Scott,R.E. (1980). Plate-induced tumors of BALB/3T3 cells exhibiting foci of differentiation into pericytes, chondrocytes, and fibroblasts. J Supramol. Struct. *14*, 233-240.

Breen,E., Falco,V.M., Absher,M., and Cutroneo,K.R. (1990). Subpopulations of rat lung fibroblasts with different amounts of type I and type III collagen mRNAs. J. Biol. Chem. *265*, 6286-6290.

Breitling,R., Amtmann,A., and Herzyk,P. (2004a). Iterative Group Analysis (iGA): a simple tool to enhance sensitivity and facilitate interpretation of microarray experiments. BMC. Bioinformatics. *5*, 34.

Breitling,R., Armengaud,P., Amtmann,A., and Herzyk,P. (2004b). Rank products: a simple, yet powerful, new method to detect differentially regulated genes in replicated microarray experiments. FEBS Lett. *573*, 83-92.

Bron,A.J. (2001). The architecture of the corneal stroma. Br. J Ophthalmol. *85*, 379-381.

Brown,R.A., Sethi,K.K., Gwanmesia,I., Raemdonck,D., Eastwood,M., and Mudera,V. (2002). Enhanced fibroblast contraction of 3D collagen lattices and integrin expression by TGF-beta1 and -beta3: mechanoregulatory growth factors? Exp. Cell Res *274*, 310-322.

Brown,T.D. (2000). Techniques for mechanical stimulation of cells in vitro: a review. J. Biomech. *33*, 3-14.

Burridge,K. and Chrzanowska-Wodnicka,M. (1996). Focal adhesions, contractility, and signaling. Annu. Rev. Cell Dev. Biol. *12*, 463-518.

Butcher,J.T., Penrod,A.M., Garcia,A.J., and Nerem,R.M. (2004). Unique morphology and focal adhesion development of valvular endothelial cells in static and fluid flow environments. Arterioscler. Thromb. Vasc. Biol. *24*, 1429-1434.

Camelliti,P., Borg,T.K., and Kohl,P. (2005). Structural and functional characterisation of cardiac fibroblasts. Cardiovasc. Res. *65*, 40-51.

Canty,E.G. and Kadler,K.E. (2002). Collagen fibril biosynthesis in tendon: a review and recent insights. Comp Biochem. Physiol A Mol. Integr. Physiol *133*, 979-985.

Caplan,A.I. (1991). Mesenchymal stem cells. J Orthop. Res. *9*, 641-650.

Caplan,A.I. and Bruder,S.P. (2001). Mesenchymal stem cells: building blocks for molecular medicine in the 21st century. Trends Mol. Med *7*, 259-264.

Carlson,E.C., Wang,I.J., Liu,C.Y., Brannan,P., Kao,C.W., and Kao,W.W. (2003). Altered KSPG expression by keratocytes following corneal injury. Mol. Vis. *9*, 615-623.

Carlson,S.S. and Hockfield,S. (1996). Extracellular Matrix., W.D.Comper, ed. (Amsterdam: Harwood), pp. 1-23.

Chapman,J.A. (1962). Fibroblasts and collagen. Br. Med Bull. *18*, 233-237.

Chavrier,P., Janssen-Timmen,U., Mattei,M.G., Zerial,M., Bravo,R., and Charnay,P. (1989). Structure, chromosome location, and expression of the mouse zinc finger gene Krox-20: multiple gene products and coregulation with the proto-oncogene c-fos. Mol. Cell Biol. *9*, 787-797.

Chavrier,P., Zerial,M., Lemaire,P., Almendral,J., Bravo,R., and Charnay,P. (1988). A gene encoding a protein with zinc fingers is activated during G0/G1 transition in cultured cells. EMBO J. *7*, 29-35.

Chen,N.X., Ryder,K.D., Pavalko,F.M., Turner,C.H., Burr,D.B., Qiu,J., and Duncan,R.L. (2000). Ca(2+) regulates fluid shear-induced cytoskeletal reorganization and gene expression in osteoblasts. Am. J. Physiol Cell Physiol *278*, C989-C997.

Chen,W., Yazicioglu,M., and Cobb,M.H. (2004). Characterization of OSR1, a member of the mammalian Ste20p/germinal center kinase subfamily. J. Biol. Chem. *279*, 11129-11136.

Chichester,C.O., Fernandez,M., and Minguell,J.J. (1993). Extracellular matrix gene expression by human bone marrow stroma and by marrow fibroblasts. Cell Adhes. Commun. *1*, 93-99.

Chiquet,M. (1999). Regulation of extracellular matrix gene expression by mechanical stress. Matrix Biol *18*, 417-426.

Chiquet,M., Renedo,A.S., Huber,F., and Fluck,M. (2003). How do fibroblasts translate mechanical signals into changes in extracellular matrix production? Matrix Biol. *22*, 73-80.

Choi,B.M., Pae,H.O., Kim,Y.M., and Chung,H.T. (2003). Nitric oxide-mediated cytoprotection of hepatocytes from glucose deprivation-induced cytotoxicity: involvement of heme oxygenase-1. Hepatology *37*, 810-823.

Choquet,D., Felsenfeld,D.P., and Sheetz,M.P. (1997). Extracellular matrix rigidity causes strengthening of integrin-cytoskeleton linkages. Cell *88*, 39-48.

Clark,I.M., Powell,L.K., and Cawston,T.E. (1994). Tissue inhibitor of metalloproteinases (TIMP-1) stimulates the secretion of collagenase from human skin fibroblasts. Biochem. Biophys. Res. Commun. *203*, 874-880.

Clarke,K.J., Zhong,Q., Schwartz,D.D., Coleman,E.S., Kemppainen,R.J., and Judd,R.L. (2003). Regulation of adiponectin secretion by endothelin-1. Biochem. Biophys. Res. Commun. *312*, 945-949.

Comper,W.D. (1996). Extracellular Matrix., W.D.Comper, ed. (Amsterdam: Harwood), pp. 1-21.

Conrad,G.W., Hamilton,C., and Haynes,E. (1977a). Differences in glycosaminoglycans synthesized by fibroblast-like cells from chick cornea, heart, and skin. J Biol Chem. *252*, 6861-6870.

Conrad,G.W., Hart,G.W., and Chen,Y. (1977b). Differences in vitro between fibroblast-like cells from cornea, heart, and skin of embryonic chicks. J Cell Sci *26*, 119-137.

Cope,L.M., Irizarry,R.A., Jaffee,H.A., Wu,Z., and Speed,T.P. (2004). A benchmark for Affymetrix GeneChip expression measures. Bioinformatics. *20*, 323-331.

Coussens,L.M. and Werb,Z. (1996). Matrix metalloproteinases and the development of cancer. Chem. Biol. *3*, 895-904.

Daly,C.H. (1982). Biomechanical properties of dermis. J Invest Dermatol. *79 Suppl 1*, 17s-20s.

Danielson,K.G., Baribault,H., Holmes,D.F., Graham,H., Kadler,K.E., and Iozzo,R.V. (1997). Targeted disruption of decorin leads to abnormal collagen fibril morphology and skin fragility. J Cell Biol *136*, 729-743.

Davies,P.F., Robotewskyj,A., and Griem,M.L. (1994). Quantitative studies of endothelial cell adhesion. Directional remodeling of focal adhesion sites in response to flow forces. J. Clin. Invest *93*, 2031-2038.

Desmouliere,A. (1995). Factors influencing myofibroblast differentiation during wound healing and fibrosis. Cell Biol. Int. *19*, 471-476.

Diehn,M., Sherlock,G., Binkley,G., Jin,H., Matese,J.C., Hernandez-Boussard,T., Rees,C.A., Cherry,J.M., Botstein,D., Brown,P.O., and Alizadeh,A.A. (2003). SOURCE: a unified genomic resource of functional annotations, ontologies, and gene expression data. Nucleic Acids Res. *31*, 219-223.

Doane,K.J., Babiarz,J.P., Fitch,J.M., Linsenmayer,T.F., and Birk,D.E. (1992). Collagen fibril assembly by corneal fibroblasts in three-dimensional collagen gel cultures: small-diameter heterotypic fibrils are deposited in the absence of keratan sulfate proteoglycan. Exp. Cell Res. *202*, 113-124.

Dressler,M.R., Butler,D.L., Wenstrup,R., Awad,H.A., Smith,F., and Boivin,G.P. (2002). A potential mechanism for age-related declines in patellar tendon biomechanics. J Orthop. Res. *20*, 1315-1322.

Dunn,M.G. and Silver,F.H. (1983). Viscoelastic behavior of human connective tissues: relative contribution of viscous and elastic components. Connect. Tissue Res. *12*, 59-70.

Dunphy,J.E. (1963). The fibroblast - A ubiquitous ally for the surgeon. N. Engl. J. Med. *268*, 1367-1377.

Eastwood,M., McGrouther,D.A., and Brown,R.A. (1998). Fibroblast responses to mechanical forces. Proc. Inst. Mech. Eng [H.] *212*, 85-92.

Eastwood,M., Porter,R., Khan,U., McGrouther,G., and Brown,R. (1996). Quantitative analysis of collagen gel contractile forces generated by dermal fibroblasts and the relationship to cell morphology. J Cell Physiol *166*, 33-42.

Elfervig,M.K., Minchew,J.T., Francke,E., Tsuzaki,M., and Banes,A.J. (2001). IL-1beta sensitizes intervertebral disc annulus cells to fluid-induced shear stress. J Cell Biochem *82*, 290-298.

Elsdale,T. and Bard,J. (1972). Collagen substrata for studies on cell behavior. J Cell Biol. *54*, 626-637.

Evans,C.E. and Trail,I.A. (2001). An in vitro comparison of human flexor and extensor tendon cells. J. Hand Surg. [Br.] *26*, 307-313.

Fanger,G.R., Johnson,N.L., and Johnson,G.L. (1997). MEK kinases are regulated by EGF and selectively interact with Rac/Cdc42. EMBO J. *16*, 4961-4972.

Ferry,G., Tellier,E., Try,A., Gres,S., Naime,I., Simon,M.F., Rodriguez,M., Boucher,J., Tack,I., Gesta,S., Chomarat,P., Dieu,M., Raes,M., Galizzi,J.P., Valet,P., Boutin,J.A., and Saulnier-Blache,J.S. (2003). Autotaxin is released from adipocytes, catalyzes lysophosphatidic acid synthesis, and activates preadipocyte proliferation. Up-regulated expression with adipocyte differentiation and obesity. J. Biol. Chem. *278*, 18162-18169.

Field,C.M. and Alberts,B.M. (1995). Anillin, a contractile ring protein that cycles from the nucleus to the cell cortex. J. Cell Biol. *131*, 165-178.

Fini,M.E., Girard,M.T., Matsubara,M., and Bartlett,J.D. (1995). Unique regulation of the matrix metalloproteinase, gelatinase B. Invest Ophthalmol. Vis. Sci *36*, 622-633.

Fiore,E., Fusco,C., Romero,P., and Stamenkovic,I. (2002). Matrix metalloproteinase 9 (MMP-9/gelatinase B) proteolytically cleaves ICAM-1 and participates in tumor cell resistance to natural killer cell-mediated cytotoxicity. Oncogene *21*, 5213-5223.

Force,T., Pombo,C.M., Avruch,J.A., Bonventre,J.V., and Kyriakis,J.M. (1996). Stress-activated protein kinases in cardiovascular disease. Circ. Res. *78*, 947-953.

Funderburgh,J.L. and Conrad,G.W. (1990). Isoforms of corneal keratan sulfate proteoglycan. J. Biol. Chem. *265*, 8297-8303.

Funderburgh,J.L., Funderburgh,M.L., Mann,M.M., and Conrad,G.W. (1991). Unique glycosylation of three keratan sulfate proteoglycan isoforms. J. Biol. Chem. *266*, 14226-14231.

Funderburgh,J.L., Mann,M.M., and Funderburgh,M.L. (2003). Keratocyte phenotype mediates proteoglycan structure: a role for fibroblasts in corneal fibrosis. J Biol. Chem. *278*, 45629-45637.

Gabbiani,G. and Rungger-Brandle,E. (1981). Handbook of Inflammation. Tissue Repair and Regeneration., L.E.Glynn, ed. (Amsterdam: Elsevier/North-Holland Biomedical Press), pp. 1-50.

Gantt,K.R., Jain,R.G., Dudek,R.W., and Pekala,P.H. (2004). HuB localizes to polysomes and alters C/EBP-beta expression in 3T3-L1 adipocytes. Biochem. Biophys. Res. Commun. *313*, 619-622.

Garrett,D.M. and Conrad,G.W. (1979). Fibroblast-like cells from embryonic chick cornea, heart, and skin are antigenically distinct. Dev. Biol *70*, 50-70.

Geiger,B. and Bershadsky,A. (2001). Assembly and mechanosensory function of focal contacts. Curr. Opin. Cell Biol. *13*, 584-592.

Gerwins,P., Blank,J.L., and Johnson,G.L. (1997). Cloning of a novel mitogen-activated protein kinase kinase kinase, MEKK4, that selectively regulates the c-Jun amino terminal kinase pathway. J. Biol. Chem. *272*, 8288-8295.

Gilbert,S.F. and Migeon,B.R. (1975). D-valine as a selective agent for normal human and rodent epithelial cells in culture. Cell *5*, 11-17.

Gomez,D.E., Alonso,D.F., Yoshiji,H., and Thorgeirsson,U.P. (1997). Tissue inhibitors of metalloproteinases: structure, regulation and biological functions. Eur. J Cell Biol. *74*, 111-122.

Goodman,A.R., Cardozo,T., Abagyan,R., Altmeyer,A., Wisniewski,H.G., and Vilcek,J. (1996). Long pentraxins: an emerging group of proteins with diverse functions. Cytokine Growth Factor Rev. *7*, 191-202.

172

Greenbaum,D., Colangelo,C., Williams,K., and Gerstein,M. (2003). Comparing protein abundance and mRNA expression levels on a genomic scale. Genome Biol. *4*, 117.

Grierson,J.P. and Meldolesi,J. (1995). Shear stress-induced [Ca2+]i transients and oscillations in mouse fibroblasts are mediated by endogenously released ATP. J. Biol. Chem. *270*, 4451-4456.

Grinnell,F. (2000). Fibroblast-collagen-matrix contraction: growth-factor signalling and mechanical loading. Trends Cell Biol. *10*, 362-365.

Guan,K.L. and Butch,E. (1995). Isolation and characterization of a novel dual specific phosphatase, HVH2, which selectively dephosphorylates the mitogen-activated protein kinase. J. Biol. Chem. *270*, 7197-7203.

Gudas,J.M., Payton,M., Thukral,S., Chen,E., Bass,M., Robinson,M.O., and Coats,S. (1999). Cyclin E2, a novel G1 cyclin that binds Cdk2 and is aberrantly expressed in human cancers. Mol. Cell Biol. *19*, 612-622.

Gunn,T.M., Azarani,A., Kim,P.H., Hyman,R.W., Davis,R.W., and Barsh,G.S. (2002). Identification and preliminary characterization of mouse Adam33. BMC. Genet. *3*, 2.

Haier,J. and Nicolson,G.L. (2002). PTEN regulates tumor cell adhesion of colon carcinoma cells under dynamic conditions of fluid flow. Oncogene *21*, 1450-1460.

Hanson,A.N. and Bentley,J.P. (1983). Quantitation of type I to type III collagen ratios in small samples of human tendon, blood vessels, and atherosclerotic plaque. Anal. Biochem. *130*, 32-40.

Harper,B.D., Beckerle,M.C., and Pomies,P. (2000). Fine mapping of the alpha-actinin binding site within cysteine-rich protein. Biochem. J. *350 Pt 1*, 269-274.

Harper,R.A. and Grove,G. (1979). Human skin fibroblasts derived from papillary and reticular dermis: differences in growth potential in vitro. Science *204*, 526-527.

Hassell,J.R., Robey,P.G., Barrach,H.J., Wilczek,J., Rennard,S.I., and Martin,G.R. (1980). Isolation of a heparan sulfate-containing proteoglycan from basement membrane. Proc. Natl. Acad. Sci. U. S. A *77*, 4494-4498.

Hayakawa,K., Sato,N., and Obinata,T. (2001). Dynamic reorientation of cultured cells and stress fibers under mechanical stress from periodic stretching. Exp. Cell Res. *268*, 104-114.

Herrmann,H., Dessau,W., Fessler,L.I., and von der,M.K. (1980). Synthesis of types I, III and AB2 collagen by chick tendon fibroblasts in vitro. Eur. J Biochem *105*, 63-74.

Hojo,Y., Saito,Y., Tanimoto,T., Hoefen,R.J., Baines,C.P., Yamamoto,K., Haendeler,J., Asmis,R., and Berk,B.C. (2002). Fluid shear stress attenuates hydrogen peroxide-induced c-Jun NH2-terminal kinase activation via a glutathione reductase-mediated mechanism. Circ. Res. *91*, 712-718.

Holt,H.H., Crosbie,R.H., Saito,F., and Campbell,K.P. (1999). Identification of Dyxin: A Novel Intracellular Binding Partner of beta-dystroglycan. Unpublished.

Huang,A.M., Montagna,C., Sharan,S., Ni,Y., Ried,T., and Sterneck,E. (2004). Loss of CCAAT/enhancer binding protein delta promotes chromosomal instability. Oncogene *23*, 1549-1557.

Hung,C.T., Allen,F.D., Pollack,S.R., Attia,E.T., Hannafin,J.A., and Torzilli,P.A. (1997). Intracellular calcium response of ACL and MCL ligament fibroblasts to fluid-induced shear stress. Cell Signal. *9*, 587-594.

Hung,C.T., Henshaw,D.R., Wang,C.C., Mauck,R.L., Raia,F., Palmer,G., Chao,P.H., Mow,V.C., Ratcliffe,A., and Valhmu,W.B. (2000). Mitogen-activated protein kinase signaling in bovine articular chondrocytes in response to fluid flow does not require calcium mobilization. J. Biomech. *33*, 73-80.

Hurskainen,T.L., Hirohata,S., Seldin,M.F., and Apte,S.S. (1999). ADAM-TS5, ADAM-TS6, and ADAM-TS7, novel members of a new family of zinc metalloproteases. General features and genomic distribution of the ADAM-TS family. J. Biol. Chem. *274*, 25555-25563.

Hynes,R. (1999). Fibronectins. In Guidebook to the Extracellular Matrix, Anchor adn Adhesion Proteins, T.Kreis and R.Vale, eds. (Oxford: Oxford University Press), pp. 422-425.

Hynes,R.O. (1996). Targeted mutations in cell adhesion genes: what have we learned from them? Dev. Biol. *180*, 402-412.

Ingber,D. (1999). How cells (might) sense microgravity. FASEB J *13 Suppl*, S3-15.

Iozzo,R.V. and Murdoch,A.D. (1996). Proteoglycans of the extracellular environment: clues from the gene and protein side offer novel perspectives in molecular diversity and function. FASEB J *10*, 598-614.

Irizarry,R.A., Hobbs,B., Collin,F., Beazer-Barclay,Y.D., Antonellis,K.J., Scherf,U., and Speed,T.P. (2003). Exploration, normalization, and summaries of high density oligonucleotide array probe level data. Biostatistics. *4*, 249-264.

Irwin,C.R., Picardo,M., Ellis,I., Sloan,P., Grey,A., McGurk,M., and Schor,S.L. (1994). Inter- and intra-site heterogeneity in the expression of fetal-like phenotypic characteristics by gingival fibroblasts: potential significance for wound healing. J Cell Sci *107 (Pt 5)*, 1333-1346.

Itoh,Y., Kajita,M., Kinoh,H., Mori,H., Okada,A., and Seiki,M. (1999). Membrane type 4 matrix metalloproteinase (MT4-MMP, MMP-17) is a glycosylphosphatidylinositol-anchored proteinase. J Biol. Chem. *274*, 34260-34266.

Jain,R.G., Andrews,L.G., McGowan,K.M., Pekala,P.H., and Keene,J.D. (1997). Ectopic expression of Hel-N1, an RNA-binding protein, increases glucose transporter (GLUT1) expression in 3T3-L1 adipocytes. Mol. Cell Biol. *17*, 954-962.

Joshi-Tope,G., Gillespie,M., Vastrik,I., D'Eustachio,P., Schmidt,E., de Bono,B., Jassal,B., Gopinath,G.R., Wu,G.R., Matthews,L., Lewis,S., Birney,E., and Stein,L. (2005). Reactome: a knowledgebase of biological pathways. Nucleic Acids Res. *33*, D428-D432.

Kabakov,A.E. and Gabai,V.L. (1995). Heat shock-induced accumulation of 70-kDa stress protein (HSP70) can protect ATP-depleted tumor cells from necrosis. Exp. Cell Res. *217*, 15-21.

Kamata,H., Honda,S., Maeda,S., Chang,L., Hirata,H., and Karin,M. (2005). Reactive oxygen species promote TNFalpha-induced death and sustained JNK activation by inhibiting MAP kinase phosphatases. Cell *120*, 649-661.

Kamezaki,K., Shimoda,K., Numata,A., Aoki,K., Kato,K., Takase,K., Nakajima,H., Ihara,K., Haro,T., Ishikawa,F., Imamura,R., Miyamoto,T., Nagafuji,K., Gondo,H., Hara,T., and Harada,M. (2003). The lipocalin 24p3, which is an essential molecule in IL-3 withdrawal-induced apoptosis, is not involved in the G-CSF withdrawal-induced apoptosis. Eur. J. Haematol. *71*, 412-417.

Kaname,S. and Ruoslahti,E. (1996). Betaglycan has multiple binding sites for transforming growth factor-beta 1. Biochem. J *315 (Pt 3)*, 815-820.

Kang,M.I., Kobayashi,A., Wakabayashi,N., Kim,S.G., and Yamamoto,M. (2004). Scaffolding of Keap1 to the actin cytoskeleton controls the function of Nrf2 as key regulator of cytoprotective phase 2 genes. Proc. Natl. Acad. Sci. U. S. A *101*, 2046-2051.

Kanwar,Y.S., Linker,A., and Farquhar,M.G. (1980). Increased permeability of the glomerular basement membrane to ferritin after removal of glycosaminoglycans (heparan sulfate) by enzyme digestion. J Cell Biol. *86*, 688-693.

Karring,H., Thogersen,I.B., Klintworth,G.K., Enghild,J.J., and Moller-Pedersen,T. (2004). Proteomic analysis of the soluble fraction from human corneal fibroblasts with reference to ocular transparency. Mol. Cell Proteomics. *3*, 660-674.

Kasperk,C.H., Borcsok,I., Schairer,H.U., Schneider,U., Nawroth,P.P., Niethard,F.U., and Ziegler,R. (1997). Endothelin-1 is a potent regulator of human bone cell metabolism in vitro. Calcif. Tissue Int. *60*, 368-374.

Katz,B.Z., Zamir,E., Bershadsky,A., Kam,Z., Yamada,K.M., and Geiger,B. (2000). Physical state of the extracellular matrix regulates the structure and molecular composition of cell-matrix adhesions. Mol. Biol. Cell *11*, 1047-1060.

Kaufman,M., Pinsky,L., Straisfeld,C., Shanfield,B., and Zilahi,B. (1975). Qualitative differences in testosterone metabolism as an indication of cellular heterogeneity in fibroblast monolayers derived from human preputial skin. Exp. Cell Res *96*, 31-36.

Keeling,S.L., Gad,J.M., and Cooper,H.M. (1997). Mouse Neogenin, a DCC-like molecule, has four splice variants and is expressed widely in the adult mouse and during embryogenesis. Oncogene *15*, 691-700.

Kessler,D., Dethlefsen,S., Haase,I., Plomann,M., Hirche,F., Krieg,T., and Eckes,B. (2001). Fibroblasts in mechanically stressed collagen lattices assume a "synthetic" phenotype. J Biol Chem. *276*, 36575-36585.

Kevorkian,L., Young,D.A., Darrah,C., Donell,S.T., Shepstone,L., Porter,S., Brockbank,S.M., Edwards,D.R., Parker,A.E., and Clark,I.M. (2004). Expression

profiling of metalloproteinases and their inhibitors in cartilage. Arthritis Rheum. *50*, 131-141.

Kikuchi,T., Abe,T., Yaekashiwa,M., Tominaga,Y., Mitsuhashi,H., Satoh,K., Nakamura,T., and Nukiwa,T. (2000). Secretory leukoprotease inhibitor augments hepatocyte growth factor production in human lung fibroblasts. Am. J. Respir. Cell Mol. Biol. *23*, 364-370.

Kim,G., Lee,T., Wynshaw-Boris,A., and Levine,R.L. (2001). Nucleotide sequence and structure of the mouse carbonic anhydrase III gene. Gene *265*, 37-44.

Kim,I., Kim,H.G., Kim,H., Kim,H.H., Park,S.K., Uhm,C.S., Lee,Z.H., and Koh,G.Y. (2000). Hepatic expression, synthesis and secretion of a novel fibrinogen/angiopoietin-related protein that prevents endothelial-cell apoptosis. Biochem. J. *346 Pt 3*, 603-610.

Kim,Y.B., Yang,B.H., Piao,Z.G., Oh,S.B., Kim,J.S., and Park,K. (2003a). Expression of Na+/HCO3- cotransporter and its role in pH regulation in mouse parotid acinar cells. Biochem. Biophys. Res. Commun. *304*, 593-598.

Kim,Y.B., Yang,B.H., Piao,Z.G., Oh,S.B., Kim,J.S., and Park,K. (2003b). Expression of Na+/HCO3- cotransporter and its role in pH regulation in mouse parotid acinar cells. Biochem. Biophys. Res. Commun. *304*, 593-598.

Kjaer,M. (2004). Role of extracellular matrix in adaptation of tendon and skeletal muscle to mechanical loading. Physiol Rev. *84*, 649-698.

Kleiner,D.E. and Stetler-Stevenson,W.G. (1994). Quantitative zymography: detection of picogram quantities of gelatinases. Anal. Biochem. *218*, 325-329.

Knauper,V., Docherty,A.J., Smith,B., Tschesche,H., and Murphy,G. (1997). Analysis of the contribution of the hinge region of human neutrophil collagenase (HNC, MMP-8) to stability and collagenolytic activity by alanine scanning mutagenesis. FEBS Lett. *405*, 60-64.

Ko,K.S. and McCulloch,C.A. (2001). Intercellular mechanotransduction: cellular circuits that coordinate tissue responses to mechanical loading. Biochem Biophys. Res Commun. *285*, 1077-1083.

Ko,S.D., Page,R.C., and Narayanan,A.S. (1977). Fibroblast heterogeneity and prostaglandin regulation of subpopulations. Proc. Natl. Acad. Sci U. S. A *74*, 3429-3432.

Kobayashi,T., Hattori,S., and Shinkai,H. (2003). Matrix metalloproteinases-2 and -9 are secreted from human fibroblasts. Acta Derm. Venereol. *83*, 105-107.

Kojima,S., Itoh,Y., Matsumoto,S., Masuho,Y., and Seiki,M. (2000). Membrane-type 6 matrix metalloproteinase (MT6-MMP, MMP-25) is the second glycosyl-phosphatidyl inositol (GPI)-anchored MMP. FEBS Lett. *480*, 142-146.

Kolodney,M.S. and Wysolmerski,R.B. (1992). Isometric contraction by fibroblasts and endothelial cells in tissue culture: a quantitative study. J Cell Biol. *117*, 73-82.

Konttinen,Y.T., Li,T.F., Hukkanen,M., Ma,J., Xu,J.W., and Virtanen,I. (2000). Fibroblast biology. Signals targeting the synovial fibroblast in arthritis. Arthritis Res. *2*, 348-355.

Kopetz,E.S., Nelson,J.B., and Carducci,M.A. (2002). Endothelin-1 as a target for therapeutic intervention in prostate cancer. Invest New Drugs *20*, 173-182.

Koumas,L., King,A.E., Critchley,H.O., Kelly,R.W., and Phipps,R.P. (2001). Fibroblast heterogeneity: existence of functionally distinct Thy 1(+) and Thy 1(-) human female reproductive tract fibroblasts. Am. J Pathol. *159*, 925-935.

Kratchmarova,I., Kalume,D.E., Blagoev,B., Scherer,P.E., Podtelejnikov,A.V., Molina,H., Bickel,P.E., Andersen,J.S., Fernandez,M.M., Bunkenborg,J., Roepstorff,P., Kristiansen,K., Lodish,H.F., Mann,M., and Pandey,A. (2002). A proteomic approach for identification of secreted proteins during the differentiation of 3T3-L1 preadipocytes to adipocytes. Mol. Cell Proteomics. *1*, 213-222.

Kunic,B., Truan,G., Breskvar,K., and Pompon,D. (2001). Functional cloning, based on azole resistance in Saccharomyces cerevisiae, and characterization of Rhizopus nigricans redox carriers that are differentially involved in the P450-dependent response to progesterone stress. Mol. Genet. Genomics *265*, 930-940.

Kuznetsov,S. and Gehron,R.P. (1996). Species differences in growth requirements for bone marrow stromal fibroblast colony formation In vitro. Calcif. Tissue Int. *59*, 265-270.

Laemmli,U.K. (1970). Cleavage of structural proteins during the assembly of the head of bacteriophage T4. Nature *227*, 680-685.

Lam,H.C., Lee,J.K., and Lai,K.H. (2000). Detection and characterization of endothelin in transformed human osteoblast cell culture medium. Endocrine. *12*, 77-80.

Lambert,C.A., Colige,A.C., Munaut,C., Lapiere,C.M., and Nusgens,B.V. (2001). Distinct pathways in the over-expression of matrix metalloproteinases in human fibroblasts by relaxation of mechanical tension. Matrix Biol *20*, 397-408.

Lander,A.D. (1999). Proteoglycans. In Guidebook to the Extracellular Matrix, Anchor, and Adhesion Proteins, T.Kreis and R.Vale, eds. (Oxford: Oxford University Press), pp. 351-356.

Lavker,R.M., Zheng,P.S., and Dong,G. (1987). Aged skin: a study by light, transmission electron, and scanning electron microscopy. J Invest Dermatol. *88*, 44s-51s.

Lee,C.H., Shin,H.J., Cho,I.H., Kang,Y.M., Kim,I.A., Park,K.D., and Shin,J.W. (2005). Nanofiber alignment and direction of mechanical strain affect the ECM production of human ACL fibroblast. Biomaterials *26*, 1261-1270.

Lee,H.G. and Eun,H.C. (1999). Differences between fibroblasts cultured from oral mucosa and normal skin: implication to wound healing. J Dermatol. Sci *21*, 176-182.

Lefrancois-Martinez,A.M., Bertherat,J., Val,P., Tournaire,C., Gallo-Payet,N., Hyndman,D., Veyssiere,G., Bertagna,X., Jean,C., and Martinez,A. (2004). Decreased

expression of cyclic adenosine monophosphate-regulated aldose reductase (AKR1B1) is associated with malignancy in human sporadic adrenocortical tumors. J Clin Endocrinol. Metab *89*, 3010-3019.

Leung,D.Y., Glagov,S., and Mathews,M.B. (1976). Cyclic stretching stimulates synthesis of matrix components by arterial smooth muscle cells in vitro. Science *191*, 475-477.

Li,S., Weidenfeld,J., and Morrisey,E.E. (2004). Transcriptional and DNA binding activity of the Foxp1/2/4 family is modulated by heterotypic and homotypic protein interactions. Mol. Cell Biol. *24*, 809-822.

Lichtinghagen,R., Musholt,P.B., Lein,M., Romer,A., Rudolph,B., Kristiansen,G., Hauptmann,S., Schnorr,D., Loening,S.A., and Jung,K. (2002). Different mRNA and protein expression of matrix metalloproteinases 2 and 9 and tissue inhibitor of metalloproteinases 1 in benign and malignant prostate tissue. Eur. Urol. *42*, 398-406.

Light,N.D. (1985). Collagen in skin: Preparation and analysis. In Methods in Skin Research, D.Skerrow and C.J.Skerrow, eds. (New York: John Wiley & Sons Ltd.), pp. 559-586.

Lin,T.W., Cardenas,L., and Soslowsky,L.J. (2004). Biomechanics of tendon injury and repair. J Biomech. *37*, 865-877.

Lindquist,S. and Craig,E.A. (1988). The heat-shock proteins. Annu. Rev. Genet. *22*, 631-677.

Liu,B. and Wu,D. (2003). The first inner loop of endothelin receptor type B is necessary for specific coupling to Galpha 13. J. Biol. Chem. *278*, 2384-2387.

Locklin,R.M., Riggs,B.L., Hicok,K.C., Horton,H.F., Byrne,M.C., and Khosla,S. (2001). Assessment of gene regulation by bone morphogenetic protein 2 in human marrow stromal cells using gene array technology. J. Bone Miner. Res. *16*, 2192-2204.

MacKenna,D., Summerour,S.R., and Villarreal,F.J. (2000). Role of mechanical factors in modulating cardiac fibroblast function and extracellular matrix synthesis. Cardiovasc. Res *46*, 257-263.

Magid,R., Murphy,T.J., and Galis,Z.S. (2003). Expression of matrix metalloproteinase-9 in endothelial cells is differentially regulated by shear stress. Role of c-Myc. J Biol. Chem. *278*, 32994-32999.

Majumdar,M.K., Thiede,M.A., Mosca,J.D., Moorman,M., and Gerson,S.L. (1998). Phenotypic and functional comparison of cultures of marrow-derived mesenchymal stem cells (MSCs) and stromal cells. J Cell Physiol *176*, 57-66.

Mandard,S., Zandbergen,F., Tan,N.S., Escher,P., Patsouris,D., Koenig,W., Kleemann,R., Bakker,A., Veenman,F., Wahli,W., Muller,M., and Kersten,S. (2004). The direct peroxisome proliferator-activated receptor target fasting-induced adipose factor (FIAF/PGAR/ANGPTL4) is present in blood plasma as a truncated protein that is increased by fenofibrate treatment. J. Biol. Chem. *279*, 34411-34420.

Marchant,J.K., Hahn,R.A., Linsenmayer,T.F., and Birk,D.E. (1996). Reduction of type V collagen using a dominant-negative strategy alters the regulation of fibrillogenesis and results in the loss of corneal-specific fibril morphology. J Cell Biol. *135*, 1415-1426.

Marchler-Bauer,A., Anderson,J.B., Cherukuri,P.F., DeWeese-Scott,C., Geer,L.Y., Gwadz,M., He,S., Hurwitz,D.I., Jackson,J.D., Ke,Z., Lanczycki,C.J., Liebert,C.A., Liu,C., Lu,F., Marchler,G.H., Mullokandov,M., Shoemaker,B.A., Simonyan,V., Song,J.S., Thiessen,P.A., Yamashita,R.A., Yin,J.J., Zhang,D., and Bryant,S.H. (2005). CDD: a Conserved Domain Database for protein classification. Nucleic Acids Res. *33 Database Issue*, D192-D196.

Marone,M., Mozzetti,S., De Ritis,D., Pierelli,L., and Scambia,G. (2001). Semiquantitative RT-PCR analysis to assess the expression levels of multiple transcripts from the same sample. Biol. Proced. Online. *3*, 19-25.

Marshall,G.E., Konstas,A.G., and Lee,W.R. (1991). Immunogold fine structural localization of extracellular matrix components in aged human cornea. II. Collagen types V and VI. Graefes Arch. Clin. Exp. Ophthalmol. *229*, 164-171.

Martin,G.M., Sprague,C.A., Norwood,T.H., and Pendergrass,W.R. (1974). Clonal selection, attenuation and differentiation in an in vitro model of hyperplasia. Am. J. Pathol. *74*, 137-154.

Matsuda,H. and Smelser,G.K. (1973). Electron microscopy of corneal wound healing. Exp. Eye Res. *16*, 427-442.

Maximow,A. (1927). Bindegewebe und blutbildende Gewebe. In Handbuch der mikroskopischen Anatomie des Menschen, W.von Mollendorff, ed. (Berlin: Springer), pp. 232-583.

McGarry,J.G., Klein-Nulend,J., and Prendergast,P.J. (2005). The effect of cytoskeletal disruption on pulsatile fluid flow-induced nitric oxide and prostaglandin E(2) release in osteocytes and osteoblasts. Biochem. Biophys. Res. Commun. *330*, 341-348.

McNeilly,C.M., Banes,A.J., Benjamin,M., and Ralphs,J.R. (1996). Tendon cells in vivo form a three dimensional network of cell processes linked by gap junctions. J Anat *189 (Pt 3)*, 593-600.

Meissner,A., Zilles,O., Varona,R., Jozefowski,K., Ritter,U., Marquez,G., Hallmann,R., and Korner,H. (2003). CC chemokine ligand 20 partially controls adhesion of naive B cells to activated endothelial cells under shear stress. Blood *102*, 2724-2727.

Melnick,A., Ahmad,K.F., Arai,S., Polinger,A., Ball,H., Borden,K.L., Carlile,G.W., Prive,G.G., and Licht,J.D. (2000). In-depth mutational analysis of the promyelocytic leukemia zinc finger BTB/POZ domain reveals motifs and residues required for biological and transcriptional functions. Mol. Cell Biol. *20*, 6550-6567.

Mercurio,F. and Manning,A.M. (1999). Multiple signals converging on NF-kappaB. Curr. Opin. Cell Biol. *11*, 226-232.

Michelacci,Y.M. (2003). Collagens and proteoglycans of the corneal extracellular matrix. Braz. J Med Biol. Res. *36*, 1037-1046.

Milunsky,A., Spielvogel,C., and Kanfer,J.N. (1972). Lysosomal enzyme variations in cultured normal skin fibroblasts. Life Sci. II *11*, 1101-1107.

Moll,R., Franke,W.W., Schiller,D.L., Geiger,B., and Krepler,R. (1982). The catalog of human cytokeratins: patterns of expression in normal epithelia, tumors and cultured cells. Cell *31*, 11-24.

Murphy,A.N., Unsworth,E.J., and Stetler-Stevenson,W.G. (1993). Tissue inhibitor of metalloproteinases-2 inhibits bFGF-induced human microvascular endothelial cell proliferation. J Cell Physiol *157*, 351-358.

Murphy,G., Nguyen,Q., Cockett,M.I., Atkinson,S.J., Allan,J.A., Knight,C.G., Willenbrock,F., and Docherty,A.J. (1994). Assessment of the role of the fibronectin-like domain of gelatinase A by analysis of a deletion mutant. J Biol. Chem. *269*, 6632-6636.

Musch,M.W., Petrof,E.O., Kojima,K., Ren,H., McKay,D.M., and Chang,E.B. (2004). Bacterial superantigen-treated intestinal epithelial cells upregulate heat shock proteins 25 and 72 and are resistant to oxidant cytotoxicity. Infect. Immun. *72*, 3187-3194.

Nagase,H. (1997). Activation mechanisms of matrix metalloproteinases. Biol. Chem. *378*, 151-160.

Nagase,H. and Woessner,J.F., Jr. (1999). Matrix metalloproteinases. J. Biol. Chem. *274*, 21491-21494.

Nakano,K., Kanai-Azuma,M., Kanai,Y., Moriyama,K., Yazaki,K., Hayashi,Y., and Kitamura,N. (2003). Cofilin phosphorylation and actin polymerization by NRK/NESK, a member of the germinal center kinase family. Exp. Cell Res. *287*, 219-227.

Nakano,K., Yamauchi,J., Nakagawa,K., Itoh,H., and Kitamura,N. (2000). NESK, a member of the germinal center kinase family that activates the c-Jun N-terminal kinase pathway and is expressed during the late stages of embryogenesis. J. Biol. Chem. *275*, 20533-20539.

Neidlinger-Wilke,C., Grood,E., Claes,L., and Brand,R. (2002). Fibroblast orientation to stretch begins within three hours. J Orthop. Res. *20*, 953-956.

Nelson,A.R., Fingleton,B., Rothenberg,M.L., and Matrisian,L.M. (2000). Matrix metalloproteinases: biologic activity and clinical implications. J Clin. Oncol. *18*, 1135-1149.

Ni,X., Ji,C., Cao,G., Cheng,H., Guo,L., Gu,S., Ying,K., Zhao,R.C., and Mao,Y. (2003). Molecular cloning and characterization of the protein 4.1O gene, a novel member of the protein 4.1 family with focal expression in ovary. J. Hum. Genet. *48*, 101-106.

Nishinaka,T. and Yabe-Nishimura,C. (2005). Transcription Factor Nrf2 Regulates Promoter Activity of Mouse Aldose Reductase (AKR1B3) Gene. J. Pharmacol. Sci. *97*, 43-51.

Ohtsubo,T., Rovira,I.I., Starost,M.F., Liu,C., and Finkel,T. (2004). Xanthine oxidoreductase is an endogenous regulator of cyclooxygenase-2. Circ. Res. *95*, 1118-1124.

Olivera,A., Rosenfeldt,H.M., Bektas,M., Wang,F., Ishii,I., Chun,J., Milstien,S., and Spiegel,S. (2003). Sphingosine kinase type 1 induces G12/13-mediated stress fiber formation, yet promotes growth and survival independent of G protein-coupled receptors. J. Biol. Chem. *278*, 46452-46460.

Osborn,M. and Weber,K. (1982). Intermediate filaments: cell-type-specific markers in differentiation and pathology. Cell *31*, 303-306.

Oxlund,H., Manschot,J., and Viidik,A. (1988). The role of elastin in the mechanical properties of skin. J Biomech. *21*, 213-218.

Parker,R.C. (1932). The functional characteristics of nine races of fibroblasts. Science *76*, 219-220.

Parker,R.C. and Fischer,A. (1929). Classification of "fibroblasts" according to their physiological properties. Proc. Soc. Exp. Biol. Med. *26*, 580-583.

Parkinson,D.B., Dickinson,S., Bhaskaran,A., Kinsella,M.T., Brophy,P.J., Sherman,D.L., Sharghi-Namini,S., Duran Alonso,M.B., Mirsky,R., and Jessen,K.R. (2003). Regulation of the myelin gene periaxin provides evidence for Krox-20-independent myelin-related signalling in Schwann cells. Mol. Cell Neurosci. *23*, 13-27.

Pasquali-Ronchetti,I. and Baccarani-Contri,M. (1997). Elastic fiber during development and aging. Microsc. Res. Tech. *38*, 428-435.

Pavalko,F.M., Chen,N.X., Turner,C.H., Burr,D.B., Atkinson,S., Hsieh,Y.F., Qiu,J., and Duncan,R.L. (1998). Fluid shear-induced mechanical signaling in MC3T3-E1 osteoblasts requires cytoskeleton-integrin interactions. Am. J. Physiol *275*, C1591-C1601.

Pearson,W.R., Reinhart,J., Sisk,S.C., Anderson,K.S., and Adler,P.N. (1988). Tissue-specific induction of murine glutathione transferase mRNAs by butylated hydroxyanisole. J. Biol. Chem. *263*, 13324-13332.

Pei,Y., Sherry,D.M., and McDermott,A.M. (2004). Thy-1 distinguishes human corneal fibroblasts and myofibroblasts from keratocytes. Exp. Eye Res. *79*, 705-712.

Petit,M.M., Meulemans,S.M., and Van de Ven,W.J. (2003). The focal adhesion and nuclear targeting capacity of the LIM-containing lipoma-preferred partner (LPP) protein. J. Biol. Chem. *278*, 2157-2168.

Petrini,S., Tessa,A., Carrozzo,R., Verardo,M., Pierini,R., Rizza,T., and Bertini,E. (2003). Human melanoma/NG2 chondroitin sulfate proteoglycan is expressed in the sarcolemma of postnatal human skeletal myofibers. Abnormal expression in merosin-negative and Duchenne muscular dystrophies. Mol. Cell Neurosci. *23*, 219-231.

Phillips,J.A., Vacanti,C.A., and Bonassar,L.J. (2003). Fibroblasts regulate contractile force independent of MMP activity in 3D-collagen. Biochem. Biophys. Res. Commun. *312*, 725-732.

Phinney,D.G., Kopen,G., Isaacson,R.L., and Prockop,D.J. (1999). Plastic adherent stromal cells from the bone marrow of commonly used strains of inbred mice: variations in yield, growth, and differentiation. J Cell Biochem. *72*, 570-585.

Pinto,d.S. and Gilula,N.B. (1972). Gap junctions in normal and transformed fibroblasts in culture. Exp. Cell Res. *71*, 393-401.

Pittenger,M.F., Mackay,A.M., Beck,S.C., Jaiswal,R.K., Douglas,R., Mosca,J.D., Moorman,M.A., Simonetti,D.W., Craig,S., and Marshak,D.R. (1999). Multilineage potential of adult human mesenchymal stem cells. Science *284*, 143-147.

Porter,K.R. and Vanamee,P. (1949). Observations on formation of connective tissue fibers. Proc. Soc. Exp. Biol. Med. *71*, 513-516.

Prajapati,R.T., Chavally-Mis,B., Herbage,D., Eastwood,M., and Brown,R.A. (2000a). Mechanical loading regulates protease production by fibroblasts in three-dimensional collagen substrates. Wound. Repair Regen. *8*, 226-237.

Prajapati,R.T., Eastwood,M., and Brown,R.A. (2000b). Duration and orientation of mechanical loads determine fibroblast cyto- mechanical activation: monitored by protease release. Wound. Repair Regen. *8*, 238-246.

Prockop,D.J. (1997). Marrow stromal cells as stem cells for nonhematopoietic tissues. Science *276*, 71-74.

Qi,C., Wheeler,J.A., Pruett,A., and Pekala,P.H. (2002). Expression of the RNA binding proteins, Mel-N1, Mel-N2, and Mel-N3 in adipose cells. Biochem. Biophys. Res. Commun. *294*, 329-333.

Quinn,J.M. and Gillespie,M.T. (2005). Modulation of osteoclast formation. Biochem. Biophys. Res. Commun. *328*, 739-745.

Rack,P.M. and Westbury,D.R. (1984). Elastic properties of the cat soleus tendon and their functional importance. J Physiol *347*, 479-495.

Radner,W., Zehetmayer,M., Aufreiter,R., and Mallinger,R. (1998). Interlacing and cross-angle distribution of collagen lamellae in the human cornea. Cornea *17*, 537-543.

Raspanti,M., Ottani,V., and Ruggeri,A. (1990). Subfibrillar architecture and functional properties of collagen: a comparative study in rat tendons. J Anat. *172*, 157-164.

Reddy,L., Wang,H.S., Keese,C.R., Giaever,I., and Smith,T.J. (1998). Assessment of rapid morphological changes associated with elevated cAMP levels in human orbital fibroblasts. Exp. Cell Res. *245*, 360-367.

Reichardt,L.F. and Tomaselli,K.J. (1991). Extracellular matrix molecules and their receptors: functions in neural development. Annu. Rev. Neurosci. *14*, 531-570.

Riederer-Henderson,M.A., Gauger,A., Olson,L., Robertson,C., and Greenlee,T.K., Jr. (1983). Attachment and extracellular matrix differences between tendon and synovial fibroblastic cells. In Vitro *19*, 127-133.

Ross,R. and Greenlee,T.K., Jr. (1966). Electron microscopy: attachment sites between connective tissue cells. Science *153*, 997-999.

Rozen,S. and Skaletsky,H. (2000). Primer3 on the WWW for general users and for biologist programmers. Methods Mol. Biol. *132* , 365-386.

Rudd,P.M., Mattu,T.S., Masure,S., Bratt,T., Van den Steen,P.E., Wormald,M.R., Kuster,B., Harvey,D.J., Borregaard,N., Van Damme,J., Dwek,R.A., and Opdenakker,G. (1999). Glycosylation of natural human neutrophil gelatinase B and neutrophil gelatinase B-associated lipocalin. Biochemistry *38*, 13937-13950.

Sachidanandan,C., Sambasivan,R., and Dhawan,J. (2002). Tristetraprolin and LPS-inducible CXC chemokine are rapidly induced in presumptive satellite cells in response to skeletal muscle injury. J. Cell Sci. *115*, 2701-2712.

Sadler,I., Crawford,A.W., Michelsen,J.W., and Beckerle,M.C. (1992). Zyxin and cCRP: two interactive LIM domain proteins associated with the cytoskeleton. J. Cell Biol. *119*, 1573-1587.

Sappino,A.P., Schurch,W., and Gabbiani,G. (1990). Differentiation repertoire of fibroblastic cells: expression of cytoskeletal proteins as marker of phenotypic modulations. Lab Invest *63*, 144-161.

Sato,H., Takino,T., Okada,Y., Cao,J., Shinagawa,A., Yamamoto,E., and Seiki,M. (1994). A matrix metalloproteinase expressed on the surface of invasive tumour cells. Nature *370*, 61-65.

Schena,M., Heller,R.A., Theriault,T.P., Konrad,K., Lachenmeier,E., and Davis,R.W. (1998). Microarrays: biotechnology's discovery platform for functional genomics. Trends Biotechnol. *16*, 301-306.

Schmidt,C., Pommerenke,H., Durr,F., Nebe,B., and Rychly,J. (1998). Mechanical stressing of integrin receptors induces enhanced tyrosine phosphorylation of cytoskeletally anchored proteins. J Biol. Chem. *273*, 5081-5085.

Schneider,E.L., Mitsui,Y., Au,K.S., and Shorr,S.S. (1977). Tissue-specific differences in cultured human diploid fibroblasts. Exp. Cell Res *108*, 1-6.

Schor,S.L., Schor,A.M., Grey,A.M., and Rushton,G. (1988). Foetal and cancer patient fibroblasts produce an autocrine migration-stimulating factor not made by normal adult cells. J Cell Sci. *90 (Pt 3)*, 391-399.

Schwann T.H. (1847). Microscopical researches into the accordance in the structure and growth of animals and plants. (London: Sydenham Society), pp. 1-268.

Schwartz,M.A., Schaller,M.D., and Ginsberg,M.H. (1995). Integrins: emerging paradigms of signal transduction. Annu. Rev. Cell Dev. Biol. *11*, 549-599.

Shen,F., Ruddy,M.J., Plamondon,P., and Gaffen,S.L. (2004). Cytokines link osteoblasts and inflammation: microarray analysis of interleukin-17- and TNF-{alpha}-induced genes in bone cells. J. Leukoc. Biol.

Shi-Wen,X., Chen,Y., Denton,C.P., Eastwood,M., Renzoni,E.A., Bou-Gharios,G., Pearson,J.D., Dashwood,M., du Bois,R.M., Black,C.M., Leask,A., and Abraham,D.J. (2004). Endothelin-1 promotes myofibroblast induction through the ETA receptor via a

rac/phosphoinositide 3-kinase/Akt-dependent pathway and is essential for the enhanced contractile phenotype of fibrotic fibroblasts. Mol. Biol. Cell *15*, 2707-2719.

Shiba,H., Mouri,Y., Komatsuzawa,H., Ouhara,K., Takeda,K., Sugai,M., Kinane,D.F., and Kurihara,H. (2003). Macrophage inflammatory protein-3alpha and beta-defensin-2 stimulate dentin sialophosphoprotein gene expression in human pulp cells. Biochem. Biophys. Res. Commun. *306*, 867-871.

Shimizu K. and Yoshizato K. (1992). Organ-dependent expression of differentiated states in fibroblasts cultured in vitro. Develop. Growth & Differ. *34*, 43-50.

Shipley,J.M., Doyle,G.A., Fliszar,C.J., Ye,Q.Z., Johnson,L.L., Shapiro,S.D., Welgus,H.G., and Senior,R.M. (1996). The structural basis for the elastolytic activity of the 92-kDa and 72-kDa gelatinases. Role of the fibronectin type II-like repeats. J Biol. Chem. *271*, 4335-4341.

Shirane,J., Nakayama,T., Nagakubo,D., Izawa,D., Hieshima,K., Shimomura,Y., and Yoshie,O. (2004). Corneal epithelial cells and stromal keratocytes efficently produce CC chemokine-ligand 20 (CCL20) and attract cells expressing its receptor CCR6 in mouse herpetic stromal keratitis. Curr. Eye Res. *28*, 297-306.

Silver,F.H., Freeman,J.W., and Seehra,G.P. (2003a). Collagen self-assembly and the development of tendon mechanical properties. J Biomech. *36*, 1529-1553.

Silver,F.H., Siperko,L.M., and Seehra,G.P. (2003b). Mechanobiology of force transduction in dermal tissue. Skin Res. Technol. *9*, 3-23.

Smith,J.B. and Herschman,H.R. (1995). Glucocorticoid-attenuated response genes encode intercellular mediators, including a new C-X-C chemokine. J. Biol. Chem. *270*, 16756-16765.

Smith,L., Parizi-Robinson,M., Zhu,M.S., Zhi,G., Fukui,R., Kamm,K.E., and Stull,J.T. (2002). Properties of long myosin light chain kinase binding to F-actin in vitro and in vivo. J. Biol. Chem. *277*, 35597-35604.

Smith,T.J., Sempowski,G.D., Wang,H.S., Del Vecchio,P.J., Lippe,S.D., and Phipps,R.P. (1995). Evidence for cellular heterogeneity in primary cultures of human orbital fibroblasts. J Clin. Endocrinol Metab *80*, 2620-2625.

Sorrell,J.M. and Caplan,A.I. (2004). Fibroblast heterogeneity: more than skin deep. J. Cell Sci. *117*, 667-675.

Spector,D.L., Goldman Robert D, and Leinwand Leslie A (1998). Cells: a laboratory manual. Cold Spring Harbor Laboratory Press).

Stark,J.M., Hu,P., Pierce,A.J., Moynahan,M.E., Ellis,N., and Jasin,M. (2002). ATP hydrolysis by mammalian RAD51 has a key role during homology-directed DNA repair. J. Biol. Chem. *277*, 20185-20194.

Stearns,M.L. (1940). Studies of the development of connective tissue transparent chambers in the rabbit ear. Am. J. Anat. *67*, 55-97.

Sternlicht,M.D. and Werb,Z. (2001). How matrix metalloproteinases regulate cell behavior. Annu. Rev. Cell Dev. Biol. *17*, 463-516.

Stevenson,M.A., Pollock,S.S., Coleman,C.N., and Calderwood,S.K. (1994). X-irradiation, phorbol esters, and H2O2 stimulate mitogen-activated protein kinase activity in NIH-3T3 cells through the formation of reactive oxygen intermediates. Cancer Res. *54*, 12-15.

Stocker,W., Grams,F., Baumann,U., Reinemer,P., Gomis-Ruth,F.X., McKay,D.B., and Bode,W. (1995). The metzincins--topological and sequential relations between the astacins, adamalysins, serralysins, and matrixins (collagenases) define a superfamily of zinc-peptidases. Protein Sci. *4*, 823-840.

Su,H.P., Nakada-Tsukui,K., Tosello-Trampont,A.C., Li,Y., Bu,G., Henson,P.M., and Ravichandran,K.S. (2002). Interaction of CED-6/GULP, an adapter protein involved in engulfment of apoptotic cells with CED-1 and CD91/low density lipoprotein receptor-related protein (LRP). J. Biol. Chem. *277*, 11772-11779.

Su,Y.C., Treisman,J.E., and Skolnik,E.Y. (1998). The Drosophila Ste20-related kinase misshapen is required for embryonic dorsal closure and acts through a JNK MAPK module on an evolutionarily conserved signaling pathway. Genes Dev. *12*, 2371-2380.

Sumi,Y., Muramatsu,H., Hata,K., Ueda,M., and Muramatsu,T. (2000). Secretory leukocyte protease inhibitor is a novel inhibitor of fibroblast-mediated collagen gel contraction. Exp. Cell Res. *256*, 203-212.

Svensson,L., Aszodi,A., Reinholt,F.P., Fassler,R., Heinegard,D., and Oldberg,A. (1999). Fibromodulin-null mice have abnormal collagen fibrils, tissue organization, and altered lumican deposition in tendon. J Biol Chem. *274*, 9636-9647.

Tajima,S. and Pinnell,S.R. (1981). Collagen synthesis by human skin fibroblasts in culture: studies of fibroblasts explanted from papillary and reticular dermis. J Invest Dermatol. *77*, 410-412.

Thompson,R.G., Nickel,B., Finlayson,S., Meuser,R., Hamerton,J.L., and Wrogemann,K. (1983). 56K fibroblast protein not specific for Duchenne muscular dystrophy but for skin biopsy site. Nature *304*, 740-741.

Torres,C., Francis,M.K., Lorenzini,A., Tresini,M., and Cristofalo,V.J. (2003). Metabolic stabilization of MAP kinase phosphatase-2 in senescence of human fibroblasts. Exp. Cell Res. *290*, 195-206.

Totsukawa,G., Wu,Y., Sasaki,Y., Hartshorne,D.J., Yamakita,Y., Yamashiro,S., and Matsumura,F. (2004). Distinct roles of MLCK and ROCK in the regulation of membrane protrusions and focal adhesion dynamics during cell migration of fibroblasts. J. Cell Biol. *164*, 427-439.

Umland,S.P., Wan,Y., Shah,H., Garlisi,C.G., Devito,K.E., Braunschweiger,K., Gheyas,F., and Del Mastro,R. (2004). Mouse ADAM33: two splice variants differ in protein maturation and localization. Am. J. Respir. Cell Mol. Biol. *30*, 530-539.

van der Pauw,M.T., Klein-Nulend,J., van den,B.T., Burger,E.H., Everts,V., and Beertsen,W. (2000). Response of periodontal ligament fibroblasts and gingival fibroblasts to pulsating fluid flow: nitric oxide and prostaglandin E2 release and expression of tissue non-specific alkaline phosphatase activity. J Periodontal Res. *35*, 335-343.

van Kooten,T.G., Schakenraad,J.M., van der Mei,H.C., and Busscher,H.J. (1992). Influence of substratum wettability on the strength of adhesion of human fibroblasts. Biomaterials *13*, 897-904.

van Kooten,T.G., Schakenraad,J.M., van der Mei,H.C., and Busscher,H.J. (1993). Influence of pulsatile flow on the behaviour of human fibroblasts adhered to glass. J. Biomater. Sci. Polym. Ed *4*, 601-614.

Van Wart,H.E. and Birkedal-Hansen,H. (1990). The cysteine switch: a principle of regulation of metalloproteinase activity with potential applicability to the entire matrix metalloproteinase gene family. Proc. Natl. Acad. Sci. U. S. A *87*, 5578-5582.

Vielmetter,J., Kayyem,J.F., Roman,J.M., and Dreyer,W.J. (1994). Neogenin, an avian cell surface protein expressed during terminal neuronal differentiation, is closely related to the human tumor suppressor molecule deleted in colorectal cancer. J. Cell Biol. *127*, 2009-2020.

Vij,N., Roberts,L., Joyce,S., and Chakravarti,S. (2004). Lumican suppresses cell proliferation and aids Fas-Fas ligand mediated apoptosis: implications in the cornea. Exp. Eye Res. *78*, 957-971.

Vogel,K.G. and Meyers,A.B. (1999). Proteins in the tensile region of adult bovine deep flexor tendon. Clin. Orthop. Relat Res. S344-S355.

Vosshenrich,C.A., Cumano,A., Muller,W., Di Santo,J.P., and Vieira,P. (2004). Pre-B cell receptor expression is necessary for thymic stromal lymphopoietin responsiveness in the bone marrow but not in the liver environment. Proc. Natl. Acad. Sci. U. S. A *101*, 11070-11075.

Waas,E.T., Lomme,R.M., DeGroot,J., Wobbes,T., and Hendriks,T. (2002). Tissue levels of active matrix metalloproteinase-2 and -9 in colorectal cancer. Br. J. Cancer *86*, 1876-1883.

Walker,G.A., Guerrero,I.A., and Leinwand,L.A. (2001). Myofibroblasts: molecular crossdressers. Curr. Top. Dev. Biol. *51*, 91-107.

Wang,J.H., Yang,G., Li,Z., and Shen,W. (2004a). Fibroblast responses to cyclic mechanical stretching depend on cell orientation to the stretching direction. J Biomech. *37*, 573-576.

Wang,X., Lee,G., Liebhaber,S.A., and Cooke,N.E. (1992). Human cysteine-rich protein. A member of the LIM/double-finger family displaying coordinate serum induction with c-myc. J. Biol. Chem. *267*, 9176-9184.

Wang,X.P., Suomalainen,M., Jorgez,C.J., Matzuk,M.M., Wankell,M., Werner,S., and Thesleff,I. (2004b). Modulation of activin/bone morphogenetic protein signaling by

follistatin is required for the morphogenesis of mouse molar teeth. Dev. Dyn. *231*, 98-108.

Welsh,I.C. and O'Brien,T.P. (2000). Loss of late primitive streak mesoderm and interruption of left-right morphogenesis in the Ednrb(s-1Acrg) mutant mouse. Dev. Biol. *225*, 151-168.

Winder,S.J. (2001). The complexities of dystroglycan. Trends Biochem. Sci. *26*, 118-124.

Wolf,N.S., Penn,P.E., Rao,D., and McKee,M.D. (2003). Intraclonal plasticity for bone, smooth muscle, and adipocyte lineages in bone marrow stroma fibroblastoid cells. Exp. Cell Res. *290*, 346-357.

Wozniak,M.A., Modzelewska,K., Kwong,L., and Keely,P.J. (2004). Focal adhesion regulation of cell behavior. Biochim. Biophys. Acta *1692*, 103-119.

Xia,C., Ma,W., Stafford,L.J., Liu,C., Gong,L., Martin,J.F., and Liu,M. (2003). GGAPs, a new family of bifunctional GTP-binding and GTPase-activating proteins. Mol. Cell Biol. *23*, 2476-2488.

Xin,Y., Yu,L., Chen,Z., Zheng,L., Fu,Q., Jiang,J., Zhang,P., Gong,R., and Zhao,S. (2001). Cloning, expression patterns, and chromosome localization of three human and two mouse homologues of GABA(A) receptor-associated protein. Genomics *74*, 408-413.

Xu,J., Zutter,M.M., Santoro,S.A., and Clark,R.A. (1998). A three-dimensional collagen lattice activates NF-kappaB in human fibroblasts: role in integrin alpha2 gene expression and tissue remodeling. J Cell Biol. *140*, 709-719.

Yamamoto,K., Dang,Q.N., Kennedy,S.P., Osathanondh,R., Kelly,R.A., and Lee,R.T. (1999). Induction of tenascin-C in cardiac myocytes by mechanical deformation. Role of reactive oxygen species. J Biol. Chem. *274*, 21840-21846.

Yang,Y., Dieter,M.Z., Chen,Y., Shertzer,H.G., Nebert,D.W., and Dalton,T.P. (2002a). Initial characterization of the glutamate-cysteine ligase modifier subunit Gclm(-/-) knockout mouse. Novel model system for a severely compromised oxidative stress response. J. Biol. Chem. *277*, 49446-49452.

Yang,Y., Sharma,R., Zimniak,P., and Awasthi,Y.C. (2002b). Role of alpha class glutathione S-transferases as antioxidant enzymes in rodent tissues. Toxicol. Appl. Pharmacol. *182*, 105-115.

Yao,H.H., Matzuk,M.M., Jorgez,C.J., Menke,D.B., Page,D.C., Swain,A., and Capel,B. (2004). Follistatin operates downstream of Wnt4 in mammalian ovary organogenesis. Dev. Dyn. *230*, 210-215.

Yi,C.E., Bekker,J.M., Miller,G., Hill,K.L., and Crosbie,R.H. (2003). Specific and potent RNA interference in terminally differentiated myotubes. J. Biol. Chem. *278*, 934-939.

Yokota,H., Goldring,M.B., and Sun,H.B. (2003). CITED2-mediated regulation of MMP-1 and MMP-13 in human chondrocytes under flow shear. J. Biol. Chem. *278*, 47275-47280.

Yoon,J.C., Chickering,T.W., Rosen,E.D., Dussault,B., Qin,Y., Soukas,A., Friedman,J.M., Holmes,W.E., and Spiegelman,B.M. (2000). Peroxisome proliferator-activated receptor gamma target gene encoding a novel angiopoietin-related protein associated with adipose differentiation. Mol. Cell Biol. *20*, 5343-5349.

Yoshinaka,T., Nishii,K., Yamada,K., Sawada,H., Nishiwaki,E., Smith,K., Yoshino,K., Ishiguro,H., and Higashiyama,S. (2002). Identification and characterization of novel mouse and human ADAM33s with potential metalloprotease activity. Gene *282*, 227-236.

Young,K.G., Pool,M., and Kothary,R. (2003). Bpag1 localization to actin filaments and to the nucleus is regulated by its N-terminus. J. Cell Sci. *116*, 4543-4555.

Zamir,E., Katz,B.Z., Aota,S., Yamada,K.M., Geiger,B., and Kam,Z. (1999). Molecular diversity of cell-matrix adhesions. J Cell Sci. *112 (Pt 11)*, 1655-1669.

Zhao,W.Q., Li,H., Yamashita,K., Guo,X.K., Hoshino,T., Yoshida,S., Shinya,T., and Hayakawa,T. (1998). Cell cycle-associated accumulation of tissue inhibitor of metalloproteinases-1 (TIMP-1) in the nuclei of human gingival fibroblasts. J Cell Sci. *111 (Pt 9)*, 1147-1153.

Zhao,Y.G., Xiao,A.Z., Newcomer,R.G., Park,H.I., Kang,T., Chung,L.W., Swanson,M.G., Zhau,H.E., Kurhanewicz,J., and Sang,Q.X. (2003). Activation of pro-gelatinase B by endometase/matrilysin-2 promotes invasion of human prostate cancer cells. J. Biol. Chem. *278*, 15056-15064.